NEUTRINO PROCESSES AND PAIR FORMATION IN MASSIVE STARS AND SUPERNOVAE*

WILLIAM A. FOWLER AND F. HOYLE
California Institute of Technology, Pasadena, California
St. John's College and the Department of Applied Mathematics and Theoretical Physics, Cambridge University, Cambridge, England
Received April 8, 1964

O dark dark dark. They all go into the dark,
The vacant interstellar spaces, the vacant into the vacant.

—T. S. ELIOT in *East Coker*, III (1940)

ABSTRACT

The present paper traces the physical properties of matter inside highly evolved stars, on the assumption that the whole material of the star is non-degenerate and that the star is in quasi-hydrostatic equilibrium. When these conditions are satisfied, the physical evolution of a particular element of material is insensitive to the stellar model but not to the total mass of the star. Our considerations refer explicitly to stars of mass greater than $\sim 10\, M_\odot$ but less than $\sim 10^6\, M_\odot$, at which point general relativistic considerations become paramount.

In Parts I and II neutrino-loss processes and neutrino-loss rates are examined. We conclude that $e^- + e^+ \rightarrow \nu + \bar{\nu}$ is the most important neutrino process in massive stars. In Part III a method is developed for calculating the product $\mu\beta$ as a function of temperature when electron-positron pair formation is taken into account. In this product μ is the mean molecular weight and β the ratio of gas pressure to gas plus radiation pressure. The results are used to derive relations of the form $\rho \propto (M_\odot/M)^2(T/\mu\beta)^3 \propto (M_\odot/M)^{1/2}T^3$ for massive stars. In Part IV we consider the internal energy of matter, again as a function of temperature, and including the effects of pair formation. Parts V, VI, and VII are concerned with nuclear reactions, in particular with oxygen burning, the α-process, and the e-process.

In the final Parts VIII and IX we consider the onset of a supernova of Type II in which the central core implodes while the mantle and envelope of the star explode. These considerations are tentative because the discussion now involves the structure of the whole star, and hence of the stellar model. It is emphasized that massive stars do not necessarily become Type II supernovae but can collapse to general relativistic singularities.

In the case that some form of braking mechanism, such as rotation, internal turbulence, or an entrained magnetic field, leads to core implosion followed by mantle-envelope explosion, our two main conclusions are as follows:

1. Although neutrino losses greatly speed up evolution when the temperature exceeds 10^9 ° K, the loss rate is not sufficient to produce a free-fall implosion. Free fall must await the phase change of iron group nuclei first to helium and free neutrons and finally to free protons and neutrons. Up to that point nuclear reactions which transform hydrogen into the most stable nuclei near iron are exoergic and supply the energy lost through radiation and neutrino processes.

2. Burbidge, Burbidge, Fowler, and Hoyle (1957) showed that the observed relative abundance of the iron group nuclei could be understood in terms of an equilibrium process, provided two parameters were appropriately chosen—the temperature and the ratio of the densities of free neutrons and protons. Other choices for these parameters did not lead to a satisfactory correspondence with the observed abundances. In this early work, no explanation could be given of why the two parameters should take the values necessary to explain the observed abundances. In Part VII we arrive at an explanation in terms of the evolution time scale set by neutrino losses due to pair annihilation. We conclude in part: *The terrestrial iron-group isotopic abundance ratios strongly indicate the operation in massive stars of an energy-loss mechanism having a loss rate of the same order of magnitude as that calculated for* $e^+ + e^- \rightarrow \nu + \bar{\nu}$ *on the basis of the universal Fermi interaction strength.*

Detailed theoretical derivations and numerical results have been relegated to three appendices. Appendix A treats beta-interaction rates under stellar conditions, Appendix B treats the effects of electron-positron pair formation on stellar structure and evolution, while Appendix C presents a summary of current estimates concerning nuclear-reaction rates.

* The substance of this paper was presented by W. A. F. as the 1963 Henry Norris Russell Lecture of the American Astronomical Society at its 114th meeting at the University of Alaska, College, Alaska, on July 23, 1963.

I. INTRODUCTION TO NEUTRINO PROCESSES

Theoretical and experimental studies of the nature of the weak Fermi interactions, such as beta-decay and muon-decay, indicate that *neutrino processes* may play an important role in the evolution of stars and the onset of supernova explosions. The conserved-vector-current theory of the weak decays, proposed by Feynman and Gell-Mann (1958*a*) and Gell-Mann (1958), has successfully predicted the results of experimental tests made by Nordberg, Morinigo, and Barnes (1960, 1962), Bardin, Barnes, Fowler, and Seeger (1960, 1962), Mayer-Kuckuk and Michel (1961, 1962), Freeman, Montague, West, and White (1962), and Lee, Mo, and Wu (1963). The present paper is primarily concerned with massive stars which evolve to Type II supernovae and with the neutrino processes predicted to occur in these stars by the theory. In the immediate pre-supernova state of evolution of such stars, an important factor is the escape of neutrinos and antineutrinos produced in the annihilation of the electron-positron pairs formed at high temperatures. This paper is to be regarded as a supplement to a previous discussion by the authors (Hoyle and Fowler 1960), in which *nuclear processes* in supernovae were treated.

Neutrino emission from stars has been previously treated by Bethe (1939), Gamow and Schönberg (1941), Pontecorvo (1959), Gandel'man and Pinaev (1959), Levine (1960, 1963), Chiu and Morrison (1960), Gell-Mann (1961), Chiu and Stabler (1961), Chiu (1961*a–c*, 1963), Ritus (1961), Matinyan and Tsilosani (1961), Stothers and Chiu (1962), Sampson (1962), Stothers (1963), Adams, Ruderman, and Woo (1963), Rosenberg (1963), and Pinaev (1963). The processes suggested by these authors are listed and briefly discussed in the numbered paragraphs below.

1. *Neutrino* (ν) *emission accompanies positron* (e^+) *emission in hydrogen burning either through the proton-proton chain or the CNO bi-cycle. Four protons* (p) *are transformed into the helium nucleus or alpha-particle* (α) *by the over-all reaction:*

$$4p \rightarrow \alpha + 2e^+ + 2\nu\,.$$

2. *Neutrinos and antineutrinos* ($\bar{\nu}$) *are emitted with positrons and electrons* (e^-), *respectively, by beta-unstable nuclei produced during energy generation and nucleosynthesis in nuclear processes involving intermediate and heavy nuclei. The beta-decays are:*

$$\text{(a)}\ (Z+1, A) \rightarrow (Z, A) + e^+ + \nu\,,$$

$$\text{(b)}\ (Z-1, A) \rightarrow (Z, A) + e^- + \bar{\nu}\,.$$

Electron capture is an alternative to 2(*a*):

$$\text{(c)}\ e^- + (Z+1, A) \rightarrow (Z, A) + \nu\,.$$

Nuclei are designated by their charge and mass numbers in parentheses. Antineutrino plus negative electron emission following neutron capture in heavy element synthesis is the most important of this class of processes. In the Fermi theory of beta-decay, 2(a) takes place when a proton in the nucleus $(Z+1, A)$ transforms into a neutron, the resulting nucleus then being (Z, A). Similarly, 2(b) takes place when a free neutron or a neutron in a nucleus transforms into a proton. *The free neutron decays to a proton because it has the greater rest mass. Thus*

$$\text{(d)}\ n \rightarrow p + e^- + \bar{\nu}\,.$$

3. *In the Urca process of Gamow and Schönberg as extended by Pinaev, under equilibrium conditions at high temperature and density in stars, electron capture with neutrino emission*

by a nucleus is followed by electron emission or positron capture which restores the original nucleus. The over-all process can be written as follows:

(a) $e^- + (Z, A) \rightarrow (Z - 1, A) + \nu$,

$(Z - 1, A) \rightarrow (Z, A) + e^- + \bar{\nu}$, or $e^+ + (Z - 1, A) \rightarrow (Z, A) + \bar{\nu}$,

so that

$$e^- + (Z, A) \rightarrow (Z, A) + e^- + \nu + \bar{\nu}, \quad \text{or} \quad e^+ + e^- + (Z, A) \rightarrow (Z, A) + \nu + \bar{\nu}.$$

The corresponding Urca process for positrons in antistars, if such exist, can be written as follows:

(b) $e^+ + (\bar{Z}, A) \rightarrow (\bar{Z} + 1, A) + \bar{\nu}$,

$(\bar{Z} + 1, A) \rightarrow (\bar{Z}, A) + e^+ + \nu$, or $e^- + (\bar{Z} + 1, A) \rightarrow (\bar{Z}, A) + \nu$,

so that

$$e^+ + (\bar{Z}, A) \rightarrow (\bar{Z}, A) + e^+ + \nu + \bar{\nu}, \quad \text{or} \quad e^+ + e^- + (\bar{Z}, A) \rightarrow (\bar{Z}, A) + \nu + \bar{\nu}.$$

In these expressions $\bar{Z}$ is negative. Pinaev suggested the second alternatives in the second and third lines of (a) and (b).

4. *Pontecorvo has suggested the process of neutrino bremsstrahlung in which a neutrino pair replaces the usual photon emitted in inelastic electron scattering. The process can be written for either positrons or electrons as follows:*

$$e^{\pm} + (Z, A) \rightarrow e^{\pm} + (Z, A) + \nu + \bar{\nu}.$$

5. *Ritus and also Chiu and Stabler have suggested a photoneutrino process in which a neutrino pair replaces the scattered photon in photon-electron interactions:*

$$\gamma + e^{\pm} \rightarrow e^{\pm} + \nu + \bar{\nu}.$$

6. *Chiu and Morrison and, independently, Levine have discussed a pair-annihilation neutrino process in which a neutrino pair replaces the photons usually emitted in electron-positron annihilation:*

$$e^+ + e^- \rightarrow \nu + \bar{\nu}.$$

The electron-positron pairs are produced at high temperature in stars by the electromagnetic radiation field. Note that pair annihilation effectively occurs through the Pinaev alternative in (3).

7. *Chiu and Morrison have also suggested neutrino-pair emission in photon-photon interactions:*

(a) $\gamma + \gamma \rightarrow \nu + \bar{\nu}$,

(b) $\gamma + \gamma \rightarrow \gamma + \nu + \bar{\nu}$.

Gell-Mann has shown that 7(a) is forbidden for certain forms of the weak interaction.

8. *Matinyan and Tsilosani and also Rosenberg have discussed neutrino-pair production by photons in the Coulomb field of a nucleus:*

$$\gamma + (Z, A) \rightarrow (Z, A) + \nu + \bar{\nu}.$$

9. *Adams, Ruderman, and Woo have suggested neutrino-pair emission in the decay of plasmons (γ_{pl}) in a stellar plasma:*

$$\gamma_{\rm pl} \rightarrow \nu + \bar{\nu} .$$

It will be noted in processes (4)–(9) that neutrino-pair emission replaces photon emission, singly or in pairs. The theoretical and experimental foundations of these processes and of processes (1)–(3) merit attention at the onset of this discussion. Processes (1)–(3), involving electron or positron emission and electron capture by nuclei, have been known for many years. Our understanding of these processes and our knowledge of their reaction rates have been greatly enhanced by the overthrow of parity conservation and the subsequent quantitative progress made possible by that event. For an excellent review of this exciting chapter in the modern history of physics, the reader is referred to the contribution by Wu (1961) to the Pauli Memorial Volume. Chapter xv of *Physics of the Nucleus* by Preston (1962) gives the theory of weak interaction processes in some detail. Even before the overthrow of parity, processes (1)–(3) were shown to involve neutrinos or antineutrinos by the experiments of Cowan, Reines, and their collaborators (see Reines [1960] for a review discussion). These investigators showed that the antineutrinos produced in fission reactors by process (2b) are absorbed in hydrogen. We add this process to those listed above.

10. *Antineutrino absorption stimulates proton decay with positron emission according to the reaction:*

$$\text{(a)}\quad \bar{\nu} + p \rightarrow n + e^{+} .$$

Reaction (10a) results in two detectable effects, the radiative annihilation of the positron and the radiative capture of the neutron by nuclei in the material of the experimental apparatus. The detection of these radiations is taken as observational proof that antineutrinos are emitted in 2(b). For the other processes in (1)–(3) the emission of neutrinos and antineutrinos remains to a certain extent a matter of inference. *Thus neutrino absorption by neutrons in nuclei (stimulated neutron decay) has not been observed because high-intensity neutrino sources (fission reactors are antineutrino sources!) are not available terrestrially. However, for completeness we list this process as follows:*

$$\text{(b)}\quad \nu + n \rightarrow p + e^{-} .$$

The cross-sections and mean free paths for neutrino and antineutrino absorption will be discussed at the beginning of Part II of this paper.

It will be observed that process (2d) for the free neutron is the spontaneous process corresponding to process (10b). In fact reaction (10b) is obtained from process (2d) merely by transposing the antineutrino to the left-hand side of process (2d) and changing it into its antiparticle, the neutrino. In general, when a particle from one side of a reaction is transposed to the other, it will be replaced by its antiparticle. Thus the equations for antinucleons corresponding to reactions (10a) and (10b) can be immediately written out, if desired, by transposing the proton and changing it to the negative proton and by transposing the neutron and changing it to the antineutron. Similar operations can be performed on processes (2a) and (2b). We will not have occasion to deal with antinucleons in this paper, but it will be realized that stars composed of antimatter, again if such exist, will undergo the same processes as stars composed of matter, with antineutrinos replacing neutrinos and vice versa and, in fact, in all cases, antiparticles replacing the corresponding particles and vice versa.

Before the Cowan-Reines experiments the existence of neutrinos and antineutrinos had an *implicit* basis in the experimental confirmation that these particles were required to conserve energy, angular momentum, linear momentum, and statistics in beta-decay as first suggested by Pauli and so successfully exploited by Fermi (see Wu 1961). In

this connection, it is perhaps not irrelevant to note that neutrinos were also thought necessary to "conserve parity" before it became apparent that parity was not conserved in weak interactions. Neutrinos have survived the non-conservation of parity even though they were introduced in part in order to conserve parity.

The situation in regard to processes (4)–(9) is quite different than for processes (1), (2), (3), and (10). To obtain a clear appreciation of this situation, it is necessary to appraise briefly the current status of the theory of the weak interactions. On theoretical grounds, Feynman and Gell-Mann (1958*a*), Sudarshan and Marshak (1958), and Sakurai (1958) proposed that the Fermi interactions have a universal form and a universal strength. The form is polar vector minus axial vector, customarily designated "V-A" since the phrase "polar-vector interaction" is usually shortened to "vector." It will be recalled that the electric field is a polar-vector field, while the magnetic field is an axial-vector field. The word "minus" in the description of the Fermi interactions appropriately describes the nature of the interference effects which frequently arise between the polar-vector interaction and the axial-vector interaction. In addition, Feynman and Gell-Mann (1958) and Gell-Mann (1958) proposed that the polar-vector part of the weak interaction current is conserved, i.e., it is unchanged on renormalization in the case of nucleons which have strong nucleonic interactions. This is accomplished by including pion contributions as well as nucleon contributions in nuclear beta-decay. The same remarks are also true for the electric field: that produced by the proton is the same as that produced by the positron, i.e., these particles have the same electric charge. The electric charge of the proton is independent of the proton's strong nucleonic interaction.

On the basis of universality the polar-vector coupling strength in nuclear beta-decay should equal the coupling in muon decay, which requires no renormalization since muons do not enjoy the strong nucleonic interactions. This is not the case for the axial-vector interaction which is expected to be changed upon renormalization in the case of nucleons, although an unambiguous theoretical calculation cannot be made. Empirically the fact that the axial-vector coupling strength is 20 per cent greater in amplitude than the polar-vector coupling in nuclear beta-decay can be attributed to renormalization effects. Similarly the proton and neutron do not have the Dirac values for their magnetic moments. Renormalization does change the magnetic moments of the proton and neutron but not their electric charges.

The V-A form of the Fermi interactions is in excellent agreement with experiments on parity non-conservation and lepton conservation (see Konopinski [1959] for a review discussion). The universality of the coupling strength has been demonstrated in that the coupling constant (analogous to electric charge in electromagnetism) in muon decay has indeed been found to be very nearly equal experimentally to the vector-coupling constant in the decay of the radioactive nucleus, O^{14}. This last decay has certain properties which make it less dependent than in most cases on detailed knowledge of the internal structure of O^{14} and of the radioactive product, the excited state of N^{14} which is the isotopic spin counterpart of O^{14}. The experimental discrepancy according to Bardin *et al.* (1960, 1962) in the equality of the muon and vector coupling is 2.0 ± 0.2 per cent, or ten times the probable error of measurement. In a number of similar decays the discrepancy is 2.2 ± 0.2 per cent according to Freeman *et al.* (1962, 1964). However, these discrepancies are probably due to poor estimation of theoretical corrections to the decay rates, to a weak charge-dependent nuclear force (Blin-Stoyle and Le Tourneux 1961), to a finite mass for the vector boson which may serve as the exchanged "quantum" in the weak interactions (Lee 1962), or to the fact that the muon coupling constant may include a small strangeness–non-conserving term as well as the strangeness-conserving vector coupling term (Feynman and Gell-Mann 1958*b*, Cabibbo 1963).

The conserved-vector-coupling hypothesis has also been found to be in agreement with observations on small theoretically predicted effects in the mirror decays Li^8, B^8 (Nordberg *et al.* 1960, 1962) and B^{12}, N^{12} (Mayer-Kuckuk and Michel 1961, 1962; Lee

et al. 1963). In addition the theory predicts the right order of magnitude ($\sim 10^{-8}$) for the ratio of pion beta-decays, $\pi^+ \rightarrow \pi^o + e^+ + \nu$, to normal pion decays, $\pi^+ \rightarrow \mu^+ + \nu'$ (Bacastow, Elioff, Larsen, Wiegand, and Ypsilantis 1962).

The situation, then, is that a fairly complete theory of the weak Fermi interactions has been verified in many details. However, processes (4)–(9) have not been observed in the laboratory because the very low cross-sections to be expected theoretically place them below the limit of detectability at the present time. The essential point theoretically comes down to the question of the extent of the universality of the interaction, as will become clear in the following paragraphs.

The weak Fermi interactions are "point" or, at most, very short-range ($\lesssim 4 \times 10^{-14}$ cm) interactions between fermions in groups of four. This is apparent in the processes previously listed except for processes (7a) and (7b), which are induced by a pair of photons which are bosons and not fermions. Process (9) involves a single plasmon. However, processes (7a), (7b), and (9) occur through an intermediate pair of virtual fermions, e.g., an electron and a positron, which are not indicated in the symbolic reaction. The four interacting fermions occur in pairs:

(1) *antineutron-proton* ($\bar{n}p$), (2) *negative proton–neutron* ($\bar{p}n$),
(3) *positive electron–neutrino* ($\bar{e}\nu$), (4) *antineutrino–negative electron* ($\bar{\nu}e$),
(5) *positive muon–neutrino* ($\bar{\mu}\nu'$), and (6) *antineutrino–negative muon* ($\bar{\nu}'\mu$).

Here we use $e = e^-$, $\bar{e} = e^+$, $\mu = \mu^-$, and $\bar{\mu} = \mu^+$, and the neutrinos associated with muons are distinguished by a prime superscript. The particle-antiparticle combinations guarantee the conservation of nucleons and the conservation of leptons (electrons, muons, neutrinos) in all the interactions. Thus, for example, the negative proton-neutron combination can transform into the antineutrino-negative electron combination, and when the negative proton is transferred to the final stage of the process becoming a proton, the final transformation describes ordinary neutron decay (2d). Transposing the antineutrino to the initial stage and changing it into a neutrino yields stimulated neutron decay (10b), a process in which only particles and no antiparticles are involved. From these considerations it will be clear that the antineutron-proton combination can be interpreted as the *destruction* of a neutron with the *production* of a positive proton. In the mathematical formalism (2), (4), and (6) are represented by the Hermitean conjugates of (1), (3), and (5).

Recent experiments by Danby, Gaillard, Goulianos, Lederman, Mistry, Schwartz, and Steinberger (1962) indicate that the neutrinos associated with muons are not identical with those associated with electrons, but the present considerations are independent of this point. It is known that pairs of the so-called strange particles, e.g., kaons, do not share the full strength of the interaction between ordinary fermions, but again the present considerations are unaffected one way or the other except in that the muon coupling constant may be slightly greater than the vector coupling constant if it includes a strangeness–non-conserving term.

In calculating the transition probability or rate of any one of the Fermi interactions using the Feynman–Gell-Mann theory, it is first necessary to evaluate the transition amplitude as the "square" of a Fermi interaction current. Formally, the interaction current, J_μ with $\mu = 1, 2, 3, 4$, or x, y, z, t, must be multiplied by a propagator, $D_{\mu\nu}$, and then by its Hermitean conjugate, $J_\nu{}^+$. In the considerations which follow we can ignore the propagator. Contributions to the current come from terms stipulating the appropriate operations on the wave functions of each of the coupled pairs mentioned above. Thus the interaction current is given by

$$J_\mu = (\bar{n}\gamma_\mu a p) + (\bar{e}\gamma_\mu a \nu) + (\bar{\mu}\gamma_\mu a \nu') , \tag{1}$$

where γ_μ is a Dirac operator, $a = \frac{1}{2}(1 + i\gamma_5)$ with $\gamma_5 = \gamma_1\,\gamma_2\,\gamma_3\,\gamma_4$, and the particle symbols represent the appropriate wave functions. Similarly

$$J_\nu^+ = (\bar{n}\gamma_\nu a p)^+ + \ldots = (\bar{p}\gamma_\nu \bar{a} n) + \ldots \tag{2}$$

with $\bar{a} = \frac{1}{2}(1 - i\gamma_5)$. The polar-vector coupling is represented by $\gamma_\mu/2$ and the axial vector by $-i\gamma_\mu\gamma_5/2$.

On the principle of universality the terms are all weighted equally in the total sum for the current. Additional pion terms must be added to the nucleonic terms to give no change on renormalization for the polar-vector coupling. Physically these pion terms correspond to the observed decay of charged pions. This decay can appropriately be added to our list of processes.

11. *Charged pions decay through a pair of virtual nucleons to muons and neutrinos as follows:*

(a) $\pi^+ \rightarrow (p + \bar{n}) \rightarrow (n + \mu^+ + \nu' + \bar{n})$ or $(p + \mu^+ + \nu' + \bar{p}) \rightarrow \mu^+ + \nu'$,

(b) $\pi^- \rightarrow (\bar{p} + n) \rightarrow (\bar{n} + \mu^- + \bar{\nu}' + n)$ or $(\bar{p} + \mu^- + \bar{\nu}' + p) \rightarrow \mu^- + \bar{\nu}'$.

Annihilation of nucleons and antinucleons occurs in the intermediate stage.

It will be clear that the "square" of the current contains cross terms as well as square terms. For simplicity we ignore the operators, $\gamma_\mu a$, and then the cross term, $(\bar{n}p)(\bar{e}\nu)^+ = (\bar{n}p)(\bar{\nu}e)$, can be read as the destruction of a neutron and a neutrino with the creation of a positive proton and a negative electron which is just process (10b), or after transposition of the neutrino, just neutron decay (2d). The cross term $(\bar{e}\nu)(\bar{n}p)^+ = (\bar{e}\nu)(\bar{p}n)$ represents electron capture by protons or proton decay after transposition of the electron. In a sense this term is redundant since it is just the reverse process to the first cross term discussed.

The two other cross terms, excluding redundancies, correspond to muon decay $(\bar{\mu}\nu')(\bar{\nu}e)$ and muon capture $(\bar{\mu}\nu')(\bar{p}n)$. Although we will not discuss muon processes in this paper, they may eventually prove of interest in stars if very high temperatures are attained. Thus muon processes can be added to our list.

12. *Muons decay to electrons, neutrinos, and antineutrinos as follows:*

(a) $\mu^- \rightarrow e^- + \nu' + \bar{\nu}$,

(b) $\mu^+ \rightarrow e^+ + \bar{\nu}' + \nu$.

13. *Muons are captured by protons and neutrons as follows:*

(a) $\mu^- + p \rightarrow n + \nu'$,

(b) $\mu^+ + n \rightarrow p + \bar{\nu}'$.

The capturing proton and neutron can, of course, occur as nucleons in nuclei. Examples of cross terms and square terms are presented briefly in Tables 1 and 2.

The present observational situation indicates that the transition amplitudes in processes (1)–(3) and (10)–(13), which involve representative nucleonic, pionic, electronic, and muonic cross terms, do have a universal value. However, "square" terms and, in particular, $(\bar{e}\nu)(\bar{e}\nu)^+ = (\bar{e}\nu)(\bar{\nu}e)$, are involved in processes (4)–(9). Thus process (6) can be described by first writing $(\bar{e}\nu)(\bar{\nu}e)$ which describes neutrino scattering by electrons, $\nu + e^- \rightarrow \nu + e^-$, and then transposing the electron on the right-hand side so that a positive electron as well as a negative electron occurs in the initial stage and finally transposing the neutrino on the left-hand side so that an antineutrino as well as a neutrino occurs in the final stage. The result is $e^+ + e^- \rightarrow \nu + \bar{\nu}$. As another example, trans-

pose both neutrinos to obtain antineutrino scattering by electrons, $\bar{\nu} + e^- \rightarrow \bar{\nu} + e^-$. Because of experimental difficulties arising from the smallness of the cross-sections involved relative to the corresponding cross-sections for photon emission, these processes involving "square" terms have not been observed. The Feynman–Gell-Mann theory states that the "square" terms appear in a straightforward way and that the interactions they describe share the universal coupling. A contrary theory might well be formulated in which, for example, an interaction current did not serve as the starting point. However, for the present, the simplest hypothesis is to begin with an interaction current and to extend the universality observed for the cross terms to the "square" terms. Then unambiguous and explicit calculations can be made on the reaction rates of processes (4)–(9).

Experimental proof of the "square" terms will be difficult. The "square" of the nucleonic terms $(\bar{n}p)(\bar{n}p)^+ = (\bar{n}p)(\bar{p}n)$ describes nuclear scatterings and reactions induced by the weak interaction. These nuclear processes will not conserve parity, whereas nuclear processes induced by the strong nuclear forces are believed to conserve parity strictly. The parity–non-conserving amplitudes will be small compared to the parity-conserving ones, but measurements of the interference between these amplitudes may eventually prove successful (Michel 1964). The establishment of one type of "square" term would strongly point to the existence of the others. There is another interesting possibility for experimental investigations. If the weak interactions are due to an *uxl* (vector boson) acting as a quantum just as the photon does in the case of the electromagnetic interaction, then the interaction current theory follows directly, again just as in the electromagnetic case.

14. *The interactions of charged* uxl*'s or vector bosons (excluding muon and kaon interactions) can be represented as follows:*

$$\text{(a)}\quad p^+ + \bar{n} \rightarrow U^+ \rightarrow \mu^+ + \nu' \rightarrow e^+ + \nu\,,$$

$$\text{(b)}\quad p^- + n \rightarrow U^- \rightarrow \mu^- + \bar{\nu}' \rightarrow e^- + \bar{\nu}\,,$$

TABLE 1

THE WEAK INTERACTION: CROSS TERMS
(UNIVERSAL STRENGTH OBSERVED)

$(\bar{n}p)(\bar{\nu}e)$	$n+\nu \rightarrow p+e^-$	
	or $n \rightarrow p+e^-+\bar{\nu}$	Observed beta decay
$(\bar{\mu}\nu')(\bar{p}n)$	$\mu^-+p \rightarrow n+\nu'$	Observed muon capture
$(\bar{\mu}\nu')(\bar{\nu}e)$	$\mu^-+\nu \rightarrow e^-+\nu'$	
	or $\mu^- \rightarrow e^-+\nu'+\bar{\nu}$	Observed muon decay

TABLE 2

THE WEAK INTERACTION: SQUARE TERMS
(UNIVERSAL STRENGTH ASSUMED)

$(\bar{\nu}e)(\bar{e}\nu)$	$\nu+e^- \rightarrow \nu+e^-$	Unobserved neutrino-electron scattering
	or $e^++e^- \rightarrow \nu+\bar{\nu}$	Unobserved annihilation with neutrino emission
	competes with	
	$e^++e^- \rightarrow \gamma+\gamma$	Observed annihilation with photon emission
	$[G/(e^2/\hbar c)]^2 \sim 10^{-19}$	Fractional competition
$(\bar{p}n)(\bar{n}p)$	$p+n \rightarrow p+n$	Nucleon scattering with parity violation

where γ_μ is a Dirac operator, $a = \frac{1}{2}(1 + i\gamma_5)$ with $\gamma_5 = \gamma_1\,\gamma_2\,\gamma_3\,\gamma_4$, and the particle symbols represent the appropriate wave functions. Similarly

$$J_\nu^+ = (\bar{n}\gamma_\nu a\bar{p})^+ + \ldots = (\bar{p}\gamma_\nu \bar{a}n) + \ldots \tag{2}$$

with $\bar{a} = \frac{1}{2}(1 - i\gamma_5)$. The polar-vector coupling is represented by $\gamma_\mu/2$ and the axial vector by $-i\gamma_\mu\gamma_5/2$.

On the principle of universality the terms are all weighted equally in the total sum for the current. Additional pion terms must be added to the nucleonic terms to give no change on renormalization for the polar-vector coupling. Physically these pion terms correspond to the observed decay of charged pions. This decay can appropriately be added to our list of processes.

11. *Charged pions decay through a pair of virtual nucleons to muons and neutrinos as follows:*

(a) $\pi^+ \rightarrow (p + \bar{n}) \rightarrow (n + \mu^+ + \nu' + \bar{n})$ or $(p + \mu^+ + \nu' + \bar{p}) \rightarrow \mu^+ + \nu'$,

(b) $\pi^- \rightarrow (\bar{p} + n) \rightarrow (\bar{n} + \mu^- + \bar{\nu}' + n)$ or $(\bar{p} + \mu^- + \bar{\nu}' + p) \rightarrow \mu^- + \bar{\nu}'$.

Annihilation of nucleons and antinucleons occurs in the intermediate stage.

It will be clear that the "square" of the current contains cross terms as well as square terms. For simplicity we ignore the operators, $\gamma_\mu a$, and then the cross term, $(\bar{n}p)(\bar{e}\nu)^+ = (\bar{n}p)(\bar{\nu}e)$, can be read as the destruction of a neutron and a neutrino with the creation of a positive proton and a negative electron which is just process (10b), or after transposition of the neutrino, just neutron decay (2d). The cross term $(\bar{e}\nu)(\bar{n}p)^+ = (\bar{e}\nu)(\bar{p}n)$ represents electron capture by protons or proton decay after transposition of the electron. In a sense this term is redundant since it is just the reverse process to the first cross term discussed.

The two other cross terms, excluding redundancies, correspond to muon decay $(\bar{\mu}\nu')(\bar{\nu}e)$ and muon capture $(\bar{\mu}\nu')(\bar{p}n)$. Although we will not discuss muon processes in this paper, they may eventually prove of interest in stars if very high temperatures are attained. Thus muon processes can be added to our list.

12. *Muons decay to electrons, neutrinos, and antineutrinos as follows:*

(a) $\mu^- \rightarrow e^- + \nu' + \bar{\nu}$,

(b) $\mu^+ \rightarrow e^+ + \bar{\nu}' + \nu$.

13. *Muons are captured by protons and neutrons as follows:*

(a) $\mu^- + p \rightarrow n + \nu'$,

(b) $\mu^+ + n \rightarrow p + \bar{\nu}'$.

The capturing proton and neutron can, of course, occur as nucleons in nuclei. Examples of cross terms and square terms are presented briefly in Tables 1 and 2.

The present observational situation indicates that the transition amplitudes in processes (1)–(3) and (10)–(13), which involve representative nucleonic, pionic, electronic, and muonic cross terms, do have a universal value. However, "square" terms and, in particular, $(\bar{e}\nu)(\bar{e}\nu)^+ = (\bar{e}\nu)(\bar{\nu}e)$, are involved in processes (4)–(9). Thus process (6) can be described by first writing $(\bar{e}\nu)(\bar{\nu}e)$ which describes neutrino scattering by electrons, $\nu + e^- \rightarrow \nu + e^-$, and then transposing the electron on the right-hand side so that a positive electron as well as a negative electron occurs in the initial stage and finally transposing the neutrino on the left-hand side so that an antineutrino as well as a neutrino occurs in the final stage. The result is $e^+ + e^- \rightarrow \nu + \bar{\nu}$. As another example, trans-

neutrino typically receive kinetic energies around 1.4 MeV. Thus the loss is 1.4 MeV/22.8 MeV $\sim$ 6 per cent. In the r-process in Type I supernovae (B^{2}FH 1957; Becker and Fowler 1959) approximately three capture gamma rays of considerably lower energy, $\sim$5 MeV total, are followed by a much more energetic beta-decay in which antineutrino and electron energies are about 6 MeV each so the direct energy loss is 6 MeV/17 MeV $\sim$ 35 per cent of the total. These losses are not as critical as others to be described and will not be elaborated upon at this time. The point is that some nuclear energy is made available in the interior of a star by these processes even though some escape as neutrinos.

In 1941, Gamow and Schönberg proposed process (3) as the mechanism for energy loss which could lead to catastrophic implosion in supernova events. Losses of the order of 10^{11} erg gm^{-1} sec^{-1} arise in the equilibrium involving $_{26}Fe^{56}$ or (26, 56) as (Z, A) in process (3) and $_{25}Mn^{56}$ or (25, 56) as ($Z-1$, A) in pre-supernova stars with central temperatures near $T = 7 \times 10^9$ degrees and density $\rho = 10^7$ gm cm^{-3}. Hoyle (1946) and Hoyle and Fowler (1960) showed that this process was not nearly as effective a mechanism for refrigeration as the photodisintegration of iron-group nuclei into alpha-particles and neutrons which occurs at the temperature and density just indicated and which is discussed in some detail in Part VIII of this paper. However, with the discovery of processes (4)–(9) the question has been reopened by Pontecorvo and others.

It is now generally agreed on the basis of the universal theory of the weak Fermi interaction, the foundations for which were discussed in detail in Part I, that process (6) is by far the most effective of all the neutrino loss mechanisms in *massive* stars with $M \gtrsim 10\, M_\odot$. It alone will be discussed in the sequel. As far as the present authors are aware, the cross-section for this process was first derived by Levine (1960, 1963) who found

$$\sigma = \frac{1}{3\pi} G^2 \left(\frac{\hbar}{m_e c}\right)^2 \left(\frac{c}{v}\right)\left[(\omega^2 - 1) - \tfrac{1}{2}\left(\frac{m_e}{m_b}\right)^2(\omega^4 - 2\omega^2 - 2) + \ldots\right]$$
$$\approx 1.424 \times 10^{-45}\left(\frac{c}{v}\right)(\omega^2 - 1)\,\mathrm{cm}^2, \tag{3}$$

where $W = \omega m_e c^2$ is the total energy (rest mass and kinetic) of the annihilating electron and positron in their center-of-momentum coordinate system and v is their relative velocity, while m_b is the mass of the vector boson and $G = 3.00 \pm 0.03 \times 10^{-12}$ is the dimensionless interaction constant for the polar-vector beta-decay which, as discussed in Part I, is experimentally and theoretically close in value to the coupling constant for the muon decay. The numerical value of G is the average of the experimental results of Bardin *et al.* (1960, 1962) and of Freeman *et al.* (1962, 1964). The numerical value given can also be expressed non-dimensionally as $G = 1.00 \pm 0.01 \times 10^{-5}\ (m_e/M_u)^2$, where $M_u = 1822\, m_e$ is the atomic mass unit while in cgs units $G\hbar^3/m_e^2 c = 1.41 \pm 0.01 \times 10^{-49}$ erg cm^3. The other symbols have their customary meanings; $\hbar/m_e c = 3.8614 \times 10^{-11}$ cm is just the Compton wavelength/2π of the electron. The numerical form of equation (3) neglects the term in $(m_e/m_b)^2 \lesssim 10^{-6}$. The cross-section for annihilation with photon emission is proportional to $(e^2/m_e c^2)^2$. Thus the ratio of neutrino emission to photon emission is of order $(G\hbar c/e^2)^2 \sim (137 \times 3 \times 10^{-12})^2 \sim 10^{-19}$.

Using equation (3), Levine (1960, 1963) and Chiu and Stabler (1961) have calculated the neutrino luminosity of stellar material starting with the equation

$$\frac{du_\nu}{dt} = n_+ n_- \langle \sigma v W \rangle \qquad \text{erg cm}^{-3}\,\text{sec}^{-1}, \tag{4}$$

where n_+ and n_- are the positron and electron number densities per cm^3 and the average indicated is taken over the distribution in total energy, W, and relative velocity, v, of the positron-electron pair. Similarly, one can write

$$\frac{dU_\nu}{dt} = \rho N_+ N_- \langle \sigma v W \rangle \qquad \text{erg gm}^{-1}\,\text{sec}^{-1}, \tag{5}$$

where $\rho\, dU_\nu/dt = du_\nu/dt$, ρ is the density in gm cm^{-3}, and $N_+ = n_+/\rho$ and $N_- = n_-/\rho$ are the positron and electron number densities per gram. (In regard to notation, lower-case letters will be used for symbols designating quantities per cm^3 and capital letters for quantities per gm.) Numerically, one has before averaging

$$\sigma v W = 3.49 \times 10^{-41}\,(\omega^3 - \omega) \qquad \text{erg cm}^3\,\text{sec}^{-1}\,. \tag{6}$$

The Fermi-Dirac number densities of positrons and electrons in equilibrium with the radiation field and with nuclei are

$$\begin{aligned} n_\pm = \rho N_\pm &= \frac{1}{\pi^2}\left(\frac{m_e c}{\hbar}\right)^3 \int_0^\infty \frac{\eta^2 d\eta}{\exp[\,z\,(\eta^2+1)^{1/2} \pm \varphi\,] + 1} \\ &= \frac{1}{\pi^2}\left(\frac{m_e c}{\hbar}\right)^3 \int_1^\infty \frac{\omega\,(\omega^2-1)^{1/2} d\omega}{\exp(\,z\omega \pm \varphi) + 1}\,, \end{aligned} \tag{7}$$

where $z = m_e c^2/kT = 5.930/T_9$ with $T_9 = T/10^9$ degrees, η is the positron or electron momentum in units of $m_e c$, ω is the total energy in units of $m_e c^2$, $\varphi = \Phi/kT$ is the chemical potential for positrons (use + sign) and electrons (use − sign) in units kT. The chemical potential can be determined by using the auxiliary condition

$$n_0 = n_- - n_+\,, \tag{8}$$

where $n_0 = \rho N_0 = Z n_N = \rho Z/AM_u$ is the number of ionization electrons per cm^3 associated with nuclei of charge number Z, mass number A, and number density n_N per cm^3, N_0 is the number of electrons per gram, M_u is the atomic mass unit on the new $C^{12} = 12$ scale, and A/Z is the mean molecular weight per electron in the absence of electron-positron pairs. Appropriate averages can be taken in the case of mixed nuclear content.

This paper is concerned principally with Type II supernovae, which, according to Hoyle and Fowler (1960), occur as the final evolutionary stage of massive stars ($M \gtrsim 10\,M_\odot$). In the pre-supernova stages of such stars the electrons and positrons are non-degenerate, for which the inequality $\exp[z(\eta^2+1)^{1/2} \pm \varphi] \gg 1$ holds in the region where the maximum of the integrand occurs in equation (7). In what follows this approximation will be employed so that

$$n_\pm = \rho N_\pm \approx n_1 \exp(\mp \varphi)\,, \tag{9}$$

where

$$\begin{aligned} n_1 = \rho N_1 &= \frac{1}{\pi^2}\left(\frac{m_e c}{\hbar}\right)^3 \int_0^\infty \exp[\,-z\,(\eta^2+1)^{1/2}\,]\,\eta^2 d\eta \\ &= \frac{1}{\pi^2}\left(\frac{m_e c}{\hbar}\right)^3 \int_1^\infty \exp(\,-z\omega)\left(\frac{v}{c}\right)\omega^2 d\omega \\ &= \frac{1}{\pi^2}\left(\frac{m_e c}{\hbar}\right)^3 \left(\frac{kT}{m_e c^2}\right) K_2(z) = \frac{2}{\pi^2}\left(\frac{kT}{\hbar c}\right)^3 \bar{K}_2(z) \\ &= 1.688 \times 10^{28} T_9^3 \bar{K}_2(z)\,\text{cm}^{-3}\,. \end{aligned} \tag{10}$$

In the last expressions $\bar{K}_2(z) = \bar{K}_2(5.93/T_9) = \frac{1}{2}z^2\,K_2(z)$, where $K_2(z)$ is the modified Bessel function of second order. Figure 1 shows $\bar{K}_2$ as a function of $T = m_e c^2/kz$. In the extreme relativistic (ER) non-degenerate case one has

$$\bar{K}_2 \approx 1 \qquad kT > m_e c^2\,, \qquad \text{ER} \tag{11}$$

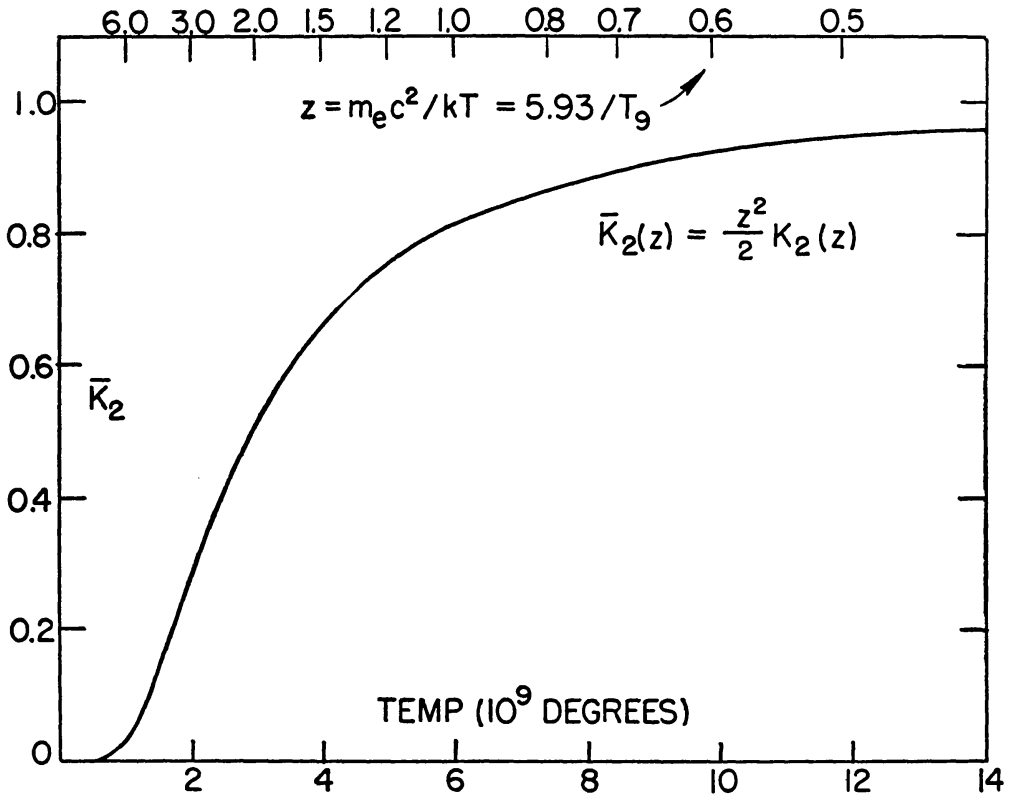

FIG. 1.—The function $\bar{K}_2(z) = (z^2/2)K_2(z)$ plotted versus temperature in 10^9 °. $K_2(z)$ is the modified Bessel function of second order and $z = m_e c^2/kT = 5.93/T_9$. $\bar{K}_2(z)$ is useful in determining the number density of electrons and positrons in non-degenerate stellar matter.

while in the non-relativistic (NR) non-degenerate case

$$\bar{K}_2 \approx \left(\frac{\pi z^3}{8}\right)^{1/2} \exp(-z)\left(1+\frac{15}{8z}+\frac{105}{128z^2}+\ldots\right)$$

$$\approx \frac{9.08}{T_9^{3/2}} \exp\left(-\frac{5.93}{T_9}\right)(1+0.316T_9+0.023T_9^2+\ldots) \quad kT < m_e c^2. \quad \text{NR} \quad (12)$$

In the first case

$$n_1 \approx 1.688 \times 10^{28}\, T_9^3 \text{ cm}^{-3}, \quad \text{ER} \quad (13)$$

while in the second case

$$n_1 \approx 1.521 \times 10^{29} T_9^{3/2} \exp\left(-\frac{5.93}{T_9}\right) \text{cm}^{-3}. \quad \text{NR} \quad (14)$$

The non-degenerate approximations yield

$$n_+ n_- \approx n_1^2$$

or

$$N_+ N_- \approx N_1^2, \quad (15)$$

and

$$n_+/n_- = N_+/N_- \approx \exp(-2\varphi)$$

or

$$\varphi = \frac{\Phi}{kT} \approx \tfrac{1}{2} \ln \frac{n_-}{n_+} = \tfrac{1}{2} \ln \frac{N_-}{N_+} \approx \ln \frac{N_-}{N_1} \approx \ln \frac{N_1}{N_+}. \quad (16)$$

Equation (15) shows that the product of the number densities is independent of the density (n_0) of electrons associated with nuclei. This is a most important non-degenerate result, since the product occurs in equation (4) for the neutrino luminosity. Equation (16) yields the chemical potential if the number densities of electrons and positrons are known. Chiu and Stabler (1961) combine equations similar to equations (8), (9), and (10) to derive explicit values for these densities as follows:

$$n_\pm = \rho N_\pm \approx \mp (n_0/2) + [(n_0/2)^2 + n_1^2]^{1/2}, \tag{17}$$

so that the total number of electrons and positrons is given by

$$n_e = \rho\, N_e = n_- + n_+ = [n_0^2 + 4n_1^2]^{1/2} = \rho\, [N_0^2 + 4N_1^2]^{1/2}. \tag{18}$$

For $n_0 \gg n_1$, $n_- \sim n_0$ and $n_+ \sim n_1^2/n_0$, while for $n_1 \gg n_0$, $n_\pm \sim n_1$, $n_e = n_- + n_+ = 2n_1$. Equations similar to (9), (15), (17), and (18) can be written down for N_+ and N_- in terms of N_0 and N_1, all of which are number densities per gram. Higher order approximations for $n_\pm$ and $N_\pm$ are discussed in Appendix B.

Figure 2 illustrates the temperature dependence for n_+n_-, $\langle \sigma v W \rangle$, and du_ν/dt. The non-degenerate integral for du_ν/dt has been evaluated in terms of modified Hankel functions by Talbot (1964) and the high and low temperature approximations given by Levine (1960, 1963) and Chiu and Stabler (1961) have been confirmed. One has

$$\begin{aligned} du_\nu/dt &= \rho\, dU_\nu/dt \\ &= \frac{1}{\pi^5} G^2 \left(\frac{m_e c}{\hbar}\right)^4 m_e c^3 \left(\frac{1}{z}\right)^3 \left(2zK_1K_2 + 5K_2^2 + 2K_1K_3 + \frac{8}{z} K_2K_3\right) \\ &= 0.325 \times 10^{21} \left(\frac{1}{z}\right)^3 \left(2zK_1K_2 + 5K_2^2 + 2K_1K_3 + \frac{8}{z} K_2K_3\right) \\ &\sim 1.02 \times 10^{21} \left(\frac{1}{z}\right)^3 \exp(-2z)\ \text{erg cm}^{-3}\,\text{sec}^{-1} \\ &\sim 4.89 \times 10^{18} T_9^3 \exp(-11.86/T_9) \end{aligned} \tag{19}$$

for $kT < m_e c^2/2$ or $T_9 < 3$,

and

$$\begin{aligned} du_\nu/dt &= \rho\, dU_\nu/dt \\ &= \frac{128}{\pi^5} G^2 \left(\frac{m_e c}{\hbar}\right)^4 m_e c^3 \left(\frac{1}{z}\right)^9 (\bar{K}_2\bar{K}_3 + \tfrac{1}{8} z^2 \bar{K}_1\bar{K}_3 + \tfrac{5}{32} z^2 \bar{K}_2^2 + \tfrac{1}{32} z^4 \bar{K}_1\bar{K}_2) \\ &= 4.16 \times 10^{22} \left(\frac{1}{z}\right)^9 (\bar{K}_2\bar{K}_3 + \tfrac{1}{8} z^2 \bar{K}_1\bar{K}_3 + \tfrac{5}{32} z^2 \bar{K}_2^2 + \tfrac{1}{32} z^4 \bar{K}_1\bar{K}_2) \\ &\sim 4.16 \times 10^{22} \left(\frac{1}{z}\right)^9 \text{erg cm}^{-3}\,\text{sec}^{-1} \\ &\sim 4.58 \times 10^{15} T_9^9 \end{aligned} \tag{20}$$

for $kT > m_e c^2/2$ or $T_9 > 3$.

In these expressions $\bar{K}_1(z) = z\bar{K}_1(z)$, $\bar{K}_2(z) = \frac{1}{2}z^2K_2(z)$ and $\bar{K}_3(z) = \frac{1}{8}z^3K_3(z)$ with $K_n(z) \to (\pi/2z)^{1/2} \exp(-z)$ at low temperature ($z > 1$) and $\bar{K}_n(z) \to 1$ at high temperature ($z < 1$).

Expression (20) serves as a rough approximation down to $T_9 = 3$ where it is about 50 per cent high. At $T_9 = 6$ it is high by 10 per cent. The asymptotic proportionality of du_ν/dt with the ninth power of the temperature arises from the fact that $n_+n_- \approx n_1^2$ varies as T^6 at high temperatures as indicated in equation (10), while σvW varies as W^3 and thus $\langle \sigma vW \rangle$ as $(kT)^3$ at high temperature. In general under stellar conditions $\rho \propto T^3$ so $dU_\nu/dt \propto T^6$ for the neutrino luminosity in erg gm^{-1} sec^{-1}. In the sequel, for a star having an evolved core with mass $\sim 20\ M_\odot$ we find ρ related numerically to T^3 in such a way that

$$dU_\nu/dt \sim 6 \times 10^{10}\ T_9^6 \qquad \text{erg gm}^{-1}\ \text{sec}^{-1}\ . \tag{21}$$

Actually, equation (21) is a better approximation than equation (20), since we find that ρ increases somewhat faster than T^3. Equation (21) gives a neutrino loss high by about a factor of 2 at $T_9 = 2$. It is to be emphasized that the number of positrons and

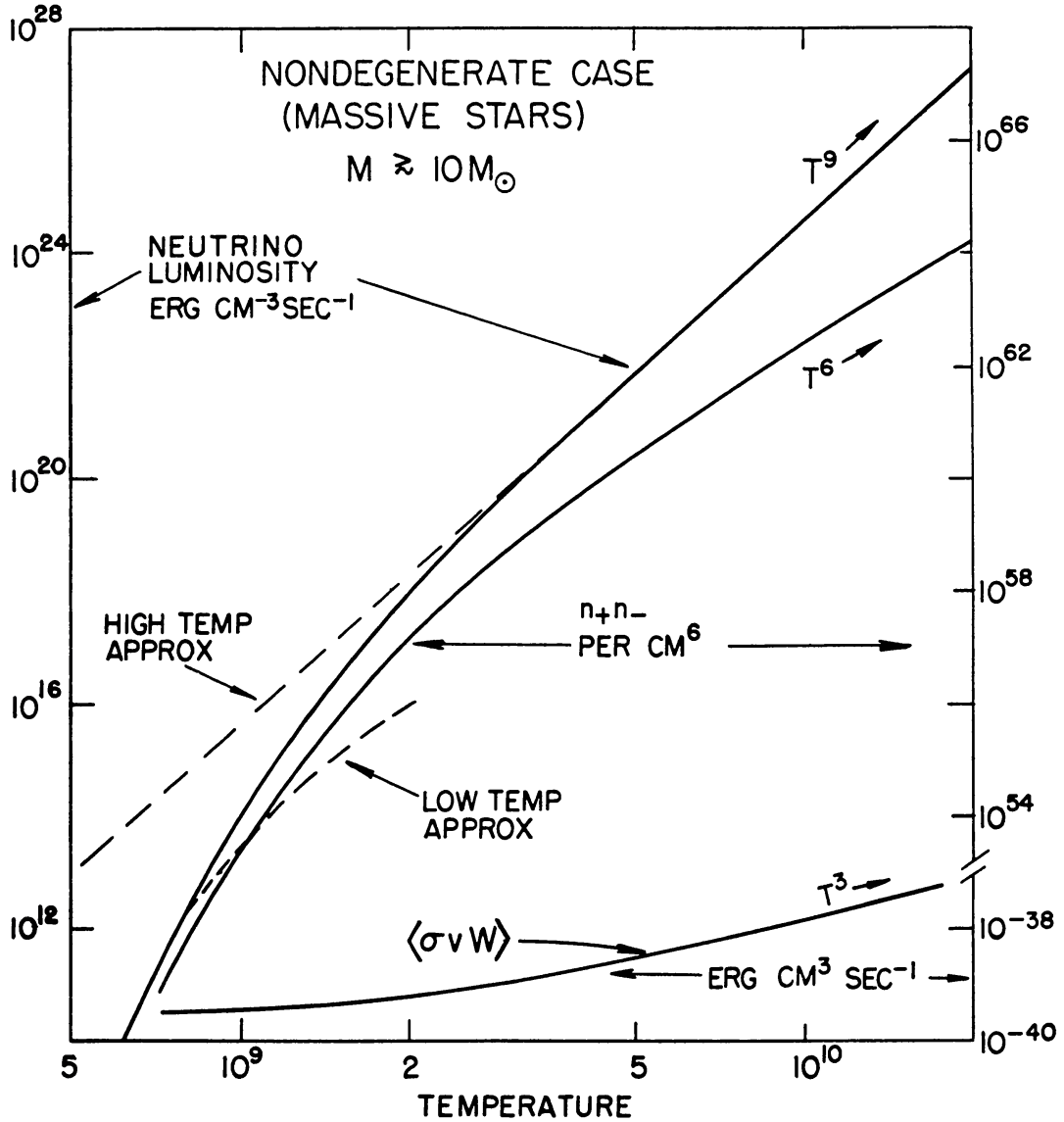

FIG. 2.—The neutrino luminosity and the quantities n_+n_- and $\langle \sigma vW \rangle$ for non-degenerate stars plotted versus temperature.

thus the neutrino luminosity are considerably reduced when stellar material becomes degenerate. This point is discussed by Chiu and Stabler (1961).

It will be immediately apparent from Figure 2 and equation (21) that the neutrino luminosity of a massive star becomes considerably greater than the photon luminosity when high temperatures are reached during advanced stages of evolution. Thus when 1 solar mass of the star to which equation (21) applies reaches $T_9 = 3.5$, one finds a total neutrino luminosity of 4×10^{47} erg sec^{-1}, which is 10^{14} times that of the Sun. For comparison, supergiants have photon luminosities in solar units of the order of 10^4. In general neutrino luminosity takes over from photon luminosity in stars when the central temperature becomes $T_9 \sim 0.5$. Chiu and his collaborators have discussed this matter in considerable detail, and we will confine our considerations to very advanced stages of stellar evolution for massive stars—Type II supernovae.

III. THE DENSITY-TEMPERATURE RELATION FOR MASSIVE STELLAR CORES BEFORE IMPLOSION: EFFECTS OF ELECTRON-POSITRON PAIRS

The basic aim of this paper requires that neutrino losses in massive stellar cores preceding and during Type II supernovae events be compared with nuclear-energy emission and absorption and that both neutrino and nuclear energetics be compared with the internal energy content of the star and with the work done by gravitational forces. These comparisons can only be made in the context of a specified density-temperature relation for the internal material of the star in question. In our first discussion of Type II supernovae (Hoyle and Fowler 1960), we took the pre-supernova star to be massive enough, $M \gtrsim 10\ M_\odot$, that its core remained non-degenerate and thus subject at its center to implosion at the onset of the energy-absorbing, iron-to-helium–neutron phase change. The explosion of light nuclear fuel in the incompletely evolved material of the outer portion or mantle of the core was taken as the characteristic Type II supernova event. The pre-supernova giant star was assigned a core of mass, now to be designated by M_c, equal to $\sim\frac{2}{3}$ of the total mass, M, with a structure corresponding to polytrope index, $n = 3$, for which $\rho \propto T^3$. Specifically by M_c we mean the mass of the core at the termination of hydrogen and helium burning in the star. It will subsequently be necessary to differentiate the mantle of the core from its central region. Outside the core, the envelope with mass $M_c \sim \frac{1}{3} M$ was taken to consist primarily of hydrogen and helium in the ratio, 2:1 by mass, characteristic of Population I material. The discontinuity in mean molecular weight between the unevolved envelope and evolved core material was considered to separate the extended envelope from the contracted core to such an extent that the core could be taken to be gravitationally independent of the envelope and to have an internal structure as a function of radius and time appropriate to that of a star of mass M_c. Thus M_c will serve as an *effective* mass value in density-temperature relations such as equation (28) below. Because of some uncertainty in the ratio, M_c/M, we shall use M_c in what follows rather than $\frac{2}{3} M$ used in Hoyle and Fowler (1960). In order to obtain explicit results we shall take $M_c = 20\ M_\odot$ in the numerical example corresponding to the previous choice $M \approx 30\ M_\odot$. On the other hand $M_c = 20\ M_\odot$ may well apply more accurately to M as high as $60\ M_\odot$. The important point is that the results reached in the specific example $M_c = 20\ M_\odot$, independent of the exact value for M, can be taken to hold in general for stars with cores massive enough that electron degeneracy does not set in until the final stages of evolution when the *central* region ($\sim M_\odot$) of the core collapses to a degenerate configuration. We estimate that the lower limit for M_c falls in the range 5–10 $M_\odot$ so that the lower limit for the total mass is $M \sim 10\ M_\odot$. Some calculations have also been made for $M_c = 10$, 40, and 100 $M_\odot$ or $M \approx 15$, 60, and 150 $M_\odot$.

For a polytrope of index $n = 3$ it is well known that $\rho = \text{const.}\ (T/\mu\beta)^3$, where μ is the mean molecular weight and β is the ratio of gas pressure to total pressure which includes radiation pressure as well as that due to the gas. The constant of proportionality

in the relation just given depends only on the mass of the star, the gas constant, and the gravitational constant. The proportionality holds at all points in the star and also at all times as long as the star is in hydrostatic equilibrium. As illustrated in Figure 3, the structure of the star can be depicted in a ρ, $T/\mu\beta$ diagram as sliding along a given curve with $\rho \propto (T/\mu\beta)^3$, the central situation being given by the leading point on the curve at all stages of evolution. Figure 3 also illustrates schematically the nuclear evolution along the $(\rho, T/\mu\beta)$ path of a star with $M \approx 30\,M_\odot$. This evolution will be discussed in detail in succeeding portions of this paper.

The new element introduced by the creation of electron-positron pairs in increasing number with increasing temperature is now that $\mu \propto 1/N$ clearly decreases with tem-

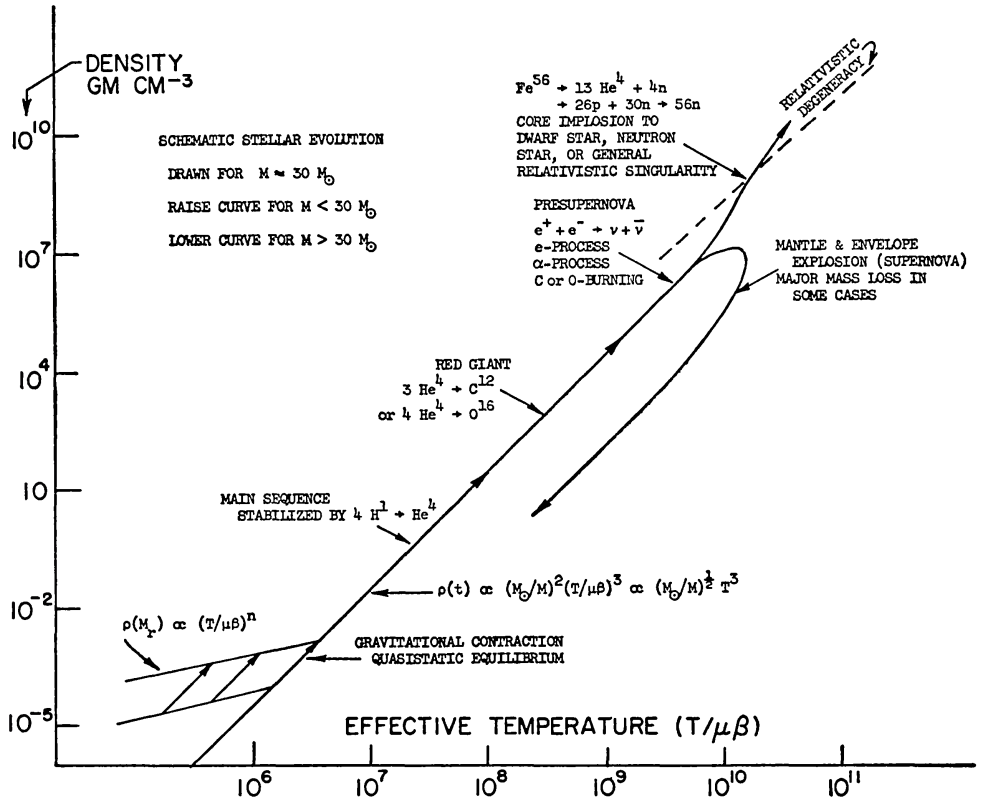

FIG. 3.—Schematic diagram of the nuclear evolution of a star with $M \approx 30\,M_\odot$. The effective mass has been set equal to $M_e = 20\,M_\odot$ and has been taken constant throughout the evolution.

perature. It will be found in what follows that β increases with temperature, but the overall result is a slight decrease in the product $\mu\beta$ and hence in $(\mu\beta)^3$, so that ρ increases somewhat more rapidly than T^3. It is now required to ascertain $(\mu\beta)^3$ as a function of temperature and thus to make the appropriate modifications in our work in Hoyle and Fowler (1960) where we considered $(\mu\beta)^3$ to be a constant. These modifications are discussed in detail in Appendix B and are found to be quite interesting in regard to the response of the internal structure of the star to pair formation but do not change in an essential way our previous picture of pre-supernova evolution.

It will, of course, be clear that the problem here put forth can be solved accurately and completely only by a detailed integration of the differential equations governing the internal structure of a star. Since this is a matter of considerable time and expense even employing the most rapid, efficient, and economical of modern computers, it must suffice at this point to employ polytropic models to reach conclusions which it is to be hoped

are not too wide of the truth. In the development which follows we essentially assume that only the equations for hydrostatic equilibrium and the perfect gas law need to be taken into account as a star contracts through a continuous series of quasi-equilibrium conditions. Neutrino losses reduce the time scale for contraction to the point where radiation transfer can be neglected. On the other hand, the time scale for pressure adjustment under gravitational forces will be found to be short compared to the characteristic time for energy loss by neutrino processes. This brings us then to the consideration of polytropic gas spheres in which pressure equilibrium under gravitational forces is the basic physical consideration. In our analysis we have been fortunate to be able to fall back on the general principles presented by Eddington (1930) and Chandrasekhar (1939). In particular the treatment in this paper can be considered as a moderate extension of the fundamental work of Chandrasekhar to take into account electron-positron pair formation at high temperature. This will be especially apparent if reference is made to the general discussion in Appendix B.

Chandrasekhar emphasizes that even for relativistic energies, Boyle's Law is identically true for non-degenerate electrons, nuclei, etc. It will be taken that this applies when electron-positron pairs are created with relativistic energies under non-degenerate circumstances. In other words, the mixture of non-relativistic nuclei and relativistic electrons and positrons is a perfect gas. The immediate sequel follows Eddington (1930, p. 116) closely, with appropriate modification for variable μ and β. Eddington (1930, p. 128) treated the case of variable molecular weight.

Even with variable μ, β the pressure p in a perfect gas is given by

$$p = \frac{\rho \Re T}{\mu\beta} = \frac{aT^4}{3(1-\beta)}, \tag{22}$$

so that

$$\rho = \frac{a\mu\beta}{3\Re(1-\beta)} T^3 \tag{23}$$

with the gas constant, $\Re = k/M_u = 8.314 \times 10^{16}$ erg mole^{-1} $(10^9\ °)^{-1}$ and the Stefan-Boltzmann constant, $a = (\pi^2/15)(k^4/\hbar^3c^3) = 7.565 \times 10^{21}$ erg cm^{-3} $(10^9\ °)^{-4}$. Eliminating T

$$p = \left\{\frac{3\Re^4(1-\beta)}{a\mu^4\beta^4}\right\}^{1/3} \rho^{4/3}. \tag{24}$$

If the structure of the star (or stellar core in the case at hand) is to correspond to that of a polytrope of index n in which $p \propto \rho^{1+1/n}$, then the factor in braces must depend in a very specific way on ρ, namely, as $\rho^{3/n-1}$. This is now assumed and constitutes the essential departure from the detailed calculation mentioned above which must eventually be made.

If the factor of proportionality in the pressure-density relation is designated by κ, then

$$p = \kappa\rho^{1+1/n}, \tag{25}$$

where

$$\kappa = \frac{\Re T}{\mu\beta\rho^{1/n}} = \left[\frac{3\Re^4(1-\beta)}{a\mu^4\beta^4\rho^{3/n-1}}\right]^{1/3}$$

$$= \frac{\Re T_o}{\mu_o\beta_o\rho_o^{1/n}} = \left[\frac{3\Re^4(1-\beta_o)}{a\mu_o^4\beta_o^4\rho_o^{3/n-1}}\right]^{1/3}. \tag{26}$$

In the last equation the factor κ is written out for reference in terms of parameters describing conditions at the center of the core which are here designated with subscript o.

Gravitational effects are introduced in terms of boundary conditions *at the center* by combining Eddington's equations (57.2) and (58.3) to obtain

$$\left(\frac{M_c}{M_n}\right)^2 = \frac{\kappa^n}{4\pi}\left(\frac{n+1}{G}\right)^3\left(\frac{\mu_o\beta_o}{\Re T_o}\right)^{n-3}, \tag{27}$$

where M_n is a constant of integration characteristic of the polytrope with index n. Eddington designated this parameter by M'. The total mass of a star is proportional to M_n if the star is a polytrope of index n. Solving for the density-temperature relation yields

$$\rho = \frac{1}{4\pi}\left(\frac{n+1}{G}\right)^3\left(\frac{M_n}{M_c}\right)^2\left(\frac{\Re T_o}{\mu_o\beta_o}\right)^{3-n}\left(\frac{\Re T}{\mu\beta}\right)^n \tag{28}$$

$$= \frac{1}{4\pi}\left(\frac{n+1}{G}\right)^3\left(\frac{M_n}{M_c}\right)^2\left(\frac{\mu\beta T_o}{\mu_o\beta_o T}\right)^{3-n}\left(\frac{\Re T}{\mu\beta}\right)^3. \tag{29}$$

In terms of conditions at the center of the star

$$\rho = \rho_o\left(\frac{\mu_o\beta_o T}{\mu\beta T_o}\right)^n, \tag{30}$$

where

$$\rho_o = \frac{1}{4\pi}\left(\frac{n+1}{G}\right)^3\left(\frac{M_n}{M_c}\right)^2\left(\frac{\Re T_o}{\mu_o\beta_o}\right)^3 = 3.90\times 10^4 a_n\left(\frac{M_\odot}{M_c}\right)^2\left(\frac{T_9}{\mu\beta}\right)_o^3 \text{ gm cm}^{-3} \tag{31}$$

with $a_n = (n+1)^3 M_n^2$. Representative values for a_n are $a_0 = 24.0$, $a_1 = 78.9$, $a_{1.5} = 115$, $a_2 = 157$, $a_{2.5} = 206$, $a_3 = 260.4$, $a_{3.5} = 327$, $a_4 = 404$, $a_5 = 648$, $a_\infty = 696$.

Equation (31) stipulates that the central density varies as $(T/\mu\beta)_o^3$ during contraction of the star as long as the polytrope index remains a constant. The factor of proportionality clearly depends on the value of the polytropic index. Consider now the variation of density for any particular sample of stellar material, not just that at the center. We can designate such a particular sample as the increment in mass dM_r just external to the sphere which always contains mass M_r. Now for all polytropes it is well known that M_r can be taken as the independent variable in place of the radius, r, throughout the structure of the star. For each specified value of M_r/M_n one finds that ρ/ρ_o and $(T/\mu\beta)/(T/\mu\beta)_o$ are fixed throughout the contraction as long as n remains unchanged. Thus equation (29) shows that for any particular sample of the stellar material $\rho \propto (T/\mu\beta)^3$ as the star contracts, but now with a factor of proportionality which depends not only on the index n but on the location in the star. Chandrasekhar (1939) points out that this result was originally due to Ritter. This means that each point on the curve in the ρ, T-plane for *any* polytrope of constant index n moves along a contour given by $\rho(\mu\beta/T)^3 =$ constant as a polytrope contracts (or expands) between quasi-equilibrium configurations. The polytrope $n = 3$ slides along a single contour, while the polytropes with $n \neq 3$ sweep out an area in the ρ, T-plane. Equation (22) can be used to show that for a given element of mass, $p \propto \rho^{4/3} \propto (T/\mu\beta)^4$ as the star contracts again for any fixed n. The situation is illustrated for $n = 1.5$ in the lower left-hand corner of Figure 3.

In the sequel we will derive and use an important relation, equation (69), which depends only on the fact that the exponent in the "evolutionary" power law relation between ρ and $T/\mu\beta$ is equal to 3 and not on the factor of proportionality, and thus not on the index n or the particular mass element in the star. However, other important relations do depend on n, so some value for this index must be chosen. The range of n can be restricted to $1.5 < n < 5$, however. Convection at the speed of sound sets in if n falls appreciably below 1.5. The resulting very rapid loss of energy from the core then modifies the stellar model, in the sense of cutting back the convection. Hence 1.5 may be taken as a reasonable lower limit for n. The upper limit arises because polytropes

with $n > 5$ do not possess finite radius. It follows that the range of a_n in equation (31) amounts to a factor less than 6. And if we choose $n = 3$ as an explicit case the value of a_3 lies within a factor 2.5 of a_n for all other physically permissible polytropes. This choice also has the advantage that $\rho \propto (T/\mu\beta)^3$ holds good with the same constant of proportionality everywhere throughout the star at all times. Thus, with $M_3 = 2.018$, $a_3 = 260$, it is found that

$$\rho = \frac{16}{\pi G^3}\left(\frac{M_3}{M_c}\right)^2\left(\frac{\Re T}{\mu\beta}\right)^3. \tag{32}$$

Numerically,

$$\rho = 1.016 \times 10^7 \left(\frac{M_\odot}{M_c}\right)^2\left(\frac{T_9}{\mu\beta}\right)^3 \text{ gm cm}^{-3}$$

$$= 2.54 \times 10^4 \left(\frac{T_9}{\mu\beta}\right)^3 \text{ gm cm}^{-3} \text{ for } M_c = 20M_\odot,\ M \approx 30M_\odot. \tag{33}$$

We shall use equations (33) not only at a particular moment of time but throughout the evolution of the star. It would be possible to consider n as varying with time. For material near the center, which is our main concern, such a variation would produce a change with time of the numerical coefficient in equation (33), this being just the change of a_n in equation (31). The change is limited, however, as we have seen, to a factor of about 2.5, and this is not of importance to the following considerations. In the absence of precise evolutionary computations, equation (33) gives a very satisfactory approximation to the relation between ρ and T for a non-degenerate star of nearly uniform molecular weight. It is the nature of the path in the ρ, T-plane which is important in determining the nuclear evolution of a star; given $\rho = f(T)$ one variable is removed from nuclear-reaction rate equations.

The adoption of the case $n = 3$ requires $(1 - \beta)/\mu^4\beta^4$ to be a constant, independent both of time and of position within the star. In the past it has been possible to use this fact with $\mu = A/(Z + 1)$ to determine β. However, μ is a variable when pairs are produced at elevated temperatures.

It is thus required to express $(\mu\beta)^3$ in terms of ρ and/or T in order to obtain an explicit ρ, T-relation. This can be done straightforwardly. The mean molecular weight can be found from

$$\frac{1}{\mu} = NM_u = \frac{nM_u}{\rho} = (N_N + N_e)M_u = \frac{1}{A} + \frac{Z}{A}\left[1 + \left(\frac{2N_1}{N_0}\right)^2\right]^{1/2}, \tag{34}$$

where N is the total number of particles per gram including nuclei (N_N) and electrons plus positrons ($N_e = N_+ + N_-$). (Note that we express μ in the same atomic mass unit, M_u, in which atomic weights are expressed and *not* in terms of the mass of the hydrogen atom.) The nuclei are taken to be completely stripped of electrons at the temperatures of interest. We have used $N_0 = ZN_N = Z/AM_u$ in equation (18). The reciprocal of β is given by

$$\frac{1}{\beta} = 1 + \frac{aT^3}{3\rho Nk}, \tag{35}$$

so that equations (34) and (35) give

$$\frac{1}{\mu\beta} = NM_u + \frac{aT^3}{3\Re\rho} = \frac{1}{A} + \frac{Z}{A}\left[1 + \left(\frac{2N_1}{N_0}\right)^2\right]^{1/2} + \frac{aT^3}{3\Re\rho}. \tag{36}$$

The nuclear term $(1/A)$ can usually be neglected and will be in what follows. Equation (10) yields

$$\frac{2N_1}{N_0} = \frac{4}{\pi^2}\frac{AM_u}{Z}\left(\frac{k}{\hbar c}\right)^3\frac{T^3}{\rho}\bar{K}_2(z) = 5.604 \times 10^4 \frac{A}{Z}\frac{T_9^3}{\rho}\bar{K}_2(5.93/T_9). \tag{37}$$

When equation (33) for the polytrope with $n = 3$ is introduced, this becomes

$$\frac{2N_1}{N_0} = \frac{M_u^4}{4\pi}\frac{A}{Z}\left(\frac{M_c}{M_3}\right)^2\left(\frac{G\mu\beta}{\hbar c}\right)^3 \bar{K}_2(z)$$

$$= 5.51\times 10^{-3}\frac{A}{Z}\left(\frac{M_c}{M_\odot}\right)^2(\mu\beta)^3\bar{K}_2(5.93/T_9) \tag{38}$$

$$= 4.41(\mu\beta)^3\bar{K}_2(5.93/T_9) \text{ for } A = 2Z,\ M_c = 20M_\odot .$$

The numerical coefficient in equation (38) becomes 4.75 for $A = 56$, $Z = 26$.

From equations (32) and (33) we also have

$$\frac{aT^3}{3\Re\rho} = 3.033\times 10^4 T_9^3/\rho = \frac{\pi^3 M_u^4}{5\times 3^2\times 2^4}\left(\frac{M_c}{M_3}\right)^2\left(\frac{G\mu\beta}{\hbar c}\right)^3$$

$$= 2.98\times 10^{-3}\left(\frac{M_c}{M_\odot}\right)^2(\mu\beta)^3 \tag{39}$$

$$= 1.19(\mu\beta)^3 \text{ for } M_c = 20M_\odot,\ M \approx 30M_\odot .$$

Equations (36), (38), and (39) can be combined to give an expression for $\mu\beta$ as a function of $z = 5.93/T_9$ in terms of the mass M_c of the stellar core and the composition factor A/Z. After some rearrangement one finds

$$\left[\left(\frac{180}{\pi^4}\right)^2\bar{K}_2^2(z) - 1\right](\mu\beta)^8 + 2\eta_3(\mu\beta)^4 + \left(\frac{Z}{A}\eta_3\right)^2(\mu\beta)^2 - \eta_3^2 = 0, \tag{40}$$

where

$$\eta_3 = \frac{720}{\pi^3 M_u^4}\left(\frac{\hbar c}{G}\right)^3\left(\frac{M_3}{M_c}\right)^2 = \frac{48}{\pi}\frac{\Re^4}{aG^3}\left(\frac{M_3}{M_c}\right)^2 = 335.2\left(\frac{M_\odot}{M_c}\right)^2 \tag{41}$$

$$= 0.838 \quad \text{for} \quad M_c = 20M_\odot, \quad M \approx 30M_\odot .$$

Actually it is only a matter of tedious algebra to derive equation (41) for a polytrope of index n just as we have done for the special case $n = 3$. We give only the result

$$\left(\frac{180}{\pi^4}\right)^2\bar{K}_2^2(z)\left(\frac{\mu_o\beta_o T}{T_o}\right)^{6-2n}(\mu\beta)^{2n+2}$$

$$-\left[\eta_n\left(1-\frac{Z}{A}\mu\beta\right)-\left(\frac{\mu_o\beta_o T}{T_o}\right)^{3-n}(\mu\beta)^{n+1}\right]\left[\eta_n\left(1+\frac{Z}{A}\mu\beta\right)-\left(\frac{\mu_o\beta_o T}{T_o}\right)^{3-n}(\mu\beta)^{n+1}\right] \tag{42}$$

$$=\left(\frac{180}{\pi^4}\right)^2\bar{K}_2^2(z)\left(\frac{\mu_o\beta_o T}{\mu\beta T_o}\right)^{6-2n}(\mu\beta)^8$$

$$-\left[\eta_n\left(1-\frac{Z}{A}\mu\beta\right)-\left(\frac{\mu_o\beta_o T}{\mu\beta T_o}\right)^{3-n}(\mu\beta)^4\right]\left[\eta_n\left(1+\frac{Z}{A}\mu\beta\right)-\left(\frac{\mu_o\beta_o T}{\mu\beta T_o}\right)^{3-n}(\mu\beta)^4\right] = 0,$$

where

$$\eta_n = \frac{45}{4\pi^3}\frac{(n+1)^3}{M_u^4}\left(\frac{\hbar c}{G}\right)^3\left(\frac{M_n}{M_c}\right)^2 = \frac{3}{4\pi}(n+1)^3\frac{\Re^4}{aG^3}\left(\frac{M_n}{M_c}\right)^2 . \tag{43}$$

For $n = 3$ equation (42) becomes

$$\left(\frac{180}{\pi^4}\right)^2\bar{K}_2^2(z)(\mu\beta)^8-\left[\eta_3\left(1-\frac{Z}{A}\mu\beta\right)-(\mu\beta)^4\right]\left[\eta_3\left(1+\frac{Z}{A}\mu\beta\right)-(\mu\beta)^4\right]=0, \tag{44}$$

which is just another form for equation (40).

We can now see that equations (40) and (44) reduce to the famous quartic equation derived by Eddington (1930, p. 117). If we set $\bar{K}_2(z) = 0$ and $\mu = A/Z$ in equation (44) then, setting the first bracketed term equal to zero, it is found for $n = 3$ that

$$1-\beta=\frac{(\mu\beta)^4}{\eta_3}=\frac{\pi^3}{720}\left(\frac{G}{\hbar c}\right)^3(\mu\beta M_u)^4\left(\frac{M_c}{M_3}\right)^2$$
$$=\frac{\pi}{48}\frac{aG^3}{\Re^4}(\mu\beta)^4\left(\frac{M_c}{M_3}\right)^2=2.98\times10^{-3}\left(\frac{M_c}{M_\odot}\right)^2(\mu\beta)^4, \tag{45}$$

which is just the quartic equation. The second bracketed term is not equal to zero. It must be emphasized that equation (45) is true even in the general case with pair formation, but it is not immediately useful in this case. Use of equations (34) and (35) with equation (45) leads directly to equations (40) or (44).

Note also that for *all* polytropes one has an equation at the center similar to equation (44),

$$\left(\frac{180}{\pi^4}\right)^2\bar{K}_2^2(z_o)(\mu_o\beta_o)^8-\left[\eta_n\left(1-\frac{Z}{A}\mu_o\beta_o\right)-(\mu_o\beta_o)^4\right]$$
$$\times\left[\eta_n\left(1+\frac{Z}{A}\mu_o\beta_o\right)-(\mu_o\beta_o)^4\right]=0, \tag{46}$$

and for $\bar{K}_2^2(z_o) = 0$ and $\mu_o = A/Z$,

$$1-\beta_o=\frac{(\mu\beta)_o^4}{\eta_n}. \tag{47}$$

This generalized quartic equation holds at the center of all polytropes even at temperatures where pair formation takes place.

In massive stars at low density when the electron-positron pairs greatly out-number the original electrons, $N_0 = Z/AM_u$, we can neglect $Z\mu\beta/A$ in the above expressions to establish the useful approximate relations

$$(\mu\beta)^{n+1}\approx\eta_n\left(\frac{\mu_o\beta_oT}{T_o}\right)^{n-3}\left[1+\frac{180}{\pi^4}\bar{K}_2(z)\right]^{-1}$$

or

$$\mu\beta\sim\mu_o\beta_o\left(\frac{T}{T_o}\right)^{(n-3)/(n+1)}\sim\eta_n^{1/4}\left(\frac{T}{T_o}\right)^{(n-3)/(n+1)} \qquad \bar{K}_2(z)\sim0 \tag{48}$$

and

$$(\mu_o\beta_o)^4\approx\eta_n\left[1+\frac{180}{\pi^4}\bar{K}_2(z)\right]^{-1} \qquad \text{at center, all polytropes} \tag{49}$$
$$\sim\eta_n \qquad \bar{K}_2(z)\sim0$$

For $n = 3$

$$(\mu\beta)^4\approx\eta_3\left[1+\frac{180}{\pi^4}\bar{K}_2(z)\right]^{-1}$$
$$\sim\eta_3 \qquad \bar{K}_2(z)\sim0$$
$$\approx335.2\left(\frac{M_\odot}{M_c}\right)^2\left[1+\frac{180}{\pi^4}\bar{K}_2(z)\right]^{-1} \qquad \text{all } r,\ n=3 \tag{50}$$

Equations (34), (37), (35), and (32) then give

$$\mu\approx335.2\left(\frac{M_\odot}{M_c}\right)^{1/2}\left[1+\frac{180}{\pi^4}\bar{K}_2(z)\right]^{3/4}\left[\frac{180}{\pi^4}\bar{K}_2(z)\right]^{-1}, \qquad n=3 \tag{51}$$

$$\beta \approx \frac{180}{\pi^4}\bar{K}_2(z)\left[1+\frac{180}{\pi^4}\bar{K}_2(z)\right]^{-1}, \tag{52}$$

$$\rho \approx \frac{1}{(4\pi)^{1/4}}\left(\frac{4a}{3G}\right)^{3/4}\left(\frac{M_3}{M_c}\right)^{1/2}\left[1+\frac{180}{\pi^4}\bar{K}_2(z)\right]^{3/4}T^3,$$

$$\approx 1.298\times 10^5\left(\frac{M_\odot}{M_c}\right)^{1/2}\left[1+\frac{180}{\pi^4}\bar{K}_2(z)\right]^{3/4}T_9{}^3\ \mathrm{gm\ cm^{-3}}, \quad n=3. \tag{53}$$

Equation (52) is independent of the polytropic index n. All of the approximations (48)–(53) hold numerically only for massive stars ($M \geq 10^3\ M_\odot$). However, the relation $\rho/T^3 \propto M_c^{-1/2}$ is more accurate than $\rho/T^3 \propto M_c^{-2}$ for $M > 10\ M_\odot$. General relativistic effects make these equations only very approximate above $M \geq 10^6\ M_\odot$.

The numerical evaluation of equation (40) for $M_c = 20\ M_\odot$, $M \approx 30\ M_\odot$ leads to

$$[\bar{K}_2{}^2(5.93/T_9)-0.293](\mu\beta)^8+0.491(\mu\beta)^4+0.206\left(\frac{Z}{A}\right)^2(\mu\beta)^2-0.206=0. \tag{54}$$

Table 3 presents approximate numerical solutions of equations (33) and (54) for the case $M_c = 20\ M_\odot$, $M \approx 30\ M_\odot$. The quantity $z = 5.93/T_9$ has been taken as the independent variable since $\bar{K}_2$ is an explicit function of z and the ultimate object becomes the determination of the density as a function of temperature (tenth column). For $z \geq 2$ or $T_9 < 3$, $A/Z = 2$ has been used on the basis that C^{12}, O^{16}, . . . , Ni^{56} will successively be the most probable nuclear forms as evolution of the core proceeds. Near $z \sim 1.5$ or $T_9 \sim 4$, Ni^{56} transforms to Fe^{56} and for lower z and higher T_9, $A/Z = 56/26$ has been used. Once $(\mu\beta)$ has been obtained from equation (54), equations (38), (18), (17), (34), (35), and (33) can be used to obtain $2N_1$, N_e, $N_\pm$, μ, β, and ρ, respectively, as given in the table. The first part of equation (36) solved for $N \approx N_e$ can be employed as a check on the value for N_e found from equation(18). The adiabatic coefficients Γ_1, Γ_2, and Γ_3 can be determined using equations (B95), (B96), and (B97), respectively. The

TABLE 3

THE RUN OF VARIOUS QUANTITIES WITH TEMPERATURE IN A STAR WITH $M_c = 20\ M_\odot$, $M \approx 30\ M_\odot$ TAKEN AS A POLYTROPE OF INDEX, $n = 3$, WITH ALLOWANCE FOR ELECTRON-POSITRON PAIR CREATION BUT NOT FOR IMPLOSION

(For $0 < T_9 < 3.95$, $A/Z = 2$; for $3.95 < T_9 < \infty$, $A/Z = 56/26 = 2.15$)

z	T_9	$\bar{K}_2$	x	c_v	$\mu\beta$	$(\mu\beta)^3$	μ	β	$\log\rho$	Γ_1	Γ_2	Γ_3
∞	0	0	1.50	1.50	0.834	0.581	2.00	0.417	$-\infty$	1.4085	1.3442	1.3607
6	0.99	0.030	1.76	1.99	.834	.580	1.99	.418	4.63	1.3751	1.3374	1.3469
5	1.19	0.066	1.81	2.06	.832	.577	1.97	.422	4.87	1.3577	1.3295	1.3365
4	1.48	0.139	1.87	2.16	.827	.566	1.89	.436	5.16	1.3323	1.3129	1.3175
3.5	1.69	0.198	1.91	2.22	.820	.551	1.79	.457	5.34	1.3233	1.3027	1.3074
3	1.98	0.277	1.96	2.29	.809	.530	1.67	.484	5.57	1.3209	1.2943	1.3003
2.5	2.37	0.380	2.02	2.37	.794	.501	1.52	.523	5.83	1.3272	1.2910	1.2992
2	2.96	0.508	2.10	2.48	.776	.467	1.37	.565	6.15	1.3365	1.2936	1.3034
1.5	3.95	0.657	2.21	2.60	.756	.431	1.24	.612	6.56	1.3448	1.3014	1.3115
1.5	3.95	0.657	2.21	2.60	.758	.436	1.26	.601	6.55	1.3439	1.3007	1.3107
1.0	5.93	0.812	2.37	2.75	.739	.404	1.15	.642	7.12	1.3459	1.3134	1.3212
0.85	6.98	0.868	2.43	2.80	.732	.392	1.12	.654	7.34	1.3440	1.3176	1.3239
0.7	8.47	0.897	2.50	2.85	.730	.389	1.10	.663	7.60	1.3427	1.3217	1.3268
0.5	11.86	0.943	2.61	2.91	.724	.381	1.08	.670	8.04	1.3395	1.3267	1.3299
0	∞	1.000	3.00	3.00	0.718	0.370	1.05	0.682	∞	1.3333	1.3333	1.3333

TABLE 3—*Continued*

T_9	ρ_6	ρ_4/T_9^3	$2N_1/10^{23}$	$N_0/10^{23}$	$N_-/10^{23}$	$N_+/10^{23}$	$\exp\varphi$	$\varphi/(x+z)$	dQ/dT (10^{16} erg/gm-10^9 deg)	log dU_p/dt (erg gm^{-1} sec^{-1})
0	0	4.33	0	3.01	3.01	0	∞	1	+6.22	$-\infty$
0.99	0.0425	4.34	0.24	3.02	3.02	0.005	25.1	0.420	3.69	9.34
1.19	0.0735	4.37	0.52	3.05	3.03	0.02	11.7	0.361	2.19	10.25
1.48	0.145	4.45	1.06	3.19	3.10	0.09	5.85	0.301	−0.10	11.28
1.69	0.220	4.57	1.47	3.36	3.18	0.18	4.33	0.271	−1.08	11.81
1.98	0.369	4.76	1.98	3.60	3.30	0.30	3.34	0.243	−1.39	12.35
2.37	0.668	5.03	2.56	3.96	3.48	0.48	2.72	0.221	−0.73	12.93
2.96	1.42	5.42	3.18	4.39	3.70	0.69	2.33	0.206	+0.37	13.60
3.95	3.62	5.84	3.82	4.86	3.93	0.93	2.06	0.195	1.20	14.39
3.95	3.58	5.80	3.88	4.78	3.79	0.99	1.96	0.181	1.21	14.40
5.93	13.1	6.29	4.42	5.23	4.01	1.22	1.82	0.178	1.41	15.48
6.98	22.0	6.48	4.59	5.37	4.09	1.28	1.78	0.177	1.23	15.86
8.47	39.6	6.52	4.71	5.48	4.14	1.34	1.76	0.177	0.93	16.25
11.86	111	6.64	4.84	5.57	4.18	1.39	1.73	0.176	0.37	17.21
∞	∞	6.82	5.00	5.72	4.26	1.46	1.70	0.176	0	∞

quantities ρ/T_9^3, $\exp\varphi = N_-/N_1$, and $\varphi/(x+z)$ can also be computed. Figures 4 and 5 show μ, β, and $\mu\beta$ and the ρ, T-path found in the calculations presented in Table 3. In Figure 5 the ρ, T-path discussed here holds up to $T_9 \sim 6$ and has been extended to $T_9 \sim 9$. Figure 6 shows the ρ, T-paths for $M_c = 10$, 20, 40, and 100 $M_\odot$ or $M \approx 15$, 30, 60, and 150 $M_\odot$.

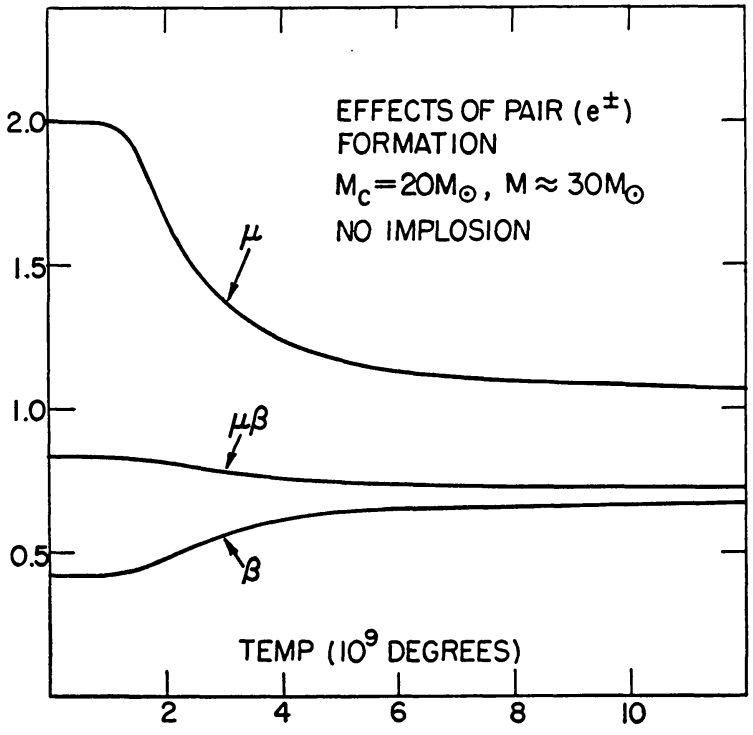

FIG. 4.—The quantities μ, β, and $\mu\beta$ plotted as a function of temperature in 10^9 degrees for the case of no implosion in a star with $M \approx 30\ M_\odot$.

It must be emphasized, however, that the iron-to-helium-neutron phase change and the helium-to-neutron-proton phase change, to be discussed in Part VIII, cause the core to implode. Equation (33) is then no longer valid, and the actual density substantially deviates from that calculated here for $T_9 > 6$. The results obtained in Part VIII are tabulated in Table 4 and illustrated in Figures 5 and 6 for $T_9 > 6$. As a final comment on the ρ, T-relation we note that ρ/T_9^3 varies from 4.33×10^4 at $T_9 \sim 0$ to 6.30×10^4 at $T_9 \sim 6$. In Hoyle and Fowler (1960) we used $\rho/T_9^3 = 4.3 \times 10^4$ showing that the new considerations have not introduced major modifications, even though the number of electronic particles has increased by ~75 per cent at $T_9 \sim 6$. The increase in β has partially compensated for the fall in μ. As a crude approximation over T_9 from 1 to 6 we have $\mu\beta \sim T_9^{-0.07}$ and $\rho \sim 4.3 \times 10^4\ T_9^{3.2}$.

In concluding this discussion of density-temperature relations, it must be emphasized

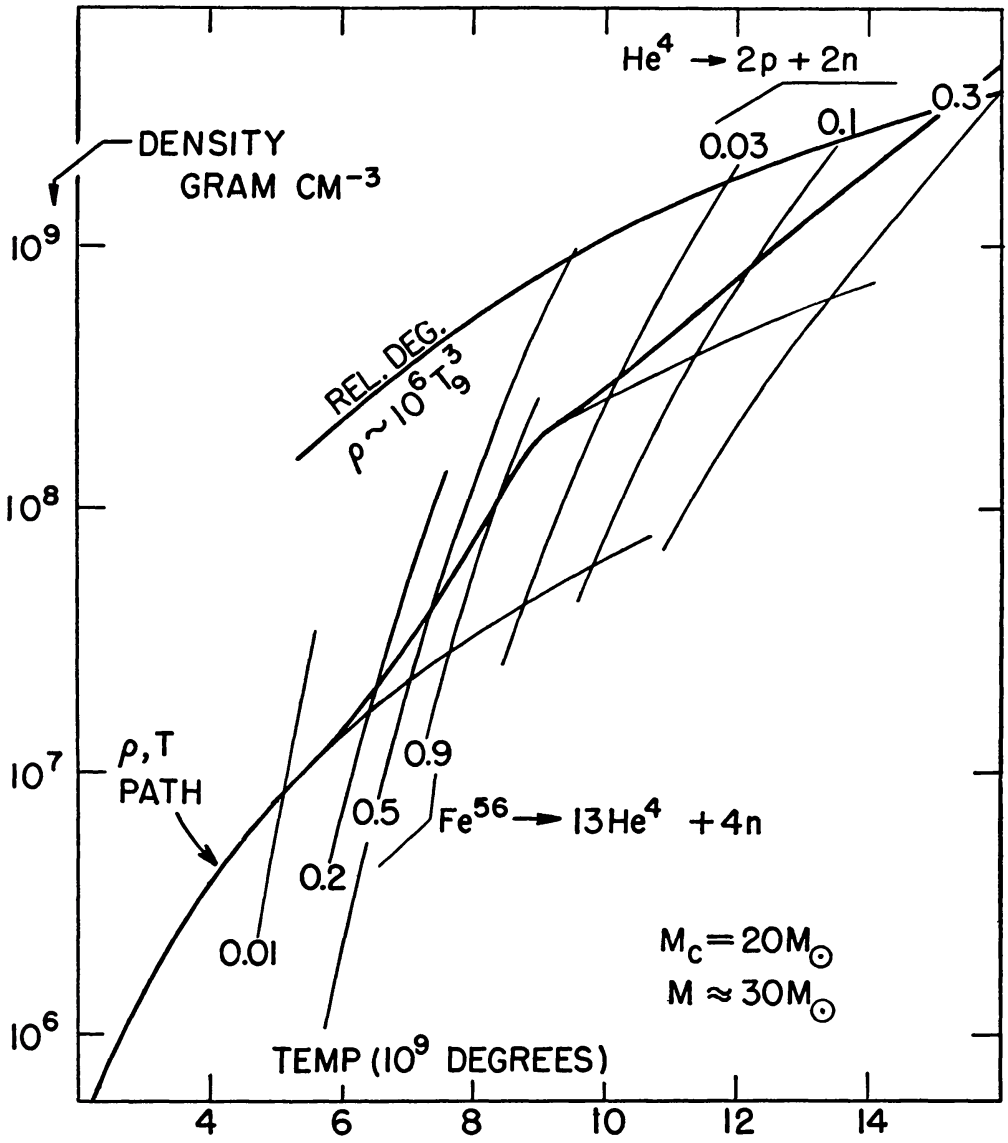

FIG. 5.—The ρ, T path for a star with $M_c = 20\ M_\odot$, $M \approx 30\ M_\odot$. The almost vertical curve segments give the fraction by mass of iron group elements converted to helium and neutrons or of helium converted to protons and neutrons. The curve above which the electrons are relativistically degenerate is also shown.

that equations (33), (53), and others of similar nature must not be used for a star of mass M with M_c/M considered to be a constant throughout the evolutionary life of the star. In the initial main-sequence stage $M_c \approx M$, during the red-giant stage $M_c \sim \frac{1}{5} M$ may be a fair approximation, while in the pre-supernova stage of primary interest here we have taken $M_c \sim \frac{2}{3} M$. Some judgment must be utilized in choosing M_c/M at a given stage of interest. Nonetheless, equations (33) and (53) are still very useful, especially for massive stars where equation (50) indicates that $\mu\beta \propto M_c^{-1/2}$ and thus $\rho/T^3 \propto M_c^{-2}$ $(\mu\beta)^{-3} \propto M_c^{-1/2}$ as explicitly indicated in equation (53). In addition it must also be emphasized that these relations are fair approximations at the center of the star where nuclear and neutrino processes are important but fail completely in the outer regions of stars, especially in the case of the extended envelopes of red giants and pre-supernova stars. We hope these words of caution to the wise will be sufficient.

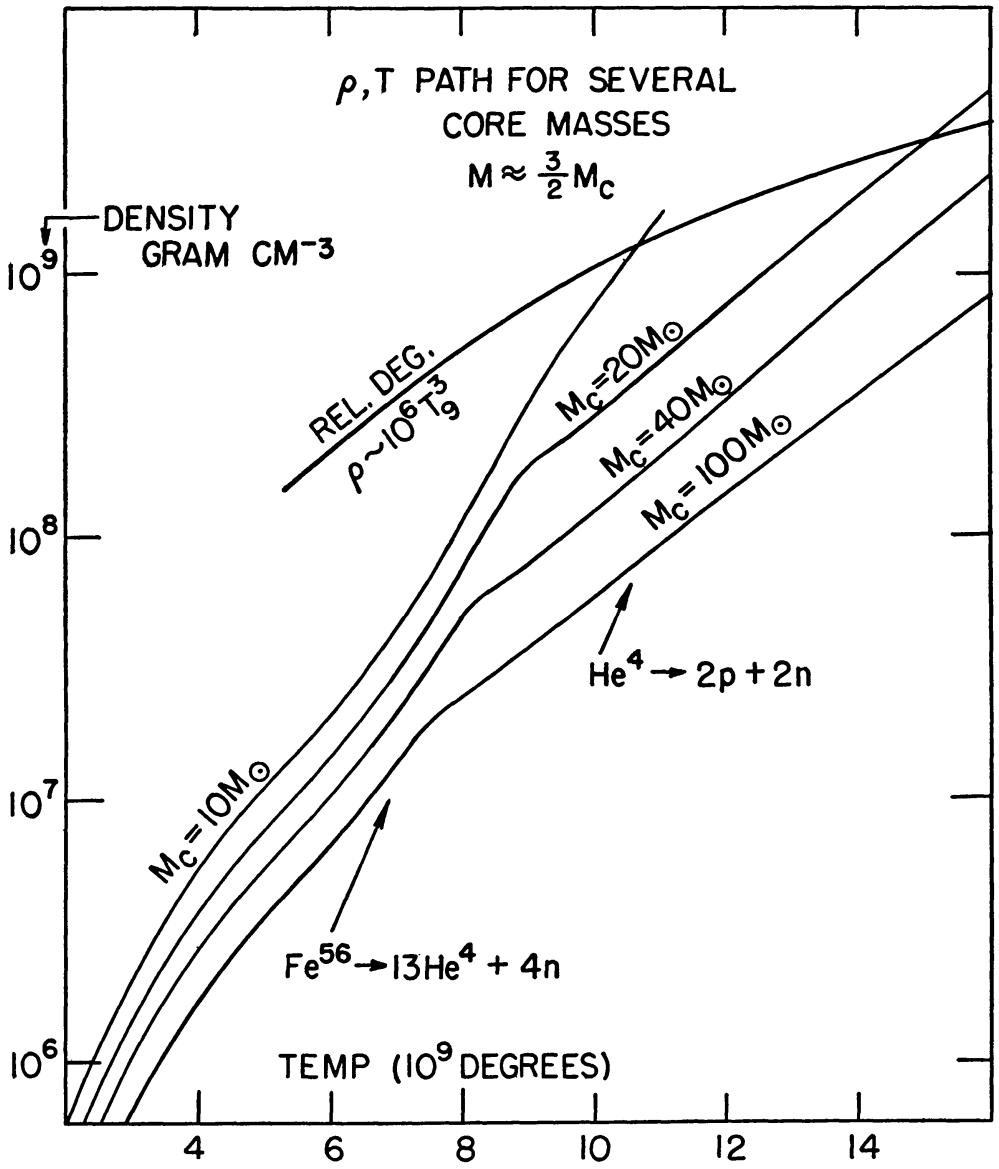

FIG. 6.—The ρ, T paths for stars with M_c = 10, 20, 40, 100 $M_\odot$ or $M \approx$ 15, 30, 60, 150 $M_\odot$

IV. GRAVITATIONAL AND INTERNAL ENERGY RELATIONS FOR NON-DEGENERATE GASES CONTAINING ELECTRONS AND POSITRONS; COMPARISON WITH NEUTRINO ENERGY LOSSES

With methods for determining the ρ, T-relation in massive, non-degenerate stellar cores containing positrons as well as electrons and nuclei now established, it is possible to consider the work done by gravity and the changes of internal energy that occur as the core evolves along one of the curves illustrated in Figures 5 and 6. Continuing to

TABLE 4

IMPLOSION CONDITIONS

$M_c = 20\ M_\odot$, $M \approx 30\ M_\odot$

	T_9	log ρ	log dQ/dT (erg gm^{-1}/ 10^9 deg)	log dU_ν/dt (erg gm^{-1}/ sec)
	$\gamma + Fe^{56} \rightarrow 13He^4 + 4n - 2.14 \times 10^{18}$ erg gm^{-1}			
Q_N/Q'_{Fe} (per cent):				
0	4.18			
		4.68	6.80	16.33	14.78
1	5.18			
		5.68	7.08	17.28	15.28
10	6.18			
		6.39	7.28	17.71	15.55
20	6.60			
		6.76	7.40	17.84	15.65
30	6.91			
		7.06	7.51	17.87	15.72
40	7.20			
		7.33	7.61	17.93	15.76
50	7.45			
		7.57	7.70	17.95	15.79
60	7.69			
		7.82	7.81	17.92	15.81
70	7.95			
		8.09	7.92	17.88	15.83
80	8.23			
		8.39	8.05	17.81	15.83
90	8.56			
		8.78	8.20	17.64	15.83
99	9.0			
	$\gamma + He^4 \rightarrow 2p + 2n - 6.82 \times 10^{-18}$ erg gm^{-1}			
Q_N/Q'_α (per cent):				
0	9.24			
		9.74	8.40	17.31	16.05
3	10.24			
		10.58	8.57	17.31	16.29
5	10.91			
		11.63	8.80	17.37	16.43
10	12.35			
		13.13	9.12	17.34	16.57
15	13.90			
		14.75	9.45	17.30	16.70
20	15.60			

employ the temperature as independent variable, we now wish to calculate the quantity

$$\frac{dQ}{dT} = -p\frac{dV}{dT} - \frac{dU}{dT}, \tag{55}$$

where $-pdV$ is the increment of work done by gravity on the stellar core material in erg gm^{-1}, p is the pressure exerted by gas and radiation, and dU is the incremental change in internal energy in erg gm^{-1} for an increase in temperature dT. Our treatment derives from that of Chandrasekhar (1939, p. 394), for non-degenerate, relativistic electrons, although the notation has been changed to allow for the presence of positrons. The approximations involved in what follows are discussed in detail in Appendix B. The quantities of primary interest are the work and energy per gram rather than per cm^3 so that it is convenient to take $V = 1/\rho$ and transform equation (55) to

$$\frac{dQ}{dT} = \frac{p}{\rho^2}\frac{d\rho}{dT} - \frac{dU}{dT}. \tag{56}$$

The sign convention used in equations (55) and (56) is opposite to Chandrasekhar's. Our dQ is the negative of his. It will be apparent that dQ in equations (55) and (56) is the increment in *available* gravitational energy above that needed to maintain the internal energy. Dynamical energies have not been included. In classical non-relativistic dynamics the internal energies of a particular sample of material are independent of the accelerations and bulk motion of that sample. The pressure must be known as a function $p(\rho, T)$. In quasi-static equilibrium the polytropic equations yield $\rho(T)$. In dynamic collapse or explosion methods for determining $\rho(T)$ will be developed as required.

As the star evolves it is possible to compute $dQ/dt = (dQ/dT)(dT/dt)$ once dQ/dT is known from equation (56) and once the rate of temperature change during the evolution is known. Note that dU/dT is the total derivative equal to $\partial U/\partial T + (\partial U/\partial\rho)(d\rho/dT)$.

Since Boyle's Law is obeyed for the gas pressure in the non-degenerate approximation, relativistic or non-relativistic, and, since radiation pressure must be included in the total pressure, this latter quantity is given by

$$\begin{aligned} p &= \rho NkT + \tfrac{1}{3}aT^4 = \rho N_e kT + \rho N_N kT + \tfrac{1}{3}aT^4 \\ &= \frac{\rho\Re T}{\mu\beta} = 0.8314\times 10^{17}\frac{\rho T_9}{\mu\beta} \\ &= \frac{aT^4}{3(1-\beta)} = 2.522\times 10^{21}\frac{T_9^4}{1-\beta}\ \text{dyne cm}^{-2}\ \text{or erg cm}^{-3}. \end{aligned} \tag{57}$$

Thus

$$\frac{p}{\rho^2}\frac{d\rho}{dT} = \left(N_e k + N_N k + \tfrac{1}{3}\frac{aT^3}{\rho}\right)\frac{d\ \ln\rho}{d\ \ln T} = \frac{Nk}{\beta}\frac{d\ \ln\rho}{d\ \ln T} = \frac{\Re}{\mu\beta}\frac{d\ \ln\rho}{d\ \ln T}. \tag{58}$$

The internal energy per gram including radiative energy, kinetic energy of all particles, and rest-mass energies of electron-positron pairs but *not* of nuclei and ionization electrons is

$$\begin{aligned} U = \frac{u}{\rho} &= xN_e kT + \tfrac{3}{2}N_N kT + (N_e - N_0)m_e c^2 + aT^4/\rho \\ &= 1.381\times 10^{-7}T_9[xN_e + \tfrac{3}{2}N_N + (N_e - N_0)z] \\ &\qquad + 0.7565\times 10^{22}T_9^4/\rho\ \text{erg gm}^{-1} \\ &= 0.8314\times 10^{17}\frac{T_9}{\mu}\left(x\frac{N_e}{N} + \tfrac{3}{2}\frac{N_N}{N} + \frac{N_e - N_0}{N}z\right) \\ &\qquad + 0.7565\times 10^{22}T_9^4/\rho\ \text{erg gm}^{-1}. \end{aligned} \tag{59}$$

Reasons for this restricted choice of the internal energy are presented in Sections (*a*) and (*c*) of Appendix B. Nuclear energy from transmutations will be treated quite separately, as will changes in N_N through nuclear reactions except in respect to the appropriate change in internal kinetic energy. The stellar material is to be taken as completely ionized so that N_0 also can change only through nuclear processes such as electron-positron capture or emission. In the transmutation $2\ O^{16} \rightarrow S^{32}$, $N_N = 1/AM_u$ changes but $N_0 = Z/AM_u$ does not. On the other hand, in the transmutation $Ni^{56} + 2e^- \rightarrow Fe^{56} + 2\nu$, N_0 does change. For the mean kinetic energy per nucleus we have employed $\frac{3}{2}\,kT$, which is appropriate for non-relativistic particles. At $T_9 \sim 10$ the mean kinetic energy of an iron nucleus is only 2×10^{-5} of its rest-mass energy. The mean kinetic energy in units kT per relativistic electron or positron has been designated by the symbol x. The mean kinetic energy per relativistic electron in the non-degenerate case is given by Chandrasekhar (1939) in his equation (236) (p. 396) and is tabulated in his notation as $U/PV = U/NkT$ in his Table 24 (p. 397). The mean kinetic energy is derived by inserting the kinetic energy in the integrand of an equation corresponding to our equation (7) and carrying out the indicated integration and averaging. It will be clear from equation (7) that in the non-degenerate case the result will be the same for positrons as for electrons. In our notation x is given by

$$x = z\left[\frac{3K_3(z) + K_1(z)}{4K_2(z)} - 1\right], \tag{60}$$

where $K_\nu(z)$ is the modified Bessel function of order ν. In Appendix B, x is designated by x_e. The properties of the Bessel functions are such that the following useful relations (see eq. [68] and [69] below) can be derived

$$\begin{aligned} 3 - x - z &= 2 - \frac{z}{2}\left[\frac{K_3(z) + K_1(z)}{K_2(z)}\right] = 2 + \frac{d\ \ln K_2}{d\ \ln z} \\ &= \frac{d\ \ln \bar{K}_2}{d\ \ln z} = -\frac{d\ \ln \bar{K}_2}{d\ \ln T}. \end{aligned} \tag{61}$$

The differentiation of U, equation (59), with respect to T is quite straightforward if it is remembered that N_e and N_N and ρ are functions of T. N_N changes as heavier nuclei (fewer in number) are fused from lighter nuclei as T increases. Differentiation of the first term on the right-hand side of equation (59) introduces the specific heat per electron at constant volume given by $c_v = d(xT)/dT$ and tabulated by Chandrasekhar (1939) as C_V/Nk in his notation in Table 24 (p. 397). It will be recalled that in the non-relativistic case $c_v = x = \frac{3}{2}$, while in the extreme relativistic case $c_v = x = 3$. The extreme non-degenerate, extreme relativistic values, $c_v = x = 3.151$ are derived in Appendix B.

The final result for dU/dT is

$$\frac{dU}{dT} = kN_e\left(c_v + (x+z)\frac{d\ \ln N_e}{d\ \ln T}\right) + \tfrac{3}{2}kN_N\left(1 + \frac{d\ \ln N_N}{d\ \ln T}\right) + \frac{aT^3}{\rho}\left(4 - \frac{d\ \ln \rho}{d\ \ln T}\right). \tag{62}$$

Equations (58) and (62) can then be used in equation (56) to give

$$\begin{aligned} \frac{dQ}{dT} = kN_e\left[\frac{d\ \ln \rho}{d\ \ln T} - c_v - (x+z)\frac{d\ \ln N_e}{d\ \ln T}\right] + kN_N\left(\frac{d\ \ln \rho}{d\ \ln T} - \tfrac{3}{2} - \tfrac{3}{2}\frac{d\ \ln N_N}{d\ \ln T}\right) \\ + \frac{4aT^3}{3\rho}\left(\frac{d\ \ln \rho}{d\ \ln T} - 3\right). \end{aligned} \tag{63}$$

It will be noted that equation (63) reduces to the customary form for N_e = constant and N_N = constant. The radiation term in equation (63) can be combined with the other terms by employing the relation $4aT^3/3k\rho N = 4(1-\beta)/\beta$. Then

$$\frac{dQ}{dT} = kN_e\left[3 - c_v - (x+z)\frac{d\ln N_e}{d\ln T} + \left(\frac{4-3\beta}{\beta}\right)\left(\frac{d\ln\rho}{d\ln T} - 3\right)\right] + kN_N\left[\tfrac{3}{2} - \tfrac{3}{2}\frac{d\ln N_N}{d\ln T} + \left(\frac{4-3\beta}{\beta}\right)\left(\frac{d\ln\rho}{d\ln T} - 3\right)\right]. \tag{64}$$

It will be clear from equation (64) that dQ/dT can be calculated as a function of temperature for any given path in the ρ, T-plane since all terms can be evaluated once ρ as a function of T is given. We shall now work out the necessary expressions for the case of the evolutionary path of a massive stellar core in the ρ, T-plane given by equation (32). In this case, under the assumption M_c = constant, one has

$$\frac{d\ln\rho}{d\ln T} = 3 - 3\frac{d\ln\mu\beta}{d\ln T}. \tag{65}$$

As long as ρ and T and $\mu\beta$ apply to the same element of mass, equation (65) is independent of the polytrope index n. The same will be true of the *form* of the remaining equations in this part. Now the first form of equation (36) can be differentiated to show that

$$\frac{d\ln\mu\beta}{d\ln T} = -\left(\frac{\beta}{4-3\beta}\right)\frac{d\ln N}{d\ln T} = -\left(\frac{\beta}{4-3\beta}\right)\left(\frac{N_e}{N}\frac{d\ln N_e}{d\ln T} + \frac{N_N}{N}\frac{d\ln N_N}{d\ln T}\right), \tag{66}$$

so that

$$3\frac{d\ln N}{d\ln T} = \left(\frac{4-3\beta}{\beta}\right)\left(\frac{d\ln\rho}{d\ln T} - 3\right), \tag{67}$$

and upon substitution of equation (67) into equation (64) one finds

$$\frac{dQ}{dT} = kN_e\left[3 - c_v + (3-x-z)\frac{d\ln N_e}{d\ln T}\right] + kN_N\left(\tfrac{3}{2} + \tfrac{3}{2}\frac{d\ln N_N}{d\ln T}\right). \tag{68}$$

The usefulness of expression (61) will now be apparent. An alternative form of equation (68) which is of some interest can be written as

$$\frac{dQ}{dT} = kT\left[(3-c_v)\left(\frac{N_e}{T}\right) + (3-x-z)\frac{dN_e}{dT}\right] + kT\left(\tfrac{3}{2}\frac{N_N}{T} + \tfrac{3}{2}\frac{dN_N}{dT}\right). \tag{69}$$

It is instructive to consider the meaning of the various terms in equations (68) and (69). For unit increment in temperature we have:

1. Work done by gravitational forces on existing e^- and $e^\pm = 3kN_e$
2. Work done by gravitational forces on newly created $e^\pm = 3kT(dN_e/dT)$
3. Increase in internal kinetic energy of existing e^- and $e^\pm = c_v kN_e$
4. Energy necessary to create kinetic energy and rest mass of new $e^\pm$

$$= (x+z)\,kT\frac{dN_e}{dT} = (xkT + m_e c^2)\frac{dN_e}{dT}$$

5. Work done on nuclei minus increase in their kinetic energy

$$= 3kN_N - \tfrac{3}{2}kN_N = \tfrac{3}{2}kN_N$$

6. Work done on new nuclei minus increase in their kinetic energy

$$= \tfrac{3}{2} kT \frac{dN_N}{dT}.$$

Note once again that the change in nuclear rest-mass energy has not been included but will be treated separately. The nuclear density N_N decreases with increasing T roughly as T^{-1} so that $N_N/T + dN_N/dT \sim 0$ and the nuclear term in equation (69) can be neglected in good approximation as will be done in what follows. It will be noted that radiation terms do not appear in equations (68) and (69). This is in agreement with the well-known fact that the work done against radiation pressure is just equal to the increase in internal radiation energy. The same is true for extremely relativistic particles ($z \to 0$, $x \to c_v \to 3$).

In using equation (68) to compute dQ/dT as a function of temperature, it is required, among other things, to evaluate $d \ln N_e/d \ln T$. This can be done most simply by using equations (10), (18), and (61) to derive

$$\frac{d \ln N_e}{d \ln T} = \left(\frac{2N_1}{N_e}\right)^2 \frac{d \ln N_1}{d \ln T} = \left(\frac{2N_1}{N_e}\right)^2 \left(x + z - \frac{d \ln \rho}{d \ln T}\right). \tag{70}$$

Equations (67) and (70) can be used to eliminate $d \ln \rho/d \ln T$ to yield

$$\frac{d \ln N_e}{d \ln T} = \frac{x + z - 3}{(N_e/2N_1)^2 + 3\beta/(4 - 3\beta)} = \frac{x + z - 3}{(N_0/2N_1)^2 + 4/(4 - 3\beta)}, \tag{71}$$

where the approximation $N_e \approx N$ has been employed.

Before discussing the actual computations made using equation (68) we derive an expression for dQ/dT which has proven useful in the eventual implosion of the stellar core. By substituting equation (70) into equation (63) it is found that

$$\frac{dQ}{dT} = kN_e \left\{\left[1 + (x + z)\left(\frac{2N_1}{N_e}\right)^2\right]\frac{d \ln \rho}{d \ln T} - c_v - (x + z)^2 \left(\frac{2N_1}{N_e}\right)^2\right\}$$
$$+ kN_N \left(\frac{d \ln \rho}{d \ln T} - \tfrac{3}{2} - \tfrac{3}{2} \frac{d \ln N_N}{d \ln T}\right) + \frac{4aT^3}{3\rho}\left(\frac{d \ln \rho}{d \ln T} - 3\right). \tag{72}$$

The factor $(2N_1/N_e)^2 = [1 + (N_0/2N_1)^2]^{-1}$ is a function only of temperature and can be evaluated directly using equation (37). Equation (72) is much more general than (68) or (69). No relation such as (28) or (32) has been used, so that equation (72) does not depend on the star's being in mechanical equilibrium.

Table 3 includes the calculation of dQ/dT using equations (68) and (71) for the quasi static ρ, T-path for a star with $M_c = 20\ M_\odot$, $M \approx 30\ M_\odot$ illustrated in Figure 5 for $T_9 < 6$. The results for the various electron-positron contributions to dQ/dT, items 1–6 above are shown in Figure 7, while dQ/dT and $Q = \int (dQ/dT)dT$ are shown in Figure 8. For illustrative purposes the quasi-static calculations have been carried beyond the point where the implosion of the core, to be described in Part VIII, takes place. These portions of the curves are shown as dashed lines in Figure 8 and apply for the hypothetical case of no implosion. For the implosion case, dQ/dT has been calculated using the methods of Part VIII, and the results have been incorporated in Table 4 and shown graphically in Figure 9. Figure 9 also shows the corresponding nuclear and neutrino terms, dQ_N/dT and dU_ν/dt.

The most remarkable result of these calculations is that dQ/dT vanishes near $T_9 = 1.5$, reaches a negative value with magnitude $\sim 10^{16}$ erg gm^{-1} per 10^9 degrees at $T_9 \sim$ and returns to zero and thence positive value near $T_9 \sim 3$. As long as a quasi-stat

$\rho \propto (T/\mu\beta)^3$ curve is followed, the gravitational energy which the stellar core can call upon by contracting is *not* sufficient to supply the energy necessary to create the new electron-positron pairs, the rate of production for which reaches a maximum around $T_9 = 2$, as indicated by the total energy curve for new $e^{\pm}$ in Figure 7. The pronounced effect of the tail of the Planck distribution for radiation is evidenced by the fact that this maximum occurs at $kT \sim \frac{1}{2}m_e c^2$ and not at $kT = 2m_e c^2$.

Table 3 also gives the neutrino luminosity from equation (21) for the ρ, T-path under consideration. It will be clear that the neutrino luminosity is moderately large in the temperature range, $T_9 \sim 2$ to 3, with $du_\nu/dt \sim 10^{18}$ erg cm^{-3} sec^{-1} or $dU_\nu/dt \sim 10^{12}$ erg gm^{-1} sec^{-1}.

If the stellar core were not able to call upon another source of energy, ρ would rise much more rapidly than T^3 because of the energy needed for pair creation. In short, implosion would begin near $T_9 \sim 2$. This has led Chiu (1961*a*, *b*) to suggest that neutrino loss from $e^+ + e^- \rightarrow \nu + \bar{\nu}$ is a possible cause of core implosion in Type II supernovae and that the core material may never reach the stage where the iron to helium-neutron phase change of Hoyle and Fowler (1960) becomes effective. It will be shown

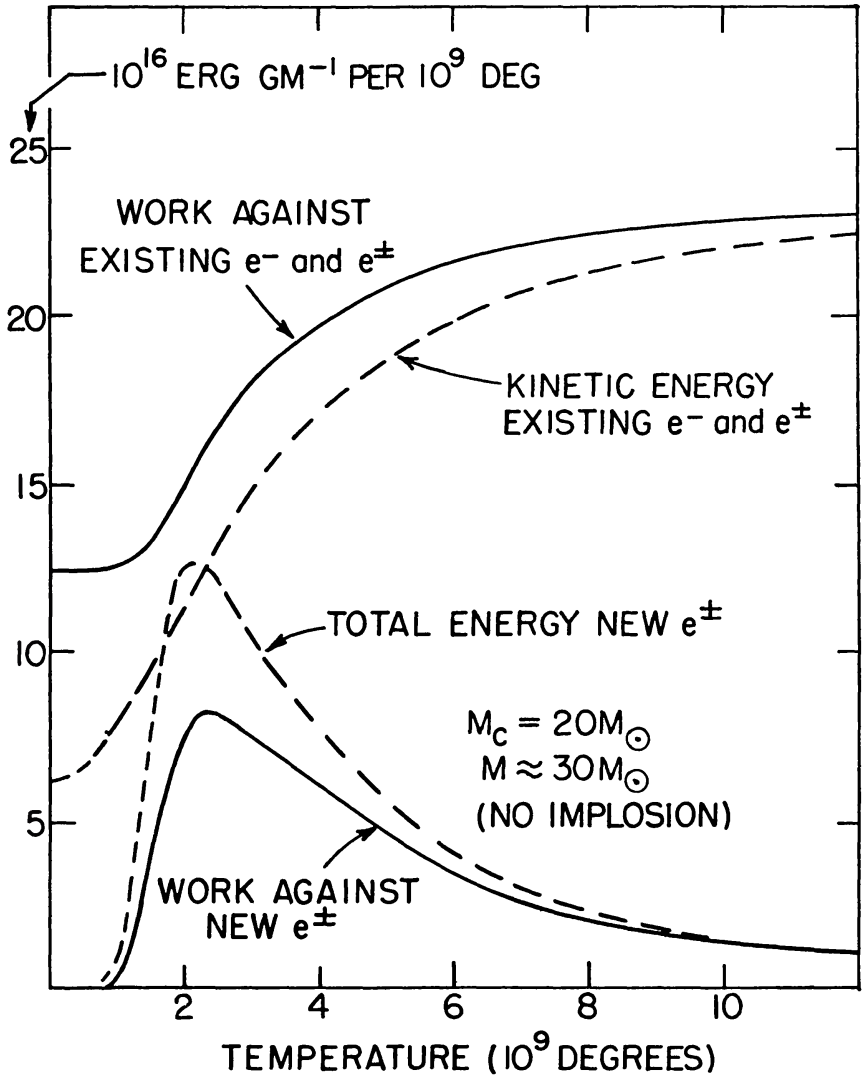

FIG. 7.—Various electron-positron contributions to the quantity dQ/dT for a star with $M \approx 30\ M_\odot$ in the case of no implosion.

in the sequel that there is indeed an important source of energy upon which the stellar core can call in order to postpone implosion, namely, nuclear energy of the rapidly evolving core material. However, it may be well to recall, at this point, our argument for the strong requirement that the iron-to-helium-neutron phase change must be the cause of implosion in Type II supernovae.

The argument is based on our point of view that Type II supernovae are the site of the equilibrium or *e*-process in which the iron-group elements are synthesized. The iron-group elements are more abundant than their immediate predecessors in the periodic table and very much more abundant than all of the heavier elements. It is reasonable to associate their production with the explosion of the *massive* Type II supernovae. In the model discussed in Hoyle and Fowler (1960) we regarded the iron-group elements as having been synthesized in the layers of the star situated immediately below the seat of the explosion and just outside the imploding region. A self-consistent picture results if the central region of the supernova core implodes at the onset of the iron-to-helium-

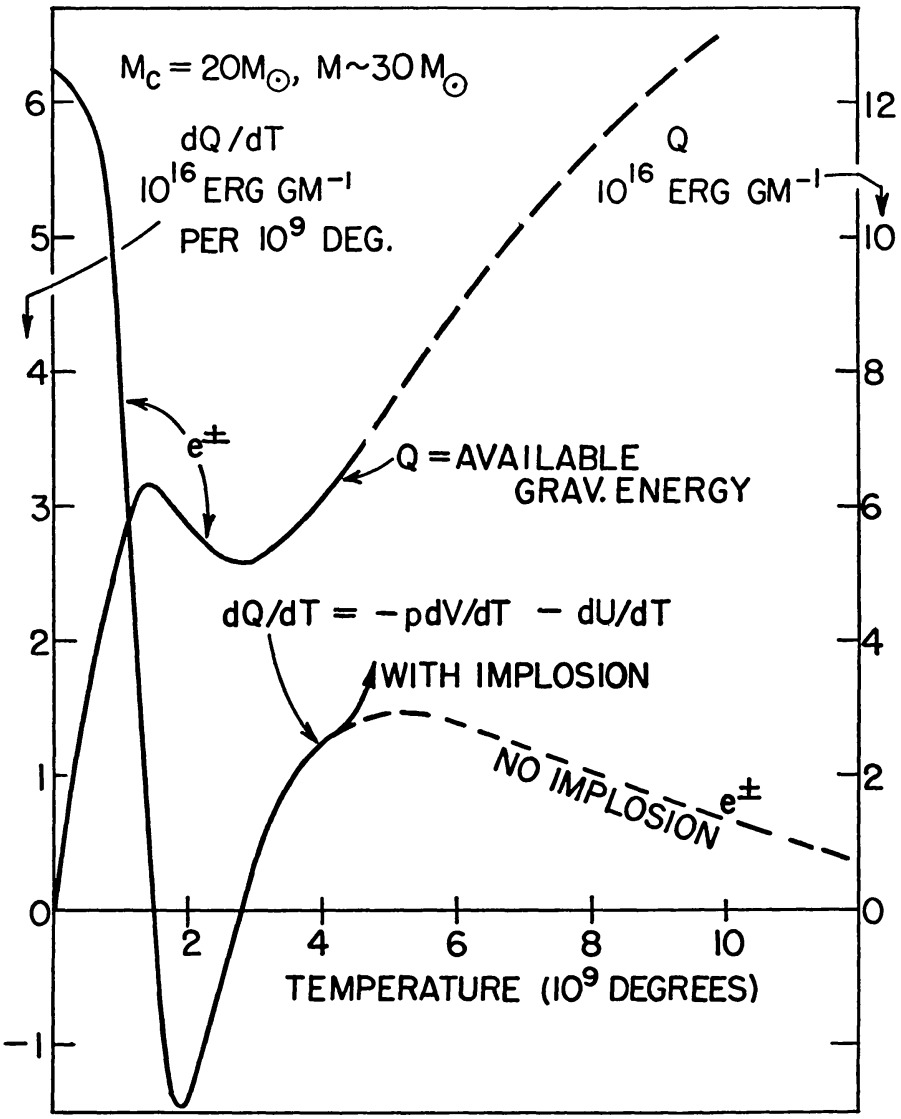

FIG. 8.—The quantities dQ/dT and Q plotted as a function of temperature in 10^9 degrees for a star with $M \approx 30\ M_\odot$ in the case of no implosion.

neutron phase change and if the outer region of the core (still iron-group) is swept up and out in the explosion of the fuel-rich envelope. Since all of this occurs about $T_9 \sim 4$, it would not seem to be possible to incorporate iron-group production in the Chiu model in which implosion occurs at $T_9 \sim 2$, a temperature well below that at which iron-group nuclei are synthesized. If the observational evidence on the great abundance and the equilibrium distribution in relative abundances of the iron-group nuclei are to be taken as relevant and authoritative, then we are most *reluctant* to give up Type II supernovae as the site of synthesis, since these supernovae so well meet requirements in regard to the amount of material synthesized and in regard to furnishing appropriate physical circumstances for the synthesis. The detailed analysis presented in the following parts of this paper would seem to justify this *reluctance* completely.

V. NUCLEAR REACTIONS AS THE SOURCE OF ENERGY FOR NEUTRINO EMISSION BY MASSIVE STARS IN THE PRE-SUPERNOVA STAGE

Stars are thermonuclear fusion reactors in which nuclear-energy generation takes place as hydrogen is fused into successively heavier nuclei until the iron-group elements

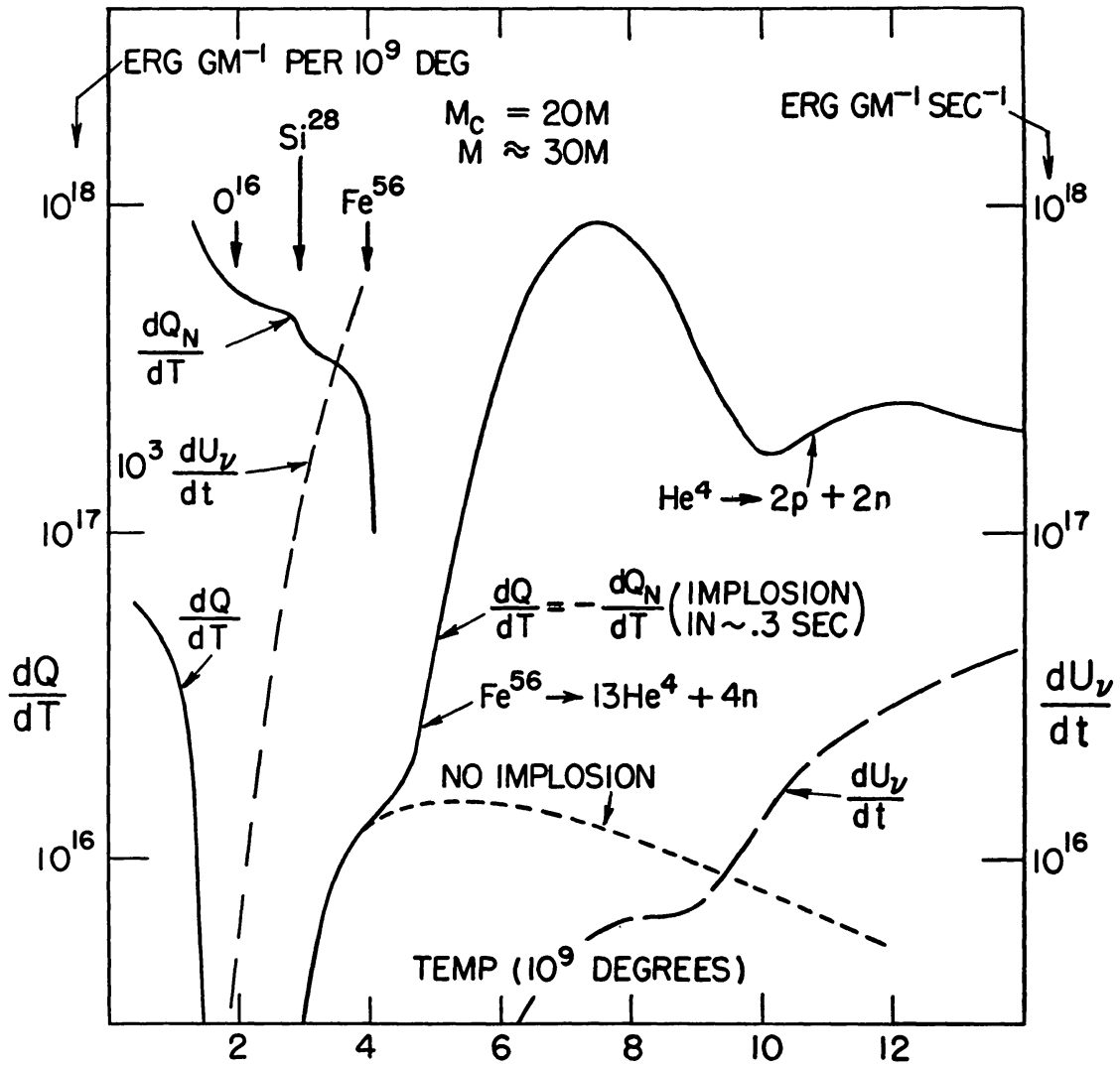

FIG. 9.—The quantities dQ_N/dT, dQ/dT, and $dU\nu/dt$ as a function of temperature in 10^9 degrees for a star with $M \approx 30\ M_\odot$.

are reached. The nuclei of the iron-group are the most stable forms of nuclear matter, i.e., the nuclei in which the constituent nucleons have the minimum internal energy. (The internal energy, potential plus kinetic, is of course negative so that its absolute magnitude, usually termed the *binding energy*, is positive and reaches maximum value at the iron-group nuclei.) The minimum in energy and maximum in binding energy occur as the result of the fact that the nuclear-surface energy decreases with atomic mass while the Coulomb energy increases.

In a star nuclear-energy generation ceases when nuclei at the minimum energy are reached. At this point the nuclear resources of the star are exhausted. In this part a brief account is given of the various stages in hydrogen-to-iron fusion in the evolution of massive stars with special emphasis on nuclear-fusion reactions as the source of energy for neutrino emission by such stars.

During the main sequence stage a massive star burns hydrogen through the CNO bi-cycle rather than the *proton-proton* chain unless the CNO abundance is very low indeed. The CNO bi-cycle is in general more effective at the high internal temperatures ($T_7 > 2$) of main-sequence stars only slightly heavier than the Sun, since the bi-cycle is far more temperature dependent with rate proportional to T^{15} than the pp-chain with rate proportional to T^4. New tables for the rate of energy generation by the CNO bi-cycle have been recently prepared by Caughlan and Fowler (1962). In the bi-cycle the over-all result is

$$4\mathrm{H}^1 \rightarrow \mathrm{He}^4 + 25.0 \text{ MeV } (5.98 \times 10^{18} \text{ erg gm}^{-1} \text{ excluding } \nu\text{-loss}) . \quad (73)$$

The energy release is given by $q = 1.602 \times 10^{-6}\, Q/\Sigma A_i M_u = 0.965 \times 10^{18}\, Q/\Sigma A_i$ erg gm^{-1}, where $Q = 25.0$ MeV is the energy release in MeV per process and $\Sigma A_i \approx 4$ is the sum of the masses of the interacting nuclei in atomic mass units. See Section (j) of Appendix C for additional discussion in regard to the energy emission per reaction and per gram. The mean lifetime in seconds for hydrogen to CNO burning in massive stars is given by

$$\log \tau_{\mathrm{CNO}}(H^1) = -8.43 - \log \rho x_{\mathrm{CNO}} + \tfrac{2}{3} \log T_7 + 30.70/T_7^{1/3} , \quad (74)$$

and the energy generation in erg gm^{-1} sec^{-1} in the bi-cycle is given by

$$\log \epsilon_{\mathrm{HCNO}} = 27.21 + \log \rho x_{\mathrm{H}} x_{\mathrm{CNO}} - \tfrac{2}{3} \log T_7 - 30.70/T_7^{1/3} . \quad (75)$$

Here and hereafter we neglect screening factors. This is justified in massive stars which have relatively low densities for a given temperature.

When hydrogen is exhausted in 10–50 per cent of the stellar interior, core contraction occurs and central temperatures and densities are reached which result in the ignition of helium. The initial stage in the helium burning is the Salpeter-Hoyle process: $\mathrm{He}^4(\alpha)\mathrm{Be}^8(\alpha)\mathrm{C}^{12*}$ ($\gamma\gamma$ or $e^{\pm}$)C^{12}. This is a three-body process which takes place in two resonant stages. The unbound ground state of Be^8 serves as one resonance and the 7.65-MeV excited state of C^{12} as the other. The over-all result is

$$3\ \mathrm{He}^4 \rightarrow \mathrm{C}^{12} + 7.28 \text{ MeV } (5.85 \times 10^{17} \text{ erg gm}^{-1}) . \quad (76)$$

The results of B^{2}FH (1957) for the mean lifetimes of He^4 to this process must be modified by the experimental findings of Fregeau (1956), Alburger (1960, 1961), Ajzenberg-Selove and Stelson (1960), Seeger and Kavanagh (1963), and Hall and Tanner (1964). The combined efforts of these workers establish $\Gamma_\gamma + \Gamma_{e^\pm} = (2.4 \pm 1.5) \times 10^{-3}$ eV so that the second equation on page 566 of B^{2}FH (1957) yields the following expression for the He^4 mean lifetime in seconds

$$\log \tau_{3\alpha}(\mathrm{He}^4) = 6.25 - 2 \log \rho x_\alpha + 3 \log T_8 + 18.75/T_8 . \quad (77)$$

Equation (77) corresponds to a reduction of 0.38 in the logarithm of the mean lifetime given in the second column of Table III, 3 of B^{2}FH (1957).

Under appropriate circumstances the production of C^{12} is followed by $C^{12}(\alpha, \gamma)O^{16} + 7.162$ MeV and, it was thought at one time, by $O^{16}(\alpha, \gamma)Ne^{20} + 4.730$ MeV. However, it has been recently shown by Gove, Litherland, and Ferguson (1961) that the excited state in Ne^{20} at 4.97 MeV which had been considered to serve as a thermonuclear resonance in $O^{16}(\alpha, \gamma)Ne^{20}$ at 240 keV has spin and parity 2^-, and thus cannot be produced by the combination of O^{16} and He^4. The ground states of these two nuclei have spin and parity O^+, and the parity associated with two units of orbital angular momentum is even (as indicated by the superscript +). States with spin and parity combinations (0^+, 1^-, 2^+, 3^-, etc.) permitting breakup into O^{16} and He^4 occur at 5.63 and 5.80 MeV but require temperatures well over $T_8 \sim 3$ to become effective. It develops then that $O^{16}(\alpha, \gamma)$-Ne^{20} does not occur significantly in stars except under such special circumstances as the occurrence of very high temperatures in *low-mass* stars for a short period when degeneracy is suddenly removed at the onset of helium burning. Helium does not become degenerate in massive stars during the contraction of the core. Deinzer and Salpeter (1964) have shown that small amounts ($\sim$ 10 per cent) of Ne^{20} and Mg^{24} are produced in the final stages of helium burning when $3He^4 \rightarrow C^{12}$ is inhibited by the low concentration of He^4. Above 50 $M_\odot$ they find even larger amounts of Mg^{24}. Our discussion is restricted to $10\ M_\odot < M < 50\ M_\odot$.

For the record, the partial lifetimes in seconds for O^{16} to helium burning are the following for off-resonance processes, for resonance at the 5.63-MeV state ($E_r = 0.90$ MeV, $\omega\Gamma_\alpha\Gamma_\gamma/\Gamma = 0.001$ eV) in Ne^{20}:

$$\begin{aligned}\log \tau_\alpha(O^{16}) &= -10.2 - \log \theta_\alpha^2 - \log \rho x_\alpha + \tfrac{2}{3} \log T_8 + 37.2/T_8^{1/3} \text{ (off-resonant)} \\ &= -2.3 - \log \rho x_\alpha + \tfrac{3}{2} \log T_8 + 45.4/T_8 \text{ (via } Ne^{20*} \text{ [5.63 MeV])} .\end{aligned} \tag{78}$$

The reciprocal of the sum of the reciprocals of these partial lifetimes is the over-all lifetime for $T_8 < 30$. For the value of the reduced alpha-particle width, θ_α^2, see the discussion below concerning the corresponding width for $C^{12}(\alpha, \gamma)$. The minimum off-resonant lifetime is given by $\theta_\alpha^2 = 1$. With this value the off-resonant contribution to the reaction rate dominates up to $T_8 \sim 3$.

The question of the relative production of C^{12} and O^{16} in helium burning in massive stars now remains. It will be clear that the rate for $3\ He^4 \rightarrow C^{12}$ is reduced relative to that for $C^{12}(\alpha, \gamma)O^{16}$ at the same temperature in going from low-mass to high-mass stars. This is because in equation (32) density decreases with stellar mass for a given temperature. The rate of the three-body process, $3\ He^4 \rightarrow C^{12}$, is proportional to ρ^3 while that for the two body process is proportional to ρ^2. The mean lifetime in seconds of C^{12} nuclei to helium burning is given by modifying the results of B^{2}FH (1957) by the experimental findings of Swann and Metzger (1957) as follows

$$\begin{aligned}\log \tau_\alpha(C^{12}) &= -10.84 - \log \theta_\alpha^2 - \log \rho x_\alpha + 2 \log T_8 + 30.08/T_8^{1/3} + 0.18/T_8^{2/3} \\ &= -10.73 - \log \rho x_\alpha + 2 \log T_8 + 30.08/T_8^{1/3} + 0.18/T_8^{2/3} .\end{aligned} \tag{79}$$

The modification is necessitated by the fact that Swann and Metzger improved on their 1956 results to give a final value $\Gamma_\gamma = 0.066 \pm 0.02$ eV rather than 0.13 eV for the gamma-width of the 7.116 MeV excited state in O^{16} which dominates the low-energy cross-section for $C^{12}(\alpha, \gamma)O^{16}$. In addition B^{2}FH (1957) took the reduced width for alpha-particle emission, $\theta_\alpha^2 = 0.1$. However, the 7.116 MeV excited state in O^{16} is well described by the alpha-particle model for O^{16} (Dennison 1954; Kameny 1956) and on this basis $\theta_\alpha^2 \sim 1$ is to be expected. On the cluster model of light nuclei, Roth and Wildermuth (1960) show that the low-lying excited states of O^{16} consist primarily of the cluster

$C^{12} + He^4$ with both components in their ground states or of the cluster C^{12*} (2^+, 4.43-MeV excitation) + He^4. Three of the states which are best described by the cluster $C^{12} + He^4$ have reduced alpha-particle widths equal to 0.73, 0.76, and 0.85. The average of these values is $\theta_a^2 = 0.78$. Roth and Wildermuth (1960) assign the 7.116-MeV state in O^{16} to the cluster $C^{12} + He^4$, so we use $\theta_a^2 = 0.78$ in obtaining equation (79). For the $C^{12*} + He^4$ cluster states the average reduced-ground-state alpha-particle width is $\theta_a^2 = 0.024$. It is small as expected. Had we employed this value, the constant in equation (79) would be -9.22 rather than -10.73. We believe that there is very little likelihood that the 7.116-MeV state in O^{16} is represented by the cluster $C^{12*} + He^4$. There is no justification for averaging all reduced widths as done by some authors. Our choice requires that 0.60 be subtracted from the mean lifetimes given in the third column of Table III, 3 of B²FH (1957). In stars of low mass where $C^{12}(\alpha, \gamma)$ does not follow $3\ He^4 \rightarrow C^{12}$ the energy generation in erg gm^{-1} sec^{-1} is

$$\log \epsilon_{3\alpha} = 11.52 + 2 \log \rho + 3 \log x_a - 3 \log T_8 - 18.75/T_8 . \tag{80}$$

Hoyle (1954) showed that if the quantity

$$k = x_a \frac{\tau_{3\alpha}(He^4)}{\tau_a(C^{12})} \tag{81}$$

exceeds the value $\frac{1}{3}$ then $C^{12}(\alpha, \gamma)O^{16}$ invariably follows $3\ He^4 \rightarrow C^{12}$ in the long run and helium burning results in the production of O^{16} only, with no C^{12}. This quantity has the Briggs logarithm

$$\log k = 16.98 - \log \rho + \log T_8 - 30.08/T_8^{1/3} - 0.18/T_8^{2/3} + 18.75/T_8 , \tag{82}$$

and $\log k$ must exceed -0.48 for pure O^{16} production. For $k = 0$, only C^{12} is produced. In addition, for example, $k = \frac{1}{9}$ yields $O^{16}/C^{12} = 2$. In the case that only O^{16} is produced the general process can be represented by

$$4\ He^4 \rightarrow O^{16} + 14.44\ \text{MeV}\ (8.70 \times 10^{17}\ \text{erg gm}^{-1}) . \tag{83}$$

Effectively the mean lifetime of He^4 in seconds is given by

$$\log \tau_{4\alpha}(He^4) = 6.12 - 2 \log \rho x_a + 3 \log T_8 + 18.75/T_8 , \tag{84}$$

and the rate of energy generation in erg gm^{-1} sec^{-1}, after appropriately modifying B²FH (1957), is given by

$$\log \epsilon_{4\alpha} = 11.82 + 2 \log \rho + 3 \log x_a - 3 \log T_8 - 18.75/T_8 . \tag{85}$$

This expression does not hold when x_a becomes small especially in very massive stars where some Ne^{20} and considerable Mg^{24} is produced at the end of helium burning (Deinzer and Salpeter 1964).

Massive stars of the type under specific consideration ($30\ M\odot$) are approximately 10^5 times as luminous as the Sun. The central energy generation in the Sun is $\sim$30 erg gm^{-1} sec^{-1}, so that scaling up this value by the luminosity to mass ratio (3000) leads to $\epsilon_{4\alpha} \sim 10^5$ erg gm^{-1} sec^{-1}. In order to express ρ in terms of temperature we employ equation (32), noting that $\mu = 1.6$ when $x_a = 0.5$ at the midway point in helium burning. These values lead to $\beta = 0.5$ and $\rho = 50\ T_8^3$. Returning to equation (85), we then find that the helium burning gives the required energy generation at $T_8 \sim 1.8$, $\rho \sim 300$ gm cm^{-3} over a period of 8.7×10^{17} erg $gm^{-1} \div 10^5$ erg gm^{-1} $sec^{-1} \sim 9 \times 10^{12}$ sec or 3×10^5 yr. Under these conditions neutrino energy loss is negligible. More importantly

equation (81) yields $k \sim 2$, well over the value $\frac{1}{3}$ above which 4 $He^4 \rightarrow O^{16}$ occurs. This conclusion, of course, depends on the choice $\theta_\alpha^2 = 0.78$ made previously for the alpha-reduced width of the 7.116 MeV excited state in O^{16}. However, even for $\theta^2 \sim 0.1$, $O^{16}/C^{12} \sim 2$ and we will take it until further data become available that O^{16} is the main product of helium burning in *massive* stars. It will become clear that this conclusion is most important in determining the time scale in massive stars for the nuclear evolution from the end of helium burning to the production of intermediate mass nuclei, Ne^{20} to S^{32}. However, it is not critical to the discussion in Parts VI and VII of the subsequent α- and e-processes.

Helium burning in massive stars where O^{16} is the main product is thus in marked contrast to the corresponding burning in low-mass stars where both C^{12} and O^{16} are produced. This dependence of helium-burning products on stellar mass may have an important bearing on the C/O abundance ratios produced under varying astrophysical circumstances. We continue with the nuclear evolution in massive stars illustrated in Figure 3.

Oxygen burning takes place through the reactions $O^{16}(O^{16}, \gamma)S^{32} + 16.54$ MeV, $O^{16}(O^{16}, n)S^{31} + 1.46$ MeV, $O^{16}(O^{16}, p)P^{31} + 7.68$ MeV, $O^{16}(O^{16}, \alpha)Si^{28} + 9.59$ MeV, plus a number of more complicated reactions which primarily occur through exchange mechanisms. Typical of these exchange reactions are $O^{16}(O^{16}, O^{15})O^{17} - 11.53$ MeV in which a neutron is exchanged and $O^{16}(O^{16}, C^{12})Ne^{20} - 2.43$ MeV in which an alpha-particle is exchanged. In general these exchange reactions are endoergic and are not as important at low-interaction energies in stars as the exoergic mechanisms first mentioned. It will be noted that these first-mentioned reactions require considerable amalgamation of the two interacting O^{16} nuclei and thus primarily proceed through compound nucleus formation.

Carbon burning, which succeeds helium burning in stars of relatively low mass, has been discussed by Reeves and Salpeter (1959). The neutron emitting reaction, $C^{12}(C^{12}, n)Mg^{23} - 2.604$ MeV, is endoergic so that $C^{12}(C^{12}, p)Na^{23} + 2.238$ MeV and $C^{12}(C^{12}, \alpha)Ne^{20} + 4.616$ MeV are the two most important primary reactions. The protons and alpha-particles are captured initially by C^{12} to form N^{13} and O^{16}. At a reasonable temperature for carbon burning, $T = 6 \times 10^8$ degrees, N^{13} decays to C^{13} before photodisintegration and the reaction $C^{13}(\alpha, n)O^{16} + 2.202$ MeV then produces additional O^{16}. Eventually the protons and alpha-particles react with Na^{23} and Ne^{20} to produce Mg^{24}, which is the most abundant product at the end of the carbon burning. However, the over-all result is a considerable spread in abundance over the nuclei from O^{16} to Si^{28}.

In contrast, in oxygen burning, the neutron-emitting reaction is exoergic and thus competes successfully with those primary reactions in which protons and alpha-particles are emitted. If neutrons and protons are produced in equal numbers, as can reasonably be expected to be at least approximately the case, then the nuclei which result from the secondary capture of the emitted, p, n, and α will be close to the stability line along which $Z = N = A/2$. Initially the emitted p, n, α are captured by O^{16} to form F^{17}, O^{17}, and Ne^{20}. However, at the temperature at which oxygen burning occurs in massive stars, $T \sim 2 \times 10^9$ degrees (see discussion to follow) these nuclei very quickly undergo photodisintegration through $F^{17}(\gamma, p)O^{16} - 0.598$ MeV, $O^{17}(\gamma, n)O^{16} - 4.142$ MeV, and $Ne^{20}(\gamma, \alpha)O^{16} - 4.73$ MeV. Nucleons and alpha-particles are not tightly bound to the closed shell nucleus O^{16}. Thus the primary reaction products are eventually captured by P^{31} and Si^{28} to form S^{32}. S^{31} decays with a mean lifetime of 3.7 sec to P^{31}. S^{32} is quite stable to photodisintegration at 2×10^9 degrees while slightly heavier nuclei are not. Thus the first stage of oxygen burning results principally in the production of S^{32} with some spread in abundance over nearby atomic masses. The over-all process can be represented by

$$2\ O^{16} \rightarrow S^{32} + 16.54\ \text{MeV}\ (4.98 \times 10^{17}\ \text{erg gm}^{-1})\ . \qquad (86)$$

Near the termination of oxygen burning as the temperature rises above 2×10^9 degrees it will be found in Part VI that considerable Si^{28} and Ar^{36} are produced.

In Appendix C on nuclear-reaction rates, formulae are developed for computing the lifetime of nuclei involved in continuum processes such as (86) and for computing the reaction and energy generation rate of such processes. Since all primary processes except scattering lead eventually to S^{32}, it is the lifetime of O^{16} to compound nucleus formation in $O^{16} + O^{16}$ which is required. Scattering by re-emission of the original nuclei after formation of the compound nucleus is rare. Taking the interactions to be "black" and with $R = 1.54\,(A_0^{1/3} + A_1^{1/3}) = 7.76$ fermis, it is found from equation (C66) that the "instantaneous" mean lifetime in seconds when the O^{16} concentration by mass is x_{16} is given by

$$\log \tau_{16}(O^{16}) = -38.0 - \log \rho x_{16} + \tfrac{2}{3} \log T_9 + \frac{59.04}{T_9^{1/3}}(1 + 0.080 T_9)^{1/3}. \quad (87)$$

In this and all equations to follow we take $f_o = 1$ and $\langle \beta_l \rangle = 1$ (see Appendix C). The coefficient, 1.54 fermis, in the expression for the interaction radius, R, has been taken from the heavy-ion scattering experiments of Bromley, Kuehner, and Almqvist (1960). A small term designated by B^{2}FH (1957) as $a_l E_o$ has been incorporated as the term proportional to T_9 in the last bracket in equation (87). In the situation under discussion initially $x_{16} = 1$. Note that the concept of "lifetime" must be used carefully in cases where it depends on the concentration of the nuclei to which it applies. Even for constant ρ, T the decrease in number is not exponential in time.

The corresponding mean lifetime in seconds for C^{12} in the reaction

$$2\,C^{12} \rightarrow Mg^{24} + 13.93\ \text{MeV}\ (5.60 \times 10^{17}\ \text{erg gm}^{-1}) \quad (88)$$

is, with $R = 7.05$ fermis,

$$\log \tau_{12}(C^{12}) = -26.9 - \log \rho x_{12} + \tfrac{2}{3} \log T_9 + \frac{36.57}{T_9^{1/3}}(1 + 0.080 T_9)^{1/3}. \quad (89)$$

The rates of energy generation in erg gm^{-1} sec^{-1} for processes (86) and (88) can be found by using appendix equation (C72) and are

$$\log \epsilon_{OO} = 55.7 + \log \rho x_{16}^2 - \tfrac{2}{3} \log T_9 - \frac{59.04}{T_9^{1/3}}(1 + 0.080 T_9)^{1/3} \quad (90)$$

and

$$\log \epsilon_{CC} = 44.7 + \log \rho x_{12}^2 - \tfrac{2}{3} \log T_9 - \frac{36.57}{T_9^{1/3}}(1 + 0.080 T_9)^{1/3}. \quad (91)$$

As a matter of interest we indicate the mean lifetimes in seconds and energy generation in erg gm^{-1} sec^{-1} for $C^{12} + O^{16} \rightarrow Si^{28} + 16.75$ MeV (5.77×10^{17} erg gm^{-1}) with $R = 7.40$ fermis as follows:

$$\log \tau_{16}(C^{12}) + \log \rho x_{16} - 1.20 = \log \tau_{12}(O^{16}) + \log \rho x_{12} - 1.08 = -32.8 + \tfrac{2}{3} \log T_9 + \frac{46.30}{T_9^{1/3}}(1 + 0.080 T_9)^{1/3}, \quad (92)$$

$$\log \epsilon_{CO} = 49.7 + \log \rho x_{12} x_{16} - \tfrac{2}{3} \log T_9 - \frac{46.30}{T_9^{1/3}}(1 + 0.080 T_9)^{1/3}. \quad (93)$$

In what follows, equations (87) and (90) will be used near $T_9 = 2$ where, from Table 3, $\rho \approx 4.8 \times 10^4\, T_9^3$ in a stellar core with effective mass $M_c = 20\,M_\odot$, $M \approx 30\,M_\odot$. Thus

$$\log \tau_{16}(O^{16}) = -42.7 - \log x_{16} - \tfrac{7}{3} \log T_9 + \frac{59.04}{T_9^{1/3}}(1 + 0.080 T_9)^{1/3} \quad (94)$$

$$\text{for } M_c = 20 M_\odot,\ M \approx 30 M_\odot,$$

and

$$\log \epsilon_{OO} = 60.4 + 2 \log x_{16} + \tfrac{7}{3} \log T_9 - \frac{59.04}{T_9^{1/3}}(1 + 0.080 T_9)^{1/3} \quad (95)$$

for $M_c = 20 M_\odot$, $M \approx 30 M_\odot$.

We are now in a position to come to grips with the problem posed in Part IV. The questions at hand are (1) at what temperature does the energy generation from oxygen burning match pair-creation requirements and the neutrino loss and (2) what is the duration of the oxygen burning? The calculations will be made for conditions at the center of the star. It might appear more reasonable to average the nuclear generation and neutrino loss rates over the entire stellar interior as discussed in Section (*k*) of Appendix C and then equate these average values in order to determine the temperature and to divide the available nuclear energy (5×10^{17} erg gm^{-1}) by the average neutrino loss rate in order to determine the duration. The time scale so calculated will be longer than that determined for conditions at the center but would imply that all of the nuclear fuel in the star was expended. The average of dU_ν/dt over a polytropic structure of index $n = 3$ is found to be about 12 per cent of the central value. However, it is the fate of the central portion of the star which is important in regard to the time scale. If we take this central portion to involve $\sim$12 per cent of the stellar mass, a reasonable choice (see Parts VIII and IX), then these two factors approximately cancel and the calculations made for conditions at the center of the star will be correct in order of magnitude.

The first step is to equate ϵ_{OO} from equation (95) to dU_ν/dt from equation (14). The energy required for pair formation $\sim 2 \times 10^{16}$ erg gm^{-1} can be neglected. The result is dependent on the degree of oxygen consumption, but for $x_{16} = 1$, 0.5, 0.1, 0.01, the results are $T_9 \approx 2.1$, 2.2, 2.5, and 3.0, respectively. The neutrino loss is $\sim 5 \times 10^{12}$ erg gm^{-1} sec^{-1} and the "duration" of oxygen burning is $\sim 5 \times 10^{17}$ erg gm$^{-1} \div 5 \times 10^{12}$ erg gm^{-1} sec$^{-1} \sim 10^5$ sec $\sim$ 1 day. The neglect of photon losses ($\sim 10^6$ erg gm^{-1} sec^{-1}) which has been implicit in the calculation is justified by the large neutrino loss just determined. Had we set $\log \epsilon_{OO} = \log dU_\gamma/dt = 6$ for the photon losses alone, we would have found oxygen burning occurring at $T_9 \sim 1.5$ over an interval of $\sim 10^{12}$ sec. The neutrino losses have shortened the time scale for oxygen burning by a factor $\sim 10^7$! In fact, it will be clear as emphasized by Chiu and Stabler (1961) that neutrino losses dominate for temperatures above $T_9 \sim 0.5$, the result being a marked decrease in the time scale for the stages of stellar evolution leading up to the ultimate core collapse and envelope explosion. However, *neutrino loss does not cause final collapse.* The free fall time scale at the relevant density, $\rho \sim 6 \times 10^5$ gm cm^{-3}, is given by equation (B88) in Appendix B and is the order of 1 sec, shorter by a factor of $\sim 10^5$ than the neutrino-loss time scale.

One additional point is important; near $T_9 = 2.2$ the lifetime of O^{16} to $O^{16}(\gamma, \alpha)C^{12}$ can be shown to be $\sim 10^7$ sec so that the fusion of O^{16} with O^{16} occurs much more rapidly than the photodisintegration of O^{16}. Photodisintegration does become important near $T_9 \sim 3$.

It is gratifying from the authors' point of view that oxygen burning is competent to supply the energy necessary to sustain neutrino emission just in the temperature range where energy is not available from the work done by gravitational forces in contraction under quasi-equilibrium conditions. The nuclear energy resources of the star are sufficient to prevent catastrophic collapse even though the neutrino losses are very severe and do shorten the time scale over that calculated on the basis of photon losses alone by a very great factor $\sim 10^7$. Even so, the neutrino losses fail to induce free fall by a factor of $\sim 10^5$. Even in drastic circumstances, *exoergic* nuclear reactions still serve as stellar thermostats.

At the end of section (*g*), Appendix B, it is shown that the adiabatic coefficients dip slightly below $\frac{4}{3}$ when $dQ/dT < 0$ during oxygen burning. This is true only at the center of the stellar core. The averages over the core exceed $\frac{4}{3}$ and the core is dynamically stable. This can be ascertained by inspection of Table 3.

VI. THE ALPHA-PROCESS IN MASSIVE STARS

The termination of oxygen burning near $T_9 \sim 3$ does not lead to a change in the general state of affairs. The burden of supplying the necessary energy is taken over by what we will call the alpha-process (α-process) following B^{2}FH (1957). Nuclear energy is available until the iron-group nuclei are produced near $T_9 \sim 4$. In the run from S^{32} to the iron-group nuclei the energy released is about 2.0×10^{17} erg gm^{-1} where we have not included the energy carried away by neutrinos in the beta-processes by which two protons are ultimately changed to two neutrons in the Fe^{56}. The remainder must suffice for $e^+ + e^- \rightarrow \nu + \bar{\nu}$ over a change in temperature $\Delta T_9 \sim 1$ from $T_9 \sim 3$ to $T_9 \sim 4$ so that $\sim 2 \times 10^{17}$ erg gm^{-1} per 10^9 deg are available from the final nuclear resources. This is illustrated in Figure 9 by the curve for dQ_N/dT. This quantity is to be compared with dU_ν/dt in order to determine the time scale Δt for a significant change in ΔT to be established. Note that dU_ν/dt has been multiplied by 10^3 to bring it on scale in the range $2 < T_9 < 4$ so that the time scale is of the order of 10^3 sec in the region near the point where dQ_N/dT and $10^3\, dU_\nu/dt$ intersect. With $dQ_N/dT_9 \approx 2 \times 10^{17}$ erg gm^{-1} per 10^9 deg and $dU_\nu/dt \approx 4 \times 10^{10}\, T_9^6$ erg gm^{-1} sec^{-1} from equation (21) corrected for $T_9 \sim 3$ to 4, it is possible to reach a better estimate of the duration of the final nuclear burning by employing equation (B86) to write

$$\Delta t = \int_{\Delta T_9} \frac{dQ_N/dT_9}{dU_\nu/dt}\, dT_9 \approx [T_9^{-5}(\text{initial}) - T_9^{-5}(\text{final})] \times 10^6 \text{ sec} \qquad (96)$$

$$\approx 3000 \text{ sec for the change from } T_9 \sim 3 \text{ to } T_9 \sim 4 .$$

Equation (96) follows from equation (B86) with the small term dQ/dT_9 neglected (see Fig. 9). This calculation is replaced by more detailed calculations in what follows, but no great change in Δt results.

The value found for Δt is considerably greater than the free-fall collapse time in a stellar core which is the order of 1 sec (see Part VIII). Thus nuclear energy is ample to supply the neutrino losses *without* catastrophic gravitational implosion. Before going to the situation where nuclear processes begin to *absorb* energy from the medium, we turn to certain details of the nucleosynthesis from S^{32} to Fe^{56}.

Near the end of the oxygen burning ($x_{16} \sim 0.1$, $T_9 \sim 2.5$) a marked change occurs in the nature of the *nuclear* processes. Photodisintegration of nuclei begins to occur and with increasing temperature becomes more rapid than direct fusion processes. The mutual Coulomb barrier between S^{32} nuclei is so high, $E_C \approx 40$ MeV, that fusion processes are very rare indeed. Thus the nuclear burning does not occur through the interaction of pairs of sulfur nuclei but through a chain of reactions which B^{2}FH (1957) termed the α-process. The photodisintegration of some of the sulfur nuclei frees alpha-particles, protons, and neutrons, and these are in turn captured by other sulfur nuclei and reaction products to form heavier nuclei. We first make a determination of the relative number of alpha-particles, protons, and neutrons released in the photodisintegration of S^{32} and for this purpose turn to equations (C22) and (C7) in Appendix C. The appropriate photodisintegration reactions and energies are $S^{32}(\gamma, \alpha)Si^{28} - 6.95$ MeV, $S^{32}(\gamma, p)P^{31} - 8.86$ MeV, and $S^{32}(\gamma, n)S^{31} - 15.09$ MeV. From the experimental data on nuclear reactions involving S^{32} as summarized by Endt and van der Leun (1962) we find $\Sigma_o[(2J+1)\Gamma_1\Gamma_\gamma/\Gamma]_r \sim 10^{-5}$, 2×10^{-4}, and 10^{-3} MeV for the α, p, and n cases respectively. The effective thermal energies E_0 at which the reverse capture reactions take place are 3.14 MeV, 1.34 MeV, and ~ 0 MeV so that $Q + E_o = 10.09$, 10.20, and 15.09 MeV, respectively. It will be immediately clear from equation (C22) that proton and alpha-particle emission will dominate and it is found at $T_9 = 2.5$ that the partial lifetimes to photodisintegration are $\tau_{\gamma\alpha}(S^{32}) \sim 10^4$ sec, $\tau_{\gamma p}(S^{32}) \sim 10^3$ sec, and $\tau_{\gamma n}(S^{32}) \sim 10^{12}$ sec. On the other hand at $T_9 = 2$, $\tau_{\gamma\alpha}(S^{32}) \sim 10^8$ sec and $\tau_{\gamma p}(S^{32}) \sim 3 \times 10^7$ sec

Thus in the time scale ($\sim 3 \times 10^3$ sec) permitted by the neutrino loss rate it becomes apparent that photodisintegration of the product S^{32} becomes important in the late stages ($x_{16} < 0.1$) of oxygen burning. Overlapping of processes is to be expected at high temperatures.

The results obtained above indicate that the photodisintegration of S^{32} results primarily in proton emission which exceeds alpha-particle emission by approximately a factor of 10. However, the residual nucleus in proton emission P^{31} is rapidly photodisintegrated through $P^{31}(\gamma, p)Si^{30} - 7.29$ MeV which has a much lower threshold than $P^{31}(\gamma, \alpha)$ or $P^{31}(\gamma, n)$. In turn Si^{30} is rapidly consumed through $Si^{30}(\gamma, n)Si^{29} - 10.61$ MeV which has the lowest threshold and similarly Si^{29} goes by $Si^{29}(\gamma, n)Si^{28} - 8.48$ MeV, again neutron emission having the lowest threshold. It will be clear then that $S^{32}(\gamma, p)$ is followed rapidly by the emission of a second proton and two neutrons. These nucleons also interact rapidly at the temperature and density under consideration and the production of an alpha-particle is the ultimate result. Thus, in effect, S^{32} is photodisintegrated into $Si^{28} + He^4$ in an interval determined by the rate of the $S^{32}(\gamma, p)$ reaction. As noted above this interval is on the average 10^3 sec and is somewhat less than the time scale set by neutrino losses. Whether it proceeds by $S^{32}(\gamma, \alpha)Si^{28} - 6.95$ MeV or by $S^{32}(\gamma, 2p\ 2n)Si^{28} - 35.2$ MeV, the over-all result is still adequately described as the α-process. Let those who will, pick nits!

The ejection of an alpha-particle or four nucleons from S^{32} results in the production of Si^{28}. This nucleus is very refractory, the α, p, n, binding energies being 9.99 MeV, 11.58 MeV, and 17.18 MeV, respectively. It will be clear that proton emission will be the most probable when photodisintegration does eventually occur, and the mean lifetime for this process according to equation (C22) is

$$\log \tau_{\gamma p}(Si^{28}) = -17.5 + 3.36/T_9^{1/3} + 58.3/T_9\,, \tag{97}$$

where we have taken $\Sigma_o[(2J + 1)\Gamma_1\Gamma_\gamma/\Gamma]_r \sim 2 \times 10^{-4}$ MeV again from Endt and van der Leun (1962). Equation (97) yields $\tau_{\gamma p}(Si^{28}) = 10^8$ sec, 10^4 sec, 10^2 sec, and 1 sec at $T_9 = 2.5$, 3.0, 3.4, and 3.8, respectively. Thus Si^{28} is not photodisintegrated within the neutrino-loss time scale until the temperature is somewhat over 3×10^9 degrees. The upshot is the occurrence of a temperature interval $2.5 < T_9 < 3$ in which S^{32} is subject to rapid photodisintegration but Si^{28} is not. When Si^{28} is eventually destroyed the over-all result is $Si^{28}(\gamma, p)(-11.58\ \text{MeV})Al^{27}(\gamma, p)(-8.27\ \text{MeV})Mg^{26}(\gamma, n)(-11.10\ \text{MeV})Mg^{25}(\gamma, n)(-7.33\ \text{MeV})$ or $Si^{28}(\gamma, 2p\ 2n)Mg^{24} - 38.3$ MeV which is quickly followed by $2p + 2n \rightarrow \alpha + 28.3$ MeV. $Si^{28}(\gamma, \alpha)Mg^{24}$ also occurs directly.

The alpha-particles freed by the photodisintegration of some S^{32} nuclei are captured by other S^{32} nuclei to form A^{36}, the over-all result being

$$2\ S^{32} \rightarrow Si^{28} + A^{36} - 0.31\ \text{MeV}\,. \tag{98}$$

In addition some synthesis of Ca^{40}, Ti^{44}, and heavier nuclei in decreasing amounts occurs. However, as long as Si^{28} remains refractory, equation (98) is the primary process and Si^{28} and Ar^{36} are the major products. Early in this stage of burning S^{32} is more abundant than the first Ar^{36} produced and captures the main bulk of the alpha-particles. Furthermore, equation (C9) shows that capture rates decrease with increasing charge number because of the increasing Coulomb repulsion. Thus the synthesis tails off rapidly with increasing atomic mass. It might be argued that Ar^{36} eventually becomes more abundant than S^{32}, and at the end of this stage of the burning produces a significant amount of Ca^{40}, etc. However, if one applies equation (1) of Hoyle and Fowler (1960) to process (98) it is found that the equilibrium ratios are $S^{32}/Si^{28} = S^{32}/Ar^{36} \sim 2$ in the interval $2.5 < T_9 < 3$, i.e., only one-half of the S^{32} is converted into $Si^{28} + A^{36}$. In a sense, S^{32} and Ar^{36} survive beyond the temperature at which they would otherwise be

photodisintegrated just because they come into equilibrium through (γ, α) or $(\gamma, 2p\ 2n)$ and (α, γ) with refractory Si^{28}. We note that $Ar^{36}(\gamma, \alpha)S^{32} - 6.64$ MeV. Studies of equilibria such as $3\ S^{32} \rightarrow 2\ Si^{28} + Ca^{40}$, $4\ S^{32} \rightarrow 3\ Si^{28} + Ti^{44}$, etc., yield amounts of Ca^{40}, Ti^{44} comparable to but less than Ar^{36}. The time scale is short at this point, and it is doubtful if equilibrium is reached.

Above $T_9 \sim 3$ the photodisintegration of Si^{28} sets in through $Si^{28}(\gamma, 2p\ 2n)Mg^{24}$. Mg^{24} has an alpha-particle binding energy equal to 9.31 MeV, or 0.68 MeV less than Si^{28}. The result is that the Mg^{24} lifetime to effective alpha-particle loss is less than 10 per cent that of Si^{28}. Ne^{20}, O^{16} and C^{12} have even shorter lifetimes and Be^{8} is spontaneously unstable to alpha-particle breakup. Thus the photodisintegration of each Si^{28} nucleus results in complete breakdown and the copious production of alpha-particles. When Si^{28} begins to break up, the restriction which made equation (98) the major process is removed, and in fact S^{32} and Ar^{36} are also subject to complete alpha breakup. The time scale for the breakup of all components, Si^{28}, S^{32}, and Ar^{36}, is determined primarily by the Si^{28} lifetime given by equation (97).

The alpha-particles resulting from the breakdown of some nuclei will be captured by others to form heavier nuclei. As long as energy is gained in the process the "equilibrium" will shift toward greater atomic weight, A. The synthesis will mainly involve the stable nuclei with $A = 2Z = 2N = 4n$ (n an integer) and will terminate when the most stable nucleus of this form is reached. This presupposes that beta-processes, electron capture, or positron emission, are not rapid enough to permit transformations to the even more stable nuclei having several more neutrons than protons. This point will be elaborated later in this discussion. We also emphasize once again that protons and neutrons will be involved in the breakdown and buildup process and that correspondingly other nuclei than those with $A = 4n$, with n an integer, will be involved. We neglect this complication since the general results will be much the same as for a pure α-process. Furthermore, if beta-processes do not occur, then the total number of protons and neutrons, free and bound, remain equal and nuclei with $Z = N$ will appear most abundantly in the synthesis processes.

Until recently there has been some question concerning the identity of the most stable nucleus with $Z = N$. Of those for which direct experimental information was available up till late in 1963, Fe^{52} is the most stable with a mean binding energy per nucleon equal to 8.609 MeV. However, it was realized that Ni^{56} is almost certainly even more stable since it is doubly magic, having both neutron and proton shells closed at $Z = N = 28$. An estimate based on beta-decay systematics was given by Way, Gove, McGinnis, and Nakasima (1961) and yielded a mean binding energy of 8.644 MeV per nucleon on the basis that the Ni^{56}-Co^{56} mass-energy difference is $\sim$2.1 MeV. This estimate has been found to be remarkably accurate in two experimental determinations of this mass-energy difference. Hoot, Kondo, and Rickey (1963) find Ni^{56}-$Co^{56} = 2.092 \pm 0.024$ MeV, while Miller, Kavanagh, and Goldring (1963) find 2.114 ± 0.0222 MeV, yielding a mean value 2.103 ± 0.016 MeV.

It must be shown that the alpha-particle capture rates are rapid enough up to Ni^{56} and somewhat beyond so that an equilibrium distribution will be formed around Ni^{56} as the most abundant nucleus. Calculation of these capture rates required a knowledge of the number density n_α for alpha-particles. An equilibrium calculation based on

$$\gamma + (Z,\ A) \rightleftarrows \frac{A}{4}\,He^4 \tag{99}$$

will not be wide of the mark as the synthesis changes the most abundant nuclear species from Si^{28} through (Z, A) to Ni^{56}. This assumes that enough Si^{28} remains throughout this stage to maintain the equilibrium abundance of alpha-particles. We calculate the alpha-abundance from the quasi-equilibrium equation for those nuclei which have reached a

stationary maximum abundance at a given time. Equation (1) of Hoyle and Fowler (1960) yields, for $x_A \sim 1$, and $\log \rho = 4.7 + 3 \log T_9$

$$\log n_\alpha \sim 34.7 - \frac{1}{A}(21 + 10 \log A) + \tfrac{3}{2}\left(1 + \frac{4}{A}\right) \log T_9 - \frac{5.04}{T_9} \bar{Q}_\alpha$$

$$\sim 34 + 1.6 \log T_9 - \frac{5.04}{T_9} \bar{Q}_\alpha, \qquad 32 \leq A \leq 56, \tag{100}$$

where $\bar{Q}_\alpha$ is the *average* binding energy for alpha-particles in (Z, A). For example $\bar{Q}_\alpha = 5.67$ MeV for S^{32} and 6.14 MeV for Fe^{52}. The result is $\log n_\alpha \sim 26$ or $\rho x_\alpha \sim 10^3$ during the α-process approximately independent of (Z, A). With $\log f_o \langle \beta \rangle_l \sim 0$, equations (C66) and (100) yield

$$\log \tau_{\alpha\gamma}(Z, A) \sim -19 - 3.6\, Z^{1/2} - \tfrac{4}{3} \log 2Z + 31/T_9 + 4.9\, Z^{2/3}/T_9^{1/3}. \tag{101}$$

For $Fe^{52}(\alpha, \gamma)Ni^{56}$ equation (101) gives $\tau_{\alpha\gamma} \sim 0.5$ sec at $T_9 \sim 3$ which is short compared to the Si^{28} breakup period. It is probably preferable to use (C60′), rather than (C60), in (C66) in which case $\tau_{\alpha\gamma} \sim 10$ sec; and this is still short compared to the breakup period of Si^{28}.

Thus the rate of breakdown and buildup through the α-process under discussion is determined principally by $\tau_{\gamma p}(Si^{28})$. If we exclude the ultimate beta transitions which follow the formation of Ni^{56}, then the over-all transformations involving only the $A = 2Z = 2N = 4n$ nuclei can be represented by

$$2\ Si^{28} \rightarrow Ni^{56} + 0.196 \text{ MeV per nucleon } (1.89 \times 10^{17} \text{ erg gm}^{-1}). \tag{102}$$

If we recall that some S^{32}, Ar^{36}, etc., have been produced by processes (86) and (98), then the net energy release during this stage is only 1.6×10^{17} erg gm^{-1}. From the arguments just presented it will be clear then that the rate of energy generation in process (102) is from equation (C71) with $A_1 = 0$,

$$\log \epsilon_{\alpha\text{-proc}} = \log xq/\tau_{\gamma p}(Si^{28}) = +34.7 + \log x - 3.36/T_9^{1/3} - 58.3/T_9, \tag{103}$$

where $q \approx 1.6 \times 10^{17}$ erg gm^{-1} and x represents the time-dependent abundance of all three of the nuclei S^{32}, Si^{28}, and Ar^{36} which are produced in processes (86) and (98) and are transformed into heavier nuclei near Ni^{56} as x varies from 1 to 0.

The time scale for the α-process to Ni^{56} can now be calculated in the customary way. We equate $\log \epsilon_{\alpha\text{-proc}}$ to $\log dU_\nu/dt = 10.6 + 6 \log T_9$ from equation (21) corrected for $T_9 \sim 3$ to 4 and find $x = 1$, 0.1, and 0.01 at $T_9 = 3.1$, 3.3, and 3.5, respectively. The burning occurs mainly between $T_9 = 3.1$ and 3.2 so that

$$\Delta t_{\alpha\text{-proc}} = 1.6 \times 10^{17}/4 \times 10^{10}\, T_9^6 \approx 4000 \text{ sec}. \tag{104}$$

This result agrees approximately with that found in equation (96). The essential point is that nuclear processes, which have been discussed in detail, produce the energy emitted by the star in the form of neutrinos up to $T_9 = 3.5$.

VII. THE EQUILIBRIUM PROCESS IN MASSIVE STARS

The formation through the α-process of the most stable nuclei in a medium, where the total numbers of protons and neutrons are equal, temporarily terminates abundance changes and energy generation at $T_9 = 3.5$. The α-process comes to an end. Energy loss by neutrino emission leads to a mild contraction of the stellar core and a slight rise in temperature and density. At this point beta-processes, positron emission and electron

capture, begin to play a role in the transformation to nuclei which have a greater number of neutrons than protons, e.g., Fe^{56}, and which are more stable than those with equal numbers, e.g., Ni^{56}. It is thus necessary to investigate the rate of these beta-processes, given in Appendix A, for the specific nuclei involved at this stage of the nucleosynthesis.

The pertinent question is this: In the time scale permitted by the neutrino losses, how far will the beta-processes go in producing nuclei with a neutron excess? In other words, in the "equilibrium" or *e*-process in which the iron-group abundances are finally determined, does the material come to the complete equilibrium corresponding to the ambient temperature and density or does the limited reaction rate of the beta-processes impose an additional constraint? It has been emphasized by B²FH (1957) and Hoyle and Fowler (1960) that the abundances of the iron-group nuclei found in the solar system (particularly, terrestrial isotopic abundances) show definite effects of such a rate limitation. We take it that solar-system iron-group nuclei are typical of nuclei produced in the *e*-process just outside the imploding central regions of Type II supernovae. These nuclei reside in the material which is swept out by the explosion of mantle and envelope to be discussed later. This explosion occurs in such a short time interval that the quasi-equilibrium abundances reached before the implosion-explosion are essentially unchanged. In what follows we will find a most significant connection between iron-group abundances and the time scale set by neutrino losses during the stellar stage just prior to core implosion and mantle-envelope explosion.

The measure of beta-interaction rates appropriate for our present purposes is the rate of change of one-half the average neutron-proton difference per nucleus. This can be calculated from

$$\tfrac{1}{2}\frac{d(\bar{N}-\bar{Z})}{dt}=\frac{d\bar{N}}{dt}=-\frac{d\bar{Z}}{dt}=\frac{\Sigma\pm n(N,Z)/\tau(N,Z)}{\Sigma n(N,Z)}, \tag{105}$$

where $\bar{N}=\Sigma Nn(N,Z)/\Sigma n(N,Z)$, $\bar{Z}=\Sigma Zn(N,Z)/\Sigma n(N,Z)$, $n(N,Z)$ is the number of nuclei containing N neutrons and Z protons, and $\tau(N,Z)$ is the mean lifetime of these nuclei for beta-interactions. (We use here the notation $n[N,Z]=n[A-Z,Z]$ rather than $n[A,Z]$ for obvious reasons.) The positive sign is to be used for positron emission or electron capture and the negative sign for electron emission or positron capture. The problem at hand involves first of all the calculation of $n(N,Z)$ as a function of the ratio of protons to neutrons, $\bar{Z}/\bar{N}$. This is a task of considerable magnitude if temperature and density are also varied, and a computer program to accomplish the purpose has been undertaken by Clifford and Tayler (1964) at Cambridge University. Here we will fix on a temperature and density using some of their results and will discuss only in a general way what is essentially the "approach" to equilibrium in stellar nuclear processes.

Since B²FH (1957) found that equilibrium calculations at $T_9=3.8$ gave excellent agreement with solar-system iron-group abundances, and since this temperature is just slightly above that at which the pure α-process ends, we will use this value in what follows. Then in a steller core with effective mass $M_c=20\,M_\odot$ we have on interpolation in Table 3, $\rho_6=3.1$, $N_e=4.8\times10^{23}$ gm^{-1}, $n_e=1.50\times10^{30}$ cm^{-3}, $N_-=3.9\times10^{23}$ electrons gm^{-1}, $n_-=1.22\times10^{30}$ electrons cm^{-3}, $N_+=0.9\times10^{23}$ positrons gm^{-1}, and $n_+=0.28\times10^{30}$ positrons cm^{-3}. The electron-positron numbers will change slightly as Ni^{56} changes to Fe^{56} as the dominant nucleus during the operation of the *e*-process. The double entry for $z=mc_e^2/kT=1.5$, $T_9=3.95$ in Table 3 illustrates the change in N_e, for example.

The termination of the α-process at $T_9=3.5$ followed by a slight rise in temperature and density upon contraction brings the material to $T_9=3.8$ with $\bar{Z}/\bar{N}=1$ and Ni^{56} the most abundant nucleus. Beta-processes will now lower $\bar{Z}/\bar{N}$. For substitution in equation (105) one thus needs relative values for n(N, Z) for a series of values for $\bar{Z}/\bar{N}$ at $T_9=3.8$. A fixed value for $\bar{Z}/\bar{N}$ serves as a constraint on the equilibrium process in the manner described by B²FH (1957; see pp. 577, 578). Dr. Tayler and Mr. Clifford

have carried out abundance calculations for $\bar{Z}/\bar{N} = 1.00$, 0.975, 0.950, 0.925, 0.900, 0.875, 0.8725, 0.870, 0.865, and 0.860 as part of their general program. The interval between successive values corresponds to $\Delta\bar{N} = 0.4$ neutrons per nucleus when $\Delta(\bar{Z}/\bar{N}) = 0.025$. A total change of ~ 2 neutrons per nucleus is thus covered as expected for the typical case ${}_{28}Ni_{28}^{56} \rightarrow {}_{26}Fe_{30}^{56}$. Table 5 lists the principal components of the material for various values of $\bar{Z}/\bar{N}$.

Methods for calculations of the $\tau(N, Z)$ under stellar conditions are described in Appendix A. It will be clear that electron capture and positron emission are the important beta-processes since the trend in stability is toward nuclei with a neutron excess. Under terrestrial laboratory conditions positron emission is more rapid than electron capture if sufficient energy is available in the nuclear transformation to produce the positron rest mass and give the positron kinetic energy at least comparable to its rest-mass equivalent energy. However, in dense stellar interiors the electron density at the nucleus is considerably greater than in the undisturbed atom so that the rate of electron capture is greatly enhanced. This effect is discussed in detail in Appendix A. The result is that the proton-to-neutron change in radioactive nuclei which normally capture electrons or emit positrons is increased in rate and even stable nuclei, e.g., Ni^{58}, have fairly short lifetimes for capture of electrons having high energy in the tail of the thermal energy distribution.

Reference to Table 5 indicates that the nuclei which make important contributions in equation (105) are: Ni^{56} (2×10^3 sec), Ni^{57} (2×10^3 sec), Ni^{58} (5×10^4 sec), and Fe^{54} (4×10^4 sec). The proton (4×10^3 sec), Co^{55} (2×10^3 sec), and Fe^{55} (10^4 sec) also contribute. In general the transformation from $\bar{Z}/\bar{N} = 1.00$ to smaller values can be followed in Figure 10. At $\bar{Z}/\bar{N} = 1$ the principal constituents are Ni^{56}, Ni^{57}, and Co^{55}. These capture electrons or emit positrons to become Co^{56}, Co^{57}, and Fe^{55}, respectively. The Co^{56} immediately becomes Fe^{54} and Ni^{58} through fast nuclear processes since $2\ Co^{56} \rightarrow Fe^{54} + Ni^{58} + 4.45$ MeV. Fe^{54} and Ni^{58} capture electrons to become Mn^{54} and

TABLE 5

A. THE APPROACH TO EQUILIBRIUM AT $T = 3.8 \times 10^9$, $\rho = 3.1 \times 10^6$, $M_c = 20\ M_\odot$, $M \approx 30\ M_\odot$

	$\frac{1}{4}(\bar{N}-\bar{Z})$	$\bar{Z}/\bar{N}$	$\log \frac{n_p/n_n}{\theta}$	Time (10^4 sec)	
1.....	0.0	1.000	8.62		0.0
				0.1	
2.....	0.4	0.975	7.36		0.1
				0.1	
3.....	0.8	0.950	6.61		0.2
				0.2	
4.....	1.2	0.925	5.18		0.4
				0.8	
5.....	1.6	0.900	4.04		1.2
				1.6	
6.....	2.0	0.875	2.94		2.8
				0.4	
7.....	2.04	0.8725	2.74		3.2
				0.5	
8.....	2.08	0.870	2.48		3.7
				18.0 { 1.3	
9.....	2.16	0.865	1.76		5.0
				3.0	
10.....	2.24	0.860	1.17		8.0
				12.8	
11.....	2.40	0.850	.....		20.8

TABLE 5—*Continued*

B. ABUNDANCE IN PER CENT BY MASS

(Naturally Radioactive Nuclei in Parentheses)

Nucleus	(Co^{55})	(Ni^{56})	(Ni^{57})	Ni^{58}	Fe^{54}	(Fe^{55})	Fe^{56}	Fe^{57}	Fe^{58}
Product	(Fe^{55})Mn^{55}	(Co^{56})Fe^{56}	(Co^{57})Fe^{57}	(Co^{58})	(Mn^{54})	Mn^{55}	(Mn^{56})	.....	.....
Energy diff. (MeV)	3.46	2.10	3.24	−0.38	−0.69	0.23	−3.71	.....	.....
τ_{star} (sec)	2×10^{3}	2×10^{3}	2×10^{3}	5×10^{4}	4×10^{4}	10^{4}	10^{8}	.....	.....
1	3.3	89.1	2.9	0.7	1.7	3×10^{-3}	6×10^{-5}	.....	.....
2	8.7	54.3	7.5	7.9	19.3	0.2	1×10^{-2}	.....	.....
3	8.2	21.4	6.8	16.7	43.4	0.9	0.1	.....	.....
4	2.1	1.0	1.5	18.5	60.1	6.0	4.1	2×10^{-3}	.....
5	0.3	3×10^{-2}	0.2	8.3	34.0	12.0	29.2	6×10^{-2}	4×10^{-3}
6	2×10^{-2}	5×10^{-4}	9×10^{-3}	1.2	6.8	7.9	62.9	0.4	0.1
7	8×10^{-3}	2×10^{-4}	5×10^{-3}	0.8	4.7	6.7	66.2	0.5	0.2
8	4×10^{-3}	.....	2×10^{-3}	0.4	2.8	5.3	69.2	0.7	0.3
9	4×10^{-4}	.....	2×10^{-4}	0.1	0.6	2.5	70.5	1.5	1.2
10	.....	.....	.....	2×10^{-2}	0.2	1.2	64.5	2.7	4.0

Co^{58} which change by fast nuclear processes to Cr^{52}, Fe^{56}, and Ni^{60}. Fe^{55} and Co^{57} produce Mn^{55} and Fe^{57}. Eventually nuclear processes produce the equilibrium abundances which mainly reside in the stable nuclei which form the shaded "steps" in Figure 10, namely, $Cr^{52,53,54}$, Mn^{55}, $Fe^{56,57,58}$, Co^{59}, and $Ni^{60,61,62}$ (the last two nuclei are not shown). Some material remains as stable Fe^{54} and Ni^{58} and also as stable Cr^{50} (not shown) and the other rare iron-group nuclei.

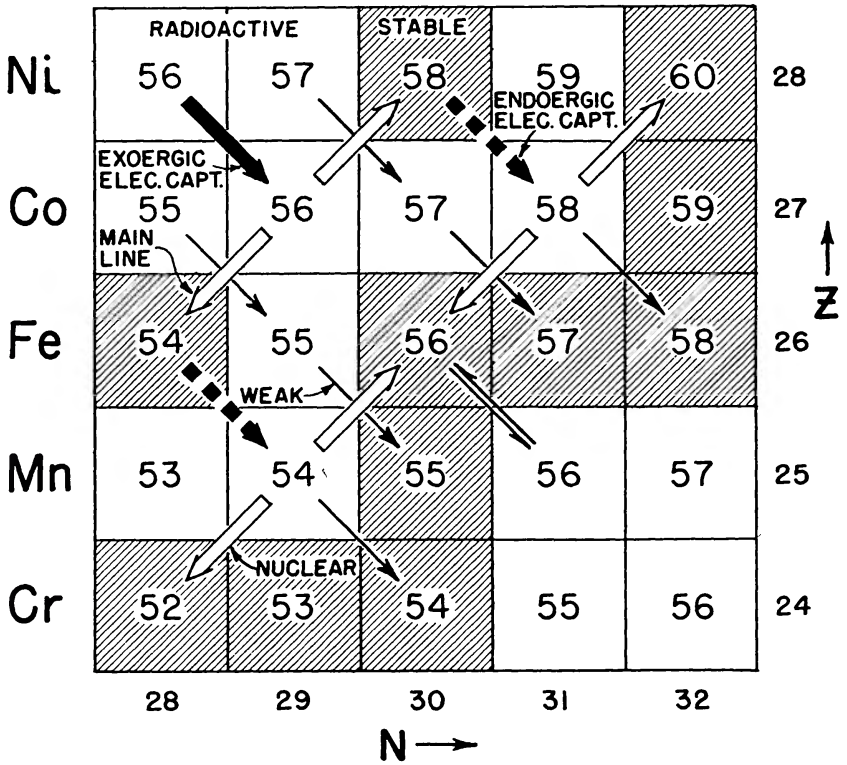

FIG. 10.—The flow of nuclear material in the N, Z-plane during the equilibrium or e-process showing the effects of the slow beta-interactions and the rapid nuclear interactions. The α-process results mainly in the production of Ni^{56} with about 10 per cent Co^{55}, Ni^{57}, Fe^{54}, and Fe^{52} (not shown).

Table 5 gives the time intervals calculated using equation (105) for the changes through $\bar{Z}/\bar{N} = 1.00, 0.975, \ldots,$ to 0.860, and the total time to each value. Table 5 also gives the quantity $\theta = \log_{10} n_p/n_n$, the logarithm to the base 10 of the ratio of densities of free protons to free neutrons external to the complex nuclei. As pointed out by B²FH (1957) equilibrium calculations can be made quite simply using θ as a parameter. It will be clear, however, that $\bar{Z}/\bar{N}$ is the more significant parameter. The computer program of Clifford and Tayler (1964) essentially finds the values of θ which yield the chosen values of $\bar{Z}/\bar{N}$ and calculates the corresponding equilibrium abundances. It will be noted immediately that, as expected, very large ratios of free protons to free neutrons are required external to the complex nuclei to maintain the larger values for $\bar{Z}/\bar{N}$, e.g., $\theta = 8.62$ for $\bar{Z}/\bar{N} = 1.00$. In simple physical terms a dense atmosphere of protons is necessary to prevent the nuclei with $Z = N$ from decaying to the more stable nuclei with $Z < N$. The electrostatic repulsion between protons in the nucleus which leads to increased stability for $Z < N$ is seen to have a powerful effect.

TABLE 6

IRON ISOTOPES—PER CENT OF TOTAL *e*-PROCESS ABUNDANCE BY MASS

($M_c = 20\ M_\odot$, $M \approx 30\ M_\odot$)

$\bar{Z}/\bar{N}$	log n_p/n_n	Fe^{54}	Fe^{56}	Fe^{57}	Fe^{58}	Electron Capture Time (10^4 sec)
1.000	8.6	1.7	89.1	2.9	0.0	0.0
0.950	6.6	43.4	21.9	7.2	0.0	0.2
0.900	4.0	34.0	29.6	4.7	0.04	1.2
0.872*	2.7	4.3	66.6	2.5	0.23	3.2
0.860	1.2	0.2	64.5	3.0	4.0	8.0
0.850	.....	.....	.....	.....	.....	20.8
Solar-terr values		4.2	67.2	1.6	0.25	

* Interpolated from calculated values at 0.8725 and 0.870.

B²FH (1957) found the optimum correspondence between solar system iron-group abundances and the calculated values for the case $T_9 = 3.8$ and $\theta = 2.5$ illustrated in their Figure IV, 1, on page 579. We have already seen that $T_9 = 3.8$ is reached naturally in the stellar and nuclear evolution under discussion. The new calculations of Clifford and Tayler (1964) yield optimum results at $\theta = 2.7$ which differs insignificantly from the B²FH values. Correspondingly $\bar{Z}/\bar{N} = 0.872$ and $\frac{1}{2}\Delta(\bar{N} - \bar{Z}) \approx 2.0$, showing that the beta-processes changed approximately two neutrons into protons in the transformation from material with Ni^{56} the most abundant nucleus to material with Fe^{56} the most abundant.

The correspondence between the observations and the calculations of Clifford and Tayler (1964) is illustrated for the stable iron isotopes $Fe^{54,56,57,58}$ in Table 6. The solar-terrestrial values are those found first by dividing the iron abundance by mass by the abundance of all the equilibrium process elements (V, Cr, Mn, Fe, Co, Ni) using the *solar* spectroscopic data given by Aller (1961). The resulting value 73 per cent was then divided among the iron isotopes according to the *terrestrial* isotopic abundance ratios. The chondritic iron abundance given by Suess and Urey (1956) is somewhat higher than

the solar value. This higher value can be obtained from the equilibrium-process calculations by employing a slightly lower value for the temperature without changing the isotope ratios significantly. The calculated values in Table 6 have been obtained from the abundances of Clifford and Tayler (1964) given in part in Table 5 by assigning all of the material at mass 56 to Fe^{56}, for example, on the basis that if the equilibrium process terminated at a given value for $\bar{Z}/\bar{N}$ then Ni^{56} and Co^{56} would subsequently decay to Fe^{56} and so forth.

The table shows that almost exact correspondence is obtained at $\bar{Z}/\bar{N} = 0.872$ or $\theta = \log n_p/n_n = 2.7$ as noted previously. The time required for the electron captures up to this point is seen to be 3.2×10^4 sec. This value holds for a star of mass $M \approx 30\ M\odot$ with core mass $M_c = 20\ M\odot$ where $T_9 = 3.8$ and $\rho_6 = 3.1$ are the assumed equilibrium conditions. In the calculations, positron emission, electron emission, and positron capture have been neglected relative to electron capture. The detailed treatment in Appendix A justifies this neglect. At still lower $\bar{Z}/\bar{N}$, as complete equilibrium is attained, all processes, in particular positron capture, must be considered. The time required for the fast nuclear reactions to re-establish equilibrium as the electron captures take place has also been neglected. This is justified since, for example, the lifetime of Co^{56} to Co^{56} $(\gamma, n)Co^{55} - 10.07$ MeV is $\sim 10^{-4}$ sec at $T_9 = 3.8$, $\rho_6 = 3.1$.

It will be noted that the time required for a given change in $\bar{Z}/\bar{N}$ or in $\frac{1}{2}(\bar{N} - \bar{Z})$ rapidly increases after $\bar{Z}/\bar{N} = 0.872$. Table 5 shows that the change 0.875–0.850 requires more than ten times the interval required for the change 0.900–0.875. Table 6 shows that the total time from 1.000 to 0.850 is more than six times that required to reach 0.872. Thus we are in position to reach an answer to the question posed in the second paragraph of this part of this paper. In the time scale permitted by the neutrino losses, how far will the beta-processes go in producing nuclei with a neutron excess?

To answer this question it is necessary to compute the neutrino time scale under the conditions of temperature and density which have been reached in a star with $M \approx 30\ M\odot$ when the beta-processes operate to change Ni^{56} and other $Z = N$ nuclei produced in the α-process to nuclei such as Fe^{56} with $\frac{1}{2}(N - Z) = 2$. In the Ni^{56}–Fe^{56} transformation the energy release is 6.6 MeV or 1.13×10^{17} erg gm^{-1} which is reduced to $\sim 10^{17}$ erg gm^{-1} by direct neutrino losses. At $T_9 = 3.8$ and $\rho_6 = 3.1$, $dU_\nu/dt \sim 10^{14}$ erg gm^{-1} sec^{-1} so the time scale is $t_\nu \sim 10^{17}/10^{14} \sim 1000$ sec ~ 17 min. This calculation underestimates t_ν. Some Ni^{56} begins to decay as soon as it is first produced at the beginning of the α-process. Thus an upper limit for t_ν is the sum of the interval for the α-process plus that for the Ni^{56}–Fe^{56} transformation. This sum is 4000 sec + 1000 sec = 5000 sec. As an intermediate value we tentatively adopt $t_\nu \sim 3000$ sec.

The value just adopted tentatively holds for the time scale at the center of the star. Since the neutrino loss decreases rapidly with decreasing temperature the time scale, from the considerations of section (k), Appendix C, will be somewhat longer throughout the central region in which the Ni^{56}–Fe^{56} transformation is taking place. Rough calculations lead us to adopt $t_\nu \sim 6000$ sec finally. The Ni^{56}–Fe^{56} transformation is relatively insensitive to temperature, and no correction is necessary.

Thus we find $t_\nu \sim 6000$ sec is considerably shorter than $t_e \sim 3 \times 10^4$ sec. However, it must be recalled that our calculations have been made for a particular example, $M \approx 30\ M\odot$ or $M_c = 20\ M\odot$, of the type of stars which Hoyle and Fowler (1960) suggested would evolve to become Type II supernovae, namely, stars for which $10\ M\odot < M < 50\ M\odot$. Return now to a perusal of equation (53) in Part III. This equation indicates that for a given temperature and polytropic structure the central density is proportional to $M_c^{-1/2}$. The neutrino loss rates per gram at a given temperature vary inversely with the density, while the electron capture rates vary almost directly as the density. The ratio of the neutrino-loss time scale to the electron capture time scale thus varies as ρ^2 or M_c^{-1}. We require larger ρ or smaller M_c. The two time scales can thus be brought into correspondence in a variety of ways. The lower range of stellar masses may well

have contributed relatively more e-process material than the higher range. Second, our choice of $M_c \approx (\frac{2}{3})\, M$ may be too large. Third, the numerical coefficient in our ρ, T-relation may be low.

Thus, it would seem that quite close correspondence in the time scales exists for $e^- + e^+ \rightarrow \nu + \bar{\nu}$ and for $Ni^{56} + 2e^- \rightarrow Fe^{56} + 2\nu$ with a universal Fermi interaction for these two types of beta-interactions if the stars in which solar system e-process material was produced had masses 10–50 $M_\odot$ as originally contemplated by Hoyle and Fowler (1960). All of the processes, resources, losses, and time scales discussed in Parts V–VII and VIII to follow are listed in Table 7 for $M \approx 30\, M_\odot$.

The point under discussion here can be sharpened by a consideration of the time scale if $e^- + e^+ \rightarrow \nu + \bar{\nu}$ was not operative. Photon losses in the interval $3 < T_9 < 4$ can be estimated to be $\sim 10^7$ erg gm^{-1} sec^{-1} rather than the value $\sim 10^{14}$ erg gm^{-1} sec^{-1} for

TABLE 7

NEUTRINO LOSS AND PHASE-CHANGE TIME INTERVALS
($M_c = 20\, M_\odot$, $M \approx 30\, M_\odot$)

Temperature	Process*	Nuclear Resources (erg gm^{-1})	Neutrino Loss (erg gm^{-1} sec^{-1})	Core Interval (sec)
$2 \rightarrow 3 \times 10^9$	$2\ O^{16} \rightarrow Si^{28} + He^4$	5×10^{17}	5×10^{12}	10^5
$3 \rightarrow 4 \times 10^9$	$2\ Si^{28} \rightarrow Ni^{56}$ (α)	2×10^{17}	6×10^{13}	5000
4×10^9	$Ni^{56} \rightarrow Fe^{56}$ (e)	10^{17}		
$4 \rightarrow 14 \times 10^9$	$Fe^{56} \rightarrow 13\ \alpha + 4n$	-2×10^{18}	5×10^{15}	
	$\alpha \rightarrow 2p + 2n$	-7×10^{18}	4×10^{16}	0.3 free fall

* For $Ni^{56} \rightarrow Fe^{56}$ effective interval $\sim$ 6000 sec.

dU_ν/dt. Thus the photon-loss time scale for Ni^{56} to Fe^{56} is $\sim 6 \times 10^{10}$ sec $\sim$ 2000 years or ample time for the beta-interactions to reduce $\bar{Z}/\bar{N}$ well below the last values tabulated in Tables 5 and 6. The result, as shown in Table 6, would be, among other things, an enhancement in Fe^{58} and a decrease in Fe^{54} completely in variance with the terrestrial ratio. Clearly the time scale was not this long. Photon losses by the stellar material were not competent to decrease the time scale to the necessary value. On the other hand the neutrino time scale set by assigning the universal Fermi interaction strength to the process $e^+ + e^- \rightarrow \nu + \bar{\nu}$ in the pre-supernova stage of massive stars is closely that required to match the electron capture times involved in the formation of the Fe-isotopes and the other iron group nuclei. The isotopic abundance ratios in any sample of terrestrial iron are circumstantial evidence for the universality of the beta interactions.

This much can be asserted with some certainty: *The terrestrial iron group isotopic abundance ratios strongly indicate the operation in massive stars of an energy loss mechanism having a loss rate of the same order of magnitude as that calculated for* $e^+ + e^- \rightarrow \nu + \bar{\nu}$ *on the basis of the universal Fermi interaction strength. If this process does not occur directly through the universal coupling then the Pinaev* (1963) *modification of the Urca process* (*process* [3] *in Part I*) *is probably the most likely alternative. It does not require universality in the weak interactions but has a somewhat smaller reaction rate than the direct pair annihilation.*

A comment on the ultimate values for $\bar{Z}/\bar{N}$ or $\theta = \log n_p/n_n$ reached when the beta-interactions are in complete equilibrium is in order at this point. B^{2}FH (1957) estimated $\theta = 1.4$ from a consideration of the equilibrium between free neutrons and free protons and electrons. This value is only an approximation at best. It does in principle cover

the equilibrium between free protons and free neutrons and positrons. The difficulty involves the fact that neutrinos and antineutrinos escape and do not enter into reverse reactions once produced. This means, among other things, that energy must be supplied to maintain equilibrium at a given density and temperature. Granted this energy supply the equilibrium will depend more on the properties of the heavy nuclei than on those of the free neutrons and protons. The electron-positron ratio will be given as calculated previously in this paper on the basis $\gamma \rightleftarrows e^+ + e^-$. Then when electron capture and positron emission are balanced exactly by positron capture and electron emission, equilibrium in the beta-interactions will have been reached. We found above that it was not necessary to carry the calculations this far. In principle this could be done but would of necessity include all beta-processes involving all nuclei and would be fairly complicated in detail.

The preceding analysis has been based on the assumption that a unique abundance distribution characteristic of a particular final value for $\bar{Z}/\bar{N}$ or θ can match the observations reasonably well. However, it has also become clear in the discussion that the value reached by $\bar{Z}/\bar{N}$ through beta-interactions depends on the time interval available for the e-process and thus on the mass of the pre-supernova stellar core. Hence, different abundance distributions are produced in supernovae of different masses and the solar system iron-group abundances represent an appropriate averaging over abundance distributions characteristic of a range of supernovae masses. We do not propose to carry out a detailed calculation along these lines at the present time but do wish to make some comments on the possibilities inherent in this line of attack.

Clifford and Tayler (1964) have confirmed the findings of B^{2}FH (1957) that the calculated results for θ near 2.7 yield too low values for the abundances of Cr^{50} and Ni^{58} by a factor of the order of 10. Averaging over a range of distributions characteristic of varying time scales may serve to correct this defect in the calculated results. Consider a mixed abundance distribution with contributions from low-mass supernovae (10–35 $M\odot$) and from high-mass supernovae (35–50 $M\odot$). The first contribution will dominate on the reasonable basis that the lower-mass stars are sufficiently greater in number such that a greater total mass has been processed in lower-mass supernovae than in those of higher mass. The major contribution will be characterized by a value for θ slightly lower than the unique value which gives the optimum fit as described above. Take $\bar{Z}/\bar{N} = 0.870$, $\theta = 2.48$, $\frac{1}{2}(\bar{N}/\bar{Z}) = 2.08$ as a possibility for this case. Then, for example, Fe^{58} will be somewhat greater than observed and Fe^{54} somewhat less.

Now dilute this abundance distribution with that from very massive supernovae ($\sim 10^3\ M\odot$) in which the time scale is not only too short for many beta-interactions to occur but is also too short for certain nuclear processes. As Ni^{56} decays to Co^{56} the nuclear processes will quickly convert the Co^{56} into the more stable nuclei having the same $N - Z$ value, namely, 2. These are Cr^{50}, Fe^{54}, and Ni^{58}. Zn^{62} with $N - Z = 2$ is not very stable and hence not very abundant at equilibrium. The conversion of the Co^{56} is mainly accomplished by the ejection of p and n from some Co^{56} nuclei and the addition of these p and n to others. As long as the numbers of free p and n are not changed this results in the mean molecular weight per nucleus remaining fixed at $\sim$56. Actually equilibrium calculations indicate that n_p (free protons) tends to decrease through capture so that the mean atomic weight $\bar{A}$ tends to increase for this reason. On the other hand the light nuclei Si^{28}, S^{32}, Ar^{36}, Ca^{40} can serve as seed nuclei for the synthesis of new iron-group nuclei by capturing p, n, α and the mean molecular weight in the iron group might thus be changed. However, the equilibrium abundance of these nuclei is too small for this process to be effective.

New iron-group nuclei can also be made by the formation of C^{12} from three alpha-particles followed by subsequent p, n, α captures. Because of the low equilibrium density of alpha-particles this process will be infrequent on short time scale. Another possibility, but also much too infrequent to be effective, is the complete photodisintegration of Co^{56}

nuclei into p, n, α with reassembly into nuclei which do not necessarily have $\bar{A} = 56$. Given a long enough time scale this process does operate to decrease $\bar{A}$ below 56. It would seem that nuclear processes which will change $\bar{A}$ are too slow when t_ν becomes very short. Thus complete equilibrium will not be reached and the transformation of the Co^{56} must keep $\bar{A} = 56$ or slightly increase it because of free proton capture. It will be clear that one Ni^{58} is needed for each Fe^{54} and three for each Cr^{50} if $\bar{A}$ remains fixed at 56, again neglecting Zn^{62}. As stated previously it can be reasonably expected that Ni^{58} and Fe^{54} will be the most abundant in the short time-scale distribution, with Cr^{50} enhanced over the abundance expected on a complete equilibrium calculation. Clearly the addition of such a contribution will tend to remedy the deficiency in Cr^{50}, Ni^{58}, and Fe^{54} previously mentioned. This is borne out by the calculations in Table 5 for $\bar{Z}/\bar{N} = 0.925$ where complete nuclear equilibrium is assumed, but even so the results show considerable enhancement in Ni^{58} and Fe^{54}. Furthermore, the addition of some Ni^{56} which has not decayed but which eventually becomes Fe^{56} will restore the Fe^{58}/Fe^{56} ratio to a value close to that observed. In fact, this dilution improves practically all ratios since with the notable exceptions of Cr^{50}, Fe^{54}, and Ni^{58} the calculated ratios to Fe^{56} are in general high by $\sim$50 per cent for $\theta = 2.48$. Rough calculations indicate that one part short time-scale distribution plus two parts long time-scale distribution will give improved agreement with the observations. Our basic conclusion previously reached is reinforced, but now it is necessary to postulate some e-process contribution from stars with M up to $\sim 10^3\, M_\odot$ as well as from $M \sim$ 10–50 $M_\odot$.

A general comment on the comparison of e-process calculations with iron-group elemental abundances is in order at this point. Isotopic abundances for a given element depend primarily on the ultimate value reached for $\bar{Z}/\bar{N}$ or for θ. We have stressed iron isotope abundances, computed versus observed, in this discussion. Similar results hold for the four isotopes of chromium. On the other hand, the general shape of the iron-group peak, as determined by *elemental* abundances depends primarily on the value for T_9, the temperature at equilibrium. The B^{2}FH (1957) choice, $T_9 = 3.8$, was determined by fitting to the solar spectroscopic values believed to be correct at that time. Meteoritic iron-group abundances seem to indicate a relatively greater iron abundance, i.e., a sharper iron-group peak. This can be obtained theoretically by choosing a slightly lower temperature. Conversely the choice of a higher temperature tends to flatten the peak. (See, however, the paper "The Iron Group Elements and the Equilibrium Process in Nucleosynthesis" presented by W. A. F. at the I.A.U. Symposium on "Abundance Determination from Stellar Spectra" held in Utrecht, August 10–14, 1964.)

It remains only to inquire whether beta-processes were fast enough during the run from Si^{28} to the iron-group nuclei with time scale $\sim$4000 sec to change $\bar{Z}/\bar{N}$ significantly from unity. In particular would ${}_{21}Sc_{21}^{42}$ ($\bar{\tau} = 1.0$ sec), ${}_{23}V_{23}^{46}$ ($\bar{\tau} = 0.6$ sec), ${}_{25}Mn_{25}^{50}$ ($\bar{\tau} = 0.4$ sec) or ${}_{27}Co_{27}^{54}$ ($\bar{\tau} = 0.3$ sec) be sufficiently abundant to bring about the necessary number of beta-transformations? We investigate this problem by assuming, for example, that V^{46} has its maximum abundance when the material is essentially equally divided between Ti^{44} and Cr^{48} on the way from S^{32} to the iron group nuclei. Then under equilibrium conditions

$$\log \frac{V^{46}}{Ti^{44} + Cr^{48}} = \log \frac{V^{46}}{2(Ti^{44}Cr^{48})^{1/2}} = \log \frac{\omega(46)}{2[\omega(44)\omega(48)]^{1/2}} - \frac{5.04}{T_9} \times 3.545 \tag{106}$$

$$= 0.77 - \frac{17.9}{T_9} = -4.8 \text{ at } T_9 = 3.2\,,$$

where $M(V^{46}) - \frac{1}{2} M(Ti^{44}) - \frac{1}{2} M(V^{48}) = 3.545$ MeV/c^2 and the ω's are statistical weight factors. Since $Ti^{44} + Cr^{48}$ will not constitute all of the material this is an upper limit on the V^{46} abundance. With $\bar{\tau}(V^{46}) = 0.6$ sec the effective processing time becomes

$>4 \times 10^4$ sec, say $\sim 10^5$ sec. This is to be compared with that portion of the time, say, $\sim 4 \times 10^2$ sec, when the material has maximum concentration near $A = 44$–48. This large discrepancy of 250 cannot be made up by the arguments involving $\rho^2 \propto M_c^{-1}$ advanced earlier in this section, and we conclude that $\bar{Z}/\bar{N} \approx 1$ up to $A = 56$.

VIII. CENTRAL CORE IMPLOSION

The production of the iron group nuclei, principally Fe^{56}, at $T_9 \sim 4$ exhausts the nuclear resources of a star. In fact, at higher temperatures the energy flow is reversed and endoergic photodisintegration replaces exoergic fusion. Because of the great stability of the alpha-particle, the iron-group nuclei are not immediately broken up into protons and neutrons. A preliminary stage occurs in which the nucleus (A, Z) is photodisintegrated according to

$$\gamma + (A, Z) \rightarrow \frac{Z}{2}\mathrm{He}^4 + (A - 2Z)n . \tag{107}$$

Through what follows calculations will be made for Fe^{56} for which equation (107) becomes

$$\gamma + \mathrm{Fe}^{56} \rightarrow 13\ \mathrm{He}^4 + 4n - 124.4\ \mathrm{MeV}\ (-\ 2.14 \times 10^{18}\ \mathrm{erg\ gm^{-1}}) . \tag{108}$$

Eventually even the alpha-particles are photodisintegrated according to

$$\gamma + \mathrm{He}^4 \rightarrow 2p + 2n - 28.3\ \mathrm{MeV}\ (-\ 6.82 \times 10^{18}\ \mathrm{erg\ gm^{-1}}) , \tag{109}$$

so that the complete photodisintegration can be represented by

$$\gamma + \mathrm{Fe}^{56} \rightarrow 26p + 30n - 492.3\ \mathrm{MeV}\ (-\ 8.48 \times 10^{18}\ \mathrm{erg\ gm^{-1}}) . \tag{110}$$

Even this breakdown is an oversimplification, but it is sufficient for most purposes. The energy losses are much more severe than the neutrino losses and must be made up from the gravitational-energy store of the star. This can only be done through an extremely rapid rise in density or, in other words, through the implosion of the central regions of the star affected by the nuclear photodisintegrations.

Eventually the stellar matter becomes degenerate, and the equations developed in this paper are no longer adequate. The final stage involves capture of the electrons by protons to form a neutron core. A consideration of the properties of such a core lies outside the scope of this paper. *Static* neutron stars have been considered by Oppenheimer and Volkoff (1939), Harrison, Wakano, and Wheeler (1958), Cameron (1959*a*), Salpeter (1960), Hamada and Salpeter (1961), Saakyan (1963), and Morton (1964).

A lower limit for the time of collapse arising from the photorefrigeration is set by the time for free fall. For this to be the case the sum of the mean photodisintegration times for Fe^{56} and subsequent products must be less than the free-fall time. At the start of the photodisintegrations at $T_9 \sim 4$ the use of equation (C22) indicates that the mean lifetimes of Fe^{56}, and the first few products are comparable to that calculated previously for Si^{28}, namely, 1 sec, so that the total time is at most 10 sec. As the process proceeds and the temperature rises, the individual times decrease markedly, the total time typically being the order of 10^{-6} sec at $T_9 = 7$. The free-fall times (see equation [B88], Appendix B) are given by

$$t_{ff} = \rho/\dot{\rho} = \frac{1}{(24\pi G\rho)^{1/2}} \approx \frac{446}{\rho^{1/2}}\ \mathrm{sec} . \tag{111}$$

At $T_9 = 4$, $\rho = 3.6 \times 10^6$ so that $t_{ff} \sim 0.2$ sec, while at $T_9 = 7$ we shall find $\rho \approx 3 \times 10^7$ so that $t_{ff} \sim 0.1$ sec. Thus the photodisintegration rate may be somewhat of a limitation at the start of the implosion but not at all as the temperature rises.

It is now proposed to make an approximate calculation of the ρ, T-path during the implosion resulting from the iron-to-helium-neutron phase change and part of the subsequent change to the proton-neutron phase. In this calculation we use equation (72) for dQ/dT. On the assumption that the implosion is too rapid for neutrino and photon losses to be appreciable, we would then set $dQ/dT = 0$ for an adiabatic process. However, it will be recalled that in the derivation of equation (72) from equation (56) we neglected the nuclear energy in equation (59) preferring to introduce this energy as a separate term at this point. When this is done the adiabatic equation becomes

$$\frac{dQ}{dT} + \frac{dQ_N}{dT} = 0 . \tag{112}$$

In this equation we have followed the usual convention in nuclear physics in taking changes in Q_N as positive for exoergic reactions and negative for endoergic reactions such as equations (108) and (109). On the basis that Q_N is a part of the internal energy U it would be preferable to use the opposite convention. The temperature derivative of Q_N will be calculated from the equilibrium abundances as a function of T as detailed below.

Conventions aside, it is important to realize that equation (112) with equation (72) for dQ/dT is the correct energy equation for each element of material even when acceleration up to free fall occurs. With initial conditions given by the hydrostatic equilibrium solutions before implosion, equation (72) will give the correct ρ, T-path when substituted in equation (112). We are interested primarily in that part of the core which implodes homologously. Homologous collapse occurs over the region in which the acceleration due to gravity, g, is linear in radial distance. It is well known that g starts linearly in all polytropes, flattens out to a maximum value, and then decreases. For $n = 3$ the maximum occurs at $r/R = 0.22$ or $M_r/M = 0.31$ where M_r is the mass interior to radius r. The linear relation holds to 20 per cent out to $M_r/M = 0.1$ so that approximately $\frac{1}{10}$ of the core collapses homologously along the same ρ, T-path. It is, of course, true that equation (112) does not include the work done by gravity in accelerating the material. Use of the dynamical equation

$$\rho \frac{d^2r}{dt^2} = -\frac{dp}{dr} - \rho \frac{GM_r}{r^2} \tag{113}$$

is required to calculate the dynamical energy of motion, $\frac{1}{2}\rho(dr/dt)^2$, imparted by gravity. Knowledge of the ρ, T-path and the equation of state of the material yields the p, ρ-path for use in equation (113). However, for our purposes equation (112) is sufficient for the calculation of the ρ, T-path of the homologously collapsing central regions of the core. This calculation will now be made for the two stages governed by reactions (108) and (109).

In the case of reaction (108)

$$\frac{Q_N}{Q'_{Fe}} = 1 - x_{Fe} , \tag{114}$$

with x_{Fe} equal to the abundance by mass of the iron-group elements centered on Fe^{56} and $Q'_{Fe} = -2.14 \times 10^{18}$ erg gm^{-1}. The prime on Q'_{Fe} is used to designate the partial breakdown of Fe into alpha-particles and neutrons. For the complete breakdown into protons and neutrons, $Q_{Fe} = -8.48 \times 10^{18}$ erg gm^{-1}. As reaction (108) proceeds and x_{Fe} decreases from ~ 1 to ~ 0 the equilibrium equation governing this reaction yields one relation between ρ and T for the collapsing material. By the use of equations (1) and (1′) in Hoyle and Fowler (1960) this relation is found to be

$$\ln \rho = 26.04 - \tfrac{17}{16} \ln(1 - x_{Fe}) + \tfrac{1}{16} \ln x_{Fe} + \tfrac{3}{2} \ln T_9 - \frac{90.2}{T_9} , \tag{115}$$

since $x_\alpha = \frac{13}{14}(1 - x_{56})$ and $x_n = \frac{1}{14}(1 - x_{56})$ with $x_{56} + x_\alpha + x_n = 1$. In terms of Briggs logarithms one has

$$\log \rho = 11.32 - \tfrac{17}{16}\log(1 - x_{\mathrm{Fe}}) + \tfrac{1}{16}\log x_{\mathrm{Fe}} + \tfrac{3}{2}\log T_9 - \frac{39.17}{T_9}. \tag{116}$$

With the substitution of equation (114) the equation in Naperian logarithms becomes

$$\ln \rho = 26.04 - \tfrac{17}{16}\ln \frac{Q_{\mathrm{N}}}{Q'_{\mathrm{Fe}}} + \tfrac{1}{16}\ln\left(1 - \frac{Q_{\mathrm{N}}}{Q'_{\mathrm{Fe}}}\right) + \tfrac{3}{2}\ln T_9 - \frac{90.2}{T_9}. \tag{117}$$

Differentiation yields

$$\frac{d \ln \rho}{d \ln T} = \frac{d \ln \rho}{d \ln T_9} = -\frac{1}{\varphi(Q_{\mathrm{N}})}\frac{d \ln Q_{\mathrm{N}}}{d \ln T_9} + \tfrac{3}{2} + \frac{90.2}{T_9}, \tag{118}$$

where

$$\varphi(Q_{\mathrm{N}}) = (Q'_{\mathrm{Fe}} - Q_{\mathrm{N}})/(\tfrac{17}{16}Q'_{\mathrm{Fe}} - Q_{\mathrm{N}}) = x_{\mathrm{Fe}}/(x_{\mathrm{Fe}} + \tfrac{1}{16}).$$

At this point it is convenient to set the term $d \ln Q_{\mathrm{N}}/d \ln T_9 = d \ln Q_{\mathrm{N}}/d \ln T = (T/Q_{\mathrm{N}})\, d Q_{\mathrm{N}}/dT$ in equation (118) equal to $-(T/Q_{\mathrm{N}})\, dQ/dT$ using equation (112) and then to substitute for dQ/dT by the use of equation (72) with the approximation that the nuclear term containing kN_n can be neglected. After some algebraic manipulation it is found that

$$\frac{d \ln \rho}{d \ln T} = \frac{-[\tfrac{3}{2} + (90.2 \times 10^9/T)](Q_{\mathrm{N}}/T)\varphi(Q_{\mathrm{N}}) + kN_e c'_v + 4aT^3/\rho}{-(Q_{\mathrm{N}}/T)\varphi(Q_{\mathrm{N}}) + kN_e c_v'' + 4aT^3/3\rho}, \tag{119}$$

where

$$c'_v = c_v + (x + z)^2\left(\frac{2N_1}{N_e}\right)^2, \tag{120}$$

$$c''_v = 1 + (x + z)\left(\frac{2N_1}{N_e}\right)^2. \tag{121}$$

Equations (117) and (119), respectively, give a relation between ρ, T and the slope of the ρ, T-curve as a function of the independent variable Q_{N} which runs from ~ 0 to $\sim Q'_{\mathrm{Fe}}$ as the collapse proceeds. Thus the ρ, T-curve can be constructed by numerical methods, and this has been done approximately with the results given in Table 4 and illustrated in Figures 5 and 6 ($6 < T_9 < 9$). Fifty per cent of the Fe^{56} is disintegrated at $T_9 = 7.45$ $\log \rho = 7.65$ while only 1 per cent remains at $T_9 = 9.0$, $\log \rho = 8.3$. In general the behavior of the ρ, T-curve discussed by Hoyle and Fowler (1960) is followed.

A similar analysis of reaction (109) leads to the following equations:

$$\frac{Q_{\mathrm{N}}}{Q'_\alpha} = 1 - \tfrac{14}{13}x_\alpha, \tag{122}$$

with $Q'_\alpha = \frac{13}{14}Q_\alpha = -6.34 \times 10^{18}$ erg gm^{-1}. The maximum value for the fractional abundance of helium after completion of reaction (108) is $x_\alpha = \frac{13}{14}$. In our notation $Q_{\mathrm{Fe}} = Q'_{\mathrm{Fe}} + Q'_\alpha = -8.48 \times 10^{18}$ erg gm^{-1}. Then

$$\ln \rho = 22.29 - \tfrac{2}{3}\ln\left(\tfrac{13}{28} - \frac{x_\alpha}{2}\right)\left(\tfrac{15}{28} - \frac{x_\alpha}{2}\right) + \tfrac{1}{3}\ln x_\alpha + \tfrac{3}{2}\ln T_9 - \frac{109.3}{T_9} \tag{123}$$

$$= 23.29 - \tfrac{2}{3}\ln\frac{Q_{\mathrm{N}}}{Q'_\alpha}\left(\frac{Q_{\mathrm{N}}}{Q'_\alpha} + \tfrac{2}{13}\right) + \tfrac{1}{3}\ln\left(1 - \frac{Q_{\mathrm{N}}}{Q'_\alpha}\right) + \tfrac{3}{2}\ln T_9 - \frac{109.3}{T_9}, \tag{124}$$

or

$$\log\rho = 10.13 - \tfrac{2}{3}\log\frac{Q_N}{Q'_a}\left(\frac{Q_N}{Q'_a}+\tfrac{2}{13}\right)+\tfrac{1}{3}\log\left(1-\frac{Q_N}{Q'_a}\right)+\tfrac{3}{2}\log T_9 - \frac{47.5}{T_9}, \quad (125)$$

$$\frac{d\ln\rho}{d\ln T}=\frac{d\ln\rho}{d\ln T_9}=-\frac{1}{\psi(Q_N)}\frac{d\ln Q_N}{d\ln T_9}+\tfrac{3}{2}+\frac{109.3}{T_9}, \quad (126)$$

where

$$\psi(Q_N) = 3(Q'_a - Q_N)(2Q'_a + 13Q_N)/(4Q'^2_a + 50Q'_aQ_N - 39Q_N^2), \quad (127)$$

and finally

$$-\frac{d\ln\rho}{d\ln T}=\frac{-[\tfrac{3}{2}+(109.3\times 10^9/T)](Q_N/T)\psi(Q_N)+kN_ec'_v+4aT^3/\rho}{-(Q_N/T)\psi(Q_N)+kN_ec''_v+4aT^3/3\rho}. \quad (128)$$

The ρ, T-curve up to $Q_N = 0.2\ Q'_a$ has been constructed approximately with the results given in Table 4 and illustrated in Figures 5 and 6 ($T_9 > 9$). The material becomes relativistically degenerate at $T_9 \sim 15$, $\log\rho \sim 9.5$. The curve for relativistic degeneracy is given approximately by $\rho = 10^6\ T_9^3$ gm cm^{-3} by equation (B140) of Appendix B. Table 4 also includes a column for $dQ/dT = -dQ_N/dT$ during implosion calculated using equation (112). The neutrino loss dU_ν/dt is given for comparison. The results are illustrated in Figure 9 for $T_9 > 6$.

Figures 5 and 6 show that core collapse begins at $\rho \sim 3 \times 10^7$ gm cm^{-3}. The collapse time can be estimated approximately by use of the free-fall equation (B88) given in Appendix B. If the e-folding time for r (or $\rho^{1/3} \propto T$) is employed this equation yields $\tau_{ff} \approx 1338\ \rho^{-1/2}$ sec ~ 0.3 sec. Thus the central core implosion is very fast indeed. In fact, $\Delta T_9 \sim 1$ requires only the order of $\sim$0.1 sec so that dU_ν/dt in Figure 9 for $T_9 > 6$ should be multiplied by $\sim$0.1 for comparison with $dQ/dT = -dQ_N/dT$.

IX. MANTLE AND ENVELOPE EXPLOSION

The implosion of the central portion of the stellar core described in Part VIII leads to the detonation and ejection of the outer regions of the star. This subject has been previously discussed by Hoyle and Fowler (1960), and the discussion to follow constitutes a revision based primarily on the effects of neutrino losses in speeding up the pre-supernova evolution of the central regions relative to the main bulk of the star.

The effect of neutrino losses must at first tend to prevent the temperature from rising in the central regions. The star can moderate the losses by growing an isothermal central region in the core. However, it is known that in non-degenerate conditions such an isothermal region cannot contain more than about 10 per cent of the total mass. This was shown originally by Schönberg and Chandrasekhar (1942) and has been confirmed in recent years by other workers, using numerical methods. The same result can, moreover, be demonstrated analytically. We shall therefore regard the discussion of Parts VII and VIII as applying to an *inner core* of mass $\sim$0.1 M. It is in this region that the iron-group elements are built. The central part of this region implodes as described in Part VIII while an overlying shell is swept outward in the subsequent explosion resulting in the distribution of the iron-group elements (Part VII) into the interstellar medium.

A considerable fraction of the outer region of the star consists of potentially explosive O^{16}. A precise computation of the early, pre-neutrino, evolution is necessary to determine the exact amount of O^{16}. It is suggested that it will correspond approximately to the convective zones that must develop during H and He burning. Such zones have the effect of synthesizing and mixing, first He^4 and then O^{16}, through a substantial fraction of the stellar mass. For the fairly massive stars (10–50 $M_\odot$) under consideration in this paper the convective zones are large, and throughout this paper we have assumed the

convective core mass to be $\frac{2}{3}$ M and the unevolved envelope mass to be $\frac{1}{3}$ M. When an inner core with mass 0.1 M develops, this leaves 0.57 M for what we will call the mantle of the core. Thus the structure of the star can be taken to be as follows:

Inner core of rapidly evolving material.....	$\sim 0.1\ M$
Mantle composed of O^{16}.....	$\sim 0.57\ M$
Outer shell composed of original H and He.....	$\sim 0.33\ M$

These regions are illustrated in Figure 11 for various stages of a supernova event.

When the inner core has grown to $\sim 0.1\ M$, and an isothermal structure can no longer be maintained, the central temperature rises again. Neutrino losses produce a situation

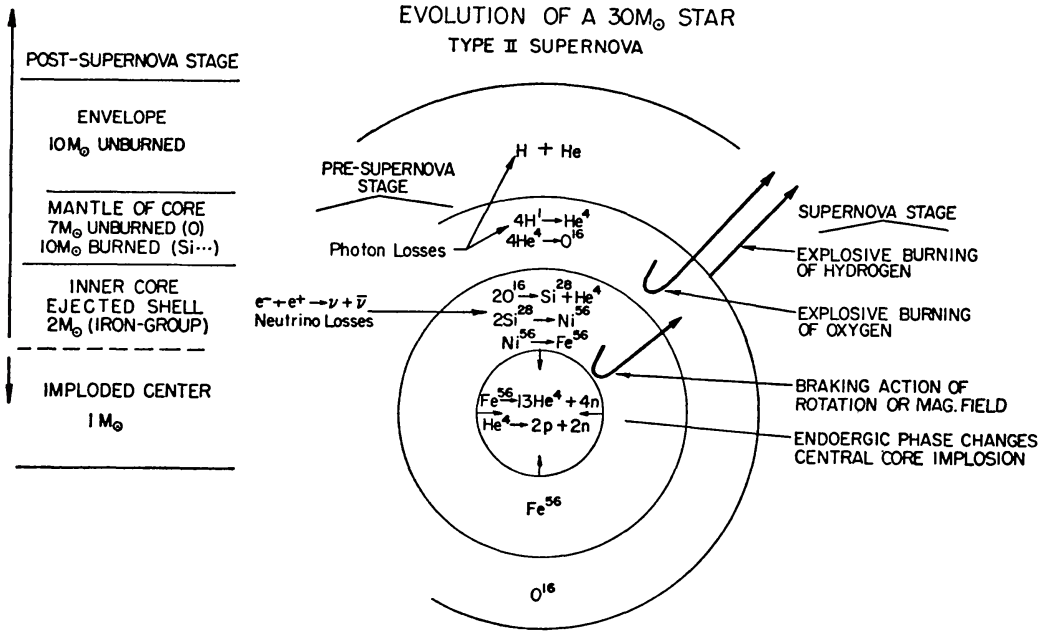

FIG. 11.—The evolution of a star with $M \approx 30\ M_{\odot}$ illustrating the pre-supernova, Type II supernova, and post-supernova stages. It is assumed that braking action due to rotation or some other mechanism ultimately leads to mantle-envelope explosion following core implosion caused by endoergic nuclear phase changes. The explosive burning of previously unburned oxygen is taken to be the source of energy in the explosion. The explosion results in the ejection of unburned "primordial" material plus products of hydrogen burning, helium burning, oxygen burning, the α-process, and the e-process.

in which evolution accelerates as it proceeds; the more advanced material runs further and further ahead of the rest. This causes the inner core to develop far ahead of the oxygen mantle. The development of the inner core requires a time of the order of only 1 day ($\sim 10^5$ sec). When implosion consequent on the phase change of iron-group elements to helium takes place, the inner core withdraws from the rest of the star. The outer part, comprising 90 per cent of the mass, can be regarded as an almost separate star in which oxygen in the mantle is compressed to explosion point at $T_9 \approx 2$.

The question now arises as to whether a spreading detonation of the oxygen can produce an outburst of the whole mantle and envelope of the star. To decide whether this is possible, it is necessary to construct an energy budget, as was done formerly by Hoyle and Fowler (1960). The situation here is different from the previous discussion, however, in that the fraction of the star now in the mantle and envelope is much greater than before—a situation caused by the neutrino losses and by the retreat of the core.

The model we shall adopt for drawing up the energy budget is one in which the star

is a polytrope of index 3 possessing central temperature $T_9 \approx 2.5$. This temperature is chosen because it is that temperature at which oxygen burning is 90 per cent or almost entirely complete at the stellar center according to the calculations of Part V. Above this temperature the development and isolation of the inner core take place. In calculating the gravitational binding energy which must be supplied to disrupt the star, an upper limit is $\frac{3}{2} GM^2/R$ where M is the total mass and R is calculated for polytropic index 3. However, the "giant" envelope is much less loosely bound than implied by this expression and the gravitational binding energy of the imploding regions need not be included at all. As a better compromise we will evaluate the mean gravitational potential as $\frac{3}{2} GM_c/R_c$, where $M_c = \frac{2}{3}M$ is the core mass and R_c is the core radius, but then multiply by M to obtain the gravitational energy.

1. *Gravitational energy before detonation.*—Equation (B124) of Appendix B yields

$$\frac{GM_c}{R_c} = 1.17 \left(\frac{\Re T}{\mu\beta}\right)_o \approx 10^{17} \left(\frac{T_9}{\mu\beta}\right)_o \text{ erg gm}^{-1} \approx 3.1 \times 10^{17} \text{ erg gm}^{-1} \tag{129}$$

for $(T_9)_o \approx 2.5$ and $(\mu\beta)_o \approx 0.79$ from Table 3. From this the gravitational binding energy according to our prescription is $|\Omega| \approx 4.6 \times 10^{17} M \approx 9.2 \times 10^{50} M/M_\odot$ ergs. This expression and others to follow is evaluated for $M \approx 30 M_\odot$ in Table 8.

TABLE 8

ENERGY BUDGET, TYPE II SUPERNOVA EXPLOSION

$M_c = 20 M_\odot$, $M \approx 30 M_\odot$

		Ergs
Gravitational energy required	$\lvert\Omega\rvert = \frac{3}{2}(GM_c/R_c)M$	$= 2.8 \times 10^{52}$
Thermal energy available	$(1 - 0.24\,\beta)\ \lvert\Omega\rvert$	$= 2.5 \times 10^{52}$
Balance required	$0.24\,\beta\ \lvert\Omega\rvert$	$= 0.3 \times 10^{52}$
Explosive energy at 5000 km sec^{-1}	$\frac{1}{2}Mv^2$	$= 0.7 \times 10^{52}$
Total required		$= 1.0 \times 10^{52}$
Erg/$M_\odot$ 2 $O^{16} \rightarrow Si^{28} + He^4$	$5 \times 10^{17} \times 2 \times 10^{33}$	$= 10^{51}$
Oxygen burning required		$= 10\ M_\odot$

2. *Thermal energy before detonation.*—From the virial theorem, the absolute magnitude of the gravitational energy is three times the volume integral of the total pressure as indicated in equation (B143) of Appendix B. The thermal energy of matter plus radiation is obtained by multiplying the pressure by the factor given by equation (B70) with $q \approx 1$ and $n_e \approx n$:

$$\frac{u}{p} = 3 - \beta\left[3 - x - z\left(1 - \frac{n_0}{n_e}\right)\right] \approx 3 - \beta\left[3 - 1.91 - 3.5\left(1 - \frac{3.01}{3.36}\right)\right] \approx 3(1 - 0.24\beta) \approx 2.67\,, \tag{130}$$

where the entries for $\beta = 0.457$, etc., at $T_9 = 1.69$ in Table 3 have been taken as appropriate averages over the mantle. Hence the internal thermal energy is a fraction of order $1 - 0.24\ \beta \approx 0.89$ of the gravitational binding energy. Thus the thermal energy is $0.89\ |\Omega| \approx 4.1 \times 10^{17} M \approx 8.2 \times 10^{50} M/M_\odot$ erg.

3. *Binding energy before detonation.*—The difference between the gravitational energy and the thermal energy is $0.11\ |\Omega| \approx 0.5 \times 10^{17} M \approx 1.0 \times 10^{50} M/M_\odot$ erg.

4. *Detonation energy.*—The energy released in $2\ O^{16} \rightarrow S^{32}$ is 5.0×10^{17} erg gm^{-1}. Although the mantle of the core contains 0.57 M gm of oxygen, not all of this will be burned in the detonation. A realistic estimate for the fraction burned would seem to be about ~60 per cent of the mantle material or $\sim\frac{1}{3}$ the mass of the star so that the overall energy release is $1.7 \times 10^7\ M \approx 3.4 \times 10^{50}\ M/M_\odot$ ergs.

5. *Energy excess.*—Taking the difference between the detonation energy and the binding energy, the energy excess for detonation of the estimated amount of O^{16} is $\sim 1.2 \times 10^{17}\ M$ erg. If converted into dynamical energy this would endow the whole mantle plus envelope with an average explosion speed of ~5000 km sec^{-1}, in good agreement with the observed expansion speeds of Type II supernovae.

The margin by which the detonation energy exceeds the binding energy is adequate but not great. It depends both on a fairly high assessment for the detonation efficiency and the amount of O^{16} involved such that the total quantity of O^{16} burned is of order $\frac{1}{3}\ M$. It is possible in some cases that either the detonation is not complete enough or that the amount of O^{16} is not sufficient to give excess positive energy to the whole envelope. In such cases we would still expect some expulsion of matter into space, through the outward propagation of shock waves from the detonation region to the surface. The shock-wave problem has been discussed by Colgate and Johnson (1960), Ôno, Sakashita, and Ohyama (1961), and by Ohyama (1963).

There is also a problem associated with the requirement of some braking action which will prevent the oxygen mantle from imploding along with the inner core before it can burn and produce enough nuclear energy for explosion. There is some question whether the internal pressures can support the mantle for the burning period and it may be that rotation, internal turbulence, or an entrained magnetic field, plays the dominant role as a brake on the mantle implosion. If this is the case not all stars in the range 10–50 $M_\odot$ would be expected to become Type II supernovae but only those with sufficient rotation, internal turbulence, or entrained magnetic field at formation. It is now realized that there is no problem in massive stars imploding without loss of mass to the gravitational limit in contrast to the previous belief, widely held, that all mass in excess of $\sim M_\odot$ had to be ejected at some evolutionary stage. This matter is considered in some detail by HFB[2] (1964).

Only in the case of a complete expulsion of the whole mantle plus envelope can the iron-group elements be ejected from the star. With the mantle plus envelope removed, and perhaps with some of the detonation energy carried inward through shock waves, we expect the outer parts of the core to join the outward-moving gases. Again, tentatively, we set the quantity of iron-group elements as $\sim 2\ M_\odot$ for $M \approx 30\ M_\odot$ on the basis that the imploding central part of the core must be of the order of a solar mass. This is somewhat less than the value $\sim 3\ M_\odot$ given previously by Hoyle and Fowler (1960). The galactic enrichment of iron-group elements over a period of 10^{10} years, even at a rate of 1 supernova per 10^3 years, is $\sim 2 \times 10^7\ M_\odot$, giving ~0.02 per cent of the total mass of the Galaxy, a result in good agreement with present observational estimates by Aller (1961).

Finally, we point out that the ratio of Fe group elements to the products of O^{16} burning, the Si group, is $2\ M_\odot/10\ M_\odot$ for $M \approx 30\ M_\odot$ or approximately $\frac{1}{5}$, a value again in good agreement with observation. Thus Aller (1961) gives a table (8–3, p. 192) for solar system abundances for which, after slight modification for other sources of evidence, we find Si group $= 1.3 \times 10^{-3}$ by mass and Fe group $= 2.5 \times 10^{-4}$. On the other hand, we note that Type II supernovae cannot contribute very much to He or CNONe synthesis, since these groups are much more abundant than the Si or Fe groups and on the basis of the arguments given here only a relatively small amount of He^4 and O^{16} or other light elements remains unburned during the explosion.

X. SUMMARY

The nature of neutrino processes in stars, and energy loss rates resulting from neutrino emission, have been reviewed in the first two parts of the paper. On the assumption that the universal Fermi strength applies to four-lepton interactions, it is found that neutrino-antineutrino emission by electron-positron pair annihilation is the most important neutrino process in massive stars ($M > 10\ M_\odot$). From the discussion of the effects of neutrino emission by this process in pre-supernova stars, two conclusions stand out as requiring special emphasis:

1. Although neutrino losses greatly speed up evolution when T_9 exceeds ~ 1, the loss rate is not sufficient to produce a free-fall implosion. Free-fall must await the phase change of iron-group nuclei first to helium and free neutrons and ultimately to free protons and free neutrons.

2. In B^{2}FH (1957) it was shown that the observed relative abundance of the iron-group nuclei could be understood in terms of an equilibrium or *e*-process, provided two parameters were appropriately chosen—the temperature and the ratio of the densities of free neutrons and protons, with logarithm denoted by $\theta = \log n_p/n_n$. Other choices for these parameters did not lead to a satisfactory correspondence with the observed abundances. In this early work, no satisfactory explanation could be given to show *why* $T_9 = 3.8$, $\theta = 2.5$ are the particular values necessary to explain the observed abundances. In Part VII of the present paper we arrive at an explanation, however. The explanation turns out to lie in a relation of the evolution time scale, as set by neutrino losses, to the time required for certain nuclei on the proton-rich side of the stability line to move toward the stability line. The indicated temperature is reached at the end of the α-process which produces nuclei such as Ni^{56} having the maximum stability for equal numbers of protons and neutrons ($Z = N$). To arrive at an appropriate value for θ in the typical transformation from Ni^{56} to Fe^{56} by electron capture, *it is necessary that neutrino losses take place at a rate of the order calculated from the universal Fermi interaction strength.* An order of magnitude deviation from the universal interaction would lead to a wrong value for θ. The Pinaev (1963) modification of the Urca process does not require universality and may be rapid enough to result in the required limit on the time scale. Exact calculations for the Pinaev process require more accurate knowledge of the relevant beta-interactions than now available.

Evolution proceeds most rapidly at the center of the star. If radiation transfer is neglected and if temperature is chosen as the independent variable, then the time scale under neutrino loss is determined by the equation

$$\frac{dt}{dT} = \left(\frac{p}{\rho^2}\frac{d\rho}{dT} - \frac{dU}{dT} + \frac{dQ_N}{dT}\right) \Big/ \frac{dU_\nu}{dt}, \tag{131}$$

in which U is the internal energy per gram, including matter and radiation and also the rest-mass energy of electron-positron pairs produced by the radiation field, dQ_N/dT is the nuclear energy released per gram per unit rise of temperature, and dU_ν/dt is the neutrino loss rate per gram *per unit time*. Formulae for dU_ν/dt by pair annihilation are given in Part II. It is convenient to take the first two terms in brackets together, writing

$$\frac{dQ}{dT} = \frac{p}{\rho^2}\frac{d\rho}{dT} - \frac{dU}{dT}. \tag{132}$$

Here dQ/dT is the energy made available per gram per unit increase of temperature by the compression of the evolving material. The first step in evaluating dQ/dT is to obtain a formula relating the density ρ to the temperature T. This question is considered in Part III and Appendix B where arguments are presented to show that ρ and T can satis-

factorily be related by equation (33), $\rho \approx 10^7 \, (M\odot/M_c)^2 \, (T_9/\mu\beta)^3$ gm cm^{-3}, so long as the star is in quasi-hydrostatic equilibrium. This equation involves not only the effective core mass of the star, which may be considered known, but also the product $\mu\beta$. In the non-degenerate case the gas law for the pressure p also involves $\mu\beta$. A determination of this product is complicated by pair creation. This problem is also considered in Part III, where it is shown that the well-known quartic equation for $\mu\beta$, applicable in the absence of pair creation, is now replaced by a quartic equation for $(\mu\beta)^2$ in which the modified Bessel function, $K_2(m_ec^2/kT)$, appears. The formulas developed allow $\mu\beta$ and also μ and β individually to be evaluated. Equation (53), in which $\rho \sim 10^5 \, (M\odot/M_c)^{1/2} \, T_9{}^3$ gm cm^{-3}, is the approximate result for massive stars. Hence the $(p/\rho^2) \, d\rho/dT$ term in equation (132) can be calculated when the temperature and the mass of the star and its chemical composition are specified. (The latter is known from nuclear considerations.)

Turning now to the internal energy U, formulae are obtained in Part IV which allow dU/dT also to be calculated when the temperature and the mass of the star and its composition are specified. Results for a mass, $M_c = 20 \, M\odot$, $M \approx 30 \, M\odot$, are shown in Figure 8. The remarkable feature emerges that dQ/dT is negative for $T_9 \sim 2$. There is an energy deficit amounting to $\sim 10^{16}$ erg gm^{-1} $(10^9 \text{ deg})^{-1}$ arising from pair creation at temperatures near this value. If dQ_N/dT were zero, equation (131) would lead to a negative time scale for evolution, an impossible conclusion. The inference would be that equations (33) or (53), based on a quasi-equilibrium of the star, had become invalid. In short, the star would implode when the central temperature reached about 2×10^9 degrees. However, dQ_N/dT is not zero. Nuclear reactions, in particular oxygen burning, are taking place, and these give $\sim 5 \times 10^{17}$ erg gm^{-1} over the relevant temperature range, more than ten times what is needed for the pair creation. Using the value of dU_ν/dt appropriate to $T_9 \sim 2$ we find $(Tdt/dT)^{-1} \sim 10^5$ sec, so that evolution in the temperature range important for pair creation takes about a day. Although this is very short compared to normal time scales for stellar evolution, it is still long compared to the time of free fall, about 1 sec. Quasi-static equilibrium is still maintained and ρ and T can still be related by equations (33) or (53). *Nuclear reactions serve as stellar thermostats.*

Nuclear energy continues to be supplied by nuclear processes up to $T_9 \sim 3.5$. The α-process discussed in Part VI follows oxygen burning. However, the energy yield from the α-process is less than that from oxygen burning. Also the neutrino loss rate increases with the temperature. The effect is to shorten the time scale for evolution to $\sim 5 \times 10^3$ sec. But this is still much longer than the time of free fall. There is still no implosion—in the sense that dynamical velocities do not develop in excess of the speed of sound.

As the temperature rises above $T_9 \sim 3.5$ exoergic nuclear reactions effectively cease. Until endoergic reactions set in a $T_9 \sim 6$ the dQ_N/dT term in equation (131) may be taken zero. The only source of energy is then from compression—i.e., the dQ/dT term of equation (132). But at $T_9 > 3.5$ this term has again become positive. For example, at $T_9 \sim 5$ we obtain $dQ/dT \sim 10^{17}$ erg gm^{-1} $(10^9 \text{ deg})^{-1}$. At this temperature $dU_\nu/dt \sim 10^{15}$ erg gm^{-1} sec^{-1}. Hence the time required for evolution to lift the temperature from $T_9 = 5$ to $T_9 = 6$ is about 100 sec, still longer than free-fall time, now <1 sec. We conclude that quasi-equilibrium is maintained up to the onset of endoergic reactions.

Endoergic reactions imply that dQ_N/dT becomes strongly negative. Equation (131) yields the impossible result of a negative time scale, implying that quasi-equilibrium ceases, and that the density and temperature can no longer be related by equations (33) or (53). The time scale for evolution is no longer set by neutrino losses but by the free-fall time. Indeed, neutrino losses can now be neglected. The equation

$$\frac{dQ}{dt} + \frac{dQ_N}{dt} = 0 \tag{133}$$

determines the density-temperature relation during the implosion. The path of material in a ρ, T-diagram is shown in Figures 5 and 6 for several stellar masses up to the onset

of relativistic degeneracy. The equations given in Part IV for calculating dQ/dT cease to be valid under conditions of relativistic degeneracy.

The discussion given in Parts VI and VII of the α-process and e-process, respectively, is an important by-product of the argument. With a knowledge of the evolutionary time scale determined by equation (131) it is possible to gain additional insight into these processes. We define the termination of the α-process as being set by the complete photonuclear disintegration of Si^{28}. This occurs at $T_9 \sim 3.5$, a value slightly below that found by B^{2}FH (1957) as the best operating temperature of the e-process, $T_9 \sim 3.8$. Our point of view is that the sample of e-process material most likely to escape from a supernova is that which lies just below the region in which the α-process takes place and just above the region where implosion is induced by endoergic nuclear reactions as shown in Figure 11. This will be material only slightly above the α-process temperature, i.e., slightly above $T_9 \sim 3.5$, in agreement with B^{2}FH (1957).

Following the photodisintegration of Si^{28} a rapid synthesis occurs in which the initial equality of the total neutron and total proton densities plays a dominant role. Thus the most abundant nucleus initially is Ni^{56}, not Fe^{56}, as in terrestrial iron-group material. However, the Ni^{56} decays to Fe^{56} by electron capture in the time scale, $t_e \sim 3 \times 10^4$ sec, comparable to the evolution time determined by neutrino losses, $t_\nu \sim 6000$ seconds in a star with mass $M \sim 30\ M_\odot$. If stars with somewhat lower masses are considered or if core masses somewhat less than $M_c \sim \frac{2}{3} M$ are specified, then t_e and t_ν are very closely equal. The decay of Ni^{56} to Co^{56} changes the ratio of proton and neutron densities, and this is equivalent to changing the value of the parameter θ. This in turn changes the equilibrium abundances. Hence the evolution with respect to neutrino losses is equivalent to an evolution with respect to θ. It turns out that as the former speeds up θ tends toward a limiting value. In stars of 10–35 $M_\odot$ the limiting value is close to just that obtained by B^{2}FH (1957). In stars of larger mass θ reaches a limiting value that corresponds to a distribution of iron-group elements systematically more "proton rich" than terrestrial material. It seems then that the iron-group elements of the solar system were mainly derived from stars of mass 10–35 $M_\odot$, rather than from more massive stars. It is of considerable interest, however, that the equilibrium distribution for 10–35 $M_\odot$ is notably deficient in two typically proton rich nuclei, Cr^{50} and Ni^{58}. To explain the abundances of these isotopes, it is necessary to suppose that, while the terrestrial e-process elements were mainly derived from stars of masses in the range 10–35 $M_\odot$, a smaller component was also derived from stars of larger mass.

So far we have been concerned with the physics of a particular element of material. The evolution of a particular element is not much affected by uncertainties concerning the structure of the whole star. However, the explosive outburst of a supernova is much affected by the over-all structure. Until more is known about the development of the model, a discussion of the outburst can of necessity only be qualitative. We expect the accelerating evolution to produce a situation analogous to that found in subgiants, where a dense core, not containing more than 10 per cent of the total mass, develops at the center. We suspect that neutrino losses have the effect of significantly reducing the mass of the imploding inner region below that estimated by Hoyle and Fowler (1960).

Material outside the core with temperature less than $T_9 \sim 2$ at the moment of implosion will fall inward and will experience compression. A rise of temperature to $T_9 \sim 3$ produces an explosive burning of oxygen—i.e., a time scale for oxygen burning less than the time required for a sound wave to travel through a star. Consideration of an individual element shows that the density cannot exceed $\sim 10^6$ gm cm^{-3} during oxygen burning, which implies that explosive burning occurs long before the outer part of the star collapses onto the imploding core. Hence the energy from the nuclear reactions, amounting to $\sim 5 \times 10^{17}$ erg gm^{-1}, is released at a stage where the gravitational binding of the outer mantle has not increased appreciably above its value at the onset of implosion. A general energy budget suggests that the total binding of the mantle and of the outer envelope

can become negative—a necessary condition for explosion. We find that the energy excess can exceed 10^{17} erg gm^{-1}. If this excess is converted into the dynamical velocity of outburst, the resulting speed is of order 5000 km sec^{-1}, in agreement with the observed speeds of Type II supernova shells.

We have regarded a discussion of the dynamical behaviors of the imploding core as lying outside the scope of the present paper. There is also a problem associated with the requirement of some braking action which will prevent the oxygen mantle from imploding along with the inner core before it can burn and produce enough nuclear energy for explosion. There is some question whether the internal pressures can support the mantle for the duration of burning period and it may be that rotation, internal turbulence, or an entrained magnetic field plays the dominant role as a brake on the mantle implosion. If this is the case not all stars in the range 10–50 $M_\odot$ would be expected to become Type II supernovae but only those with sufficient rotation, internal turbulence, or entrained magnetic field at formation. It is now realized that there is no problem in massive stars imploding without loss of mass to the gravitational limit in contrast to the previous belief, widely held, that all mass in excess of $\sim M_\odot$ had to be ejected at some evolutionary stage. This matter is considered in some detail by Hoyle, Fowler, Burbidge and Burbidge (1964). At this point we conclude this "Handbuch der *Eav*-Prozesse."

The material presented in this monograph was first discussed in part by the authors at the Herstmonceux Conference, April 17, 1962, at the Royal Greenwich Naval Observatory, Herstmonceux Castle, Hailsham, Sussex. One of the authors (W. A. F.) incorporated part of this material into the Henry Norris Russell Lecture delivered before the 114th meeting of the American Astronomical Society at the University of Alaska, College, Alaska, July 23, 1963.

The authors are indebted to Dr. R. J. Tayler and Mr. F. E. Clifford for discussions of the *e*-process, for communicating their own results before publication, and for recalculating the special *e*-process distributions originally presented in B²FH (1957). In addition they are indebted to Professor C. C. Lauritsen, Professor G. R. Burbidge, and Dr. E. M. Burbidge for general discussions of the content of the paper, to Professor M. Gell-Mann for discussions of neutrino processes, to Dr. M. J. Levine for communicating his calculation of the pair-annihilation cross-section before publication, to Dr. J. N. Bahcall for his discussions of beta-interactions in stars, to Dr. A. Boury, Dr. I. Iben, Jr., Dr. M. Schmidt, and Dr. R. L. Sears for discussions of stellar structure and evolution, to Barbara Zimmerman, R. J. Talbot, and Henry Abarbanel for carrying out numerical computations, to Jan Rasmussen and Evaline Gibbs for secretarial and editorial assistance, and to Professor J. L. Greenstein, the eminent T. S. Eliot scholar, for suggesting the introductory quotation.

F. H. is grateful to the California Institute of Technology and W. A. F. is grateful to St. John's College and the Department of Applied Mathematics and Theoretical Physics, Cambridge University, for hospitality during the period in which these studies were undertaken. W. A. F. acknowledges with gratitude the grant of a fellowship by the John Simon Guggenheim Memorial Foundation during 1961–1962 when these studies were first undertaken. The work has been supported in part by the Office of Naval Research (Nonr-220[47]) and the National Aeronautics and Space Administration (NGR-OS-002-028).

APPENDIX A

BETA-INTERACTION RATES

a) General Equations

In this appendix we discuss the rates of the weak interactions involving nuclei. These are known collectively as the beta-interactions and include electron-antineutrino emis-

sion, positron-neutrino emission, electron capture with neutrino emission, and positron capture with antineutrino emission. In the first and fourth of these, a nuclear neutron is transformed into a proton ($Z \rightarrow Z + 1$), while in the second and third, a proton is transformed into a neutron ($Z \rightarrow Z - 1$).

The rates of these interactions in stars can depart considerably from the terrestrial rates. A comprehensive discussion and bibliography has been given recently by Bahcall (1964). For the purposes of Part VII of this paper, we can limit the present discussion in regard to stars to the case of completely ionized, non-degenerate, non-relativistic nuclei, and non-degenerate but relativistic ($E \gtrsim m_e c^2$, $v \gtrsim 0.87\ c$) electrons and positrons. No discussion is included for very low-energy electron emission where atomic binding-energy contributions to the terrestrial energy release and terrestrial bound-state decay complicate the terrestrial-stellar comparison. The effect of the exclusion principle is negligible at the temperature and density of interest. Screening and certain nuclear size effects have been neglected. In a private communication Bahcall (1963) has pointed out that the electron concentration under consideration here, $\sim 10^{30}$ cm^{-3}, is about a factor of 100 greater than the electron concentration surrounding Fe atoms under terrestrial conditions; this electron concentration is in fact about equal to the concentration surrounding U atoms under normal terrestrial conditions. Reitz (1950) has shown that screening changes electron and positron decay probabilities by less than 20 per cent for particles emitted from U atoms with energies of the order of 300 to 400 keV ($kT \sim 4 \times 10^9$ degrees K). This indicates that screening is not very important for stellar atoms in the Fe peak at the temperature and density under consideration here. Bahcall (1964) has also estimated that nuclear size effects increase the capture rates calculated in this paper by approximately 15 per cent. Relativistic Coulomb effects have been included only in a multiplicative factor which is a rough approximation near $Z = 26$. Only allowed transitions in which the lepton pairs have zero orbital angular momentum in the non-relativistic approximation will be considered; antiparallel spins for the pair then corresponds to the vector Fermi transition and parallel spins to the axial vector Gamow-Teller transition. The selection rules on the change in spin and parity in the nuclear transition are therefore $\Delta J = 0$, $\Delta\Pi = 0$ for the Fermi case and $\Delta J = 0, \pm 1$ (no $0 \rightarrow 0$), $\Delta\Pi = 0$ for the Gamow-Teller case. Bahcall (1964) has investigated forbidden decays in the most important of the specific cases discussed in (*e*) and has found the allowed decays to be faster.

Under the restrictions stipulated in the preceding paragraph, it can be stated that the electron or positron *emission* rates for a transition between given initial and final nuclear states are not greatly different in stars from those in the terrestrial case. We have specifically excluded from our discussion the case of degenerate stellar material where electron or positron final states may be partially or completely occupied so that the exclusion principle serves to inhibit the emission rates. However, even in the case of non-degenerate stellar material which is the primary interest of this paper, we will find, as is intuitively obvious, that stellar electron and positron *capture* rates are very sensitive to temperature and density and for a given transition can differ considerably from terrestrial values.

There is one important respect in which the stellar situation always differs from the terrestrial case. At thermodynamic equilibrium in stars, nuclei exist in all their various excited states as well as in the ground and isomeric states for which it is possible to measure beta-decay rates in terrestrial laboratories. This fact has been known for many years (see, e.g., Chandrasekhar and Henrich [1942]) and was taken into account by B^{2}FH (1957) in their discussion of the equilibrium (*e*) process. These authors did not include excited state abundances in their treatment of neutron capture processes (*s* and *r*), since they took the temperatures for these processes to be low enough that excitation of nuclei could be neglected in first approximations. In a discussion of neutron processes at higher temperatures, Cameron (1959*b*) pointed out that the excited states of a nucleus may have quite different beta-decay rates than the ground state of the nucleus.

For each excited state of a nucleus, it is necessary to calculate the beta-decay rate by the method to be discussed in what follows. Then, to obtain an effective decay rate, this calculated value must be multiplied by the relative population factor for the state. This factor is given by

$$s = \frac{(2J+1)\exp -E^*/kT}{\Sigma_i (2J_i+1)\exp -E_i^*/kT}, \tag{A1}$$

where J is the angular momentum of the state and E^* is its excitation energy above the ground state for which $E^* = 0$. The sum of the effective decay rates over all states will then give the over-all decay rate for the nucleus in question.

With the above preliminaries aside, we now turn to the case of allowed $\beta^{\pm}$ emission. The differential decay rate, $d\lambda$, for allowed $\beta^{\pm}$ emission in the energy interval $d\omega_\beta$ is given by (see Preston [1962])

$$d\lambda(\beta^{\pm}) = \Sigma C^2 |M|^2 F_{\pm}(Z, \omega_\beta)\omega_\nu p_\nu \omega_\beta p_\beta d\omega_\beta , \tag{A2}$$

where ω is total energy in units $m_e c^2$, p is momentum in units $m_e c$, subscript ν applies to neutrino or antineutrino, subscript β applies to electron or positron, $F_{\pm}$ is a relativistic Coulomb factor, the energy $\times$ momentum products come from phase-space factors for the emitted leptons and

$$\Sigma C^2 |M|^2 = C_V{}^2 |M_F|^2 + C_A{}^2 |M_{GT}|^2 \tag{A3}$$

with

$$C_V{}^2 = \frac{G_V{}^2}{2\pi^3 \hbar / m_e c^2} = 1.13 \times 10^{-4}\,\mathrm{sec}^{-1},$$

M_F = Fermi nuclear matrix element, $G_V{}^2$ = square of dimensionless vector interaction constant = $0.90 \pm 0.01 \times 10^{-23}$ corresponding to the square of the absolute constant,

$$g_V{}^2 = G_V{}^2 (m_e c^2)^2 (\hbar / m_e c)^6 = 2.00 \pm 0.02 \times 10^{-98}\ \mathrm{erg}^2\ \mathrm{cm}^6 ,$$

and

$$C_A{}^2 = \frac{G_A{}^2}{2\pi^3 \hbar / m_e c^2} = 1.58 \times 10^{-4}\,\mathrm{sec}^{-1},$$

M_{GT} = Gamow-Teller nuclear matrix element, $G_A{}^2$ = square of dimensionless axial vector interaction constant = $1.26 \pm 0.05 \times 10^{-23}$ corresponding to the square of the absolute constant

$$g_A{}^2 = G_A{}^2 (m_e c^2)^2\ (\hbar / m_e c)^6 = 1.40 \pm 0.08\ g_V{}^2 = 2.80 \pm 0.10 \times 10^{-98}\ \mathrm{erg}^2\ \mathrm{cm}^6 .$$

If the maximum total energy available to the electron or positron be designated by ω_o in units $m_e c^2$, then $p_\nu = \omega_\nu = \omega_o - \omega_\beta = \omega_o - \omega$ on dropping the superfluous subscript. In the non-relativistic limit

$$F_{\pm}(Z, \omega) = \frac{2\pi\eta}{|\exp \pm 2\pi\eta - 1|}, \tag{A4}$$

where

$$\eta = \frac{Z e^2}{\hbar v} = \alpha Z \frac{c}{v} = \alpha Z \frac{\omega}{p} \tag{A4'}$$

is a positive quantity for both electron and positron emission with v the electron or positron velocity, $\alpha = \frac{1}{137}$ the fine structure constant, and Z the charge number of the final nucleus. The relativistically correct expression for $F_{\pm}$ is known but is somewhat complicated and $(v/c)F_{\pm} = (p/\omega)F_{\pm} = 2\pi\ \alpha Z(F_{\pm}/2\pi\eta)$ has been tabulated by Rose,

Dismuke, Perry, and Bell (1955). It is convenient to abstract the term $2\pi\eta$ from $F_\pm$ so that

$$d\lambda(\beta^\pm) = 2\pi aZ\Sigma C^2 |M|^2 \left(\frac{F_\pm}{2\pi\eta}\right)(\omega_o - \omega)^2\omega^2 d\omega . \tag{A5}$$

Upon integration over ω from unity to ω_o, the following expressions for decay rate (λ), mean lifetime (τ), and halflife (t) result:

$$\lambda(\beta^\pm) = \frac{1}{\tau(\beta^\pm)} = \frac{\ln 2}{t(\beta^\pm)} = \Sigma C^2 |M|^2 f(\beta^\pm), \tag{A6}$$

with

$$f(\beta^\pm) = 2\pi aZ \left\langle \frac{F_\pm}{2\pi\eta} \right\rangle \left(\frac{\omega_o^5}{30} - \frac{\omega_o^2}{3} + \frac{\omega_o}{2} - \frac{1}{5}\right) \tag{A7}$$

$$= 2\pi aZ \left\langle \frac{F_\pm}{2\pi\eta} \right\rangle \left(\frac{q_n^5}{30} - \frac{q_n^2}{3} + \frac{q_n}{2} - \frac{1}{5}\right) \tag{A8}$$

$$= 2\pi aZ \left\langle \frac{F_\pm}{2\pi\eta} \right\rangle \left(\frac{\epsilon_o^5}{30} + \frac{\epsilon_o^4}{6} + \frac{\epsilon_o^3}{3}\right), \tag{A9}$$

$$f(\beta^+) = 2\pi aZ \left\langle \frac{F_+}{2\pi\eta} \right\rangle \left[\frac{(q_a-2)^5}{30} + \frac{(q_a-2)^4}{6} + \frac{(q_a-2)^3}{3}\right], \tag{A10}$$

$$f(\beta^-) = 2\pi aZ \left\langle \frac{F_-}{2\pi\eta} \right\rangle \left(\frac{q_a^5}{30} + \frac{q_a^4}{6} + \frac{q_a^3}{3}\right), \tag{A11}$$

where Z is the charge number of the final nucleus. In these expressions, $\epsilon_o = \omega_o - 1$ is the maximum $\beta^\pm$ kinetic energy in units $m_e c^2$, $q_n = Q_n/m_e c^2$ is the difference between the initial and final *nuclear* masses expressed in energy equivalent units $m_e c^2$ while $q_a = Q_a/m_e c^2$ is the corresponding difference between the initial and final *atomic* or *nuclidic* masses which are the ones customarily tabulated. Except for very small atomic rearrangement terms, $\omega_o = \epsilon_o + 1 = q_n$. It is also true that $q_a = q_n + \Delta Z - \Delta b_a \approx q_n \pm 1$ (plus for β^+ emission, minus for β^- emission) where $\Delta Z = \pm 1$ is the initial charge number minus the final, $\Delta b_a = \Delta B_a/m_e c^2$ and where $\Delta B_a = 36.6\, Z^{4/3}\, \Delta Z$ eV is the corresponding change in atomic binding energy. The quantity ΔB_a is at most only a few kilovolts in energy for the Z-values of interest and can be neglected except for very small Q_n. Thus, $\omega_o = q_a \mp 1$ and $\epsilon_o(\beta^-) = q_a$ while $\epsilon_o(\beta^+) = q_a - 2$.

It will be seen that equations (A6)–(A11) do not represent an explicit integration of equation (A5) since an appropriately weighted "mean" values for $(F_\pm/2\pi\eta)$ must in general be calculated. Fortunately, in the range of relativistic electron or positron energies, $(F_\pm/2\pi\eta)$ varies slowly with energy. The tables of $2\pi aZ(F_\pm/2\pi\eta)$ prepared by Rose *et al.* (1955) can be used when highly accurate calculations are warranted. For our purposes, we find near $Z = 26$, $\langle F_-/2\pi\eta\rangle \approx 1.6$, and $\langle F_+/2\pi\eta\rangle \approx 0.5$. Over the electron-energy range which contributes predominantly to the decay rate $(F_-/2\pi\eta)$ varies only by approximately 10 per cent so that the use of a fixed value for $\langle F_-/2\pi\eta\rangle$ is a quite good approximation. In the positron case $(F_+/2\pi\eta)$ varies by as much as 50 per cent so the approximation using a fixed $\langle F_+/2\pi\eta\rangle$ is relatively poor.

In the zero charge limit, $F_\pm(Z = 0, \omega) = 1$ and the integration of equation (A5) yields the well-known expressions

$$f_o(\beta^\pm) = (\omega_o^2 - 1)^{1/2}\left(\frac{\omega_o^4}{30} - \frac{3\omega_o^2}{20} - \frac{2}{15}\right) + \frac{\omega_o}{4}\ln[\omega_o + (\omega_o^2 - 1)^{1/2}]$$

$$\approx \frac{\omega_o^5}{30} - \frac{\omega_o^3}{6} + \ldots . \qquad Z \sim 0,\ \omega_o > 2 \tag{A12}$$

$$\approx 0.2155\epsilon_o^{7/2} + \ldots . \qquad Z \sim 0,\ \epsilon_o = \omega_o - 1 < 1 .$$

Electron capture occurs terrestrially from bound atomic orbits. The rate for bound electron (e_b^-) capture in the allowed case (K, L_I, etc.) is given by

$$\lambda(e_b^-) = \frac{1}{\tau(e_b^-)} = \Sigma C^2 |M|^2 f(e_b^-), \tag{A13}$$

with

$$f(e_b^-) = \pi^2 \left(\frac{\hbar}{m_e c}\right)^3 |\psi_e(0)|^2 \omega_\nu^2 = \pi^2 \left(\frac{\hbar}{m_e c}\right)^3 |\psi_e(0)|^2 q_a^2$$
$$= \pi^2 \left(\frac{\hbar}{m_e c}\right)^3 |\psi_e(0)|^2 (q_n + 1)^2, \tag{A13'}$$

where $\omega_\nu = q_a = q_n + 1$ is the energy (single-valued) of the emitted neutrino, q_n is the nuclear mass difference in energy equivalent units $m_e c^2$, corrected if the accuracy required is high for the atomic binding of the captured electron, q_a is the corresponding atomic mass difference, and $|\psi_e(0)|^2$ is the density at the nucleus of electrons with appropriate angular momentum for allowed capture. The factor ω_ν^2 is proportional to the phase-space factor for the emitted neutrino. Allowed capture occurs primarily from the K-shell and to a sufficient approximation

$$|\psi_e(0)|^2 = \frac{2}{\pi}\left(Z\frac{m_e c^2}{\hbar^2}\right)^3, \tag{A14}$$

where Z is the charge number of the *initial* nucleus. Thus

$$f(e_b^-) = 2\pi(aZ)^3 \; q_a^2 . \tag{A15}$$

Electron capture occurs in stars from bound and continuum orbits, and for nuclei under the conditions discussed in this paper it is the continuum capture which is important. Positron capture from continuum orbits can also occur in stars, although it is not of great importance in the considerations of interest in the main body of this paper.

The allowed differential rate for $e^\pm$ capture from the energy interval $d\omega$ in the continuum (subscript c) is given by

$$d\lambda(e_c^\pm) = \Sigma C^2 |M|^2 F_\pm \pi^2 (\omega + q_n)^2 \left(\frac{\hbar}{m_e c}\right)^3 \frac{dn_\pm}{d\omega} d\omega, \tag{A16}$$

where $\omega_\nu^2 = (\omega + q_n)^2 = (\omega + q_a \pm 1)^2$ is proportional to the phase-space factor for the emitted neutrino or antineutrino and the differential electron density,

$$\frac{dn_\pm}{d\omega} = \frac{1}{\pi^2}\left(\frac{m_e c}{\hbar}\right)^3 \left(\frac{v}{c}\right) \omega^2 \exp[-z\omega \mp \varphi] \tag{A17}$$

can be obtained from equations (7), (9), and (10) of Part II. When this is done, one has, with $z = m_e c^2/kT$ and $n_\pm/n_1 = \exp \mp \varphi$,

$$d\lambda(e_c^\pm) = 2\pi a Z \Sigma C^2 |M|^2 \left(\frac{F_\pm}{2\pi\eta}\right) \frac{n_\pm}{n_1} \exp(-z\omega)\omega^2(\omega + q_n)^2 d\omega . \tag{A18}$$

To obtain $\lambda(e_c^\pm)$ we must now distinguish two cases. In the first case let $q_n = Q_n/m_e c^2$ the nuclear energy difference in units $m_e c^2$ between the capturing state and the fina nuclear state lie in the range $q_n > -1$ so that the range of integration is $1 < \omega < \infty$ and in the second case let $q_n < -1$ so that the range of integration is $|q_n| < \omega < \infty$ Then

$$\lambda(e_c^\pm) = \Sigma C^2 |M|^2 f(e_c^\pm) \tag{A19}$$

with

$$f(e_c^{\pm}) = 2\pi aZ \left\langle \frac{F_{\pm}}{2\pi\eta} \right\rangle \frac{n_{\pm}}{n_1} I_{\pm}, \tag{A19'}$$

where Z is the charge number of the initial nucleus. From the main text, equation (10),

$$n_1 = (2/\pi^2)(kT/\hbar c)^3 \bar{K}_2(z) .$$

As $z \to 0$, $n_1 \to (2/\pi^2)(kT/\hbar c)^3$, while as $z \to \infty$,

$$n_1 \to (1/2\pi^3)^{1/2}(m_e c/\hbar)^3 (kT/m_e c^2)^{3/2} \exp(-z) = 2\left(\frac{m_e kT}{2\pi\hbar^2}\right)^{3/2} \exp(-m_e c^2/kT).$$

For $q_n > -1$,

$$I_{\pm} = \int_1^{\infty} \exp(-z\omega)\omega^2(\omega + q_n)^2 d\omega$$
$$= \frac{\exp -z}{z}\left[q_n^2\left(1+\frac{2}{z}+\frac{2}{z^2}\right)+2q_n\left(1+\frac{3}{z}+\frac{6}{z^2}+\frac{6}{z^3}\right)+\left(1+\frac{4}{z}+\frac{12}{z^2}+\frac{12}{z^3}+\frac{24}{z^4}\right)\right], \tag{A20}$$

while for $q_n < -1$,

$$I_{\pm} = \int_{|q_n|}^{\infty} \exp(-z\omega)\omega^2(\omega - |q_n|)^2 d\omega$$
$$= \frac{2\exp -|Q_n/kT|}{z^3}\left(|q_n|^2+\frac{6}{z}|q_n|+\frac{12}{z^2}\right). \tag{A20'}$$

An approximate value for the average of $(F_{\pm}/2\pi\eta) = |\exp \pm 2\pi\eta - 1|^{-1}$ can be found by employing appropriate values for $2\pi\eta$. For $q_n > -1$, it is sufficiently accurate in most cases to use the mean value for $2\pi\eta$, namely,

$$\langle F_{\pm}/2\pi\eta \rangle \approx |\exp \pm \langle 2\pi\eta \rangle - 1|^{-1},$$

with

$$\langle 2\pi\eta \rangle = 2\pi aZ\langle c/v \rangle = \frac{2\pi aZ}{K_2(z)}\left(1+\frac{2}{z}+\frac{2}{z^2}\right)\exp -z$$
$$\to 2\pi aZ\left(\frac{2z}{\pi}\right)^{1/2} = 2\pi aZ\left(\frac{2m_e c^2}{\pi kT}\right)^{1/2} \quad \text{for } z\to\infty,\ T\to 0 \tag{A21}$$
$$\to 2\pi aZ \qquad \text{for } z\to 0,\ T\to\infty .$$

For $q_n < -1$, it is sufficiently accurate in most cases to use the minimum value for $2\pi\eta$, namely, $\langle F_{\pm}/2\pi\eta \rangle \approx |\exp \pm (2\pi\eta)_{\min} - 1|^{-1}$ with

$$(2\pi\eta)_{\min} = 2\pi aZ(\omega/p)_{\min} = 2\pi aZ\frac{|q_n|}{[\,|q_n|^2-1\,]^{1/2}}$$
$$\to \frac{2\pi aZ}{(2|q_n|-2)^{1/2}} \quad \text{for } q_n \lesssim -1,\ |q_n| \gtrsim 1 \tag{A21'}$$
$$\to 2\pi aZ \qquad \text{for } |q_n| \gg 1 .$$

If $\langle 2\pi\eta \rangle$ is very large, equation (A20) will not be valid for *positron* capture since in this case the term $(\exp 2\pi\eta - 1)^{-1} \approx \exp -2\pi\eta$ must be included in the integrand in I_+. One then finds for $z > 1$, $q_n > -1$

$$f(e_c^+) \approx \frac{8}{3^{5/2}}\pi^2 n_+ \left(\frac{\hbar}{m_e c}\right)^2 (q_n+1)^2\tau^2 e^{-\tau} \tag{A22}$$

with

$$\tau = 3(\pi^2 a^2 Z^2 m_e c^2/2kT)^{1/3} = 3.48(Z^2/T_6)^{1/3}. \quad \text{(A22')}$$

There is no problem in the electron case since $(1 - \exp - 2\pi\eta)^{-1} \approx 1$ for $2\pi\eta$ large.

In the region of interest in the main text, we have chosen $\langle F_-/2\pi\eta\rangle = 1.6$ and $\langle F_+/2\pi\eta\rangle = 0.5$. In terms of atomic mass differences $q_n = q_a - 1$ in the electron-capture case and $q_n = q_a + 1$ in the positron-capture case. We are primarily interested in the electron-capture case, and so we express I_- in terms of q_a as follows:
For $q_a > 0$

$$I_- = \frac{\exp - z}{z}\left[q_a^2\left(1+\frac{2}{z}+\frac{2}{z^2}\right)+2q_a\left(\frac{1}{z}+\frac{4}{z^2}+\frac{6}{z^3}\right)+2\left(\frac{1}{z^2}+\frac{6}{z^3}+\frac{12}{z^4}\right)\right]$$

$$= \frac{\exp - z}{z}\, q_a^2\left[\left(1+\frac{2}{z}+\frac{2}{z^2}\right)+2\left(\frac{kT}{Q_a}\right)\left(1+\frac{4}{z}+\frac{6}{z^2}\right)+2\left(\frac{kT}{Q_a}\right)^2\left(1+\frac{6}{z}+\frac{12}{z^2}\right)\right]; \quad \text{(A23)}$$

while for $q_a < 0$

$$I_- = \frac{2\exp-(z+|Q_a/kT|)}{z^3}|q_a|^2\left[1+\left|\frac{2}{q_a}\right|\left(1+\frac{3}{z}\right)+\left|\frac{1}{q_a}\right|^2\left(1+\frac{6}{z}+\frac{12}{z^2}\right)\right]. \quad \text{(A23')}$$

Note that equations (A23) and (A19') yield for $kT < m_e c^2$ and $kT < Q_a$ the following expression:

$$f(e_c^-) = 2\pi^3 aZ\left\langle\frac{F_-}{2\pi\eta}\right\rangle n_-\left(\frac{\hbar}{m_e c}\right)^3\left(\frac{2m_e c^2}{\pi kT}\right)^{1/2} q_a^2. \quad \text{(A24)}$$

There is an interesting point to be noted about the case $q_n < -1$ or $Q_n < - m_e c^2$. It will be recalled that expression (A19) for $\lambda(e_c^{\pm})$ which includes the term for $I_\pm$ given by (A20') must be multiplied by s from equation (A1) to obtain the effective decay rate under stellar conditions. From s and $I_\pm$, the factor $\exp -(|Q_n| + E^*)/kT$ can be abstracted, where we recall that E^* is the excitation of the initial nucleus. Now, $|Q_n| + E^*$ is the same for transitions to a given final nucleus in a given state from all initial states for which $Q_n < -m_e c^2$. We have $|Q_n| + E^* = |Q_{ng}|$ where g designates the ground state of the initial nucleus for which $E_g^* = 0$. Thus, in the important exponential term, all initial states "bound" as far as beta-decay is concerned are equivalent. The required excitation can be supplied either by photon energy or by the captured electron's energy. The polynomial factor in equation (A20') does, of course, depend on the individual q_n or Q_n values, favoring the ground state. For $q_n > -1$, $sI_\pm$ from equation (A1) and (A20), with $Q_n = Q_{ng} + E^*$ exhibits a complicated dependence on E^*, the polynomial factor in $q_n = (Q_{ng} + E^*)/m_e c^2$ tending to compensate for the exponential factor $\exp - E^*/kT$. However, for the case of primary interest in the main text where $T_9 = 3.78$, $z = 1.57$, it can be shown that the maximum value for $I_\pm \exp - E^*/kT$ occurs for the ground state $E_g^* = 0$. Thus, if the ground state of the initial nucleus has an allowed transition to a low-lying state of the final nucleus, this transition will dominate in the decay rate. However, if an excited state has a high J-value and an allowed transition to a lower state in the final nucleus, say, the ground state, it may dominate. Other things being equal, transitions to the ground state of the final nucleus are favored.

b) Numerical Evaluation of Beta-Interaction Rates

The various beta-interaction rates which have been presented in this appendix will now be evaluated numerically. We define an effective matrix element squared by

$$|M|^2 = |M_F|^2 + \left(\frac{C_A}{C_V}\right)^2 |M_{GT}|^2 = |M_F|^2 + 1.40\,|M_{GT}|^2. \quad \text{(A25)}$$

With this definition, from equations (A3), (A6), and (A13) we find

$$\log ft = 3.78 - \log |M|^2 . \tag{A25'}$$

For allowed transitions near $Z = 26$, $\log ft = 4.1$ to 5.8 and $|M|^2 = 0.5$ to 0.01. Then for all energies in MeV and all rates in sec^{-1}

$$\lambda(\beta^{\pm}) = 4.98 \times 10^{-6} Z |M|^2 \left\langle \frac{F_{\pm}}{2\pi\eta} \right\rangle (Q_n^5 - 1.33 Q_n^2 + 1.02 Q_n - 0.21), \tag{A26}$$

$$\lambda(\beta^{+}) = 2.49 \times 10^{-6} Z |M|^2 (Q_{a'}^5 + 2.56 Q_{a'}^4 + 2.61 Q_{a'}^3), \tag{A27}$$

with $Q_{a'} = Q_a - 1.022$ MeV $= Q_n - 0.511$ MeV, $Z = Z$ (final nucleus), and $\langle F_+/2\pi\eta \rangle = 0.5$. Similarly

$$\lambda(\beta^{-}) = 0.80 \times 10^{-5} Z |M|^2 (Q_a^5 + 2.56 Q_a^4 + 2.61 Q_a^3), \tag{A28}$$

with $Q_a = Q_n - 0.511$ MeV, $Z = Z$ (final nucleus), and $\langle F_-/2\pi\eta \rangle = 1.6$. Finally

$$\lambda(e_b^{-}) = 1.07 \times 10^{-9} Z^3 |M|^2 Q_a^2 , \tag{A29}$$

with $Q_a = Q_n + 0.511$ MeV, $Z = Z$ (initial nucleus).

In order to express the continuum capture rates numerically, we choose the conditions of major interest in the main text: $T_9 = 3.78$, $z = 1.57$, $\rho_6 = 3.12$, $n_- = 1.22 \times 10^{30}$ per cm^3, $n_+ = 0.28 \times 10^{30}$ per cm^3, and $n_1 = 0.58 \times 10^{30}$ per cm^3. Then, for $Q_n > -0.511$ MeV and $Z = Z$ (initial nucleus),

$$\lambda(e_c^{\pm}) = 0.82 \times 10^{-5} Z |M|^2 \left\langle \frac{F_{\pm}}{2\pi\eta} \right\rangle \left(\frac{n_{\pm}}{n_1} \right) (Q_n^2 + 2.28 Q_n + 1.57), \tag{A30}$$

and for $Q_n < -0.511$ MeV

$$\lambda(e_c^{\pm}) = 1.03 \times 10^{-5} Z |M|^2 \left\langle \frac{F_{\pm}}{2\pi\eta} \right\rangle \left(\frac{n_{\pm}}{n_1} \right) \times (|Q_n|^2 + 1.95 |Q_n| + 1.27) \exp - 3.07 |Q_n| . \tag{A31}$$

Thus, for $Q_a = Q_n + 0.511$ MeV > 0 and $\langle F_-/2\pi\eta \rangle = 1.6$,

$$\lambda(e_c^{-}) = 2.76 \times 10^{-5} Z |M|^2 (Q_a^2 + 1.26 Q_a + 0.665), \tag{A32}$$

and for $Q_a = Q_n + 0.511$ MeV < 0,

$$\lambda(e_c^{-}) = 0.724 \times 10^{-5} Z |M|^2 (|Q_a|^2 + 2.97 |Q_a| + 2.53) \exp - 3.07 |Q_a| , \tag{A33}$$

where $\exp -3.07 |Q_a| = 10^{-1.33|Q_a|}$. For consistency in numerical computations, three significant figures have been retained in the above expressions. The uncertainties arising from the factor $\langle F_{\pm}/2\pi\eta \rangle$ may be as high as 10 per cent in electron cases and 50 per cent in positron cases.

Again it must be emphasized that the decay rates given by equations (A26)–(A33) apply to a transition between a specific initial state and a specific final state. For a given initial state a sum must be performed over the transition rates to all final states. This sum must be multiplied by the statistical factor s from equation (A1). Then to determine the effective decay rate for a given nuclear species, a sum must be performed over the effective decay rates for its ground and excited states. We can represent the situation by

$$\tau_{\text{star}} = \frac{1}{\lambda_{\text{star}}} = \frac{1}{s\chi\lambda} , \tag{A34}$$

where λ is the decay rate for a specific transition of interest from an initial state having population weight s, while χ formally represents the summations of the effective decay rates over all transitions from all initial states divided by the effective decay rate $s\lambda$ for the specific transition. We will not explicitly evaluate χ in our calculations, but it is clear that χ is always greater than unity and equation (A34) will be useful only when the specific transition involved dominates the transition rate so that $\chi \sim 1$.

c) Stellar Rates Evaluated from Terrestrial Data

Calculations of electron-capture rates in stars using the preceding equations require a knowledge of the square of the nuclear matrix element for the transition or transitions involved. In some cases this is known from terrestrial measurements of the lifetime and energy of the transition. The simplest procedure is then to take the ratio of the two appropriate equations so that $|M|^2$ cancels out of the resulting relation. Thus, if the bound electron-capture rate has been measured in the laboratory, then $Q_a > 0$ and one has from the ratio of equations (A29)–(A32)

$$\frac{\lambda(e_b^-)}{\lambda(e_c^-)}=\frac{f(e_b^-)}{f(e_c^-)}=\frac{(\alpha Z)^2(q_a^2/I_-)}{\langle F_-/2\pi\eta\rangle(n_-/n_1)}=3.87\times 10^{-5}\frac{Z^2}{\left[1+\left(\frac{1.26}{Q_a}\right)+\left(\frac{0.665}{Q_a^2}\right)\right]}. \quad \text{(A35)}$$

The appropriate Q_a will be that for the ground state or long-lived isomeric state since laboratory measurements are only possible in general on the ground state or isomeric state of the capturing nucleus. It must always be borne in mind that excited states for which $\lambda(e_b^-)$ is not known may contribute significantly to the decay rate in stars, especially if the ground-state decay is forbidden and thus equation (A35) when inverted may not give the over-all $\lambda(e_c^-)$ in stars.

If the positron emission rate has been measured, then $Q_a > 1.02$ MeV and $Q_a' > 0$ and one has from the ratio of equations (A27)–(A32) taking Z(initial) $\approx$ Z(final):

$$\frac{\lambda(\beta^+)}{\lambda(e_c^-)}=\frac{f(\beta^+)}{f(e_c^-)}=\frac{\langle F_+/2\pi\eta\rangle}{\langle F_-/2\pi\eta\rangle}\frac{\left[\frac{(q_a-2)^5}{30}+\frac{(q_a-2)^4}{6}+\frac{(q_a-2)^3}{3}\right]}{(n_-/n_1)I_-} \quad \text{(A36)}$$

$$=0.090\frac{(Q_{a'}{}^5+2.56Q_{a'}{}^4+2.61Q_{a'}{}^3)}{(Q_a^2+1.26Q_a+0.665)}.$$

If it is assumed that the positron decay rate is unchanged in the star and that bound-electron capture in the star can be ignored on the assumption of complete ionization, then

$$\frac{\tau_{\rm star}(Z\to Z-1)}{\tau_{\rm terr}(Z\to Z-1)}=\frac{1}{s\chi}\frac{\lambda(e_b^-)+\lambda(\beta^+)}{\lambda(e_c^-)+\lambda(\beta^+)}=\frac{\lambda(e_b^-)}{s\chi\lambda(e_c^-)}\left[\frac{1+\lambda(\beta^+)/\lambda(e_b^-)}{1+\lambda(\beta^+)/\lambda(e_c^-)}\right] \quad \text{(A37)}$$

$$=\frac{\lambda(\beta^+)}{s\chi\lambda(e_c^-)}\left[\frac{1+\lambda(e_b^-)/\lambda(\beta^+)}{1+\lambda(\beta^+)/\lambda(e_c^-)}\right].$$

There are important cases in which the terms in brackets in one or the other of the last two terms in equation (A37) may be set equal to unity. It will be clear in this connection that a useful ratio is

$$\frac{\lambda(\beta^+)}{\lambda(e_b^-)}=\frac{2.33\times 10^3}{Z^2}\frac{(Q_{a'}{}^5+2.56Q_{a'}{}^4+2.61Q_{a'}{}^3)}{Q_a^2}. \quad \text{(A38)}$$

The statistical factor s has been introduced into equation (A37) for reasons already discussed—the state for which $\tau_{\rm terr}$ is known has relative statistical weight s in the star. We

emphasize that the ratios in equations (A35), (A36), and (A38) apply to allowed transitions between the same pair of initial and final states. The factor χ has been introduced in equation (A37) as in equation (A34) to indicate that the state for which τ_{terr} is known may not be the only one which contributes significantly to $\lambda_{star} = 1/\tau_{star}$.

If negative electron emission has been measured in the laboratory, then the stellar lifetime of the reverse reaction—endoergic continuum electron capture—can be calculated from the ratio of equations (A28)–(A33). We take $Q_a < 0$ and $Q_a > 0$ from the stellar point of view and then

$$\frac{\tau_{star}(Z \rightarrow Z-1)}{\tau_{terr}(Z \rightarrow Z-1)} = \frac{\lambda(\beta^-)}{s\chi\lambda(e_c^-)}$$
$$= \frac{1.11}{s\chi} \frac{(|Q_a|^5 + 2.56|Q_a|^4 + 2.61|Q_a|^3)}{(|Q_a|^2 + 2.97|Q_a| + 2.53)} \exp 3.07|Q_a|. \quad \text{(A39)}$$

We have used equation (A11) to determine the numerator in equation (A39). For light nuclei it is preferable to use equation (A12) without approximation.

d) Stellar Rates Evaluated from Estimated Matrix Elements

Terrestrial information is not available for certain transitions of importance in the termination of the *e*-process and in other astrophysical applications. Under these circumstances it is not possible to use equations (A35)–(A39), and it is necessary to make an estimate for $|M|^2$ which appears in equations (A26)–(A33). Moreover, in the transition between a given initial nucleus and a given final nucleus, it is necessary to make a determination on theoretical grounds of the states of these nuclei between which the most probable transitions occur. In some cases little is known about the excited states, and nuclear models must be employed to furnish some information on level structure, spacings, spins, and parities.

The procedures which we have employed will now be outlined and then applied to the decay of nuclei which are of primary interest in the main text, namely, $Ni^{56,57,58}$ and $Fe^{54,55,56}$. It is first necessary to establish those transitions which are allowed, i.e., those for which $\Delta J = 0, \pm 1$, $\Delta\Pi = 0$ for the change in spin and parity between the initial and final states. In estimating $|M|^2$ for the allowed transitions there is a further complication which is best discussed in terms of the nuclear-shell model. In this model with a simple harmonic potential, nucleons progressively fill nuclear orbitals of increasing radial quantum number and increasing orbital angular momentum, viz: $1s^+$, $1p^-$, $1d^+$, $2s^+$, $1f^-$, $2p^-$, etc., etc. Parity (Π) of the orbitals is indicated by a $\pm$ superscript. Spin-orbit splitting leads to the following ordering of the orbitals: $1s_{1/2}^+(\underline{2})$, $1p_{3/2}^-(6)$, $1p_{1/2}^-(\underline{8})$, $1d_{5/2}^+(14)$, $2s_{1/2}^+(16)$, $1d_{3/2}^+(\underline{20})$, $1f_{7/2}^-(\underline{28})$, $2p_{3/2}^-(32)$, $1f_{5/2}^-(38)$, etc., etc. The numbers in parentheses indicate the number of nucleons which can be accommodated in the filling of a given orbital and all previous ones. Those numbers underlined are the so-called magic numbers designating closed shells or important subshells in nuclei. For the iron-group nuclei and for their predecessors in the *e*-process, we have $22 \leq Z \leq 28$ and $24 \leq N \leq 34$. On the basis of the strict shell model, particularly for ground states, the outer protons fall in the $1f_{7/2}^-$ orbital while the neutrons fall in this orbital for $N \leq 28$ and in the $2p_{3/2}^-$ or $1f_{5/2}^-$ orbitals for $N > 28$. However, the configurations for excited states and even for ground states are not at all pure and can be represented by mixed percentages of $1f_{7/2}^-$, $2p_{3/2}^-$ and $1f_{5/2}^-$ orbitals. In addition, for $N > 28$ holes can occur in the $1f_{7/2}^-$ subshell. The implications of these points arise from the fact that in strictly allowed beta-interactions involving the transformation of a single nucleon from a proton into a neutron or vice versa, the orbital angular momentum of the nucleon does not change. On Fermi selection rules the leptons are emitted with zero total spin. Thus there is no nucleon spin flip and the nucleon remains in its original orbital. On Gamow-Teller

selection rules the leptons do carry off one unit of angular momentum, the result being a nucleon spin flip as for example in $1f_{7/2}^- \rightarrow 1f_{5/2}^-$ or vice versa. For the orbitals of interest at this point the l-allowed transitions are $1f_{7/2}^- \rightarrow 1f_{7/2}^-$ or $1f_{5/2}^-$, $1f_{5/2}^- \rightarrow 1f_{5/2}^-$ or $1f_{7/2}^-$ and $2p_{3/2}^-$ to $2p_{3/2}^-$. The other possibilities such as $2p_{3/2}^- 1f_{5/2}$ to are l-forbidden. In transitions allowed by $\Delta J = 0, \pm 1$, $\Delta\Pi = 0$ the actual value of the matrix element $|M|^2$ will depend, among other things, upon the possibilities for l-allowed transitions between the initial and final states. For example, ${}_{24}Cr_{24}{}^{48}(0^+)$ decays 100 per cent by bound electron capture to the 0.42-MeV state in ${}_{23}V_{25}{}^{48}(1^+)$ with a mean lifetime of 1.2×10^5 sec and an energy $Q_a = 0.98$ MeV. From equations (A29) and (A25′) we find $|M|^2 = 0.4$ and $\log ft = 4.2$. This relatively large value for $|M|^2$ can be attributed to the fact that ${}_{24}Cr_{24}{}^{48}$ predominantly has the neutron (n)-proton (p) configurations $(1f_{7/2}^-)_n{}^4$ $(1f_{7/2}^-)_p{}^4 : 0^+$ while ${}_{23}V_{25}{}^{48}$ predominantly has the configurations $(1f_{7/2}^-)_n{}^5$ $(1f_{7/2}^-)_p{}^3 : 1^+$ so that in the transition a $1f_{7/2}^-$ proton transforms into a $1f_{7/2}^-$ neutron as permitted by Fermi selection rules. On the other hand, in the discussion below of the $Fe^{55}(3/2^-)$ transition to $Mn^{55}(5/2^-)$, which is allowed on the basis of $\Delta J = 0, \pm 1$, $\Delta\Pi = 0$, we will find that l-forbiddenness is a reasonable explanation for the fact that $|M|^2 = 0.008$ and $\log ft = 5.9$.

In the cases involving nickel and iron isotopes which have been previously noted as being of primary interest we have $Z \leq 28$ and $N \geq 28$. Thus in proton to neutron transformations, the transitions between the strict shell-model orbitals $(1f_{7/2}^-)_p$ and $(2p_{3/2}^-)_n$ are forbidden. The $|M|^2$ are determined by the mixing in of other orbitals. We have made an analysis of observed $|M|^2$ values in the region $52 \leq A \leq 59$ and concluded that when substantial mixing occurs, $|M|^2 \sim 0.1$ or $\log ft \sim 4.8$. The values for allowed transitions range down to $|M|^2 \sim 0.01$ ($\log ft = 5.8$) and even lower in a few cases and this we attribute to l-forbiddenness, i.e., almost pure configurations between which l-allowed transitions cannot occur. In the detailed analysis to follow on Ni^{56}, etc., we have used the shell model as a guide in order to determine those transitions which are substantially l-allowed and have employed $|M|^2 \sim 0.1$ in these cases. These transitions are primarily those between the ground state of the initial or final nucleus and appropriate excited states of the other nucleus. We consider excitations of only one nucleon. In the excited states of the initial nucleus a proton raised to $(2p_{3/2}^-)_p$ decays to a neutron in the same orbital in the ground state of the final nucleus. Alternatively a neutron in the initial nucleus can be excited out of the $(1f_{7/2}^-)_n$ closed shell so that a $(1f_{7/2}^-)$ proton can transform to fill the shell once again in the beta-interaction. The final nucleus may have excited states containing a $(2p_{3/2}^-)$ neutron to which the $(2p_{3/2}^-)$ proton in the ground state of the initial nucleus may decay. Our procedure probably overestimates the decay rates and underestimates the decay lifetimes, but this is compensated by the fact that we probably overlook many allowed transitions and neglect forbidden transitions entirely. The lifetimes to be quoted are probably accurate to within an order of magnitude, i.e., to within a factor of 3 either way.

e) Specific Cases

The reader is referred to Way *et al.* (1961) for energy level diagrams of the nuclei discussed in the specific beta transformations which follow.

${}_{28}Ni_{28}{}^{56}$–${}_{27}Co_{29}{}^{56}$.—The ground state of Ni^{56} is described on the strict shell model by $(1f_{7/2}^-)_n{}^f$ $(1f_{7/2}^-)_p{}^f : 0^+$ where f designates a *filled* subshell when used as a superscript. Wells, Blatt, and Meyerhof (1963) have shown that Ni^{56} decays primarily ($\gtrsim 94$ per cent) to the 1.74-MeV state in Co^{56} with possible weak transitions ($\lesssim 3$ per cent) to two lower states. They find the half-life to be 6.1 *d*. Taking Ni^{56}–$Co^{56} = 2.103 \pm 0.016$ MeV from Part VI, we find $\tau_{terr} = 8.5 \times 10^5$ sec, $|M|^2 = 0.39$, $\log ft = 4.2$ for the 0.36-MeV transition to the 1.74-MeV state and $\log ft > 6$ for the other possible transitions. Equations (A29) and (A25′) have been used to obtain $|M|^2$ and $\log ft$. The 0.36-MeV transition is certainly allowed. The 1.74-MeV state in Co^{56} presumably has $J^\pi = 1^+$ arising

from the orbital $(1f_{5/2}^-)_n^{+1}$ which represents one neutron in the $1f_{5/2}^-$ subshell plus the orbital $(1f_{7/2}^-)_p^{-1}$, which represents a hole in the $1f_{7/2}^-$ subshell for protons. In the transition a $1f_{7/2}^-$ proton in Ni^{56} transforms into a $1f_{5/2}^-$ neutron in Co^{56}*. The ground state of Co^{56} is $(2p_{3/2}^-)_n^{+1}$ $(1f_{7/2}^-)_p^{-1}$: 4^+ on the shell model with spin and parity experimentally determined. Three other low-lying excited states in Co^{56} probably correspond to the 2^+, 3^+, and 5^+ states also expected for the ground-state configuration. Other low-lying states found by Miller *et al.* (1963) probably correspond to $(1f_{5/2}^-)_n^{+1}$ $(1f_{7/2}^-)_p^{-1}$: 1^+ to 6^+. The ground state of $Ni^{56}(O^+)$ has an allowed transition, as observed, only to the 1^+ state among all of these states. On the basis of the 0.36-MeV transition and neglecting the forbidden transitions we find from equations (A35) and (A37) that $\tau_{star}/\tau_{terr} = 3.1 \times 10^{-3}$ so that $\tau_{star} = 2700$ sec at $T_9 = 3.8$, $\rho_6 = 3.1$.

Experimental information has recently become available on three and possibly four excited states in Ni^{56} through the studies of Miller *et al.* (1963) and Hoot *et al.* (1963). These states may correspond to the 2^+, 3^+, 4^+, and 5^+ states expected in Ni^{56} from the excited configurations $(1f_{7/2}^-)_n^f$ $(1f_{7/2}^-)_p^{-1}$ $(2p_{3/2}^-)_p^{+1}$ or $(1f_{7/2}^-)_n^{-1}$ $(2p_{3/2}^-)_n^{+1}$ $(1f_{7/2}^-)_p^f$. The only state with low enough excitation energy to be of interest in the present discussion is the state at 2.68 ± 0.02 MeV with spin and parity probably equal to 2^+. This state can have allowed transitions with the emission of high-energy positrons to low-lying 1^+, 2^+ and 3^+ states in Co^{56}. However, the population factor is only $\sim 10^{-3}$ times that for the ground state of Ni^{56} at $T_9 = 3.8$. A rough estimate indicates that the excited state may enhance the decay rate by 20–50 per cent. Thus we adopt $\tau_{star}(Ni^{56}) \sim 2000$ sec at $T_9 = 3.8$, $\rho_6 = 3.1$.

$_{28}Ni_{29}^{57}$–$_{27}Co_{30}^{57}$.—On the strict shell model the ground state of Ni^{57} is $(2p_{3/2}^-)_n^{+1}$ $(1f_{7/2}^-)_p^f$: $3/2^-$ while that of Co^{57} is $(2p_{3/2}^-)_n^{+2}$ $(1f_{7/2}^-)_p^{-1}$: $7/2^-$ where the spin and parities have been experimentally determined. On this basis a beta-transition between the ground states is forbidden ($\Delta J > 1$) and indeed is not observed. The ground state of Ni^{57} is observed to decay with half-life $37h$ about equally by positron emission and electron capture to three excited states in Co^{57}: $3/2^-$ at 1.37 MeV, $1/2^-$ at 1.49 MeV, and $5/2^-$ at 1.90 MeV. The transition energies for electron capture are 1.87, 1.73, and 1.34 MeV with $\log ft = 5.6$, 6.1, and 5.4, respectively. The $|M|^{12}$ are of the order of 0.01. This suggests that these excited states of Co^{57} can be described in part at least by a neutron configuration $(2p_{3/2}^-)_n^{+1}$ $(1f_{5/2}^-)_n^{+1}$ in which one neutron lies in the $1f_{5/2}^-$ orbitral so that in the transition a $1f_{7/2}^-$ proton transforms into a $1f_{5/2}^-$ neutron. Alternatively the ground state of Ni^{57} may be described in part by a proton configuration $(1f_{7/2}^-)_p^{-1}$ $(2p_{3/2}^-)_p^{+1}$ so that in the transition a $2p_{3/2}^-$ proton transforms into a $2p_{3/2}^-$ neutron. Using equations (A35) and (A37) and summing over the three transitions, we find that $\tau_{star} = 7000$ sec for the ground state of Ni^{57} at $T_9 = 3.8$, $\rho_6 = 3.1$. However, there is the strong possibility that excited states of Ni^{57} based on the excited configurations $(2p_{3/2}^-)_n^{+1}$ $(1f_{7/2}^-)_p^{-1}$ $(2p_{3/2}^-)_p^{+1}$ or $(2p_{3/2}^-)_n^{+2}$ $(1f_{7/2}^-)_n^{-1}$ $(1f_{7/2}^-)_p^f$ will give a considerably smaller lifetime. In fact if we assume that several such states ($5/2^-$, $7/2^-$, $9/2^-$) cluster around an excitation energy of 1.5 MeV with $|M|^2 \sim 0.1$ we find $\tau_{star} \approx 6000$ sec for the transition to the ground state of Co^{57} alone. Combining 7000 sec and 6000 sec one finds $\tau_{star} \approx 3200$ sec. A reasonable estimate for additional transitions to the low-lying states of Co^{57} already described leads us to adopt $\tau_{star}(Ni^{57}) \sim 2000$ sec at $T_9 = 3.8$, $\rho_6 = 3.1$.

$_{28}Ni_{30}^{58}$–$_{27}Co_{31}^{58}$.—On the strict shell model the ground state of Ni^{58} is $(2p_{3/2}^-)_n^{+2}$ $(1f_{7/2}^-)_p^f$: O^+ while that of Co^{58} is $(2p_{3/2}^{-1})_n^{+3}$ $(1f_{7/2}^-)_p^{-1}$: 2^+ where the spins and parities have been experimentally determined. Ni^{58} is 0.38-MeV stable relative to Co^{58} and electron capture from the high-energy tail of the electron continuum is forbidden since $\Delta j = 2$. The first excited state of Ni^{58} at 1.45 MeV with $J^\pi = 2^+$ can be reasonably assumed to be made up in part by the configurations $(2p_{3/2}^-)_n^{+2}$ $(1f_{7/2}^-)_p^{-1}$ $(2p_{3/2}^-)_p^{+1}$: 2^+ or $(2p_{3/2}^-)_n^{+3}$ $(1f_{7/2}^-)_n^{-1}$ $(1f_{7/2}^-)_p^f$: 2^+. The transition is then allowed and $s \approx 5$ exp $(-5.0/3.8 \times 1.45) = 0.06$ in equation (A34) is not prohibitively small. With $|M|^2 =$

0.1 and $Q_a = 1.07$ MeV we find $\tau_{star} = 1/s\lambda\ (e_c^-) = 7 \times 10^4$ sec. In consideration of other possible transitions we adopt $\tau_{star}\ (Ni^{58}) \sim 5 \times 10^4$ sec at $T_9 = 3.8$, $\rho_6 = 3.1$.

$_{26}Fe_{28}^{54}$–$_{25}Mn_{29}^{54}$.—The endoergic transition (−0.69 MeV) from the stable ground state of Fe^{54}, $(1f_{7/2}^-)_n^f\ (1f_{7/2})_p^{-2}$: O^+, to the ground state of Mn^{54}, $(2p_{3/2}^-)_n^{+1}\ (1f_{7/2})_p^{-3}$: 3^+ is forbidden. Endoergic transitions to the low-lying states of Mn^{54} at 0.06, 0.18, and 0.40 MeV are also presumably forbidden since these states are probably the 2^+, 4^+, 5^+, states also expected from the ground-state configuration. It is reasonable to expect that the 2^+ excited state of Fe^{54} at 1.41 MeV is made up in part of the configurations $(1f_{7/2}^-)_n^f\ (1f_{7/2}^{-1})_p^{-3}\ (2p_{3/2}^-)_p^{+1}$: 2^+ or $(1f_{7/2}^-)_n^{-1}\ (2p^-)_n^{+1}\ (1f_{7/2})_p^{-2}$: 2^+ from both of which transitions to the 2^+ and 3^+ states of Mn^{54} are allowed. As in the case of Ni^{58} the statistical factor s is not too small and with $|M|^2 = 0.1$ for the several transitions possible we find $\tau_{star}(Fe^{54}) \sim 4 \times 10^4$ sec at $T_9 = 3.8$, $\rho = 3.1$. Transitions from the ground state of Fe^{54} to excited states ($E^* \geq 1.0$ MeV, $|Q_a| \geq 1.69$ MeV) in Mn^{54} having configurations in part describable as $(1f_{5/2})_n^{+1}\ (1f_{7/2})_p^{-3}$ do not greatly decrease the effective lifetime.

$_{26}Fe_{29}^{55}$–$_{25}Mn_{30}^{55}$ *and* $_{27}Co_{28}^{55}$–$_{26}Fe_{29}^{55}$.—The ground state of Fe^{55} is $(2p_{3/2}^-)_n^{+1}\ (1f_{7/2}^-)_p^{-2}$: $3/2^-$ while that of Mn^{55} is $(2p_{3/2}^-)_n^{+2}\ (1f_{7/2}^-)_p^{-3}$: $5/2^-$. The 0.23-MeV transition occurs 100 per cent by electron capture with half-life 2.7 year so that $|M|^2 = 0.008$ and log $ft = 5.9$. The low value for $|M|^2$ can be understood on the basis that the transition is l-forbidden. The corresponding value for τ_{star} is approximately 1.5×10^5 sec. However, Fe^{55} has excited states at 0.41, 0.93 ($5/2^-$), 1.32, 1.41 ($7/2^-$), and 1.50 MeV and numerous additional states at higher energies, while Mn^{55} has a $7/2^-$ state at 0.13 MeV. If the reasonable assumption is made that the excited states of Fe^{55} are made up in part of the configurations $(2p_{3/2}^-)_n^{+1}\ (1f_{7/2}^-)_p^{-3}\ (2p_{3/2}^-)_p^{+1}$ or $(1f_{7/2}^-)_n^{-1}\ (2p_{3/2}^-)_n^{+2}\ (1f_{7/2}^-)_p^{-2}$, then there are numerous allowed transitions to the two low states of Mn^{55}. On this basis we find $\tau_{star}(Fe^{55}) \sim 10^4$ sec at $T_9 = 3.8$, $\rho = 3.1$. For the $_{27}Co_{28}^{55}$ decay, with energy 3.46 MeV and terrestrial lifetime 26 hours, we find $\tau_{star}(Co^{55}) \sim 2 \times 10^3$ sec, again mainly due to excited states which decrease the lifetime by a factor of ~10.

$_{26}Fe_{30}^{56}$–$_{25}Mn_{31}^{56}$.—The ground state of Mn^{56}, $(2p_{3/2}^-)_n^{+3}\ (1f_{7/2}^-)_p^{-3}$: 3^+ is heavier than the ground state of Fe^{56}, $(2p_{3/2}^-)_n^{+2}\ (1f_{7/2}^-)_p^{-2}$: O^+ in mass-energy equivalent units by 3.71 MeV. The electron emission transition is forbidden terrestrially and in stars the reverse transition is very endoergic. This situation for Fe^{56} is typical for the stable nuclei Ti^{48}, Cr^{52}, Fe^{56}, Ni^{60}, and Zn ^{64}, which are reached after the nuclei resulting in the α-process such as Ni^{56} have undergone the transformation of two protons into neutrons. Electron capture by the stable nuclei such as Fe^{56} from the tail of the electron continuum can be expected to be very slow, while the electron emission from Mn^{56} is known to be relatively fast. Only when Mn^{56} is very rare compared to Fe^{56} under stellar conditions will the third proton transformation take place. This is borne out by our detailed calculations. Mn^{56} does decay by electron emission with 2.6 hour half-life to at least four excited states of Fe^{56} and in several cases $|M|^2 \sim 0.01$ to 0.1 indicating that configurations of the type discussed under Fe^{54} and Fe^{55} contribute to these excited states of Fe^{56}.

Moreover Mn^{56} has an excited state at 0.11 MeV having $J^\pi = 1^+$ so that an allowed transition to the ground state (O^+) of Fe^{56} is possible. Taking all possibilities into account we find $\tau_{star}(Fe^{56}) \sim 10^8$ sec ~ 3 years. The corresponding lifetime for the electron decay of Mn^{56} is $\tau_{star}(Mn^{56}) \sim 200$ sec if the (1^+) to (0^+) transition dominates with $|M|^2 \sim 0.1$. On the neutrino loss time scale discussed in the main text it is clear that electron capture by Fe^{56} and similar nuclei to form still more neutron rich nuclei is very slow indeed and is opposed by much more rapid electron decay by Mn^{56} and similar nuclei.

Electron capture by the proton and positron capture by the neutron.—Equation (A39) with $|Q_a| = 0.783$ MeV and $s\chi = 1$ yields

$$\tau_{star}(p) = \tau_-(p) \sim 4 \times 10^3 \text{ sec.} \qquad \text{(A40)}$$

Then for the neutron lifetime to positron capture one has

$$\tau_+(n) = \frac{n_-}{n_+} \exp(-1.294/kT)\, \tau_-(p) \sim 350 \text{ sec.} \tag{A41}$$

Combining this with the natural decay mean lifetime (1000 sec) yields

$$\tau_{\text{star}}(n) \sim 260 \text{ sec.} \tag{A42}$$

The stellar values hold for $T_9 = 3.78$, $\rho_6 = 3.12$, $n_- = 1.22 \times 10^{30}$ electrons cm^{-3} and $n_+ = 0.28 \times 10^{30}$ positrons cm^{-3}.

APPENDIX B

EFFECTS OF ELECTRON-POSITRON PAIRS ON STELLAR STRUCTURE AND EVOLUTION

a) Particle Density

In this appendix we generalize many of the relations used in Parts II and III in regard to the consequences of electron-positron pair formation in polytropic structure and evolution. We start with the exact expression for the Fermi-Dirac number densities of positrons and electrons (eq. [7] of the main text), and introduce a power series expansion for the denominator within the integrand. If the momentum P, temperature T, and chemical potential Φ are replaced by $\eta = P/m_e c$, $z = m_e c^2/kT$, and $\varphi = \Phi/kT$, then the Fermi-Dirac distribution becomes

$$n_\pm = \frac{1}{\pi^2}\left(\frac{m_e c}{\hbar}\right)^3 \int_0^\infty \frac{\eta^2 d\eta}{\exp[z(\eta^2+1)^{1/2} \pm \varphi] + 1} = \frac{1}{\pi^2}\left(\frac{m_e c}{\hbar}\right)^3 \int_0^\infty \eta^2 d\eta \Sigma(-)^{n+1} \exp[-nz(\eta^2+1)^{1/2} \mp n\varphi], \tag{B1}$$

where the summation runs over all integers from $n = 1$ to ∞. Our procedure is exactly that of Chandrasekhar (1939) and of Chandrasekhar and Henrich (1942). The positron density is included on the assumption that the equilibrium $\gamma \rightleftarrows e^+ + e^-$ implies that the chemical potentials (in units kT) obey $\varphi_+ + \varphi_- = 0$ or $\varphi_+ = -\varphi_- = -\varphi$. Integration term by term yields a summation over modified Bessel functions of second order as follows

$$n_\pm = \frac{1}{\pi^2}\left(\frac{m_e c}{\hbar}\right)^3 \sum \frac{(-)^{n+1}}{nz} \exp(\mp n\varphi) K_2(nz). \tag{B2}$$

Again the summation runs over all integers from $n = 1$ to ∞ and this will be the case throughout this appendix. To avoid the singularity in $K_2(nz)$ at $T = \infty$ or $z = m_e c^2/kT = 0$, we introduce

$$\bar{K}_2(nz) = \tfrac{1}{2}(nz)^2 K_2(nz), \tag{B3}$$

which varies from 0 to 1 as T ranges from 0 to ∞ as illustrated for $\bar{K}_2(z)$ in Figure 1. Then

$$n_\pm = \frac{2}{\pi^2}\left(\frac{kT}{\hbar c}\right)^3 \sum \frac{(-)^{n+1}}{n^3} \exp(\mp n\varphi) \bar{K}_2(nz) = 1.688 \times 10^{28} T_9^3 \sum \frac{(-)^{n+1}}{n^3} \exp(\mp n\varphi) \bar{K}_2(nz) \text{ cm}^{-3}. \tag{B4}$$

The number of pair electrons and positrons is just twice the number of positrons. The total number of electrons and positrons per cm^3 can be written

$$n_e = n_- + n_+ = \frac{4}{\pi^2}\left(\frac{kT}{\hbar c}\right)^3 \sum \frac{(-)^{n+1}}{n^3} \cosh n\varphi \bar{K}_2(nz)$$
$$= 3.375 \times 10^{28} T_9^3 \sum \frac{(-)^{n+1}}{n^3} \cosh n\varphi \bar{K}_2(nz)\,\mathrm{cm}^{-3}, \tag{B5}$$

while the difference in number of electrons and positrons per cm^3 can be written

$$n_0 = Zn_N = n_- - n_+ = \frac{4}{\pi^2}\left(\frac{kT}{\hbar c}\right)^3 \sum \frac{(-)^{n+1}}{n^3} \sinh n\varphi \bar{K}_2(nz). \tag{B6}$$

The total number of particles in the gas per cm^3 is

$$n = n_e + n_N = \frac{4}{\pi^2}\left(\frac{kT}{\hbar c}\right)^3 \sum \frac{(-)^{n+1}}{n^3}\left(\cosh n\varphi + \frac{1}{Z}\sinh n\varphi\right) \bar{K}_2(nz). \tag{B7}$$

Great care must be exercised in the use of all equations in this appendix similar to equations (B4)–(B7) as T *approaches zero. Although* $\bar{K}_2$ *goes to zero in this limit,* φ *becomes infinite. The gas becomes completely degenerate.*

Equation (B6) can be used in principle to determine the chemical potential φkT since n_0 is the number of ionization electrons per cm^3 required to neutralize the charge on nuclei, i.e.,

$$n_0 = Zn_N = \frac{\rho Z}{AM_u}, \tag{B8}$$

where n_N is the number of nuclei per cm^3 with charge number Z and atomic mass number A while ρ is the density in gm cm^{-3} and $M_u = 1.6604 \times 10^{-24}$ gm is the atomic mass unit ($C^{12} \equiv 12$). The quantity AM_u should be taken as the mass of the nucleus plus Z electrons. Thus, neglecting small atomic binding energies, tabulated *atomic* masses are sufficiently accurate and are to be employed rather than nuclear masses. A is the exact mass and not an integer.

It might be thought appropriate at this time to include the pair rest-mass energies in the mass density ρ. This can easily be done. It will be noted, however, that radiation energies and electron-positron kinetic energies are comparable to rest-mass energies at the temperatures at which pairs are created by the radiation field. The theory of general relativity indicates that all forms of mass-energy contribute to the inertial and gravitational "mass" in dynamical equations. There is thus some arbitrariness in dividing the mass-energy density into two terms, $\rho + u/c^2$, where ρ is the mass density and u is the internal energy density. We find it best to include the rest mass of particles produced by the radiation field in u/c^2 rather than in ρ. Then the total number of nuclei and associated electrons in a stellar system is invariant to structural evolution over time intervals in which no nuclear reactions (no nuclear phase change) take place. This means that ρ scales inversely as the cube of the radius of the stellar system while otherwise it would not as new particles are created. In case nuclear reactions take place the original number of nucleons remains invariant and an appropriate choice for ρ can still be made. Further considerations along these lines are beyond the scope of the present paper but are important in general relativistic situations and are discussed in HFB[2] (1964).

At this point attention will be turned to approximations valid under various circumstances, non-degenerate (ND), extreme non-degenerate (END), non-relativistic (NR), and extreme relativistic (ER). All approximations will be labeled appropriately and all approximate or limiting equalities will be indicated uniformly by $\approx$ rather than $=$,

more in a precautionary physical sense than in an attempt at spurious mathematical rigor. In those END approximations in which only the first term in the appropriate series is retained, the sign $\sim$ will be used. We do not consider degenerate situations.

The expression "extreme relativistic" requires some qualification in regard to its use throughout this paper. It applies only to electrons and positrons in the sense that $kT \gg m_e c^2$ or $T_9 \gg 6$. However, we do not consider the formation of muon or other pairs so $kT < m_\mu c^2$ or $T_9 < 10^3$. Furthermore, we never consider nuclei to be relativistic.

Non-relativistic approximations for the various number densities above can be found in terms of the low temperature ($kT < n\, m_e c^2$) approximation for the $\tilde{K}_2$, namely,

$$\tilde{K}_2(nz) \approx \left(\frac{\pi}{8}\right)^{1/2} (nz)^{3/2} \exp(-nz). \qquad \text{NR} \quad \text{(B9)}$$

In case $\tilde{K}_2(nz)$ appears with terms of order unity we frequently neglect it entirely in NR approximations. The use of equation (B9) yields

$$n_\pm \approx 2\left(\frac{m_e kT}{2\pi\hbar^2}\right)^{3/2} \sum \frac{(-)^{n+1}}{n^{3/2}} \exp(\mp n\varphi - nz), \qquad \text{NR} \quad \text{(B10)}$$

$$n_e \approx 4\left(\frac{m_e kT}{2\pi\hbar^2}\right)^{3/2} \sum \frac{(-)^{n+1}}{n^{3/2}} \cosh n\varphi \exp(-nz), \qquad \text{NR} \quad \text{(B11)}$$

and

$$n_0 \approx 4\left(\frac{m_e kT}{2\pi\hbar^2}\right)^{3/2} \sum \frac{(-)^{n+1}}{n^{3/2}} \sinh n\varphi \exp(-nz), \qquad \text{NR} \quad \text{(B12)}$$

$$n \approx 4\left(\frac{m_e kT}{2\pi\hbar^2}\right)^{3/2} \sum \frac{(-)^{n+1}}{n^{3/2}} \left(\cosh n\varphi + \frac{1}{Z}\sinh n\varphi\right) \exp(-nz)$$

$$\approx 3.054 \times 10^{29} T_9^{3/2} \sum \frac{(-)^{n+1}}{n^{3/2}} \left(\cosh n\varphi + \frac{1}{Z}\sinh n\varphi\right) \exp(-nz). \qquad \text{NR} \quad \text{(B13)}$$

It will be apparent that the series in these expressions will converge only for

$$\varphi \leq z, \qquad \text{NR} \quad \text{(B14)}$$

or in terms of the chemical potential

$$\Phi \leq m_e c^2. \qquad \text{NR} \quad \text{(B15)}$$

For φ in excess of z the series terms for large n diverge exponentially between alternate positive and negative values. These conditions for non-degeneracy will be extended to the relativistic case in the last section of this appendix. Expression (B10), when applied to positrons, is an exception to expressions (B14) and (B15). For matter as opposed to antimatter, $\varphi \geq 0$, so expression (B10) is always a fair approximation for positrons in stars (not antistars) since the terms in the series for n_+ contain exp $(-n\varphi - nz)$. In antimatter $\varphi \leq 0$ and the positrons are non-degenerate for $-\varphi \leq z$ or $|\varphi| \leq z$. For $|\varphi| > z$ either the electrons or positrons are degenerate, and in this case Peterson and Bahcall (1963) have shown that $\phi_\pm \approx \mp W_F/kT$, where W_F is the Fermi energy including rest mass.

The non-degenerate approximation for electrons used throughout the main text as appropriate for massive stars neglects unity in the integrand of equation (B1) relative to the exponential term. This is equivalent to retaining only the first term in the expression (B4), or

$$n_\pm \approx n_1 \exp(\mp\varphi), \qquad \text{ND} \quad \text{(B16)}$$

with

$$n_1 = \frac{2}{\pi^2}\left(\frac{kT}{\hbar c}\right)^3 \bar{K}_2(z) = 1.688 \times 10^{28} T_9^3 \bar{K}_2(5.930/T_9). \quad \text{ND (B17)}$$

In this approximation

$$n_0 = Z n_N \approx 2n_1 \sinh \varphi, \quad \text{ND (B18)}$$

$$n_e \approx 2n_1 \cosh \varphi \approx (n_0^2 + 4n_1^2)^{1/2}, \quad \text{ND (B19)}$$

$$n = 2n_1\left(\cosh \varphi + \frac{1}{Z}\sinh \varphi\right) \approx (n_0^2 + 4n_1^2)^{1/2} + n_0/Z. \quad \text{ND (B20)}$$

From equation (B19)

$$\varphi = \Phi/kT \approx \sinh^{-1}(n_0/2n_1) = \sinh^{-1}(N_0/2N_1). \quad \text{ND (B21)}$$

From equation (B16)

$$n_+/n_- \approx \exp(-2\varphi), \quad \text{ND (B22)}$$

or

$$\varphi \approx \tfrac{1}{2}\ln(n_-/n_+) \approx \tfrac{1}{2}\ln\frac{[(n_0/2)^2 + n_1^2]^{1/2} + n_0/2}{[(n_0/2)^2 + n_1^2]^{1/2} - n_0/2}. \quad \text{ND (B23)}$$

In equation (B21) we introduce N_0 and N_1, the number densities *per gram*, for reasons to become apparent in what follows. In the non-degenerate case with $n_0(\rho)$ given as a function of density only and $n_1(T)$ calculable from equation (B17) as a function of temperature only, it is possible to evaluate $\varphi(\rho, T)$ using equation (B21) and then to determine $n_e(\rho, T)$ and $n(\rho, T)$ from equations (B19) and (B20), respectively. The second expressions in these equations give the solutions in terms of n_0 and n_1.

Clearly the above non-degenerate expressions cannot be employed when the series of which they are the first terms do not converge. Thus it might be surmised that expressions (B14) and (B15) are the necessary conditions under which stellar material can be treated as non-degenerate, and this can indeed be rigorously shown to be the case as long as the temperature is not too high. Alternative procedures for high temperature are discussed in Sec. (*k*).

Equation (B21) for the non-degenerate case illustrates the general principle that the chemical potential is determined essentially by n_0 or N_0 and not by the pairs created by the radiation field. This leads to the result that, if stellar matter is non-degenerate for electrons at low temperature ($\varphi \leq z$), then the additional electrons created by the radiation field cannot induce degeneracy at higher temperatures since $N_0 = Z/AM_u$ remains constant, N_1 increases, and hence φ decreases with increasing temperature. Physically this is to be expected since high temperatures produce electrons with high energies and low-energy states are not filled as in the degenerate case.

In the case of very massive stars in which the density is relatively low at a given temperature it is possible (Sampson 1962) to improve on the customary non-degenerate approximation. Under the circumstance of low density at sufficiently high temperatures for pair production, it can be assumed that the number of electrons and positrons per cm^3 or gram are essentially equal and large compared to the number of electrons associated with nuclei, $n_- \approx n_+ > n_0$. From equation (B4) it will be clear that this is equivalent to setting φ equal to zero, and thus in this extreme non-degenerate approximation (B4) can be written

$$n_\pm \approx \frac{2}{\pi^2}\left(\frac{kT}{\hbar c}\right)^3 \sum \frac{(-)^{n+1}}{n^3}\bar{K}_2(nz) \sim \frac{2}{\pi^2}\left(\frac{kT}{\hbar c}\right)^3 \bar{K}_2(z). \quad \text{END (B24)}$$

In the second approximation only the first term in the series is retained. In the limit of very high temperature $kT > m_e c^2$ or $z \approx 0$ so that in the leading terms of the series in expression (B7), $\bar{K}_2(nz) \approx 1$, $\cosh n\varphi \approx 1$, $\sinh n\varphi \approx 0$, and to a sufficient approximation for the extreme relativistic case one has

$$n \approx n_e \approx 2n_\pm \approx \frac{4}{\pi^2}\left(\frac{kT}{\hbar c}\right)^3 \sum \frac{(-)^{n+1}}{n^3} = \frac{4}{\pi^2}\left(\frac{kT}{\hbar c}\right)^3 [\tfrac{3}{4}\zeta(3)]$$

$$\approx 0.9015 \times \frac{4}{\pi^2}\left(\frac{kT}{\hbar c}\right)^3 = 3.043 \times 10^{28} T_9^3 \text{ cm}^{-3}, \qquad \text{(B25)}$$

ENDER

where $\zeta(3)$ is the Riemann Zeta-Function. We note that approximation (B25) gives a 10 per cent lower value for n_e than do expressions (B19) and (B17) with $z \approx \varphi \approx 0$ and is of course more accurate under these conditions. However, equation (B19) is to be preferred under circumstances such that φ is appreciably greater than zero and z is greater than or equal to φ, i.e., $z \geq \varphi > 0$. Neither approximation is good for electrons when electron degeneracy sets in for large $\varphi > z$, but equation (B16) is then still satisfactory for positrons, i.e., for n_+.

b) Pressure

Turn now to considerations of the pressure exerted by the gas particles, electrons, positrons, and nuclei. An expression similar to equation (B1) can be obtained for the pressure excited by the electrons and positrons. It is only necessary to multiply the integrand by

$$\frac{v\eta}{3} m_e c = \frac{\eta^2}{3\omega} m_e c^2. \qquad \text{(B26)}$$

Eventually following Chandrasekhar (1939) one finds the pressure of the electrons and positrons to be given by

$$p_e = p_- + p_+ = \frac{1}{3\pi^2}\left(\frac{m_e c}{\hbar}\right)^3 m_e c^2 \left[\int_0^\infty \frac{\eta^4(\eta^2+1)^{-1/2} d\eta}{\exp[z(\eta^2+1)^{1/2} - \varphi] + 1} + \int_0^\infty \frac{\eta^4(\eta^2+1)^{-1/2}}{\exp[z(\eta^2+1)^{1/2} + \varphi] + 1}\right] \qquad \text{(B27)}$$

$$= \frac{4}{\pi^2}\left(\frac{kT}{\hbar c}\right)^3 kT \sum \frac{(-)^{n+1}}{n^4} \cosh n\varphi \bar{K}_2(nz).$$

In terms of the Stefan-Boltzmann radiation constant $a = (\pi^2/15)(k^4/\hbar^3 c^3)$

$$p_e = \frac{60}{\pi^4} aT^4 \sum \frac{(-)^{n+1}}{n^4} \cosh n\varphi \bar{K}_2(nz) \qquad \text{(B28)}$$

$$= 4.660 \times 10^{21} T_9^4 \sum \frac{(-)^{n+1}}{n^4} \cosh n\varphi \bar{K}_2(nz) \text{ dyne cm}^{-2} \text{ or erg cm}^{-3}.$$

In what follows we will frequently use aT^4 in appropriate expressions especially in relativistic approximations.

In the non-degenerate approximation corresponding to equation (B16) for $n_\pm$ the pressure is given by

$$p_e \approx \frac{4}{\pi^2}\left(\frac{kT}{\hbar c}\right)^3 kT \cosh \varphi \bar{K}_2(z), \qquad \text{(B29)}$$

ND

or

$$p_e \approx \frac{60}{\pi^4} aT^4 \cosh \varphi \bar{K}_2(z). \qquad \text{ND} \quad \text{(B30)}$$

From equations (B29), (B19), and (B17)

$$p_e \approx n_e kT, \qquad \text{ND} \quad \text{(B31)}$$

which is Boyle's Law, true relativistically or non-relativistically in the non-degenerate electron case even when positrons are included.

The gas pressure also includes that due to the nuclei for which Boyle's Law holds quite precisely in the temperature-density range under consideration in this paper. Thus

$$p_N = n_N kT = \frac{n_0}{Z} kT = \frac{4}{\pi^2}\left(\frac{kT}{\hbar c}\right)^3 \frac{kT}{Z} \sum \frac{(-)^{n+1}}{n^3} \sinh n\varphi \bar{K}_2(nz). \quad \text{(B32)}$$

The gas pressure can thus be written

$$\begin{aligned} p_g &= p_e + p_N = \frac{4}{\pi^2}\left(\frac{kT}{\hbar c}\right)^3 kT \sum \frac{(-)^{n+1}}{n^4}\left(\cosh n\varphi + \frac{n}{Z}\sinh n\varphi\right)\bar{K}_2(nz) \\ &= \frac{60}{\pi^4} aT^4 \sum \frac{(-)^{n+1}}{n^4}\left(\cosh n\varphi + \frac{n}{Z}\sinh n\varphi\right)\bar{K}_2(nz), \end{aligned} \quad \text{(B33)}$$

so that in the non-degenerate approximation

$$\begin{aligned} p_g &\approx \frac{4}{\pi^2}\left(\frac{kT}{\hbar c}\right)^3 kT\left(\cosh \varphi + \frac{1}{Z}\sinh \varphi\right)\bar{K}_2(z) \\ &\approx nkT \\ &\approx \frac{\rho \mathfrak{R} T}{\mu} = 0.8314 \times 10^{17} \frac{\rho T_9}{\mu} \text{ dyne cm}^{-2} \text{ or erg cm}^{-3}. \end{aligned} \quad \text{(B34)} \quad \text{ND}$$

The approximation for the pressure in massive stars corresponding to equation (B24) is obtained by setting all $\cosh n\varphi \approx 1$, $\sinh n\varphi \approx 0$ so that

$$p_g \approx p_e \approx \frac{60}{\pi^4} aT^4 \sum \frac{(-)^{n+1}}{n^4} \bar{K}_2(nz) \sim \frac{60}{\pi^4} aT^4 \bar{K}_2(z). \quad \text{END} \quad \text{(B35)}$$

In the limit of very high temperatures, $z \approx 0$ and all $\bar{K}_2(nz) \approx 1$ in the leading terms of the series so that

$$\begin{aligned} p_g \approx p_e &\approx \frac{60}{\pi^4} aT^4 \sum \frac{(-)^{n+1}}{n^4} = \frac{60}{\pi^4} aT^4 \left[\tfrac{7}{8}\zeta(4)\right] \\ &\approx \frac{7\pi^2}{180}\left(\frac{kT}{\hbar c}\right)^3 kT = \tfrac{7}{12} aT^4, \end{aligned} \quad \text{ENDER} \quad \text{(B36)}$$

since $\zeta(4) = \pi^4/90 = 1.0823$ and $\frac{7}{8}\zeta(4) = 7\pi^4/720 = 0.9470$. This remarkable result combined with the expression for radiation pressure $p_r = \frac{1}{3}aT^4$ indicates that in the limit under consideration

$$p_g \approx p_e \approx \tfrac{7}{4} p_r, \qquad \text{ENDER} \quad \text{(B37)}$$

and thus that the total pressure is

$$\begin{aligned} p &= p_g + p_r \approx \tfrac{11}{4} p_r \\ &\approx \tfrac{11}{12} aT^4 = 6.935 \times 10^{21} T_9^4 \text{ dyne cm}^{-2} \text{ or erg cm}^{-3}. \end{aligned} \quad \text{ENDER} \quad \text{(B38)}$$

In order to display deviations from Boyle's Law it is convenient to define two ratios as follows:

$$q_e = \frac{p_e}{n_e kT} = \frac{\sum \frac{(-)^{n+1}}{n^4} \cosh n\varphi \bar{K}_2(nz)}{\sum \frac{(-)^{n+1}}{n^3} \cosh n\varphi \bar{K}_2(nz)} \tag{B39}$$

and

$$q = \frac{p_g}{nkT} = \frac{q_e n_e + n_N}{n} = \frac{\sum \frac{(-)^{n+1}}{n^4} \left(\cosh n\varphi + \frac{n}{Z} \sinh n\varphi\right) \bar{K}_2(nz)}{\sum \frac{(-)^{n+1}}{n^3} \left(\cosh n\varphi + \frac{1}{Z} \sinh n\varphi\right) \bar{K}_2(nz)}, \tag{B40}$$

such that in various approximations

$$\begin{aligned} q &\approx q_e \approx 1 && \text{ND or NR} \\ &\approx \frac{\Sigma[(-)^{n+1}/n^4]\bar{K}_2(nz)}{\Sigma[(-)^{n+1}/n^3]\bar{K}_2(nz)} \sim 1 && \text{END} \\ &\approx \tfrac{7}{6}\zeta(4)/\zeta(3) = 1.0505. && \text{ENDER} \end{aligned} \tag{B41}$$

In the non-degenerate approximations used in this paper Boyle's Law holds to $\lesssim 5$ per cent.

Finally one has

$$p_g = q_e n_e kT + n_N kT = qnkT \tag{B42}$$

and

$$p = q_e n_e kT + n_N kT + \tfrac{1}{3}aT^4 = qnkT + \tfrac{1}{3}aT^4. \tag{B43}$$

c) *Internal Energy Density*

It is now appropriate to consider the internal energies of the gas particles. Again the results of Chandrasekhar (1939) can be extended to include positrons and the total energy density including rest mass is

$$\begin{aligned} w_\pm &= \frac{1}{\pi^2}\left(\frac{m_e c}{\hbar}\right)^3 m_e c^2 \int_0^\infty \frac{\omega^2(\omega^2-1)^{1/2}d\omega}{\exp[z\omega \pm \varphi] + 1} \\ &= \frac{1}{\pi^2}\left(\frac{m_e c}{\hbar}\right)^3 m_e c^2 \sum \frac{(-)^{n+1}}{nz} \exp(\mp n\varphi)[\tfrac{3}{4}K_3(nz) + \tfrac{1}{4}K_1(nz)], \end{aligned} \tag{B44}$$

where $K_1(nz)$ and $K_3(nz)$ are the modified Bessel functions of first and third order, respectively. These Bessel functions can be expressed in terms of $\bar{K}_2(nz)$ and its derivative as follows:

$$\tfrac{3}{4}K_3(nz) + \tfrac{1}{4}K_1(nz) = \frac{2}{(nz)^3}\left[3 - \frac{d \ln \bar{K}_2(nz)}{d \ln(nz)}\right]\bar{K}_2(nz), \tag{B45}$$

so that

$$w_\pm = \frac{2}{\pi^2}\left(\frac{kT}{\hbar c}\right)^3 kT \sum \frac{(-)^{n+1}}{n^4} \exp(\mp n\varphi)\left[3 - \frac{d \ln \bar{K}_2(nz)}{d \ln(nz)}\right]\bar{K}_2(nz). \tag{B46}$$

The internal energy of interest consists of the total kinetic and rest-mass energy of the pair electrons and positrons but only of the kinetic energy of the ionization electrons. Thus

$$u_e = w_+ + w_- - n_0 m_e c^2. \tag{B47}$$

The internal kinetic energy of the nuclei is quite simply

$$u_N = \tfrac{3}{2} n_N kT = \frac{3}{2Z} n_0 kT, \tag{B48}$$

so that the internal energy of the gas of electrons, positrons, and nuclei is

$$u_g = u_e + u_N = \frac{4}{\pi^2}\left(\frac{kT}{\hbar c}\right)^3 kT \sum \frac{(-)^{n+1}}{n^4} \times \left\{\cosh n\varphi\left[3 - \frac{d \ln \bar{K}_2(nz)}{d \ln(nz)}\right] + n\left(\frac{3}{2Z} - z\right)\sinh \varphi\right\} \bar{K}_2(nz). \tag{B49}$$

At this point it is convenient to introduce the mean kinetic energy for electrons and positrons in units kT which is given by

$$x_\pm = \frac{w_\pm - n_\pm m_e c^2}{n_\pm kT} = \frac{\sum \frac{(-)^{n+1}}{n^4} \exp(\mp n\varphi)\left[3 - nz - \frac{d \ln \bar{K}_2(nz)}{d \ln(nz)}\right]\bar{K}_2(nz)}{\sum \frac{(-)^{n+1}}{n^3} \exp(\mp n\varphi)\bar{K}_2(nz)}. \tag{B50}$$

For the combination of electrons and positrons it is possible to define

$$x_e = \frac{w_+ + w_- - n_e m_e c^2}{n_e kT} = \frac{\sum \frac{(-)^{n+1}}{n^4} \cosh n\varphi\left[3 - nz - \frac{d \ln \bar{K}_2(nz)}{d \ln(nz)}\right]\bar{K}_2(nz)}{\sum \frac{(-)^{n+1}}{n^3} \cosh n\varphi \bar{K}_2(nz)}. \tag{B51}$$

Note that in general $x_+ \neq x_- \neq x_e$. However, in the non-degenerate approximations these quantities will be approximately equal. In fact, in the non-degenerate approximation used throughout the main text in which only the first terms of the series expansions are retained we recover equation (61) of Part IV and its approximations as follows:

$$\begin{aligned} x_e \approx x_\pm &\approx 3 - z - d \ln \bar{K}_2(z)/d \ln z && \text{ND} \\ &\approx \tfrac{3}{2} && \text{NDNR} \\ &\approx 3 && \text{NDER} \\ &\approx 3\frac{\sum \frac{(-)^{n+1}}{n^4}\left[3 - nz - \frac{d \ln \bar{K}_2(nz)}{d \ln(nz)}\right]\bar{K}_2(nz)}{\sum \frac{(-)^{n+1}}{n^3}\bar{K}_2(nz)} && \text{END} \\ &\approx 3q_e \approx \tfrac{7}{2}\zeta(4)/\zeta(3) = 3.151. && \text{ENDER} \end{aligned} \tag{B52}$$

In deriving the NDNR approximation we have employed equation (B9). We wish to emphasize explicitly the important relation $x_e \approx 3q_e$ in the last approximation. In Part IV x_e is designated by x.

The specific heat at constant volume for the electrons and positrons can now be generalized. The results are

$$c_v \equiv \frac{d(x_e T)}{dT} = x_e + T\frac{dx_e}{dT}$$

$$\approx \tfrac{3}{2} \qquad \text{NDNR} \quad \text{(B53)}$$

$$\approx 3.151\,, \qquad \text{ENDER}$$

where we have used the fact that $dx_e/dT \approx 0$ in the two limiting cases.

The specific heat at constant pressure becomes

$$c_p = c_v + 1$$

$$\approx \tfrac{5}{2} \qquad \text{NDNR} \quad \text{(B54)}$$

$$\approx 4.151\,. \qquad \text{ENDER}$$

The ratio of specific heats can also be derived with the following results

$$\gamma = \frac{c_p}{c_v} = 1 + \frac{1}{c_v}$$

$$\approx \tfrac{5}{3} \qquad \text{NDNR} \quad \text{(B55)}$$

$$\approx 1.317\,. \qquad \text{ENDER}$$

Note that γ is less than $\frac{4}{3}$ in the last case.

It must be emphasized that the extreme relativistic limits for q_e, x_e, etc., depend on the degree of non-degeneracy. Only in the case of extreme non-degeneracy or pairs completely dominating are the limiting values $q_e = 1.050$, $x_e = 3.151$, etc. Otherwise limiting values intermediate between these last quoted values and $q_e = 1$, $x_e = 3$, etc., are the case.

The internal energy of the gas of electrons, positrons, and nuclei can now be written as

$$\begin{aligned} u_g &= (x_e + z)n_e kT - n_0 m_e c^2 + \tfrac{3}{2}n_{\mathrm{N}} kT \\ &= [x_e + z(1 - n_0/n_e)]n_e kT + \tfrac{3}{2}n_{\mathrm{N}} kT \\ &= xnkT + (n_e - n_0)m_e c^2 \\ &= xnkT + 2n_+ m_e c^2\,. \end{aligned} \qquad \text{(B56)}$$

In the last equalities in equation (B56) we have introduced a generalized x for both electronic and nuclear particles. (In the main text x has been used for x_e.) It will be clear that $xn = x_e n_e + \frac{3}{2} n_{\mathrm{N}}$. The non-degenerate approximation at low temperature ($n_e \approx n_0$, $x \approx \frac{3}{2}$) and at high temperature ($n_e > n_0$, $z \approx 0$, $x \approx 3$) are, respectively,

$$\begin{aligned} u_g &\approx \tfrac{3}{2}(n_e + n_{\mathrm{N}})kT = \tfrac{3}{2}nkT \qquad \text{NDNR} \\ &\approx 3n_e kT + \tfrac{3}{2}n_{\mathrm{N}} kT\,. \qquad \text{NDER} \end{aligned} \qquad \text{(B57)}$$

Equations (B56), (B8), and (34) in Part III yield

$$\begin{aligned} U_g = u_g/\rho &= \frac{\Re T}{\mu}[x + z(n_e - n_0)/n] \\ &= 0.8314 \times 10^{17}\frac{T_9}{\mu}[x + z(n_e - n_0)/n]\ \mathrm{erg\ gm^{-1}}\,. \end{aligned} \qquad \text{(B58)}$$

The approximations given in equation (B57) can be improved upon at high temperatures using the extreme non-degenerate approximation for which $\cosh n\varphi \approx 1$ and $\sinh n\varphi \approx 0$ in all the terms of equation (B49). Then

$$u_g \approx x_e n_e kT \approx \omega_+ + \omega_- \approx \frac{60}{\pi^4} aT^4 \sum \frac{(-)^{n+1}}{n^4}\left[3 - \frac{d \ln \bar{K}_2(nz)}{d \ln(nz)}\right]\bar{K}_2(nz)$$

$$\sim \frac{60}{\pi^4} aT^4\left[3 - \frac{d \ln \bar{K}_2(z)}{d \ln z}\right]\bar{K}_2(z) \qquad \text{END} \quad \text{(B59)}$$

$$\sim \frac{60}{\pi^4} aT^4(x_e + z)\bar{K}_2(z).$$

In the leading terms of this expansion at high temperature $\bar{K}_2(nz) \approx 1$, $d \ln \bar{K}_2(nz)/d \ln (nz) \approx 0$, and

$$u_g \approx \frac{180}{\pi^4} aT^4[\tfrac{7}{8}\zeta(4)] = \tfrac{7}{4} aT^4 \quad \text{(B60)}$$

$$\approx 1.324 \times 10^{22} T_9^4 \text{ erg cm}^{-3}, \qquad \text{ENDER}$$

or

$$u_g \approx 3n_e kT[\tfrac{7}{6}\zeta(4)/\zeta(3)] = 3.151\, n_e kT. \qquad \text{ENDER} \quad \text{(B61)}$$

The total internal energy including radiation becomes

$$\begin{aligned} u = u_g + u_r &= [x_e + z(1 - n_0/n_e)]n_e kT + \tfrac{3}{2} n_N kT + aT^4 \\ &= x_e n_e kT + \tfrac{3}{2} n_N kT + aT^4 + (n_e - n_0)m_e c^2 \qquad \text{(B62)} \\ &= xnkT + (n - n_N - n_0)m_e c^2 + aT^4, \end{aligned}$$

so that in the various approximations under consideration

$$\begin{aligned} u &\approx \tfrac{3}{2} nkT + aT^4 && \text{NDNR} \\ &\approx \tfrac{7}{4} aT^4 + aT^4 = \tfrac{11}{4} aT^4 && \text{ENDER} \quad \text{(B63)} \\ &\approx 2.080 \times 10^{22}\, T_9^4 \text{ erg cm}^{-3}. && \text{ENDER} \end{aligned}$$

These results along with those derived in the previous section indicate that the electron-positron pressure and energy density are just $\frac{7}{4}$ times the corresponding quantities for radiation in the extreme relativistic limit. For the total pressure and energy-density the corresponding ratio is $\frac{11}{4}$.

d) Internal Energy Density-Pressure Ratios

It is frequently required to know the ratio of internal energy density to the pressure exerted by gas and radiation. For radiation

$$\frac{u_r}{p_r} = \frac{aT^4}{\frac{1}{3} aT^4} = 3. \quad \text{(B64)}$$

For the gas, sections (*b*) and (*c*) yield

$$\frac{u_e}{p_e} = \frac{x_e + z(1 - n_0/n_e)}{q_e}, \quad \text{(B65)}$$

$$\frac{u_N}{p_N} = \tfrac{3}{2}, \quad \text{(B66)}$$

and

$$\frac{u_g}{p_g}=\frac{x_e+z(1-n_0/n_e)+3n_N/2n_e}{q_e+n_N/n_e}=\frac{x+z(n_e-n_0)/n}{q}. \tag{B67}$$

In the non-relativistic, non-degenerate approximation, $x \approx \frac{3}{2}$, $n_e \approx n_0$, so

$$\frac{u_g}{p_g}\approx\tfrac{3}{2}, \qquad \text{NDNR} \tag{B68}$$

while relativistically, $x \approx 3q$, $n_e > n_0 = Zn_N$,

$$\frac{u_g}{p_g}\approx\frac{u_e}{p_e}\approx 3. \qquad \text{ENDER} \tag{B69}$$

We emphasize the obvious point that in approximations in which the ionization electrons are neglected relative to the pairs it is also justified to neglect the nuclei.

The introduction of the ratio $\beta = p_g/p$ and $1-\beta = p_r/p$ makes it possible to incorporate equations (B64) and (B67) into

$$\begin{aligned}\frac{u}{p}=\frac{u_r+u_g}{p_r+p_g}&=3(1-\beta)+\beta\left[\frac{x+z(n_e-n_0)/n}{q}\right]\\&=3-\beta\left[3-\frac{x+z(n_e-n_0)/n}{q}\right]\end{aligned} \tag{B70}$$

or

$$\begin{aligned}\frac{u}{3p}&=1-\frac{\beta}{3}\left[\frac{3q_e-x_e-z(1-n_0/n_e)+3n_N/2n_e}{q_e+n_N/n_e}\right]\\&\approx 1-\frac{\beta}{3}\left[\frac{3q_e-x_e-z(1-n_0/n_e)}{q_e}\right] && n_e>n_N\\&\approx 1-\frac{\beta}{3}\left[\frac{3q_e-x_e-z}{q_e}\right] && n_e>n_0.\end{aligned} \tag{B71}$$

The non-relativistic and extreme relativistic approximations are respectively

$$\begin{aligned}\frac{u}{3p}&\approx 1-\frac{\beta}{2} && \text{NDNR}\\&\approx 1. && \text{ENDER}\end{aligned} \tag{B72}$$

Equations (B70), (B40), (B8), and (34) in Part III give

$$\begin{aligned}U=u/\rho&=3q\,\frac{\Re T}{\mu\beta}\left\{1-\beta\left[1-\frac{x+z(n_e-n_0)/n}{3q}\right]\right\}\\&=2.494\times 10^{17}\left(\frac{qT_9}{\mu\beta}\right)\left\{1-\beta\left[1-\frac{x+z(n_e-n_0)/n}{3q}\right]\right\}\text{erg gm}^{-1}.\end{aligned} \tag{B73}$$

It is worth noting that the last form of equation (B71) indicates that under some circumstances ($x_e \approx 3q_e$, $z > 0$) u can exceed $3p$ which can never be the case without pairs ($n_0 = n_e$, $q_e = 1$, $x_e \leq 3$).

e) Differential of the Available Energy

In the main text we have defined

$$dQ = -pdV - dU = \frac{p}{\rho^2}\,d\rho - dU, \tag{B74}$$

in which our sign convention is the opposite of that commonly used as, for example, by Chandrasekhar (1939). This choice was made primarily so that dQ could be positive during compression ($d\rho > 0$). Then when work is done in compression against the internal pressure of a given mass element, dQ is the excess energy over that stored internally in radiation, particle motion, or pair formation. The results obtained previously in this appendix make it possible to give general expressions for dQ. Since Q and $U = u/\rho$ are measured in erg gm^{-1} rather than erg cm^{-3} all of the n which have appeared above will be replaced by $N = n/\rho$.

Insertion of equations (B43) and (B62) into (B74) yields

$$dQ = q_e N_e kT\left(\frac{4-3\beta}{\beta}\right) d\ln\rho - N_e kT\left(c_v + 12 q_e \frac{1-\beta}{\beta}\right) d\ln T$$
$$- N_e kT(x_e + z)\, d\ln N_e \qquad \text{(B75)}$$
$$+ N_N kT\left(\frac{4-3\beta}{\beta}\right) d\ln\rho - N_N kT\left(\tfrac{3}{2} + 12\frac{1-\beta}{\beta}\right) d\ln T - \tfrac{3}{2} N_N kT\, d\ln N_N .$$

The coefficient of $N_N kT d\ln T$ can also be written $-3(8-7\beta)/2\beta$. It will be recalled that the rest-mass energies of the nuclei and the ionization electrons have *not* been included in U. In what follows we will not give the nuclear term explicitly. It can always be derived from the electron term by the substitution $N_e \to N_N, q_e \to 1, c_v = x_e \to \frac{3}{2}, z \to 0$.

With $N_e = N_e(\rho, T)$ equation (B75) can be transformed into

$$dQ = N_e kT\left[q_e\left(\frac{4-3\beta}{\beta}\right) - (x_e+z)\frac{\partial \ln N_e}{\partial \ln \rho}\right] d\ln\rho - N_e kT \qquad \text{(B76)}$$
$$\times\left[c_v + 12 q_e\left(\frac{1-\beta}{\beta}\right) + (x_e+z)\frac{\partial \ln N_e}{\partial \ln T}\right] d\ln T + \text{nucl. terms}.$$

If the temperature is taken as the independent variable then equation (B75) can be reduced to a form which constitutes the generalization of equation (64) of the main text, to wit,

$$\frac{dQ}{dT} = kN_e\left[3q_e - c_v - (x_e+z)\frac{d\ln N_e}{d\ln T} + q_e\left(\frac{4-3\beta}{\beta}\right)\left(\frac{d\ln\rho}{d\ln T} - 3\right)\right] \qquad \text{(B77)}$$
$$+ \text{nucl. terms}.$$

If a given mass element is followed in evolution through stages of *quasi-static equilibrium* (QSE), then from equations (65) and (66), Part IV,

$$\frac{d\ln\rho}{d\ln T} = 3 - 3\frac{d\ln\mu\beta}{d\ln T} = 3 + 3\left(\frac{\beta}{4-3\beta}\right)\frac{d\ln N}{d\ln T}. \qquad \text{QSE} \quad \text{(B78)}$$

Substitution in equation (B77) yields the generalization of equation (69) of Part IV

$$\frac{dQ}{dT} = kT\left[(3q_e - c_v)\left(\frac{N_e}{T}\right) + (3q_e - x_e - z)\frac{dN_e}{dT}\right] + \text{nucl. terms}, \quad \text{QSE} \quad \text{(B79)}$$

where $1 \le q_e \le 1.050$, $\frac{3}{2} \le x_e \le 3.151$, and $\frac{3}{2} \le c_v \le 3.151$ over the range from non-relativistic to extreme relativistic non-degenerate conditions.

When pairs are dominant in the extreme relativistic, extreme non-degenerate regime

equation (B74) takes on a particularly simple and useful form. Make use of equations (B38) and (B63) to obtain

$$dQ = \frac{p}{\rho} d \ln \rho - \rho \frac{\partial U}{\partial \rho} d \ln \rho - T \frac{\partial U}{\partial T} d \ln T$$

$$= \tfrac{11}{12} \frac{aT^4}{\rho} d \ln \rho + \tfrac{11}{4} \frac{aT^4}{\rho} d \ln \rho - 11 \frac{aT^4}{\rho} d \ln T \qquad \text{(B80)}$$

$$= \tfrac{11}{3} \frac{aT^4}{\rho} (d \ln \rho - 3 d \ln T). \qquad \text{ENDER}$$

In quasi-static equilibrium in the extreme relativistic case we will find that $\rho \propto T^3$ with $\mu\beta$ constant for a given stellar mass so that

$$dQ = 0, \qquad \text{QSEENDER (B81)}$$

which is just what is required for radiation and relativistic particles.

At this point we emphasize that dQ is the available energy calculated by a local observer co-moving with a given mass element. With the exception of equations (B78), (B79), and (B81) the expressions for dQ hold for such an observer even during accelerated contraction or expansion. If the gravitational forces and pressure gradients are not balanced the mass element may gain or lose bulk kinetic energy from or to the gravitational field. However, this will be separate in a sense from the internal energy calculations of the local observer who needs only to know the equation of state of the material and the amount of expansion or contraction to make his calculations. Powerful use can be made of this consideration in problems involving supernova core implosion and envelope explosion.

f) Time Scale for Free Expansion or Contraction

In the circumstances under discussion in this paper radiative transfer can in general be neglected compared to nuclear-energy generation and neutrino losses. Thus the conservation of energy for a given mass element over a time interval dt demands

$$dQ = (p/\rho^2) d\rho - dU = (dU_\nu/dt) dt - dQ_N. \qquad \text{(B82)}$$

In this equation $(dU_\nu/dt)dt$ is the energy lost in neutrino processes during the time interval under consideration. It is assumed that the neutrinos are not absorbed in the stellar material and are not in equilibrium with other particles and radiation. An explicit expression for dU_ν/dt as a function of ρ, T is required for use in equation (B82). In the main text we have made extensive use of equations (19) and (20) for the neutrino loss due to pair annihilation.

The differential dQ_N in equation (B82) is the energy released by nuclear reactions during the time interval under consideration. Following the conventions of nuclear physics, it is taken positive for exoergic reactions and negative for endoergic reactions. In terms of nuclear energy treated as an internal energy (U_N) one has

$$dQ_N = -dU_N, \qquad \text{(B83)}$$

with

$$U_N = N_0 m_e c^2 + N_N M_N c^2 \approx N_N M_A c^2, \qquad \text{(B84)}$$

where M_N and $M_A \approx M_N + Z m_e$ are nuclear and atomic masses, respectively. We neglect atomic binding energies and assume that the stellar material remains completely

ionized so that N_0 changes only in *nuclear* reactions through beta-emission or capture.

If the nuclear reactions have reached an equilibrium at which the reaction rates are fast enough to follow quasi-static changes, then U_N is known as an explicit function of ρ, T, and it is possible to define $Q_N = -U_N(\rho, T)$ and appropriate partial and total derivatives, e.g.,

$$\frac{dQ_N}{dT} = \frac{\partial Q_N}{\partial T} + \frac{\partial Q_N}{\partial \rho}\frac{d\rho}{dT}. \tag{B85}$$

Choosing the temperature as an independent variable, one then has the time scale for a contraction induced by neutrino loss given by

$$\Delta t = \int dt = \int \frac{dQ/dT + dQ_N/dT}{dU_\nu/dt}\, dT = (\Delta Q + \Delta Q_N)\left\langle \frac{1}{dU_\nu/dt} \right\rangle. \tag{B86}$$

If the nuclear reactions have not reached equilibrium then $dQ_N/dt = \epsilon(\rho, T)$ must be known as an explicit function of ρ, T as in equation (90), Part V, and then

$$\Delta t = \int \frac{dQ/dT}{dU_\nu/dt - dQ_N/dt}\, dT = \Delta Q \left\langle \frac{1}{dU_\nu/dt - dQ_N/dt} \right\rangle. \tag{B87}$$

In the case dU_ν/dt is greater than dQ_N/dt and in particular if the latter quantity is negative and provided dQ/dt is greater than zero, then contraction results. In the case that dQ_N/dT is positive and greater than dU_ν/dt and provided dQ/dT is greater than zero, then expansion results. In the case discussed in the main text where pair formation led to circumstances in which dQ/dT was negative it was found that dQ_N/dt was sufficiently greater than dU_ν/dt to insure quasi-static contraction.

Cases of frequent interest are those of free expansion (rise) or free contraction (fall). In these cases the pressure gradient is zero and gravitational potential energy exchanges only with the kinetic energy of bulk motion, and all internal energies in a given mass element must balance to zero. The time scale becomes that of free fall ($d\rho > 0$) or free expansion ($d\rho < 0$) given by HFB[2] (1964) as

$$\begin{aligned} dt &= \frac{1}{(\frac{8}{3}\pi G\rho)^{1/2}}\left|\frac{dr}{r}\right| = \frac{1338}{\rho^{1/2}}\left|\frac{dr}{r}\right| \text{ sec} \\ &= \frac{1}{(24\pi G\rho)^{1/2}}\left|\frac{d\rho}{\rho}\right| = \frac{446}{\rho^{1/2}}\left|\frac{d\rho}{\rho}\right| \text{ sec}. \end{aligned} \tag{B88}$$

In this expression $\rho \propto r^{-3}$ has been employed, and in addition it has been assumed that $\dot{r} = 0$ at $r = \infty$. This is, of course, not always the case, but it is frequently a good enough representation of the boundary condition on the motion to make equation (B88) a useful expression for order of magnitude estimates.

Substitution of equation (B88) in (B82) gives the equation of the implosion or explosion path. For example, in implosion induced by neutrino loss with no nuclear-energy release, equations (B80), (B82), and (B88) give

$$\tfrac{11}{3}\frac{aT^4}{\rho}(d\ln\rho - 3d\ln T) = \frac{dU_\nu/dt}{(24\pi G\rho)^{1/2}}\, d\ln\rho, \tag{B89}$$

whence

$$\frac{d\ln\rho}{d\ln T} = \frac{3}{1 - \frac{3\rho}{11aT^4}\frac{dU_\nu/dt}{(24\pi G\rho)^{1/2}}} = \frac{3}{1 - \frac{3}{11aT^4}\frac{du_\nu/dt}{(24\pi G\rho)^{1/2}}}. \tag{B90}$$

For $du_\nu/dt \propto T^9$, HFB[2] (1964) show that $\rho \propto T^{10}$ at high temperatures. Similarly in an explosion induced by positive nuclear-energy release with no neutrino loss and under the circumstances of equation (B80) one finds after free expansion is attained

$$\frac{d \ln \rho}{d \ln T} = \frac{3}{1 - \frac{3\rho}{11aT^4} \frac{dQ_N/dt}{(24\pi G\rho)^{1/2}}}. \tag{B91}$$

The minus sign occurs in the denominator since $dt = -d\rho/\rho\ (24\pi G\rho)^{1/2}$ in expansion.

In the case (B90) ρ will rise more rapidly than the third power of the temperature, while in the case (B91) ρ will initially decrease (explosion) as the temperature reaches a maximum and begins to decrease and will eventually follow in reverse a T^3 path if dQ_N/dt approaches zero as indeed will be the case at low ρ, T. This behavior has been illustrated in Figure 3. At temperatures below pair formation, but still in massive stars so that $\beta \sim 0$, one can replace $\frac{11}{3}$ by $\frac{4}{3}$ in equations (B89), (B90), and (B91). The ρ, T-behavior described here is illustrated schematically in Figure 3 for $M \approx 30\ M_\odot$.

g) The Adiabatic Coefficients

If the energy differential dQ of equation (B76) is set equal to zero and the total derivatives of the various thermodynamic variables p, ρ, T are associated in pairs, then it is possible to derive the so-called *adiabatic* coefficients for stellar material consisting of radiation, nuclei, ionization electrons and pair electrons, and positrons. In this section the ordinary non-degenerate expressions for these coefficients will be presented without enumeration of the tedious algebraic manipulations involved. The forms presented are those which reduce straightforwardly in the limit of no pairs to the expressions given by Chandrasekhar (1939). We are picayune only in not replacing c_v by $(\gamma - 1)^{-1}$. Moreover, nuclear contributions are neglected under the assumption $Z > 1$. In this case we can ignore the distinction between q and q_e and between x and x_e.

In the ordinary non-degenerate approximation $q \approx 1$, $\frac{3}{2} \lesssim x \lesssim 3$, $\frac{3}{2} \lesssim c_v \lesssim 3$ and $N_e^2 \approx N_0^2 + 4N_1^2$, this last relation being equation (18) of the main text. Changes in $N_0 = Z/AM_u$ are permitted only through nuclear transformations involving the beta-interactions and are included in dQ_N rather than the dQ of present interest. Under these circumstances the partial derivatives of $\ln N_e$ needed in equation (B76) are simply calculated using either of the identical equations (10) or (B17) and (18) or (B19) with the result

$$\frac{\partial \ln N_e}{\partial \ln \rho} \approx \lambda_1^2 \frac{\partial \ln N_1}{\partial \ln \rho} \approx -\lambda_1^2, \qquad \text{ND} \tag{B92}$$

$$\frac{\partial \ln N_e}{\partial \ln T} \approx \lambda_1^2 \frac{\partial \ln N_1}{\partial \ln T} \approx \lambda_1^2 (3 + d \ln \bar{K}_2/d \ln T) \approx \lambda_1^2 (x + z), \quad \text{ND} \tag{B93}$$

where

$$\begin{aligned} \lambda_1 &\equiv 2N_1/N_e = 2n_1/n_e \\ &\approx (1 + n_0^2/4n_1^2)^{-1/2} = (1 + N_0^2/4N_1^2)^{-1/2}. \qquad \text{ND} \end{aligned} \tag{B94}$$

The adiabatic coefficients for electrons and positrons as defined by Chandrasekhar (1939) follow

$$\begin{aligned} \Gamma_1 &\equiv d \ln p/d \ln \rho \\ &\approx \beta(1 - \lambda_1^2) + \frac{[4 - 3\beta + \beta\lambda_1^2(x+z)]^2}{\beta c_v + 12(1-\beta) + \beta\lambda_1^2(x+z)^2} && \text{ND} \\ &\approx \beta + \frac{(4-3\beta)^2}{\beta c_v + 12(1-\beta)} \sim \tfrac{4}{3} + \frac{\beta}{6} + O(\beta^2) \quad \text{No pairs}, \ \lambda_1 = 0 && \text{ND} \\ &\approx \tfrac{5}{3} && c_v = \tfrac{3}{2}, \quad \beta = 1 \quad \text{NDNR} \\ &\approx \frac{[4 - \beta(3 - x - z)]^2}{12 - \beta[12 - c_v - (x+z)^2]} \quad \text{Pairs dominant}, \ \lambda_1 = 1 && \text{ND} \\ &\approx \tfrac{4}{3} && c_v = x = 3, \ z = 0. \quad \text{NDER} \end{aligned} \tag{B95}$$

(It is obvious from $p \propto T^4$ and $\rho \propto T^3$ that the approximation $\Gamma_1 \approx \frac{4}{3}$ also holds under extreme non-degenerate, extreme relativistic [ENDER] circumstances. This will be true for the other adiabatic coefficients below.)

$$\Gamma_2 \equiv (1 - d \ln T/d \ln p)^{-1}$$

$$\approx 1 + [4 - 3\beta + \beta\lambda_1^2(x+z)] \div \beta^2 c_v(1-\lambda_1^2) + 3(1-\beta)(4+\beta)$$
$$- \lambda_1^2[12\beta(1-\beta) - \beta(7-6\beta)(x+z) - \beta^2(x+z)^2] \quad \text{ND}$$

$$\approx 1 + \frac{4-3\beta}{\beta^2 c_v + 3(1-\beta)(4+\beta)} \sim \tfrac{4}{3} + O(\beta^2) \quad \text{No pairs, } \lambda_1 = 0 \quad \text{ND} \qquad \text{(B96)}$$

$$\approx \tfrac{5}{3} \qquad c_v = \tfrac{3}{2},\ \beta = 1 \quad \text{NDNR}$$

$$\approx 1 + \frac{4 - \beta(3-x-z)}{12 - 7\beta(3-x-z) + \beta^2(3-x-z)^2} \quad \text{Pairs dominant, } \lambda_1 = 1 \quad \text{ND}$$

$$\approx \tfrac{4}{3} \qquad x = 3,\ z = 0. \quad \text{NDER}$$

$$\Gamma_3 \equiv 1 + d \ln T/d \ln \rho$$

$$\approx 1 + \frac{4 - 3\beta + \beta\lambda_1^2(x+z)}{\beta c_v + 12(1-\beta) + \beta\lambda_1^2(x+z)^2} \quad \text{ND}$$

$$\approx 1 + \frac{4-3\beta}{\beta c_v + 12(1-\beta)} \sim \tfrac{4}{3} + \frac{\beta}{24} + O(\beta^2) \quad \text{No pairs, } \lambda_1 = 0 \quad \text{ND}$$

$$\approx \tfrac{5}{3} \qquad c_v = \tfrac{3}{2},\ \beta = 1 \quad \text{NDNR} \qquad \text{(B97)}$$

$$\approx 1 + \frac{4 - \beta(3-x-z)}{12 - \beta[12 - c_v - (x+z)^2]} \quad \text{Pairs dominant, } \lambda_1 = 1 \quad \text{ND}$$

$$\approx \tfrac{4}{3} \qquad c_v = x = 3,\ z = 0. \quad \text{NDER}$$

As functions of increasing temperature the adiabatic coefficients decrease monotonically from $\frac{5}{3}$ to $\frac{4}{3}$ if pair formation is ignored. In massive stars when pair electrons and positrons become comparable in number to ionization electrons around $kT = m_e c^2/3$, $z = 3$, $x = 1.96$, $c_v = 2.29$, the adiabatic coefficients dip below $\frac{4}{3}$. For example, in Table 3, $\Gamma_1 = 1.32$, $\Gamma_2 = 1.29$, and $\Gamma_3 = 1.30$ under these conditions when a stellar core with $M = 20\ M\odot$ reaches $T_9 \approx 2$. For polytropes dQ/dT becomes negative under these circumstances. Questions concerning stability immediately arise, but in the cases considered in the main text nuclear-energy generation through oxygen burning prevents catastrophic collapse (Part V). Ultimately the adiabatic coefficient Γ_1 becomes greater than $\frac{4}{3}$ and approaches this value asymptotically at high temperatures.

h) The Quantities β, μ and the Density-Temperature Relation

The ratio of gas pressure to total pressure comes straightforwardly from equations (B33) and (B43) in a form independent of polytropic structure as follows:

$$\beta = \frac{p_g}{p} = \frac{p_g}{p_g + p_r}$$
$$= \frac{\frac{180}{\pi^4}\sum \frac{(-)^{n+1}}{n^4}\left(\cosh n\varphi + \frac{n}{Z}\sinh n\varphi\right)\bar{K}_2(nz)}{1 + \frac{180}{\pi^4}\sum \frac{(-)^{n+1}}{n^4}\left(\cosh n\varphi + \frac{n}{Z}\sinh n\varphi\right)\bar{K}_2(nz)}. \qquad \text{(B98)}$$

The various approximations under consideration in this paper become

$$\beta \approx \frac{\frac{180}{\pi^4}\left(\cosh\varphi+\frac{1}{Z}\sinh\varphi\right)\bar{K}_2(z)}{1+\frac{180}{\pi^4}\left(\cosh\varphi+\frac{1}{Z}\sinh\varphi\right)\bar{K}_2(z)} \qquad \text{ND}$$

$$\approx \frac{n_0+n_N}{n_0+n_N+aT^3/3k}=\frac{\rho(Z+1)/A}{\rho(Z+1)/A+aT^3/3\Re} \qquad \text{NDNR}$$

$$\approx \frac{\frac{180}{\pi^4}\sum\frac{(-)^{n+1}}{n^4}\bar{K}_2(nz)}{1+\frac{180}{\pi^4}\sum\frac{(-)^{n+1}}{n^4}\bar{K}_2(nz)} \sim \frac{\frac{180}{\pi^4}\bar{K}_2(z)}{1+\frac{180}{\pi^4}\bar{K}_2(z)} \qquad \text{END} \qquad \text{(B99)}$$

$$\approx \frac{\frac{180}{\pi^4}[\tfrac{7}{8}\zeta(4)]}{1+\frac{180}{\pi^4}[\tfrac{7}{8}\zeta(4)]}=\tfrac{7}{11}=0.6364. \qquad \text{ENDER}$$

The final extreme non-degenerate, extreme relativistic approximation for pairs dominant differs markedly from the customary approximation without pairs. In this latter case for massive stars β is approximately zero independent of temperature. It will now be clear from the exact equation (B98) that β approaches an extreme relativistic limit between 0 and $\frac{7}{11}$ which depends on the ratio of pair particles to ionization electrons in this limit. We will find in what follows for quasi-static equilibrium that $\rho \propto (T/\mu\beta)^3$, with $\mu\beta$ fixed in the limit so that both $n_0 = \rho Z/AM_u$ and $2n_+$ are proportional to T^3.

At this point it is necessary to give the appropriate generalization of the polytropic density-temperature relation (eq. [31] of the main text), taking into account the small deviations from Boyle's Law found above for elevated temperature. It is only necessary to introduce the quantity q to arrive at the result

$$\rho=\frac{1}{4\pi}\left(\frac{n+1}{G}\right)^3\left(\frac{M_n}{M_c}\right)^2\left(\frac{q\Re T}{\mu\beta}\right)^3. \qquad \text{(B100)}$$

In terms of

$$\eta_n=\frac{45}{4\pi^3}\frac{(n+1)^3}{M_u{}^4}\left(\frac{\hbar c}{G}\right)^3\left(\frac{M_n}{M_c}\right)^2=\frac{3}{4\pi}(n+1)^3\frac{\Re^4}{aG^3}\left(\frac{M_n}{M_c}\right)^2, \qquad \text{(B101)}$$

equation (B100) becomes

$$\rho=\frac{\pi^2}{45}M_u\eta_n\left(\frac{qkT}{\hbar c\mu\beta}\right)^3. \qquad \text{(B102)}$$

For $n = 3$

$$\eta_3=\frac{720}{\pi^3 M_u{}^4}\left(\frac{\hbar c}{G}\right)^3\left(\frac{M_3}{M_c}\right)^2=335.2\left(\frac{M_\odot}{M_c}\right)^2. \qquad \text{(B103)}$$

The numerical coefficient is 30.9 for $\eta_0(n = 0)$. The reason that the generalization can be made so simply lies in the fact that the polytropic structure equations in $\rho = \rho(r)$ are derived from the equation of hydrostatic equilibrium, $dp/dr = -\rho GM_r/r^2$, the mass conservation law, $dM_r/dr = 4\pi\rho r^2$, and the equation of state $p = \kappa\rho^{1+1/n}$ independent of any gas law relating T to ρ and p. A gas law $T = T(\rho, p)$ merely serves to give $T = T(r)$ from the polytropic equations for $\rho(r)$ and $p(r)$.

Again it is emphasized that M_c in equations (B100)–(B103) is the *effective* stellar mass

approximately equal to the mass of the central homogeneous region or core and taken throughout this paper to be given by $M_c = \frac{2}{3}M$. Equations (B100) and (B102) hold everywhere throughout a polytrope of index $n = 3$ as a function of time but only at the center for a polytrope with $n \neq 3$. To avoid a cumbersome notation, subscripts denoting the central region have not been included in equations (B100) or (B102) and will not be included in the equations to follow. *In this section* (h) *the equations presented hold as functions of the time everywhere throughout a polytrope of index* 3 *but only at the center of polytropes with* n $\neq$ 3. Equations (B98) and (B99) previously given and (B114) below are exceptions to this point.

The density-temperature relation can be made an explicit one by inclusion in equation (B102) of the expression (B98) for β and a corresponding one for the mean molecular weight μ. This is

$$\mu = \frac{1}{NM_u} = \frac{\rho}{nM_u} = \frac{\pi^2}{45}\frac{\eta_n}{n}\left(\frac{qkT}{\hbar c \mu \beta}\right)^3. \tag{B104}$$

(It is hoped that the use of the n for particle density and the subscript n for polytropic index coupled with n as a running index in summations will not lead to overwhelming confusion.) Solving for μ and using equations (B40), (B42), and (B98) leads to the result

$$\frac{\mu}{q} = \eta_n^{1/4}\frac{\left[1+\frac{180}{\pi^4}\sum\frac{(-)^{n+1}}{n^4}\left(\cosh n\varphi+\frac{n}{Z}\sinh n\varphi\right)\bar{K}_2(nz)\right]^{3/4}}{\frac{180}{\pi^4}\sum\frac{(-)^{n+1}}{n^4}\left(\cosh n\varphi+\frac{n}{Z}\sinh n\varphi\right)\bar{K}_2(nz)}. \tag{B105}$$

For $n = 3$ it will be noted that

$$\eta_3^{1/4} = 4.28\left(\frac{M_\odot}{M_c}\right)^{1/2}. \tag{B106}$$

The various approximations under consideration in this paper become

$$\frac{\mu}{q} \approx \eta_n^{1/4}\frac{\left[1+\frac{180}{\pi^4}\left(\cosh\varphi+\frac{1}{Z}\sinh\varphi\right)\bar{K}_2(z)\right]^{3/4}}{\frac{180}{\pi^4}\left(\cosh\varphi+\frac{1}{Z}\sinh\varphi\right)\bar{K}_2(z)} \qquad \text{ND}$$

$$\approx \eta_n^{1/4}\frac{\left[1+\frac{180}{\pi^4}\sum\frac{(-)^{n+1}}{n^4}\bar{K}_2(nz)\right]^{3/4}}{\frac{180}{\pi^4}\sum\frac{(-)^{n+1}}{n^4}\bar{K}_2(nz)} \sim \eta_n^{1/4}\frac{\left[1+\frac{180}{\pi^4}\bar{K}_2(z)\right]^{3/4}}{\frac{180}{\pi^4}\bar{K}_2(z)} \qquad \text{END} \tag{B107}$$

$$\approx \frac{(11/4)^{3/4}}{(7/4)}\eta_n^{1/4} = 1.220\eta_n^{1/4}. \qquad \text{ENDER}$$

For a polytrope of index $n = 3$ this last relation becomes

$$\frac{\mu}{q} \approx 5.22\left(\frac{M_\odot}{M_c}\right)^{1/2} \qquad n = 3 \text{ ENDER} \tag{B108}$$

and

$$\mu \approx 5.48\left(\frac{M_\odot}{M_c}\right)^{1/2}. \qquad n = 3 \text{ ENDER} \tag{B109}$$

In order finally to establish the ρ, T-relation the following quantity will be needed:

$$\frac{\mu\beta}{q} = \eta_n^{1/4}\left[1+\frac{180}{\pi^4}\sum\frac{(-)^{n+1}}{n^4}\left(\cosh n\varphi+\frac{n}{Z}\sinh n\varphi\right)\bar{K}_2(nz)\right]^{-1/4}; \tag{B110}$$

with these various approximations

$$\frac{\mu\beta}{q} \approx \eta_n^{1/4} \qquad \text{NDNR}$$

$$\approx \eta_n^{1/4}\left[1+\frac{180}{\pi^4}\left(\cosh\varphi+\frac{1}{Z}\sinh\varphi\right)\bar{K}_2(z)\right]^{-1/4} \qquad \text{ND}$$

$$\approx \eta_n^{1/4}\left[1+\frac{180}{\pi^4}\sum\frac{(-)^{n+1}}{n^4}\bar{K}_2(nz)\right]^{-1/4} \sim \eta_n^{1/4}\left[1+\frac{180}{\pi^4}\bar{K}_2(z)\right]^{-1/4} \qquad \text{END} \qquad \text{(B111)}$$

$$\approx \left(\frac{4}{11}\right)^{1/4}\eta_n^{1/4} = 0.777\,\eta_n^{1/4}. \qquad \text{ENDER}$$

For a polytrope of index $n = 3$

$$\frac{\mu\beta}{q} \sim 4.28\left(\frac{M_\odot}{M_c}\right)^{1/2}\left[1+\frac{180}{\pi^4}\bar{K}_2(z)\right]^{-1/4} \quad n=3 \qquad \text{END}$$

$$\approx 3.32\left(\frac{M_\odot}{M_c}\right)^{1/2}, \qquad n=3 \quad \text{ENDER} \qquad \text{(B112)}$$

and

$$\mu\beta \approx 4.28\left(\frac{M_\odot}{M_c}\right)^{1/2}, \qquad n=3 \quad \text{NDNR}$$

$$\mu\beta \approx 3.48\left(\frac{M_\odot}{M_c}\right)^{1/2}. \qquad n=3 \quad \text{ENDER} \qquad \text{(B113)}$$

It will be apparent from equation (B98) that

$$1-\beta = \left[1+\frac{180}{\pi^4}\sum\frac{(-)^{n+1}}{n^4}\left(\cosh n\varphi+\frac{n}{Z}\sinh n\varphi\right)\bar{K}_2(nz)\right]^{-1}. \qquad \text{(B114)}$$

This combined with equation (B110) leads back full circle to Eddington's quartic equation now generalized for deviations from Boyle's Law as follows:

$$\left(\frac{\mu\beta}{q}\right)^4 = \eta_n(1-\beta)$$

$$= \frac{45}{4\pi^3}\frac{(n+1)^3}{M_u^4}\left(\frac{\hbar c}{G}\right)^3\left(\frac{M_u}{M_c}\right)^2(1-\beta) \qquad \text{(B115)}$$

$$= \frac{3}{4\pi}\frac{(n+1)^3\mathfrak{R}^4}{aG^3}\left(\frac{M_n}{M_c}\right)^2(1-\beta).$$

Thus

$$\frac{\mu\beta}{q} = 4.28\left(\frac{M_\odot}{M_c}\right)^{1/2}(1-\beta)^{1/4}, \qquad n=3 \qquad \text{(B116)}$$

which is the exact equation corresponding to the first form of equation (B112) and reduces to the second form in the ENDER limit when $\beta \approx \frac{7}{11}$. In massive stars the customary procedure, ignoring pair formation, has been to set $\beta \approx 0$ in equation (B116). This is still a satisfactory approximation at low temperatures, but equation (B112) is the correct limit at high temperatures. At low temperatures in massive stars $\mu = A/(Z+1)$, $q = 1$, and equation (B116) indicates that β is small and given by

$$\beta \approx 4.28\frac{Z+1}{A}\left(\frac{M_\odot}{M}\right)^{1/2}, \qquad n=3 \quad \text{NDNR} \qquad \text{(B117)}$$

while at high temperature $\beta = \frac{7}{11}$, $q = 1.050$, and equations (B112) and (B113) indicate

$$\mu \approx 5.48 \left(\frac{M_\odot}{M_c}\right)^{1/2}. \qquad n = 3 \quad \text{ENDER} \tag{B118}$$

In this section, relations have only been given for conditions at the center for polytropes with n $\neq$ 3. The variation of $\mu\beta$ throughout a massive polytrope is given for the non-relativistic, non-degenerate ($\beta \sim 0$) approximation in equation (48) in Part III.

The substitution of equation (B110) into equation (B102) leads to the density-temperature relation

$$\begin{aligned}\rho &= \frac{4\pi^2}{180} M_u \eta_n^{1/4} \left(\frac{kT}{\hbar c}\right)^3 \\ &\quad \times \left[1 + \frac{180}{\pi^4} \sum \frac{(-)^{n+1}}{n^4} \left(\cosh n\varphi + \frac{n}{Z} \sinh n\varphi\right) \bar{K}_2(nz)\right]^{3/4} \\ &= \frac{1}{(4\pi)^{1/4}} \left[\frac{(n+1)a}{3G}\right]^{3/4} \left(\frac{M_n}{M_c}\right)^{1/2} T^3 \qquad \text{(B119)} \\ &\quad \times \left[1 + \frac{180}{\pi^4} \sum \frac{(-)^{n+1}}{n^4} \left(\cosh n\varphi + \frac{n}{Z} \sinh n\varphi\right) \bar{K}_2(nz)\right]^{3/4} \\ &= \frac{1}{(4\pi)^{1/4}} \left[\frac{(n+1)a}{3G}\right]^{3/4} \left(\frac{M_n}{M_c}\right)^{1/2} T^3/(1-\beta)^{3/4}.\end{aligned}$$

For a polytrope of index $n = 3$

$$\begin{aligned}\rho &= \frac{1}{(4\pi)^{1/4}} \left(\frac{4a}{3G}\right)^{3/4} \left(\frac{M_3}{M_c}\right)^{1/2} T^3 \\ &\quad \times \left[1 + \frac{180}{\pi^4} \sum \frac{(-)^{n+1}}{n^4} \left(\cosh n\varphi + \frac{n}{Z} \sinh n\varphi\right) \bar{K}_2(nz)\right]^{3/4} \qquad n = 3 \\ &= 1.298 \times 10^5 \left(\frac{M_\odot}{M_c}\right)^{1/2} T_9^3 \qquad \text{(B120)} \\ &\quad \times \left[1 + \frac{180}{\pi^4} \sum \frac{(-)^{n+1}}{n^4} \left(\cosh n\varphi + \frac{n}{Z} \sinh n\varphi\right) \bar{K}_2(nz)\right]^{3/4} \text{gm cm}^{-3} \; n = 3 \\ &\approx 1.298 \times 10^5 \left(\frac{M_\odot}{M_c}\right)^{1/2} T_9^3 \text{ gm cm}^{-3}. \qquad n = 3 \quad \text{NDNR}\end{aligned}$$

At the center of a polytrope of index $n = 0$ the numerical coefficient is 0.715×10^5.

The various approximations of interest give

$$\begin{aligned}\rho &\approx \frac{1}{(4\pi)^{1/4}} \left[\frac{(n+1)a}{3G}\right]^{3/4} \left(\frac{M_n}{M_c}\right)^{1/2} T^3 \qquad (\beta \ll 1) \quad \text{NDNR} \\ &\approx \frac{1}{(4\pi)^{1/4}} \left[\frac{(n+1)a}{3G}\right]^{3/4} \left(\frac{M_n}{M_c}\right)^{1/2} T^3 \\ &\quad \times \left[1 + \frac{180}{\pi^4} \left(\cosh \varphi + \frac{1}{Z} \sinh \varphi\right) \bar{K}_2(z)\right]^{3/4} \qquad \text{ND} \qquad \text{(B121)} \\ &\approx \frac{1}{(4\pi)^{1/4}} \left[\frac{(n+1)a}{3G}\right]^{3/4} \left(\frac{M_n}{M_c}\right)^{1/2} T^3 \left[1 + \frac{180}{\pi^4} \sum \frac{(-)^{n+1}}{n^4} \bar{K}_2(nz)\right]^{3/4} \text{END}\end{aligned}$$

$$\sim \frac{1}{(4\pi)^{1/4}}\left[\frac{(n+1)a}{3G}\right]^{3/4}\left(\frac{M_n}{M_c}\right)^{1/2} T^3\left[1+\frac{180}{\pi^4}\bar{K}_2(z)\right]^{3/4} \qquad \text{END}$$

$$\approx \frac{1}{(4\pi)^{1/4}}\left[\frac{11(n+1)a}{12G}\right]^{3/4}\left(\frac{M_n}{M_c}\right)^{1/2} T^3; \qquad \text{ENDER}$$

and for a polytrope of index $n = 3$

$$\rho \approx \frac{1}{(4\pi)^{1/4}}\left(\frac{11a}{3G}\right)^{3/4}\left(\frac{M_3}{M_c}\right)^{1/2} T_3 \qquad n=3 \text{ ENDER} \tag{B122}$$

$$\approx 2.78\times 10^5\left(\frac{M_\odot}{M_c}\right)^{1/2} T_9^3 \text{ gm cm}^{-3}. \qquad n=3 \text{ ENDER}$$

Note that expression (B122) contains $(\frac{11}{3})^{3/4}$ where (B120) contains $(\frac{4}{3})^{3/4}$. *At the center of a polytrope of index* n = 0 *the numerical coefficient is* 1.53×10^5.

The main effect of electron-positron pair formation on stellar structure is thus an increase in ρ/T^3 by at most a factor of $(\frac{11}{4})^{3/4} = 2.14$ in going from the non-relativistic, $\bar{K}_2(nz) = 0$, to the extreme relativistic, $\bar{K}_2(nz) = 1$, limit. The transition occurs where $\bar{K}_2(z) \sim \frac{1}{2}$ or $z \sim 2$ and $kT \sim \frac{1}{2}m_ec^2 = 255$ keV, $T_9 \sim 3$. This is correlated with the fact that β approaches the limit $\frac{7}{11}$ in the non-degenerate cases rather than remaining equal to the non-relativistic value as is the case without pair formation. The factor $(\frac{11}{4})^{3/4}$ applies accurately only for very massive stars. For stars around $M_c \sim M_\odot$ the variation in ρ/T^3 is very small over the whole temperature range. We emphasize again that these remarks apply to all parts of a polytrope of index $n = 3$ but only to the central region for other polytropes.

i) The Polytropic Radius and Mean Density

Closely associated with the polytropic density-temperature relation discussed in the previous section is the question of the dependence of the radius R_c and mean density $\bar{\rho}_c$ of a polytropic stellar core on its central temperature T_o or central density ρ_o. The relations to follow can be verified starting with the basic expressions for R and $\bar{\rho}$ given by Eddington (1930) or Chandrasekhar (1939). Since our discussion applies to a stellar core of mass M_c independent of the stellar envelope, we also append a subscript c to the symbols for the radius and the mean density. These subscripts can all be dropped in treating polytropes without envelopes. One of the constants of integration of the second-order differential equation of polytropic equilibrium has been introduced early in this paper and designated in our notation by M_n. At this point the second constant, to which the stellar radius is proportional, must be introduced and will be indicated by R_n rather than by R' as used by Eddington. Then

$$R_c = \frac{GM_cR_n}{(n+1)M_n}\left(\frac{\mu\beta}{q\Re T}\right)_o$$

$$\approx \frac{R_n}{T_o}\left(\frac{M_c}{M_n}\right)^{1/2}\left[\frac{3G}{4\pi(n+1)a}\right]^{1/4} \qquad \text{NDNR}$$

$$\approx \frac{R_n}{T_o}\left(\frac{M_c}{M_n}\right)^{1/2}\left[\frac{3G}{4\pi(n+1)a}\right]^{1/4}\left[1+\frac{180}{\pi^4}\left(\cosh\varphi+\frac{1}{Z}\sinh\varphi\right)\bar{K}_2(z)\right]_o^{-1/4} \text{ ND} \tag{B123}$$

$$\sim \frac{R_n}{T_o}\left(\frac{M_c}{M_n}\right)^{1/2}\left[\frac{3G}{4\pi(n+1)a}\right]^{1/4}\left[1+\frac{180}{\pi^4}\bar{K}_2(z_o)\right]^{-1/4} \qquad \text{END}$$

$$\approx \frac{R_n}{T_o}\left(\frac{M_c}{M_n}\right)^{1/2}\left[\frac{3G}{11\pi(n+1)a}\right]^{1/4}. \qquad \text{ENDER}$$

For a polytrope of index $n = 3$ for which $R_3 = 6.897$ and $M_3 = 2.018$

$$R_c = \frac{GM_cR_3}{4M_3}\left(\frac{\mu\beta}{q\Re T}\right)_o = 0.855GM_c\left(\frac{\mu\beta}{\Re T}\right)_o = 1.36\times 10^9\left(\frac{\mu\beta}{T_9}\right)_o\left(\frac{M_c}{M_\odot}\right)\text{cm}$$

$$\approx\frac{R_3}{T_o}\left(\frac{M_c}{M_3}\right)^{1/2}\left(\frac{3G}{16\pi a}\right)^{1/4}\left[1+\frac{180}{\pi^4}\left(\cosh\varphi+\frac{1}{Z}\sinh\varphi\right)\bar{K}_2(z)\right]_o^{-1/4} \qquad n=3 \text{ ND}$$

$$\sim\frac{R_3}{T_o}\left(\frac{M_c}{M_3}\right)^{1/2}\left(\frac{3G}{10\pi a}\right)^{1/4}\left[1+\frac{180}{\pi^4}\bar{K}_2(z_o)\right]^{-1/4} \qquad n=3 \quad \text{END}$$

$$\approx\frac{5.83\times 10^9}{(T_9)_o}\left(\frac{M_c}{M_\odot}\right)^{1/2}(1-\beta)^{1/4}\sim\frac{5.83\times 10^9}{(T_9)_o}\left(\frac{M_c}{M_\odot}\right)^{1/2}\text{cm} \qquad n=3 \text{ NDNR} \quad \text{(B124)}$$

$$\sim\frac{5.83\times 10^9}{(T_9)_o}\left(\frac{M_c}{M_\odot}\right)^{1/2}\left[1+\frac{180}{\pi^4}\bar{K}_2(z_o)\right]^{-1/4}\text{cm} \qquad n=3 \quad \text{END}$$

$$\approx\frac{R_3}{T_o}\left(\frac{M_c}{M_3}\right)^{1/2}\left[\frac{3G}{44\pi a}\right]^{1/4} \qquad n=3 \text{ ENDER}$$

$$\approx\frac{4.53\times 10^9}{(T_9)_o}\left(\frac{M_c}{M_\odot}\right)^{1/2}\text{cm}. \qquad n=3 \text{ ENDER}$$

For a polytrope of index $n = 0$ the numerical coefficients are 1.88×10^9 and 1.46×10^9 for the END and ENDER approximations, respectively. In this case $R_0 = \sqrt{6} = 2.4495$ while $M_0 = 2\sqrt{6} = 4.8990$.

The mean density can be expressed in terms of the central density in exactly the same way as is the case without pair formation, as follows:

$$\bar{\rho}_c = \frac{M_c}{\frac{4}{3}\pi R_c^3} = \frac{3M_n}{R_n^3}\rho_o$$

$$= 1.845\times 10^{-2}\rho_o \qquad n=3$$

or

$$\rho_o = 54.18\bar{\rho}_c. \qquad n=3 \quad \text{(B125)}$$

Equation (B125) can be used in connection with equations (B119)–(B122), evaluated at the center to yield explicit expressions for $\bar{\rho}_c$. M_n and R_n are tabulated accurately in Table 4 of Chandrasekhar (1939).

Important quantities in nuclear astrophysics are the number, n, of nucleons and electrons per cm^2 in a column extending from the center of a star to its surface. One finds

$$n_{\text{nucleons}} = \mu_e n_{\text{electrons}} = \frac{1}{M_u}\int\rho dr$$

$$= 1.36\,\frac{\rho_0 R}{M_u R_3} \qquad n=3 \qquad \text{(B126)}$$

$$\approx 9.0\times 10^{37}(T_9)_o^2(1-\beta_o)^{-1/2}\,\text{cm}^{-2} \qquad n=3 \quad \text{NDNR}$$

$$\approx 1.50\times 10^{38}(T_9)_o^2\,\text{cm}^{-2}. \qquad n=3 \quad \text{ENDER}$$

Note that equation (B118) must be used for $\mu_e \approx \mu$ in the ENDER approximation. The corresponding numerical coefficients for $n = 0$ are 8.1×10^{37} cm^{-2} and 1.35×10^{38} cm^{-2} for the NDNR and ENDER approximations, respectively.

j) Discussion

It is now possible to diagnose at least in part some of the effects of pair formation in stars. Equation (B99) shows the remarkable contrast between the extreme non-degenerate solutions for very massive stars and the ordinary non-degenerate solutions. In the latter case at low temperatures it will be noted that (B99, NDNR) gives β in terms of the density as well as the temperature. But the density at a given temperature in a specified polytropic structure in turn depends upon β and also on μ as indicated by equation (B102). The solution of the problem is given by Eddington's quartic equation (B115). If pair formation is ignored, this equation gives a value for β in the central regions of a star which is *independent* of ρ, T and depends only on the effective stellar mass ($\sim$ core mass), the polytropic index, and the mean molecular weight μ. Values elsewhere in the star can be easily found in terms of the polytropic structure equations. When μ changes due to ionization or nuclear reactions new values for β can be computed.

Pair formation makes μ a variable over and beyond the changes from ionization or nuclear transmutations. The solution of the problem in the non-degenerate approximation is the quartic equation in $(\mu\beta)^2$ discussed in detail in Part III. As can be anticipated on physical grounds μ decreases with temperature and β increases with temperature from the values given by Eddington's quartic equation. This is illustrated in Figure 4 for $M_c = 20\ M\odot$ where the resulting decrease in $\mu\beta$ is also illustrated as an example of the general behavior.

On the other hand, in massive stars where pairs can greatly outnumber the ionization electrons at elevated temperatures, the solutions are actually much simpler in nature, as indicated by the various equations labeled "END" and "ENDER" above. The ratio of gas to total pressure is low in value at low temperature in massive stars being proportional to $(M\odot/M_c)^{1/2}$ from equation (B117) but rises to a limiting value $\frac{7}{11}$ at high temperature. The mean molecular weight is initially $\mu = A/(Z+1)$ but tends to a low limiting value proportional to $(M\odot/M_c)^{1/2}$ at high temperatures. The product $\mu\beta$ or more exactly $\mu\beta/q$ also is proportional to $(M\odot/M_c)^{1/2}$, but the coefficient only decreases by at most the factor $(\frac{4}{11})^{1/4} = 0.78$ in the run from low temperature to high.

At this point it must be emphasized that the END and ENDER limits given in the various equations of this appendix apply only to massive stars ($M_c > 10\ M\odot$) and with good accuracy only to very massive stars ($M_c > 100\ M\odot$). The ranges of limited and high accuracy just indicated have been determined by comparing numerical computations using the ordinary non-degenerate approximation with the extreme non-degenerate values. Consider the stellar mass for which β is just $\frac{7}{11}$ at low temperature. From equation (B116) this mass is

$$M_c = \frac{27}{\mu^2} M\odot = 27 \left(\frac{Z+1}{A}\right)^2 M\odot \qquad \begin{matrix} n = 3\,, & \beta = \frac{7}{11} \\ \mu = 2\,, & \beta = \frac{7}{11} \end{matrix} \qquad \text{(B127)}$$

$$= 6.8 M\odot$$

In a star of this mass, pair formation causes an increase in β with temperature and in fact the limiting value is approximately 0.75, not $\frac{7}{11} = 0.6364$. For effective masses $M_c/M\odot = 1, 10, 20, 10^2, 10^3$, and 10^4 non-degenerate numerical calculations using equations (40), (32), (37), (34), and (35) of Part III with $n = 3$ have been made by Mr. Henry Abarbanel, and are given in Table B1 for $A/Z = 2$. Values are tabulated for $T_9 = 0$, 1.98, and ∞ corresponding to $z = \infty$, 3, and 0. Values for a more complete set of temperatures have been given for $M_c = 20\ M\odot$ in Table 3 and Figure 4. These calculations use the non-degenerate rather than the extreme non-degenerate approximations so that $q = 1$ rather than 1.0505.

Comparison with non-relativistic and extreme relativistic, extreme non-degenerate approximations are indicated in Table B1. The trends discussed in this section will be

apparent. For example, for $M_c = M_\odot$ the ratio β remains substantially constant at 0.959 while for $M_c = 10\,M_\odot$ the range is $0.55 \leq \beta \leq 0.72$. The temperatures and stellar masses at which the NDNR ($T = 0$) and ENDER ($T = \infty$) limits are useful will also become clear from perusal of Table B1. As noted previously the tabulated calculations assume $q = 1$ (NDER).

The considerations of this section have neglected general relativity. It has been found (Iben 1963) that massive stellar or polytropic systems in hydrostatic equilibrium are not bound when appropriate modifications for general relativity are made to the relation equating the pressure gradient to the gravitational force per cm^3. This result and others make it necessary to use the results of this section for $M > 10^6\,M_\odot$ with some care. This matter has been discussed in part at least by HFB[2] (1964).

TABLE B1

THE RUN OF VARIOUS QUANTITIES WITH TEMPERATURE IN STARS WITH $M_c/M_\odot = 1$–10^4 [$n = 3$, $A/(Z+1) = 2$]

$M_c/M_\odot$	T_9	$\mu\beta$	μ	β	ρ_5/T_9^3	$(M_c/M_\odot)^{1/2}\times\mu\beta$	$(M_c/M_\odot)^{1/2}\times\mu$	$(M_c/M_\odot)^{1/2}\times\beta$	$(M_c/M_\odot)^{1/2}\times\rho_5/T_9^3$
1....	0	1.9185	2.000	0.9593	14.28	1.9185	2.000	0.9593	14.28
1....	1.98	1.9181	2.000	.9591	14.31	1.9181	2.000	0.9591	14.31
1....	∞	1.9135	1.994	.9593	14.42	1.9135	1.994	0.9593	14.42
10....	0	1.1044	2.000	.5522	0.7498	3.492	6.324	1.746	2.371
10....	1.98	1.0850	1.861	.5830	0.7909	3.431	5.884	1.843	2.501
10....	∞	0.9843	1.373	.7169	1.0591	3.112	4.341	2.267	3.349
20....	0	0.8342	2.000	.4171	0.4350	3.731	8.944	1.865	1.945
20....	1.98	0.8094	1.672	.4841	0.4761	3.620	7.477	2.165	2.129
20....	∞	0.7156	1.047	.6834	0.6891	3.200	4.682	3.056	3.082
10^2....	0	0.4035	2.000	.2018	0.1537	4.035	20.0	2.018	1.537
10^2....	1.98	0.3799	1.020	.3724	0.1842	3.799	10.20	3.724	1.842
10^2....	∞	0.3269	0.499	.6550	0.2891	3.269	4.99	6.550	2.891
10^3....	0	0.1327	2.000	.0664	0.0432	4.196	63.24	2.10	1.366
10^3....	1.98	0.1216	0.3562	.3414	0.0562	3.845	11.26	10.79	1.777
10^3....	∞	0.1039	0.1593	.6520	0.0898	3.285	5.04	20.60	2.845
10^4....	0	0.0425	2.000	.0212	0.0131	4.25	200	2.12	1.31
10^4....	1.98	0.0385	0.1138	.3383	0.0177	3.85	11.38	33.83	1.77
10^4....	∞	0.0329	0.0506	0.6502	0.0284	3.29	5.06	65.02	2.84
Compare equations.....		(B112) and (B113)				(B118)	(B117)	(B120) and (B122)	

k) Conditions for Non-degeneracy

The non-degenerate approximations used throughout this paper require that

$$\exp(z\omega - \varphi) \geq 1 \tag{B128}$$

in the integrands which appear in equations (B1), (B27), and (B44) for the case of negative electrons. Clearly equation (B128) is satisfied if

$$\varphi \leq z\omega = \frac{W}{kT}, \tag{B129}$$

and the question remaining concerns what value of the total energy $W = \omega m_e c^2$ to employ in equation (B129). We adopt the customary stipulation that ω is to be taken at the maximum value of one of the integrands in equations (B1), (B27), or (B44) and

choose the pressure integrand for electrons in equation (B27) for the calculations to follow. This integrand has a maximum value when

$$3\omega\,[\exp(z\omega-\varphi)+1]=z(\omega^2-1)\exp(z\omega-\varphi)\,. \tag{B130}$$

If equations (B128) and (B129) are fulfilled this reduces to

$$z\left(\omega-\frac{1}{\omega}\right)=3\,. \tag{B131}$$

In the extreme relativistic case $\omega > 1$

$$z\omega=\frac{W}{kT}\approx 3\,. \tag{B132}$$

In the non-relativistic case $\epsilon < 1$ in $\omega = 1+\epsilon$ so that

$$z\epsilon=\frac{E}{kT}\approx\tfrac{3}{2}\,, \tag{B133}$$

where E is the kinetic energy. It will be apparent that these relations are at least approximately equivalent to using $z\omega = z + x$, where x is the mean kinetic energy of the electrons so that equation (B129) becomes

$$\varphi\leq z+x=\frac{m_e c^2+\langle E\rangle}{kT}=\frac{\langle W\rangle}{kT} \tag{B134}$$

or in terms of the chemical potential

$$\Phi\leq\langle W\rangle\,, \tag{B135}$$

which we will take as the condition for non-degeneracy. Equation (B134) is a generalization of (B14) and equation (B135) generalizes (B15).

In the non-relativistic case from equation (B21)

$$\frac{n_0}{2n_1}=\sinh\varphi\approx\tfrac{1}{2}\exp\varphi\leq\tfrac{1}{2}\exp z\,, \qquad \text{NDNR} \tag{B136}$$

so that with equations (B17) and (B9)

$$n_0\leq n_1\exp z=2\left(\frac{m_e kT}{2\pi\hbar^2}\right)^{3/2}\leq 1.53\times 10^{29}T_9^{3/2}\ \text{cm}^{-3}\,. \quad \text{NDNR} \tag{B137}$$

The maximum density at which stellar matter can be considered to be non-relativistically non-degenerate is then, with $\mu_e = A/Z$,

$$\rho=\mu_e M_u n_0\leq 2.54\times 10^5\,\mu_e T_9^{3/2}\ \text{gm cm}^{-3}\,. \qquad \text{NDNR} \tag{B138}$$

In the extreme relativistic case

$$n_0\leq 2n_1\sinh 3=\frac{40}{\pi^2}\left(\frac{kT}{\hbar c}\right)^3\leq 3.38\times 10^{29}T_9^3\ \text{cm}^{-3}\,. \quad \text{NDER} \tag{B139}$$

The maximum density at which stellar matter can be considered to be relativistically non-degenerate is then, with $\mu_e = A/Z$,

$$\rho\leq 5.60\times 10^5\,\mu_e T_9^3\ \text{gm cm}^{-3}\,. \qquad \text{NDER} \tag{B140}$$

l) Potential Energy and Total Energy of a Massive Polytrope

The potential energy of a polytrope of index n, mass M_c, and radius R_c is

$$\Omega = -\frac{3}{5-n}\frac{GM_c^2}{R_c}. \tag{B141}$$

Combined with (B123), this yields

$$\begin{aligned}
\Omega &= -\frac{3(n+1)}{5-n}\frac{M_n}{R_n}M_c\left(\frac{q\Re T}{\mu\beta}\right)_o \\
&\approx -\frac{[108\pi(n+1)]^{1/4}}{5-n}\frac{M_n^2}{R_n}\left(\frac{M_c}{M_n}\right)^{3/2}a^{1/4}G^{3/4}T_o && \text{NDNR} \\
&\approx -0.62a^{1/4}G^{3/4}M_c^{3/2}T_o && n=3 \quad \text{NDNR} \\
&\approx -6.9\times 10^{49}\left(\frac{M_c}{M_\odot}\right)^{3/2}(T_9)_o \text{ erg} && n=3 \quad \text{NDNR} \\
&\approx -\frac{[297\pi(n+1)]^{1/4}}{5-n}\frac{M_n^2}{R_n}\left(\frac{M_c}{M_n}\right)^{3/2}a^{1/4}G^{3/4}T_o && \text{ENDER} \\
&\approx -0.80a^{1/4}G^{3/4}M_c^{3/2}T_o && n=3 \quad \text{ENDER} \\
&\approx -8.8\times 10^{49}\left(\frac{M_c}{M_\odot}\right)^{3/2}(T_9)_o \text{ erg}. && n=3 \quad \text{ENDER}
\end{aligned} \tag{B142}$$

For $n = 0$ the corresponding numerical coefficients are -8.6×10^{49} and -10.9×10^{49} in the NDNR and ENDER approximations, respectively.

For $n = 5$, R_c is infinite and (B141) yields an indeterminate result. However, if we use

$$\Omega = -3\int p dV = -12\pi\int pr^2 dr, \tag{B143}$$

it can be shown that

$$\begin{aligned}
\Omega &\approx -6.0\times 10^{49}\left(\frac{M_c}{M_\odot}\right)^{3/2}(T_9)_o \text{ erg} && n=5 \quad \text{NDNR} \\
&\approx -7.5\times 10^{49}\left(\frac{M_c}{M_\odot}\right)^{3/2}(T_9)_o \text{erg}. && n=5 \quad \text{ENDER}
\end{aligned} \tag{B144}$$

The NDNR approximation holds at low temperatures for massive stars where $\beta \approx 0$, while the ENDER approximation applies to massive stars at high temperatures where $\beta \approx \frac{7}{11}$.

In both of the extreme cases described by expression (B142) the internal heat energy of the polytrope is closely equal to $|\Omega|$ and the total energy is closely equal to zero. However, in the NDNR case it is useful to determine the total energy E or binding energy E_B from

$$E = -E_B \approx -\tfrac{3}{2}\int p_o dV = -6\pi\int \beta p r^2 dr. \qquad \text{NDNR} \tag{B145}$$

Combined with equation (48) of the main text, this yields

$$E \approx -\frac{6\pi}{\mu}p_o\eta_n^{1/4}\int_0^R\left(\frac{p}{p_o}\right)\left(\frac{T/\mu\beta}{T_o/\mu_o\beta_o}\right)^{(n-3)/4}r^2dr. \qquad \text{NDNR} \tag{B146}$$

In the notation used by Eddington (1930) this equation can be reduced to

$$E \approx -\frac{3}{2M_n}\frac{M_c\Re T_o}{\mu}\int_0^{R_n}u^{(5n+1)/4}z^2dz, \qquad \text{NDNR} \tag{B147}$$

where $u = (\rho/\rho_o)^{1/n}$ is known for each polytrope as a function of the dimensionless radial variable z. For a polytrope of index $n = 3$, the integral equals $2M_3^2/R_3$ so

$$E \approx -3\frac{M_3}{R_3}\frac{M_c \Re T_o}{\mu}$$

$$\approx -0.88\frac{M_c \Re T_o}{\mu} \qquad M_3 = 2.02\,, \qquad R_3 = 6.90\,, \quad n = 3 \tag{B148}$$

$$\approx -1.46 \times 10^{50}\frac{M_c}{M_\odot}\frac{(T_9)_o}{\mu}\,\text{erg}\,. \qquad n = 3 \text{ NDNR}$$

Thus

$$\frac{E}{M_c c^2} \approx -0.88\frac{\Re T_o}{\mu c^2} \approx -0.81 \times 10^{-4}\frac{(T_9)_o}{\mu}\,\text{erg gm}^{-1}\,. \qquad n = 3 \text{ NDNR} \tag{B149}$$

For a polytrope of index $n = 0$ the numerical coefficients are -1.87×10^{50} and -1.04×10^{-4} in equations (B148) and (B149), respectively.

m) Summary of Approximations

In this appendix the following approximations have been treated:

ND: Retain only the first term ($n = 1$) in summations such as expression (B4).
END: Set $\varphi = 0$, $\cosh n\varphi = 1$, $\sinh n\varphi = 0$, $\exp(\pm n\varphi) = 1$ and retain all terms in summations. Retain only first terms for a further approximation.
NR: Use expression (B9) for $\bar{K}_2(nz)$ or set $\bar{K}_2(nz) = 0$ in comparison with terms of order unity.
ER: Set $\bar{K}_2(nz) = 1$. (The term ER applies only to electrons and positrons.)
NDNR: Use $\bar{K}_2(nz) = 0$ to eliminate terms in φ where possible.
NDER: Set $\bar{K}_2(z) = 1$ in first term approximations to summations.
ENDER: Evaluate the various summations with $\varphi = 0$, $\bar{K}_2(nz) = 1$ in terms of Riemann Zeta-Functions.

APPENDIX C

NUCLEAR-REACTION RATES

a) Average Cross-Sections

The reaction rates of the nuclear processes of interest in the main body of this paper are the subject of this appendix. The reaction and energy generation rate for processes such as reaction (86) in Part V involving one or more heavy nuclei ($A_1 + A_0 \gtrsim 24$) can be estimated by generalizing the expressions given by B^{2}FH (1957, p. 560) under case (ii). (The reader is referred to this article for further explanation of the notation employed in what now follows.) The density of excited states or levels in the heavy compound nuclei formed in the type of interactions under consideration is great enough that the cross-section at any energy can be calculated as an average over contributions from the many resonances lying in an appropriate energy interval. It is not necessary that the resonances overlap, i.e., the widths Γ may still be narrow compared to the level spacings D. In applications in physics the average over many narrow resonances is often of significance as, for example, when the energy spread in particle beams exceeds level separations. In stellar applications the average cross-sections are important when the width of the Maxwell-Boltzmann distribution, $kT = 0.0862\ T_9$ MeV, exceeds the level spacing D.

The averaging of cross-sections is done automatically in calculations with the "optical" model of nuclear reactions since in this model a complex potential well is employed

to describe the gross structure of the nucleus without regard to the detailed spectrum of individual excited states. The potential is taken to be complex so that both scattering and absorption occur.

Let the initial nuclei in a reaction be designated by indices 0 and 1 and the final nuclei by 2 and 3 (and 4, 5, . . . , if necessary). Thus the charges and atomic masses involved are Z_0, Z_1, Z_2, Z_3, and A_0, A_1, A_2, A_3. Let the initial process or channel be designated when necessary by the index 1 and the final process or channel by the index 2. Thus the partial width ($\hbar \times$ transition probability) for the initial channel involving particles 0 and 1 is designated by Γ_1 and that for the final channel involving particles 2 and 3 is designated by Γ_2. However, we will not find it necessary to append a subscript for the center of mass energy E, the reduced mass number, $A = A_0A_1/(A_0 + A_1)$, or the rationalized De Broglie wavelength, $\lambda\!\!\!^{-} = \lambda/2\pi = 4.57/(EA)^{1/2}$ fermi, for the initial channel. In what follows there is little occasion to refer to competing channels other than 1 and 2 except in the expression for the total width, $\Gamma = \Gamma_1 + \Gamma_2 + \ldots$, which must be summed over all open channels. Let the compound nucleus formed by the interacting particles have spin and parity $J\pi$. Then the average cross-section through compound nucleus formation is

$$\begin{aligned}
\bar{\sigma} &= \Sigma \bar{\sigma}_{J^\pi} , \\
\bar{\sigma}_{J^\pi} &= \left(\left\langle \frac{1}{D} \int_r \sigma dE \right\rangle \right)_{J^\pi} \\
&= 2\pi^2 \lambda\!\!\!^{-2} (\omega \Gamma_1 \Gamma_2 / D\Gamma)_{J^\pi} \qquad \text{(C1)} \\
&= \pi^2 (\hbar^2/ME)(\omega \Gamma_1 \Gamma_2 / D\Gamma)_{J^\pi} \\
&= (4.12/AE_6)(\omega \Gamma_1 \Gamma_2 / D\Gamma)_{J^\pi} \text{ barns} (10^{-24} \text{ cm}^2),
\end{aligned}$$

where $M = AM_u$ is the reduced mass in grams, $M_u = 1.660 \times 10^{-24}$ gm is the atomic mass unit, and where $\omega = (2J + 1)/(2J_0 + 1)(2J_1 + 1)$ is the statistical factor applying to the formation of the state with spin J from the interaction of the initial nuclei with spin J_0 and J_1. The integral which appears is to be taken over a single state or Breit-Wigner resonance of the J^π type and then a "local" averaging performed which introduces the mean level spacing D. In the final expressions D and the widths are taken to be smoothly varying functions of the energy, and the sign for averaging has therefore been omitted on the right-hand sides of the equations. E_6 is the energy in MeV (10^6 eV).

b) Reaction Rates Summed over Resonances with Measured Properties

The reaction rate per second per pair of interacting particles under non-degenerate stellar conditions at temperature T is given in general by

$$\begin{aligned}
\langle \sigma v \rangle &= \frac{(8/\pi)^{1/2}}{M^{1/2}(kT)^{3/2}} \int \sigma E \exp(-E/kT)\, dE \\
&= \left(\frac{8kT}{\pi M}\right)^{1/2} \int \sigma \left(\frac{E}{kT}\right) \exp\left(-\frac{E}{kT}\right) d\left(\frac{E}{kT}\right) \text{cm}^3 \text{ sec}^{-1} .
\end{aligned} \qquad \text{(C2)}$$

In the case that individual resonances due to states of the compound nucleus are narrow ($\Gamma < kT$) and provided width and spin measurements are available on each resonance, then it is convenient to replace equation (C2) by a summation over all resonances r for *all* J^π as follows:

$$\langle \sigma v \rangle = \Sigma \langle \sigma v \rangle_r = \left(\frac{2\pi\hbar^2}{MkT}\right)^{3/2} \sum\nolimits_r \left(\frac{\omega \Gamma_1 \Gamma_2}{\hbar \Gamma}\right)_r \exp(-E_r/kT), \qquad \text{(C3)}$$

or

$$\log\langle\sigma v\rangle = -12.59 - \tfrac{3}{2}\log AT_9 + \log\sum_r(\omega\Gamma_1\Gamma_2/\Gamma)_r \exp(-E_r/kT) \quad \text{(C4)}$$

for $\langle\sigma v\rangle$ in cm^3 sec^{-1} and widths in MeV. We have used

$$\int_r \sigma E dE = (\pi^2\hbar^2/M)(\omega\Gamma_1\Gamma_2/\Gamma)_r. \quad \text{(C5)}$$

The contribution of a single resonance to equation (C3) is obvious, and equation (C4) for a single resonance becomes

$$\log\langle\sigma v\rangle_r = -12.59 - \tfrac{3}{2}\log AT_9 + \log(\omega\Gamma_1\Gamma_2/\Gamma)_r - 5.04\, E_r/T_9 \quad \text{(C6)}$$

for widths and E_r in MeV.

Nuclear compilations such as Ajzenberg-Selove and Lauritsen (1959) and Endt and van der Leun (1962) give fairly complete tables of empirical values for E_r, Γ_r, J_r^π and $[(2J+1)\Gamma_1\Gamma_2/\Gamma]_r$ for a significant number of reactions. In using these tables it is convenient in practice to make use of the fact that the resonances of importance in the stellar situation at temperature T are those which lie near the effective thermal energy given by

$$E_o = [\pi a Z_1 Z_0 kT(Mc^2/2)^{1/2}]^{2/3} = 0.122\,(Z_1^2 Z_0^2 AT_9^2)^{1/3}\ \text{MeV} \quad \text{(C7)}$$

and within the effective range of thermal energy given by

$$\Delta = 4(E_o kT/3)^{1/2} = 0.237\,(Z_1^2 Z_0^2 AT_9^5)^{1/6}\ \text{MeV}. \quad \text{(C8)}$$

Below this energy range the Γ_1 are small because Coulomb barrier penetration is low while above this energy range the exponential $\exp(-E_r/kT)$ serves as a cutoff factor. Thus it is possible to make satisfactory approximate estimates using

$$\langle\sigma v\rangle \approx \left(\frac{2\pi\hbar^2}{MkT}\right)^{3/2} \exp(-E_o/kT) \sum_o \left(\frac{\omega\Gamma_1\Gamma_2}{\hbar\Gamma}\right)_r, \quad \text{(C9)}$$

where the subscript on the summation sign indicates that only those resonances with $E_r \approx E_o$ are to be included. Numerically equation (C9) yields

$$\log\langle\sigma v\rangle \approx -12.59 - \tfrac{3}{2}\log AT_9 + \log\Sigma_o(\omega\Gamma_1\Gamma_2/\Gamma)_r - 0.615\,(Z_0^2 Z_1^2 A/T_9)^{1/3}, \quad \text{(C10)}$$

where the widths are in MeV.

Reaction rates per gm per sec are related to the $\langle\sigma v\rangle$ by

$$r = \rho\frac{x_1 x_0}{M_1 M_0}\langle\sigma v\rangle \qquad \text{reactions gm}^{-1}\ \text{sec}^{-1} \quad \text{(C11)}$$

or

$$\log r = 47.56 + \log\rho x_1 x_0/A_1 A_0 + \log\langle\sigma v\rangle. \quad \text{(C12)}$$

Equation (C11) must be multiplied by $\frac{1}{2}$ on the right if 0 and 1 are identical and $\log r$ reduced by 0.30 in equation (C12). The lifetime $\tau_0(1)$ of particles 1 to interaction with particles 0 and the lifetimes $\tau_1(0)$ of particles 0 to interaction with particles 1 with production of 2 and 3 are given in sec by

$$x_0\tau_0(1)/M_0 = x_1\tau_1(0)/M_1 = [\rho\langle\sigma v\rangle]^{-1} \quad \text{(C13)}$$

or

$$\log\tau_0(1) + \log x_0/A_0 = \log\tau_1(0) + \log x_1/A_1 = -23.78 - \log\rho - \log\langle\sigma v\rangle. \quad \text{(C14)}$$

In the case of identical particles, *two* are destroyed in each reaction, and the factor of $\frac{1}{2}$ applicable to equation (C11) does *not* apply to (C13). In $\langle\sigma v\rangle$, sum over all outgoing reaction channels, $\Gamma_2 \ldots$, if total lifetimes are required.

c) Photonuclear Reactions as the Reverse of Capture Reactions

It is frequently of interest to calculate the reaction rate for a nuclear process in reverse. In the notation employed here the reaction rate for particles 2 and 3 to form 0 and 1 is sought. At low temperatures where kT is in general small compared to the energy release Q in an exoergic reaction, the reverse rate is small compared to the direct reaction rate. However, at high temperatures ($kT \sim Q$) the reaction rates can be comparable and neither can be neglected. In addition, at high temperatures, the interacting nuclei 0, 1, 2, or 3 will be present in part in excited states and the interaction of the excited nuclei may be quite different than the interaction of the nuclei in the ground state.

These considerations are of particular importance in connection with photonuclear reactions which are the reverse of capture radiation reactions. In reaction notation the two reactions can be represented by

$$(Z_0, A_0) + (Z_1, A_1) \rightleftharpoons (Z_0 + Z_1, A_0 + A_1) + \gamma\,, \tag{C15}$$

where the capture reaction reads from left to right and the photonuclear reaction from right to left. We will confine our attention to these reversible reactions in what follows, although the generalization to other cases can be made quite straightforwardly. In addition, excited states will be considered to occur only in the nucleus produced with or interacting with the gamma-ray. Designate this nucleus as particle 2 such that $Z_2 = Z_0 + Z_1$, $A_2 \approx A_0 + A_1$, and $M_0 + M_1 = M_2 + Q/c^2$, where Q is the energy released in the capture reaction or the energy threshold in the photonuclear reaction. For an excited state at E_2^* the energy release is $Q - E_2^*$ or $(Q - E_2^*)_6$ in MeV. Thermodynamics gives the decay rate or reciprocal mean lifetime for the photonuclear reaction on the nucleus *when in this state* by

$$\frac{1}{\tau_\gamma(2^*)} = \frac{(2J_0+1)(2J_1+1)}{(2J_2^*+1)}\left(\frac{MkT}{2\pi\hbar^2}\right)^{3/2}\langle\sigma v\rangle^* \exp -(Q-E_2^*)/kT \tag{C16}$$

or

$$\log \tau_\gamma(2^*) = \log (2J_2^* + 1)/(2J_0 + 1)(2J_1 + 1) - 33.77 - \log\langle\sigma v\rangle^* - \tfrac{3}{2}\log AT_9 + 5.04\,(Q - E_2^*)_6/T_9\,, \tag{C17}$$

where $\langle\sigma v^*\rangle$ is the reaction rate for the production of the excited state of 2 from the interaction of 0 and 1. This equation does not imply equilibrium. Equilibrium holds when this decay rate is equal to the production rate. If the appropriate form of equation (C3) is substituted into equation (C16), then

$$\frac{1}{\tau_\gamma(2^*)} = \frac{1}{2J_2^*+1}\sum_r\left[\frac{(2J+1)\Gamma_1\Gamma_\gamma^*}{\hbar\Gamma}\right]_r \exp -(Q+E_r-E_2^*)/kT\,, \tag{C18}$$

where Γ_γ^* is the radiation transition probability from the state E_r to the lower state E_2^* in nucleus 2. Summing over all Γ_γ^* including the ground state yields the total radiation width Γ_γ for the state at E_r.

It will be clear that the calculation of the photonuclear reaction rate for nuclei 2, including all excited states, can be made only if the distribution among these excited states is known and that this distribution can only be calculated simply if equilibrium is assumed. Equilibrium between the excited states below E_r is a fair approximation if

photoexcitation of this state occurs at all. The relative probability of excitation to E_2^* is given by

$$P(E_2^*) = \frac{(2J_2^*+1)\exp(-E_2^*/kT)}{\Sigma_*(2J_2^*+1)\exp(-E_2^*/kT)} \approx \frac{2J_2^*+1}{2J_2+1}\exp(-E_2^*/kT). \quad \text{(C19)}$$

The approximate form assumes that 2 occurs mainly in its ground state which is sufficiently accurate for our purposes. The total decay rate or reciprocal mean lifetime is then given by

$$\frac{1}{\tau_\gamma(2)} = \sum_* \frac{P(E_2^*)}{\tau_\gamma(2^*)} \approx \frac{\exp(-Q/kT)}{2J_2+1}\sum_r \left[\frac{(2J+1)\Gamma_1\Gamma_\gamma}{\hbar\Gamma}\right]_r \exp(-E_r/kT), \quad \text{(C20)}$$

where we have used $\Sigma_*\Gamma_\gamma^* = \Gamma_\gamma$. In the spirit of the approximation represented by equation (C9) this equation becomes

$$\frac{1}{\tau_\gamma(2)} \approx \frac{\exp-(Q+E_o)/kT}{2J_2+1}\sum_o \left[\frac{(2J+1)\Gamma_1\Gamma_\gamma}{\hbar\Gamma}\right]_r \quad \text{(C21)}$$

or

$$\log \tau_\gamma(2) \approx -21.18 + \log(2J_2+1) - \log \Sigma_o[(2J+1)\Gamma_1\Gamma_\gamma/\Gamma]_r + 5.04Q_6/T_9 + 0.615(Z_1^2Z_0^2A/T_9)^{1/3}, \quad \text{(C22)}$$

where the widths and Q_6 are in MeV.

Photonuclear reaction cross-sections measured in the laboratory only determine the excitation rate for the ground state and not for the excited states. Equations (C20), (C21), and (C22) show that when the photonuclear reactions are important all states must be considered since the factor exp $(-E_2^*/kT)$ which occurs in equation (C19) has been cancelled by the factor exp $(+E_2^*/kT)$ in equation (C18). These equations require that Γ_γ be the total radiation rate to all lower states in nucleus 2. This rate can be determined experimentally from the over-all cross-section for the capture of particle 1 by particle 0.

Equation (C22) is employed extensively in Parts V and VI. It is valid only when $\langle\sigma v\rangle$ can be expressed by equation (C3). The generalization to other cases does not yield as simple an expression as equation (C22) but these cases can be worked out using (C17) and (C19) as required.

d) Continuum Cross-Sections

At sufficiently high excitation, compound nuclei exhibit overlapping resonances arising as decay widths become comparable to or greater than level separations. Continuum cross-sections are the result in which the energy dependence is dominated mainly by optical model and barrier penetration factors. In treating the continuum it is sufficiently accurate to ignore the intrinsic spins of the interacting particles and to consider only the relative orbital angular momentum of the initial particles here to be designated by l in units $\hbar$. Equation (C1) is replaced by

$$\bar{\sigma} = \Sigma\,\bar{\sigma}_l, \qquad l = 0, 1, 2, 3, \ldots,$$

and

$$\bar{\sigma}_l = 2\pi^2\lambda\!\!\!^{-2}(2l+1)(\Gamma_1\Gamma_2/D\Gamma)_l, \quad \text{(C23)}$$

where D_l is now the mean separation between all states which can be formed by the same partial wave. The parities are given by $\Pi = (-)^l$.

Before continuing it is necessary to note the modifications required in equation (C23)

when identical particles are involved. In general the statistical weight factors for permitted interactions are doubled when identical particles interact (Mott and Massey 1949). However, certain spin and orbital momentum combinations are not permitted by symmetry considerations. Certain modifications arise even though we assume spin independence for the permitted interactions as above. For identical bosons with zero spin, such as $O^{16} + O^{16}$, all odd-l interactions are forbidden, so $l = 0, 2, 4, \ldots$, and the statistical weight factors are $2, 0, 10, 0, 18, \ldots$, rather than $1, 3, 5, 7, 9, \ldots$. For identical fermions with spin $\frac{1}{2}$, the even-l orbital angular momenta combine with the total spin 0 while the odd-l orbital angular momenta combine with total spin 1. The statistical weight factors are $\frac{1}{2}, \frac{9}{2}, \frac{5}{2}, \frac{21}{2}, \frac{9}{2}, \ldots$, for $l = 0, 1, 2, 3, 4, \ldots$. For identical bosons with spin 1 it is found that the statistical weight factors are $\frac{4}{3}, \frac{6}{3}, \frac{20}{3}, \frac{14}{3}, \frac{36}{3}, \ldots$, for $l = 0, 1, 2, 3, 4, \ldots$. It will be noted in all cases that the statistical weight factors fluctuate around the normal values given by $2l + 1$ and that if a sum is taken over many l-values there is little deviation from the normal sum. This will be important in what follows.

Return now to a consideration of the term $(\Gamma_1\Gamma_2/D\Gamma)_l$ in equation (C23). In a few cases of interest the incident partial width Γ_1 is larger than the other partial widths so that $\Gamma_1 \sim \Gamma$ and equation (C23) becomes

$$\bar{\sigma}_l = 2\pi^2\lambda\!\!\!^{-2}(2l + 1)(\Gamma_2/D)_l . \qquad \Gamma_1 \sim \Gamma \quad \text{(C24)}$$

Under these circumstances the barrier penetration factor for the incident particles does not appear and the $\bar{\sigma}_l$ varies relatively slowly with energy. An exception is endoergic reactions where Γ_2 may vary rapidly because of penetration factors. Such exceptions can be treated by the methods now to be discussed merely by application of the equations derived to the interaction between the final nuclei rather than to the initial nuclei and will therefore not be discussed further.

In most cases of interest Γ_1 is small because the stellar thermal interaction involves energies well below the Coulomb and centrifugal barrier heights. Thus $\Gamma_1 < \Gamma$ and Γ_1 or rather the ratio $(\Gamma_1/D)_l$ must be evaluated as a function of energy. The ratio $(\Gamma_2/\Gamma)_l$ gives the relative probability that the compound system breaks up into nuclei 2 and 3 and will be treated as a slowly varying function of energy. For a dominant outgoing channel $(\Gamma_2/\Gamma)_l \sim 1$. The exceptional case for endoergic reactions has been noted above. It is to be emphasized that $(\Gamma_2/\Gamma)_l$ may depend on l.

The optical model (Vogt 1962) yields the following expression for $(\Gamma_1/D)_l$ for use in expression (C23) for average cross-sections:

$$\left(\frac{\Gamma_1}{D}\right)_l = \frac{2}{\pi}\left[\frac{\beta T}{(1+T)^2+\Delta^2}\right]_l \approx \frac{2}{\pi}\left[\frac{\beta T}{(1+T)^2}\right]_l , \quad \text{(C25)}$$

where T_l is the barrier *transmission* factor and is related to the barrier *penetration* factor P_l (to be discussed later) by

$$T_l = \frac{P_l}{(1+\lambda\!\!\!^{-2}/\lambda\!\!\!^{-}_o{}^2)^{1/2}}$$

$$\approx \frac{\lambda\!\!\!^{-}_o}{\lambda\!\!\!^{-}} P_l \qquad \text{Low energy } \lambda\!\!\!^{-} \gg \lambda\!\!\!^{-}_o \quad \text{(C26)}$$

$$\approx 1 \qquad \text{High energy } \lambda\!\!\!^{-} \ll \lambda\!\!\!^{-}_o, \quad P_l \approx 1 ,$$

and where Δ is a small level-shift which we neglect. The quantity, $\lambda\!\!\!^{-}_o = \hbar/(2MV_o)^{1/2}$, is the wavelength ($\times \frac{1}{2}\pi$) which results when the kinetic energy of the initial nuclei is set equal to the magnitude V_o of their mutual interaction potential. Experiments show rather surprisingly that $V_o = 40$ MeV in all interactions which have been studied so far

so that $\lambda\!\!\!^{-}_o \approx 0.7/A^{1/2}$ fermis, with A the reduced mass in atomic mass units. The approximate forms at low and high kinetic energy in equation (C26) are quite straightforward if it is recalled that P_l approaches unity at energies in excess of the barrier height. B^{2}FH (1957, p. 561) failed to include $A^{-1/2}$ in $\lambda\!\!\!^{-}_o$. Tch! Tch!

The factor β_l results in the optical model from averaging over the many compound nucleus resonances but not over the "giant" or "shape" resonances resulting from the interaction potential assumed in the model. Thus contributions from the shape resonances still remain and β_l is given by

$$\beta_l = \frac{1}{2\pi} \sum_\nu \frac{W_o D_{l\nu}}{(E_{l\nu} - E)^2 + W_o^2/4}, \tag{C27}$$

where $\nu = 1, 2, 3, \ldots$, is a radial quantum number indicating the first, second, third, etc., shape resonance for orbital angular momentum l, $E_{l\nu}$ is the resonance energy, $W_o/2$ is the imaginary part of the interaction potential and $D_{l\nu}$ is the energy separation between the ν and $\nu + 1$ resonances. $D_{l\nu}$ is much larger than D_l, the separation between compound nucleus resonances. For an oscillator potential

$$E_{l\nu} = -V_o + \hbar\omega\,(2\nu + l - \tfrac{1}{2}), \tag{C28}$$

so that

$$D_{l\nu} = E_{l,\,\nu+1} - E_{l\nu} = 2\,\hbar\omega = 2\,\hbar^2/MR\lambda\!\!\!^{-}_o = 4\,(V_o\hbar^2/2MR^2)^{1/2}, \tag{C29}$$

where ω is the fundamental oscillator angular frequency which can be expressed in terms of the depth V_o and cutoff radius R of the well. For the cases of interest in this paper $D_{l\nu} \sim$ 6–20 MeV.

The factor β_l oscillates about unity between maxima at $E = E_{l\nu}$ and minima at $E = E_{l\nu} \pm D_{l\nu}/2$. Neglecting contributions from other than the nearest level or levels one finds for $D_{l\nu} > W_o$

$$\beta_l\,(\max) \approx 2\,D_{l\nu}/\pi W_o \lesssim 3 \tag{C30}$$

and

$$\beta_l\,(\min) \approx 2\,W_o/\pi D_{l\nu} \gtrsim 0.2\,. \tag{C31}$$

The numerical values are obtained with the use of the empirical values, $W_o \sim 5$ MeV and $D_{l\nu} \lesssim 20$ MeV. Thus the deviations of β_l from unity are not very great and for a "black-body" model β_l can be found by averaging over an energy interval of the order of $D_{l\nu}$ to obtain

$$\bar{\beta}_l \approx \frac{1}{2\pi D_{l\nu}} \int_{-\infty}^{+\infty} \frac{W_o D_{l\nu} dE}{(E_{l\nu} - E)^2 + W_o^2/4} \tag{C32}$$

$$\approx 1\,. \qquad \text{Black-body model}$$

Furthermore at high energies W_o tends to increase and both $\beta_l(\max)$ and $\beta_l(\min)$ approach closer to unity. For this reason β_l has been set equal to unity in the calculations made in the main body of this paper. This substitution has not been made except in high-energy expressions in this appendix.

The above considerations yield

$$\left(\frac{\Gamma_1}{D}\right)_l \approx \frac{1}{2\pi}\left(4\,\frac{\lambda\!\!\!^{-}_o}{\lambda\!\!\!^{-}} P\beta\right)_l \qquad \text{Low energy}$$

$$\approx \frac{1}{2\pi}, \qquad \text{High energy} \tag{C33}$$

and

$$\bar{\sigma}_l = \pi\lambda\!\!\!^{-2}(2l+1)\left[\frac{4T}{(1+T)^2}\beta\frac{\Gamma_2}{\Gamma}\right]_l$$

$$\approx \pi\lambda\!\!\!^{-2}(2l+1)\left(4\frac{\lambda\!\!\!^{-}_o}{\lambda\!\!\!^{-}}P\beta\frac{\Gamma_2}{\Gamma}\right)_l \qquad \text{Low energy} \qquad \text{(C34)}$$

$$\approx \pi\lambda\!\!\!^{-2}(2l+1)\left(\frac{\Gamma_2}{\Gamma}\right)_l . \qquad \text{High energy}$$

e) The Penetration Factor at Low Energy and the Reaction Radius

For the combined Coulomb and centrifugal penetration factor at low energy ($E < E_C + E_R$) we use a slight modification of the expression involving the modified Bessel function $K_{2l+1}(x)$ given by B²FH (1957, p. 560), namely,

$$P_l(E) = \frac{\pi(E_R/E)^{1/2}}{4K^2_{2l+1}(x)}\exp\left[-\frac{\pi E_C}{(E_R E)^{1/2}} - \frac{2E}{3(E_R E_C)^{1/2}}\right]$$

$$\approx \left(\frac{E_C}{E}\right)^{1/2}\exp\left[-\frac{\pi}{2}\left(\frac{E_C}{E}\right)^{1/2}x - \frac{4E}{3E_R x} + 2x - \frac{4l(l+1)}{x}\right], \qquad \text{(C35)}$$

where

$$E_R = \text{centrifugal barrier height divided by } l(l+1)$$
$$= \hbar^2/2MR^2 = 20.9/AR_f^2 \text{ MeV}, \qquad (R_f \text{ in fermis}) \qquad \text{(C36)}$$

$$E_C = \text{Coulomb barrier height},$$
$$= Z_1 Z_0 e^2/R = 1.44\, Z_1 Z_0/R_f \text{ MeV}, \qquad \text{(C37)}$$

$$x = 2(E_C/E_R)^{1/2} = 0.525\,(AZ_1Z_0R_f)^{1/2}. \qquad \text{(C38)}$$

Note that $E_o = (\pi E_C kT/2E_R^{1/2})^{2/3}$ from (C7), (C36), and (C37). Numerically, for E_6 in MeV and R_f in fermis

$$\log P_l \approx \tfrac{1}{2}\log 1.44\, Z_1Z_0/R_fE_6 - 0.430\, Z_1Z_0A^{1/2}E_6^{-1/2} - 0.053\, E_6(AR_f^3/Z_1Z_0)^{1/2}$$
$$+ 0.457\,(AZ_1Z_0R_f)^{1/2} - 3.31\, l(l+1)/(AZ_1Z_0R_f)^{1/2}. \qquad \text{(C39)}$$

In concluding this section some discussion of numerical values for R is in order. Experiments involving the interaction of pairs of heavy ions such as $C^{12} + C^{12}$, $C^{12} + O^{16}$, $O^{16} + O^{16}$ and experiments involving the interaction of protons and alpha-particles with nuclei beyond Si^{28} indicate that the numerical coefficient in the $R = R_o(A_0^{1/3} + A_1^{1/3})$ law is probably greater than the value $R_o = 1.44$ fermis used by B²FH (1957). Elastic scattering experiments, analyzed using the Blair (1954) quarter point formalism by Bromley *et al.* (1960) lead to $R_o = 1.54$ fermis when appropriate corrections are made in the analysis. The important point is that the observed deviations from the Rutherford scattering law show which partial waves interact through the nuclear potential and which do not. From what has been said before it will be clear that this is exactly the information needed. Furthermore, electron scattering experiments (Hahn, Ravenhall, and Hofstadter 1956) show that nuclei have proton distributions which extend to $(1.07\, A_0^{1/3} + 1.2)$ fermis. The addition of one-half the range of nuclear forces brings this to $(1.07\, A_0^{1/3} + 1.9)$ fermis. It is this range which marks the *breakdown* of the pure Coulomb and centrifugal potentials due to the onset of the nuclear potential, and it is

this radius which should be used in such equations as (C35) to (C39). Over the interval $27 < A_0 < 125$ ($A_0^{1/3} \sim 4$) this expression for the range is matched most closely by $R_o\, A_0^{1/3}$ with $R_o = 1.54$ fermis. Tuttle (1952) has determined effective radii, in much the same way, using electron scattering data for the interaction of p, d, t, τ, and α with light nuclei. These radii exhibit fluctuations with characteristic minima at $A_0 = 4n$, $n = 1, 2, 3, 4, 5, \ldots$. However, on the average $R_f = 1.54\ (A_0^{1/3} + A_1^{1/3})$ also fits Tuttle's curves quite well and we have used this prescription in the calculations in the main body of this paper.

The factor $(AR_f^3/Z_1Z_0)^{1/2}$ appears in certain equations to follow. With the value for R_f adopted here it becomes

$$(AR_f^3/Z_1Z_0)^{1/2} \sim 2^{1/2}(1.54)^{3/2} \sim 2.7 \qquad A \sim A_1 \sim Z_1 < A_0 \sim 2Z_0$$

and (C40)

$$\sim 4\ (1.54)^{3/2} \sim 7.6 \qquad A \sim \tfrac{1}{2}A_1 \sim \tfrac{1}{2}A_0 \sim Z_1 \sim Z_0\,.$$

Thus this quantity varies by only a factor of less than 3 over the full range of interest in interacting nuclei.

f) Continuum Cross-Section for Compound Nucleus Formation

There are circumstances when it is of interest to compute the total interaction cross-section through compound nucleus formation. This is equivalent to summing Γ_2 over all possible final pairs of nuclei including re-emission of the initial nuclei. The sum is just Γ, and so the average continuum cross-section $\bar{\sigma}_l(C)$ for compound nucleus formation through partial wave l is just

$$\begin{aligned}
\bar{\sigma}_l(C) &= 2\pi^2\lambda\!\!\!^{-2}(2l+1)(\Gamma_1/D)_l \\
&= \pi\lambda\!\!\!^{-2}(2l+1)\left[\frac{4T\beta}{(1+T)^2}\right]_l \\
&\approx \pi\lambda\!\!\!^{-2}(2l+1)\left(\frac{4\lambda\!\!\!^{-}_o}{\lambda\!\!\!^{-}}P\beta\right)_o \qquad \text{Low energy} \\
&\approx \pi\lambda\!\!\!^{-2}(2l+1)\,. \qquad \text{High energy}
\end{aligned} \tag{C41}$$

Total cross-sections for compound nucleus formation or for any particular final process are obtained by summing over all partial waves, $\bar{\sigma}(C) = \Sigma\bar{\sigma}_l(C)$ and $\bar{\sigma} = \Sigma\bar{\sigma}_l$. The result for $\bar{\sigma}\,(C)$ at high energies is well known. At such energies, $\lambda\!\!\!^{-} < R$, and the particle trajectories are essentially classical with each partial wave confined to a cylindrical region having radii between $l\lambda\!\!\!^{-}$ and $(l+1)\lambda\!\!\!^{-}$. It is generally assumed that $\beta_l = 1$ if the radius R overlaps $l\lambda\!\!\!^{-}$ and $\beta_l = 0$ if it does not. If the interacting nuclei come into contact complete absorption occurs; if the trajectory falls outside the range of the nuclear interaction there is no absorption. Then if the maximum l for interaction is $L = R/\lambda\!\!\!^{-}$ one finds

$$\bar{\sigma}\,(C) = \sum_0^L \pi\lambda\!\!\!^{-2}(2l+1) = \pi\lambda\!\!\!^{-2}(L+1)^2 = \pi(R+\lambda\!\!\!^{-})^2\,. \tag{C42}$$

The same result is obtained if the summation is replaced by an integral over l from $-\frac{1}{2}$ to $L + \frac{1}{2}$. This is just the result to be expected in the optical analogy for the absorption of light of wavelength $\lambda\!\!\!^{-}$ by a "black" target of radius R. If $\beta_l \neq 1$ for $l \leq L$ then it is possible to write formally

$$\bar{\sigma}_C = \pi(R + \lambda\!\!\!^{-})^2\,\langle\beta\rangle_l\,. \tag{C43}$$

It will also be clear that the following relation holds formally

$$\bar{\sigma} = \pi(R+\lambda\!\!\!^{-})^2 \left\langle \beta \frac{\Gamma_2}{\Gamma} \right\rangle_l , \tag{C44}$$

where in equations (C43) and (C44) the indicated averages must be taken in an appropriate way over $0 \leq l \leq L$. The factors $\pi(R+\lambda\!\!\!^{-})^2$ give the dimensions and rough order of magnitude of $\bar{\sigma}$. The averages $\langle\beta\rangle_l$ or $\langle\beta\Gamma_2/\Gamma\rangle_l$ can only be calculated from experimental data. For dominant reactions at high enough energies $(\beta\Gamma_2/\Gamma)_l \approx 1$ for all $l \leq L$. Equations (C42)–(C44) are well established for neutron interactions above several MeV.

g) Total Continuum Cross-Sections for All Partial Waves in Charged Particle Interactions

We propose now a prescription in the case of charged particle interactions for carrying out the summation over l at low energies where $\bar{\sigma}_l$ is extremely energy dependent through the penetration factor P_l. It will be clear from equation (C35) that P_l can be expressed in terms of P_0, the penetration factor for $l = 0$, by the approximate relation *independent of energy*

$$\frac{P_l}{P_0} \approx \exp\left[-\frac{4l(l+1)}{x} \right], \tag{C45}$$

where x, defined in equation (C38), is a parameter measuring the relative strengths of the Coulomb and centrifugal potentials. If equation (C45) is substituted into the low-energy case in (C34) and the first summation in equation (C23) is replaced by an integration from $l = -\frac{1}{2}$ to $L + \frac{1}{2}$ one finds

$$\bar{\sigma} = \pi\lambda\!\!\!^{-2} \left(\frac{x\lambda\!\!\!^{-}_o}{\lambda\!\!\!^{-}} P_0 \right) \left\langle \beta \frac{\Gamma_2}{\Gamma} \right\rangle_l \left[\exp\frac{1}{x} - \exp - \frac{4(L+\frac{1}{2})(L+\frac{3}{2})}{x} \right] \tag{C46}$$

$$\approx \pi(R+\lambda\!\!\!^{-})^2 \left(\frac{4\lambda\!\!\!^{-}_o}{\lambda\!\!\!^{-}} P_0 \right) \left\langle \beta \frac{\Gamma_2}{\Gamma} \right\rangle_{l \leq L} \tag{C47}$$

$$\text{for } L^2 < l_c^2 = \frac{x}{4} \text{ or } E < \tfrac{1}{2}(E_C E_R)^{1/2} \sim \tfrac{1}{2} \text{ MeV}$$

$$\approx \pi\lambda\!\!\!^{-2} \left(\frac{x\lambda\!\!\!^{-}_o}{\lambda\!\!\!^{-}} P_0 \right) \left\langle \beta \frac{\Gamma_2}{\Gamma} \right\rangle_{l \leq l_c} \tag{C48}$$

$$\text{for } L^2 > l_c^2 = \frac{x}{4} > 1 \text{ or } E_C > E > \tfrac{1}{2}(E_C E_R)^{1/2} \sim \tfrac{1}{2} \text{ MeV}.$$

For $x \leq 4$, only the $l = 0$ partial wave is effective and equation (C48) can be used with x replaced by 4. Similar expressions can be written for $\bar{\sigma}(C)$ with Γ_2/Γ replaced by unity. In the conditions for approximations (C47) and (C48) we have used the relation $L^2 = R^2/\lambda\!\!\!^{-2} = E/E_R$ and have noted that $\frac{1}{2}(E_C E_R)^{1/2} = 2.7\ (Z_1 Z_0 / A R_f^3)^{1/2}$ is of the order of $\frac{1}{2}$ MeV independent of charge, mass, and radius for all interactions with $R_f = R_o(A_0^{1/3} + A_1^{1/3})$ and $R_o \sim 1.2$ to 1.6 fermis. It will be clear in these approximations that a critical partial wave, $l_c = \frac{1}{2}x^{1/2}$, is involved. For $l \leq l_c$, $P_l \sim P_0$. When the interaction energy is less than $\sim\frac{1}{2}$ MeV as in equation (C47), then $L < l_c$ or $R < l_c\lambda\!\!\!^{-}$ and the target area is more than covered by the partial waves $0 \leq l \leq l_c$. This implies that $P_l \sim P_0$ for all interacting partial waves and so the full "optical" area $\pi(R+\lambda\!\!\!^{-})^2$ appears in expression (C47) for $\bar{\sigma}$. However, when the interaction energy is greater than $\sim\frac{1}{2}$ MeV, then the wavelength is such that $l_c\lambda\!\!\!^{-} < R$ and only partial waves with $l \leq l_c$ have $P_l \sim P_0$ and contribute significantly to $\bar{\sigma}$, the formal result being given in

fair approximation by equation (C48). In equation (C48) note that x replaces 4 in $\bar{\sigma}_0$ from equation (C34) and an average over appropriate l-values replaces $(\beta\ \Gamma_2/\Gamma)_0$.

Basic to the calculation just made is the validity of approximation (C45). It holds strictly only for zero energy of interaction, and even then the numerical coefficient in the exponent is in general somewhat less than 4. Furthermore, as the energy of interaction increases all of the P_l for $l > 0$ increase more rapidly than P_0, and this can be simulated by a decrease in the numerical coefficient with energy. However, in equation (C48) we see that $x/4$ replaces unity when equation (C34) is summed over l, and so the only error involved is that the numerator of equation (C48) ought to be somewhat smaller or $\bar{\sigma}$ somewhat larger. But in going from equation (C46) to equation (C48) we replace the term in the square brackets, which is less than unity, by unity so some compensation is thereby achieved. In view of other uncertainties such as the sensitivity of P_0 to the exact choice of radius R it will be clear that equations (C47) and (C48) are adequate approximations for practical use. The important point is that they follow from the same basic assumption which underlies equation (C42), namely the optical analogy for charged particle processes at high energies or for neutrons at intermediate energies.

In regard to $\bar{\sigma}$ and $\bar{\sigma}(C)$ for reactions involving identical particles it suffices to note that the various modifications noted previously tend to compensate. For example, in the case of identical bosons with zero spin, only one-half of the possible interactions occur, namely, those with even l, but the statistical weight factor for each interaction is doubled. Exact compensation occurs only for large values of x, but in the case $O^{16} + O^{16}$, for example, $x \approx 33$ which is adequately large since then $l_c \sim 3$.

The effective interaction energy for charged particle reactions in stellar interiors is given by $E_o = 0.122\ (Z_1^2 Z_0^2 A T_9^2)^{1/3}$ MeV. Thus even for protons ($Z_1 = 1$, $A \approx 1$) interacting at $T_9 > 1$ with nuclei with $Z_0 > 8$ it is true that $E_o > \frac{1}{2}$ MeV. In this paper, where we are concerned with interactions with $Z_1 Z_0 > 14$ and $T_9 > 2$, it will be clear that equation (C48) is the appropriate approximation to employ.

h) Reaction Rates and Mean Lifetimes

Among the results so far obtained, equations (C48) and the low-energy version of (C34) have the major applications in this paper and the stellar reaction rates corresponding to them will now be derived. When equation (C35) is substituted into the low-energy version of equation (C34), the result can be written

$$\bar{\sigma}_l = \frac{\bar{S}_l}{E} \exp(-2\pi\eta), \tag{C49}$$

where

$$2\pi\eta = \frac{\pi E_C}{(E_R E)^{1/2}} = 0.989 Z_1 Z_0 A^{1/2} E_6^{-1/2} = 31.28 Z_1 Z_0 A^{1/2} E_3^{-1/2} \tag{C50}$$

and

$$\begin{aligned} \bar{S}_l &\approx \frac{\pi\hbar^2}{2M}(2l+1)\left(\frac{4\lambda\!\!\!^{-}_o}{\lambda\!\!\!^{-}} P_l \exp 2\pi\eta\right)\left(\beta\frac{\Gamma_2}{\Gamma}\right)_l \\ &\approx \frac{2\pi\hbar^2}{M}(2l+1)\left(\beta\frac{\Gamma_2}{\Gamma}\right)_l \left(\frac{E_C}{V_o}\right)^{1/2} \exp\left[2x - \frac{4E}{3E_R x} - \frac{4l(l+1)}{x}\right]. \end{aligned} \tag{C51}$$

Numerically, for $\bar{S}_l$ in MeV-barns, E_6 in MeV, and R_f in fermis,

$$\begin{aligned} \log \bar{S}_l \approx\ & -0.30 + \log(2l+1)(\beta\ \Gamma_2/\Gamma)_l + \tfrac{1}{2}\log Z_1 Z_0/A^2 R_f \\ & + 0.457\ (A Z_1 Z_0 R_f)^{1/2} - 3.31 l(l+1)/(A Z_1 Z_0 R_f)^{1/2} - 0.053\ E_6 (A R_f^3/Z_1 Z_0)^{1/2}. \end{aligned} \tag{C52}$$

When equation (C49) is substituted in equation (C2), the result is

$$\langle \bar{\sigma}_l v \rangle \approx \left(\frac{\pi}{M}\right)^{4/3} \frac{(16 e^2 \hbar^2 Z_1 Z_0)^{5/6}}{(3RV_o)^{1/2}(kT)^{2/3}} f_o(2l+1)\left(\beta \frac{\Gamma_2}{\Gamma}\right)_l \times \exp\left[2x - \tau - \frac{4l(l+1)}{x}\right], \tag{C53}$$

where $f_o = f(E_o)$ is the electron shielding factor at E_o discussed by Salpeter (1954) and is usually only slightly in excess of unity in massive stars and where

$$\begin{aligned}\tau &= 3(E_o/kT)\left[1+\frac{2kT}{3(E_C E_R)^{1/2}}\right]^{1/3} = 3\left(\frac{\pi E_C}{2E_R^{1/2}}\right)^{2/3}\left[\frac{1}{kT}+\frac{2}{3(E_C E_R)^{1/2}}\right]^{1/3} \\ &= 3\left[\pi a Z_1 Z_0 \left(\frac{Mc^2}{2kT}\right)^{1/2}\right]^{2/3}\left[1+\frac{2kT}{3}\left(\frac{2Mc^2R^3}{aZ_1Z_0\hbar^3c^3}\right)^{1/2}\right]^{1/3} \\ &= 4.248\left(Z_1^2 Z_0^2 \frac{A}{T_9}\right)^{1/3}\left[1+0.0105\left(\frac{AR_f^3}{Z_1Z_0}\right)^{1/2} T_9\right]^{1/3} \\ &= 4.248(Z_1^2Z_0^2A)^{1/3}\left[\frac{1}{T_9}+0.0105\left(\frac{AR_f^3}{Z_1Z_0}\right)^{1/2}\right]^{1/3}.\end{aligned} \tag{C54}$$

In power law expressions for $\langle \bar{\sigma}_l v \rangle$ the exponent of the temperature is $(\tau - 2)/3$. Numerically expression (C53) becomes

$$\langle \bar{\sigma}_l v \rangle \approx 6.5 \times 10^{-15} f_o(2l+1)\left(\beta \frac{\Gamma_2}{\Gamma}\right)_l \frac{(Z_1Z_0)^{5/6}}{R_f^{1/2} A^{4/3} T_9^{2/3}} \times \exp\left[2x - \tau - \frac{4l(l+1)}{x}\right] \text{cm}^3 \text{ sec}^{-1} \tag{C55}$$

or

$$\begin{aligned}\log \langle \bar{\sigma}_l v \rangle \approx\ & -14.19 + \log f_o(2l+1)(\beta\,\Gamma_2/\Gamma)_l + \tfrac{5}{6}\log Z_1Z_0 - \tfrac{4}{3}\log A - \tfrac{1}{2}\log R_f \\ & + 0.457\,(AZ_1Z_0R_f)^{1/2} - 3.31\,l(l+1)/(AZ_1Z_0R_f)^{1/2} - \tfrac{2}{3}\log T_9 \\ & - 1.845\,(Z_1^2Z_0^2\,A/T_9)^{1/3}\,[1 + 0.0105\,(AR_f^3/Z_1Z_0)^{1/2}\,T_9]^{1/3}.\end{aligned} \tag{C56}$$

Equation (C48) can be written

$$\bar{\sigma} = \Sigma \bar{\sigma}_l = \frac{\bar{S}}{E} \exp(-2\pi\eta), \tag{C57}$$

where

$$\begin{aligned}\bar{S} &= \Sigma \bar{S}_l \approx \int \bar{S}_l dl \\ &\approx \frac{x\pi\hbar^2}{2M}\left\langle \beta \frac{\Gamma_2}{\Gamma}\right\rangle \left(\frac{E_C}{V_o}\right)^{1/2} \exp\left(2x - \frac{4E}{3E_R x}\right).\end{aligned} \tag{C58}$$

Numerically, for $\bar{S}$ in MeV-barns, E_6 in MeV and R_f in fermis

$$\begin{aligned}\log \bar{S} \approx\ & -1.82 + \log \langle \beta\,\Gamma_2/\Gamma \rangle_l + \tfrac{1}{2}\log (Z_1Z_0/A) \\ & + 0.457\,(AZ_1Z_0R_f)^{1/2} - 0.053\,E_6\,(AR_f^3/Z_1Z_0)^{1/2}.\end{aligned} \tag{C59}$$

When equation (C48) is substituted in expression (C2), the result is

$$\langle \bar{\sigma} v \rangle = \Sigma \langle \bar{\sigma}_l v \rangle \approx \left(\frac{2}{M}\right)^{5/6} \left(\frac{2\hbar}{kT}\right)^{2/3} \frac{(2\pi e^2 Z_1 Z_0)^{4/3}}{(3V_o)^{1/2}} f_o \left\langle \beta \frac{\Gamma_2}{\Gamma} \right\rangle_l \exp(2x - \tau) \tag{C60}$$

$$\approx 8.5 \times 10^{-16} f_o \left\langle \beta \frac{\Gamma_2}{\Gamma} \right\rangle_l \frac{(Z_1 Z_0)^{4/3}}{A^{5/6} T_9^{2/3}} \exp(2x - \tau) \text{cm}^3 \text{ sec}^{-1}$$

or

$$\log \langle \bar{\sigma} v \rangle \approx -15.07 + \log f_o \langle \beta\, \Gamma_2/\Gamma \rangle_l + \tfrac{4}{3} \log Z_1 Z_0 - \tfrac{5}{6} \log A + 0.457 (A Z_1 Z_0 R_f)^{1/2} - \tfrac{2}{3} \log T_9 - 1.845 (Z_1^2 Z_0^2 A/T_9)^{1/3} \times [1 + 0.0105 (A R_f^3/Z_1 Z_0)^{1/2} T_9]^{1/3} . \tag{C61}$$

In the case of endoergic reactions having a threshold at E_t and for which Γ_2 rapidly approaches a constant value above threshold, equations (C53), (C55), and (C60) should be multiplied by the factor

$$\frac{1}{\pi^{1/2}} \int_{x_t}^{\infty} e^{-x^2} dx, \qquad \text{Multiplicative factor for (C53), (C55), and (C60),}$$

where $x_t = 2(E_t - E_o)/\Delta$.

The equations presented above, such as (C56) and (C61), are most useful when $\Gamma_1 < \Gamma$ but are, of course, formally correct even for $\Gamma_1 \sim \Gamma$. However, in this latter case the Γ in terms like $(\beta\, \Gamma_2/\Gamma)_l$ or $\langle \beta\, \Gamma_2/\Gamma \rangle_l$ is energy- or temperature-dependent. Actually Γ_1 will approach Γ at some energy in a specific case and above that energy the cross-section will "saturate" and no longer rise with energy thereafter. In fact $\bar{\sigma}_l \propto \pi\lambda^2 \propto E^{-1}$ and $\bar{\sigma} \propto \pi R^2 \propto E^0$. It does not seem possible to derive useful analytic expressions, and numerical integration of (C2) using empirical cross-section data is required. Some indication of the circumstances under which Γ_1 may approximate Γ is given by comparing the effective thermal interaction energy E_o with the Coulomb barrier height E_C. The ratio is

$$\frac{E_o}{E_C} = \left(\frac{\pi^2 M c^2}{2\alpha Z_1 Z_0}\right)^{1/3} \left(\frac{R}{\hbar c}\right) (kT)^{2/3} = 0.085 \left(\frac{A R_f^3}{Z_1 Z_0}\right)^{1/3} T_9^{2/3} = 0.2 T_9^{2/3} . \tag{C62}$$

Thus only for temperatures in excess of several billion degrees are the interaction energies comparable to barrier heights. However, in the case where capture radiation is the only reaction possible for protons, it will be found that $\Gamma_p \sim \Gamma_\gamma$ at energies considerably below the Coulomb barrier height and the (p, γ) cross-section then saturates. Care must be used in employing equations (C56) or (C61) in this case.

Note added in proof. Since the above was written, we have succeeded in deriving a useful analytical expression for $\langle \bar{\sigma} v \rangle$ when $\Gamma_1 \sim \Gamma$. This expression is

$$\langle \bar{\sigma} v \rangle = \pi^{3/2} x \left(\frac{\hbar^2}{2MkT^*}\right) \left(\frac{2kT}{M}\right)^{1/2} \left\langle \frac{\Gamma_2}{D} \right\rangle_l \exp(-E_0^*/kT) \qquad \text{for } \Gamma_1 \sim \Gamma \tag{C60'}$$

or

$$\log \langle \bar{\sigma} v \rangle = -14.25 + \log x - \tfrac{3}{2} \log A - \log T_9^* + \log \langle \Gamma_2/D \rangle_l + \tfrac{1}{2} \log T_9 - 5.04\, E_o^*/T_9 . \tag{C61'}$$

We have numbered these expressions as useful modifications of (C60) and (C61) when $\Gamma_1 \sim \Gamma$. In these expressions E_o^* is the effective thermal energy at which the Γ_1 for s-wave ($l = 0$) incident particles is just equal to $\Gamma/2$ or in the two-channel case at which $\Gamma_1 = \Gamma_2$. T^* is the temperature corresponding to E_o^* as given by equation (C7). It will be clear that E_o^* and T^* must be calculated from an analysis of empirical data for Γ_1, Γ_2, and $\Gamma = \Gamma_1 + \Gamma_2 + \ldots$.

It is also appropriate to emphasize at this point that the entire discussion in this appendix concerns reactions which proceed through compound nucleus formation. Direct and exchange reaction processes have been ignored entirely. Many direct or exchange reactions are endoergic with large negative Q-values. For example, $O^{16} + O^{16} \rightarrow O^{15} + O^{17} - 11.5$ MeV involves the exchange of a neutron without important Coulomb effects but the threshold energy exceeds that available in relevant stellar situations. The reaction $O^{16} + O^{16} \rightarrow C^{12} + Ne^{20} - 2.4$ MeV does not have such a high threshold energy but involves the exchange of an alpha-particle with concomitant barrier effects. In general the interesting stellar reactions are exoergic such as $O^{16} + O^{16} \rightarrow Si^{28} + \alpha + 9.6$ MeV. Clearly such a reaction requires considerable amalgamation of the two interacting O^{16} nuclei and thus must proceed primarily through compound nucleus formation.

i) Continuum Reaction Rates and Lifetimes

The reaction rate per gm per sec corresponding to equation (C60) is

$$r = \rho \frac{x_1 x_0}{M_1 M_0} \langle \sigma v \rangle = 3.63 \times 10^{47} \rho \frac{x_1 x_0}{A_1 A_0} \langle \sigma v \rangle$$

$$\approx 3.1 \times 10^{32} \rho \frac{x_1 x_0}{A_1 A_0} f_o \left\langle \beta \frac{\Gamma_2}{\Gamma} \right\rangle_l \frac{(Z_1 Z_0)^{4/3}}{A^{5/6} T_9^{2/3}} \exp(2x - \tau) \text{ reactions gm}^{-1} \text{ sec}^{-1} \quad \text{(C63)}$$

or

$$\log r \sim 32.49 + \log \rho x_1 x_0 / A_1 A_0 + \log f_o \langle \beta\, \Gamma_2/\Gamma \rangle_l + \tfrac{4}{3} \log Z_1 Z_0 - \tfrac{5}{6} \log A$$
$$+ 0.457\, (A Z_1 Z_0 R_f)^{1/2} - \tfrac{2}{3} \log T_9 - 1.845\, (Z_1^2 Z_0^2 A / T_9)^{1/3} \quad \text{(C64)}$$
$$\times [1 + 0.0105\, (A R_f^3 / Z_1 Z_0)^{1/2}\, T_9]^{1/3} .$$

For the interaction of identical particles multiply the right-hand side of expression (C63) by $\frac{1}{2}$ and subtract 0.30 from the right-hand side of expression (C64). In the first part of expression (C63) $\bar{\sigma}$ has been replaced by σ since the expression is a general one.

The lifetime for particles 0 to interaction with particles 1 for *all* outgoing reactions channels is

$$\tau_1(0) = M_1 / \rho x_1 \Sigma_2 \langle \sigma v \rangle = 1.660 \times 10^{-24} A_1 / \rho x_1 \Sigma_2 \langle \sigma v \rangle \quad \text{(C65)}$$

or

$$\log \tau_1(0) \approx -8.71 - \log \rho x_1 / A_1 - \log f_o \langle \beta \rangle_l - \tfrac{4}{3} \log Z_1 Z_0 + \tfrac{5}{6} \log A$$
$$- 0.457\, (A Z_1 Z_0 R_f)^{1/2} + \tfrac{2}{3} \log T_9 + 1.845\, (Z_1^2 Z_0^2 A / T_9)^{1/3} \quad \text{(C66)}$$
$$\times [1 + 0.0105\, (A R_f^3 / Z_1 Z_0)^{1/2}\, T_9]^{1/3} .$$

Here we have assumed that $\Gamma_1 < \Gamma$ so that $\Sigma\Gamma_2 \approx \Gamma$ for all l. When $\Gamma_1 \sim \Gamma$ use equation (C60′) in equation (C65) with Γ_2 replaced by $\Sigma\Gamma_2$.

If equation (C60) applies to a capture radiation reaction ($\Gamma_2 = \Gamma_\gamma$) then the reverse photonuclear reaction rate can be determined and the lifetime of nucleus 2 to photodisintegration with the production of 0 and 1 becomes

$$\frac{1}{\tau_\gamma(2)} = \left(\frac{MkT}{2\pi\hbar^2}\right)^{3/2} \langle \bar{\sigma} v \rangle \exp - Q/kT \quad \text{(C67)}$$

or

$$\log \tau_\gamma(2) \approx -33.77 - \tfrac{3}{2}\log AT_9 - \log\langle\bar{\sigma}v\rangle + 5.04\,Q_6/T_9 \approx -18.70$$
$$- \log f_o\langle\beta\,\Gamma_\gamma/\Gamma\rangle_l - \tfrac{4}{3}\log Z_1Z_0 - \tfrac{2}{3}\log A - 0.457\,(AZ_1Z_0R_f)^{1/2} - \tfrac{5}{6}\log T_9 \quad \text{(C68)}$$
$$+ 1.845\,(Z_1^2Z_0^2A/T_9)^{1/3}\,[1 + 0.0105\,(AR_f^3/Z_1Z_0)^{1/2}\,T_9]^{1/3} + 5.04\,Q_6/T_9\,.$$

Equation (C67) is not general in that statistical factors do not occur as would be necessary if $\bar{\sigma}$ were replaced by σ.

j) Energy Generation

The energy generation through a nuclear reaction is given by

$$\epsilon = rQ = 1.602\times10^{-6}rQ_6$$
$$= 0.581\times10^{42}\rho\,\frac{x_1x_0}{A_1A_0}\,Q_6\langle\sigma v\rangle \text{ erg gm}^{-1}\text{ sec}^{-1}, \quad \text{(C69)}$$

where Q is the energy released per reaction and is usually expressed as Q_6 in MeV. At this point define

$$q = Q/M_u\Sigma A_i = \frac{0.965\times10^{18}}{\Sigma A_i}\,Q_6 \text{ erg gm}^{-1}, \quad \text{(C70)}$$

where q is the energy released in ergs for each gram of interacting nuclei consumed and ΣA_i is the sum of the masses of the interacting nuclei in atomic mass units M_u. Then for two non-identical interacting nuclei the energy generation rate is

$$\epsilon = \frac{q}{\tau_1(0)}\,\frac{x_0(A_1+A_0)}{A_0} = \frac{q}{\tau_0(1)}\,\frac{x_1(A_1+A_0)}{A_1} \text{ erg gm}^{-1}\text{ sec}^{-1}, \quad \text{(C71)}$$

and for any number n of interacting identical particles

$$\epsilon = q\,\frac{x}{\tau} = \frac{q\,x^n}{\tau(x=1)} \text{ erg gm}^{-1}\text{ sec}^{-1}, \quad \text{(C72)}$$

where in equation (C72) we drop identifying subscripts and $\tau(x = 1)$ is the "instantaneous" mean lifetime for $x = 1$. Expression (C72) is particularly convenient when burning occurs in a one-component medium as in the case of pure hydrogen burning, pure helium burning, pure carbon burning, pure oxygen burning, etc. For the helium burning, $n = 3$; for the others, $n = 2$.

In pure helium burning with $3He^4 \rightarrow C^{12}$ alone, use the energy release q and the lifetime of He^4 appropriate to this process. When $C^{12}(\alpha, \gamma)O^{16}$ is in equilibrium with $3He^4 \rightarrow C^{12}$ so that effectively $4He^4 \rightarrow O^{16}$, use q for the over-all process and $\tau = (\frac{3}{4})\tau_{3\alpha}(He^4) = (\frac{1}{4})\tau_{12}(He^4)$. In both cases $n = 3$ if $\tau_{3\alpha}(He^4)$ for $x_\alpha = 1$ is used.

In pure hydrogen burning by the *pp*-chain the energy generation rate depends on whether one or two *pp*-reactions are required in $4H^1 \rightarrow He^4$. If two are required, as is the case when the chain is completed by $2He^3 \rightarrow He^4 + 2H^1$, then twice the lifetime of H^1 to the *pp*-reaction must be used in equation (C72). If only one is required, as is the case when the chain is completed by $He^3(\alpha, \gamma)Be^7(e^-, \nu)Li^7(p, \alpha)He^4$, then the appropriate lifetime is just that of H^1 to the *pp*-reaction. In both cases $n = 2$.

For the CNO bi-cycle equation (C71) can be used for the energy generation in any one of the interactions of the CNO isotopes with hydrogen, but for the over-all energy generation, (C72) may be used if τ is the lifetime of hydrogen at a specified CNO concentration by mass and q is taken as 5.98×10^{18} erg gm^{-1} from $4H^1 \rightarrow He^4$. At equilibrium τ is approximately equal to $\tau_{14}(H^1)$ for $N^{14}(p, \gamma)O^{15}$, since this is the slowest reaction in the main CN cycle.

k) Average Energy Generation or Loss in a Star

Equation (C69) gives the stellar energy generation for a given nuclear reaction at specified composition, density, and temperature. In what follows it will be assumed that no change in composition occurs over the reaction region in a star. This is the case in convective cores. Thus the average energy generation in a star can be calculated if the fixed composition is known and if the run of density and temperature throughout the star is known. We seek

$$\bar{\epsilon} = \frac{L}{M} = \frac{1}{M}\int \epsilon dM = \frac{4\pi}{M}\int \epsilon \rho r^2 dr\,, \tag{C73}$$

where M is the stellar mass and L is the contribution to the stellar luminosity arising from the reaction of interest.

Express the energy generation *per gram* in terms of powers of the density and temperature thus:

$$\frac{\epsilon}{\epsilon_o} = \left(\frac{\rho}{\rho_o}\right)^{u-1}\left(\frac{T}{T_o}\right)^{s}, \tag{C74}$$

where the subscript $_o$ designates central conditions. It will be clear that the power u applies to the dependence of energy generation *per cm*^{3} on density.

In a polytrope of index n it is sufficiently accurate to neglect the dependence of $\mu\beta$ on T for massive stars (see Appendix B) and so

$$\frac{\rho}{\rho_o} \approx \left(\frac{T}{T_o}\right)^{n}. \tag{C75}$$

Thus

$$L \approx 4\pi\epsilon_o\rho_o\int\left(\frac{\rho}{\rho_o}\right)^{u}\left(\frac{T}{T_o}\right)^{s} r^2 dr = 4\pi\epsilon_o\rho_o\int\left(\frac{T}{T_o}\right)^{nu+s} r^2 dr\,. \tag{C76}$$

In the notation of Chandrasekhar (1939) with $r = a\xi$ and $T/T_o = \theta$ this becomes

$$L \approx 4\pi\epsilon_o\rho_o a^3\int \theta^{nu+s}\xi^2 d\xi\,, \tag{C77}$$

where

$$a = \left[\frac{n+1}{4\pi}\left(\frac{RT}{\rho\mu\beta}\right)_o\right]^{1/2}. \tag{C78}$$

The run of the dimensionless temperature θ with the dimensionless radius ξ proceeds according to

$$\theta = \exp\left(-\frac{\xi^2}{6}\right)\left[1+\left(\frac{n}{120}-\frac{1}{72}\right)\xi^4+\ldots\right] \approx \exp\left(-\frac{\xi^2}{6}\right). \quad \xi < 1 \tag{C79}$$

The approximate form for small ξ is sufficient for calculating L, the main contribution to which comes from the high-temperature, high-density central regions where the nuclear processes are most prolific. Thus

$$L \approx 4\pi\xi_o\rho_o a^3\int \exp\left(-\frac{nu+s}{6}\xi^2\right)\xi^2 d\xi \approx 4\pi\epsilon_o\rho_o a^3\frac{(27\pi/2)^{1/2}}{(nu+s)^{3/2}}. \tag{C80}$$

The stellar mass is given by

$$M = 4\pi\int \rho r^2\, dr = 4\pi\rho_o a^3\int \theta^n\, \xi^2\, d\xi \tag{C81}$$

but cannot be determined accurately enough by use of the approximation in expression (C79). Fortunately, Chandrasekhar (1939) expresses the mass in terms of tabulated constants of integration M_n as follows:

$$M = 4\pi\rho_o a^3 M_n\,, \tag{C82}$$

so that

$$\bar{\epsilon} \approx \epsilon_o \frac{(27\pi/2)^{1/2}}{M_n(nu+s)^{3/2}}. \quad \text{(C83)}$$

Thus a mass $M\bar{\epsilon}/\epsilon_0$ is effectively providing the energy generation at the central operating conditions. For a polytrope of index $n = 3$ it is known that $M_n \approx 2$, so numerically

$$\bar{\epsilon} \approx \epsilon_o \frac{3.2}{(3u+s)^{3/2}}. \qquad n = 3 \quad \text{(C84)}$$

Similar expressions can be derived for energy losses. For pair annihilation neutrino losses where $u = 0$, $s = 9$ the average energy loss is about 12 per cent of that at the center.

REFERENCES

Adams, J. B., Ruderman, M. A., and Woo, C-H. 1963, *Phys. Rev.*, **129**, 1383.
Ajzenberg-Selove, F., and Lauritsen, T. 1959, *Nuclear Phys.*, **11**, 1.
Ajzenberg-Selove, F., and Stelson, P. H. 1960, *Phys. Rev.*, **120**, 500.
Alburger, D. E. 1960, *Phys. Rev.*, **118**, 235.
———. 1961, *ibid.*, **124**, 193.
Aller, L. H. 1961, *The Abundance of the Elements* (New York: Interscience Publishers, Inc.).
Bacastow, R., Elioff, T., Larsen, R., Wiegand, C., and Ypsilantis, T. 1962, *Phys. Rev. Letters*, **9**, 400.
Bahcall, J. N. 1963, private communication.
———. 1964, *Ap. J.*, **139**, 318. (*See also* 1962, *Phys. Rev.*, **128**, 1297; 1962, *Phys. Rev.*, **126**, 1143; 1962, *Ap. J.*, **136**, 445; and 1961, *Phys. Rev.* **124**, 495.)
Bardin, R. K., Barnes, C. A., Fowler, W. A., and Seeger, P. A. 1960, *Phys. Rev. Letters*, **5**, 323.
———. 1962, *Phys. Rev.*, **127**, 583.
Becker, R. A., and Fowler, W. A. 1959, *Phys. Rev.*, **115**, 1410.
Bell, J. S., Lovseth, J., and Veltman, M. 1963, Paper presented at the International Conference on Elementary Particles, Sienna, Italy, October, 1963.
Bethe, H. 1939, *Phys. Rev.*, **55**, 434.
Blair, J. S. 1954, *Phys. Rev.*, **95**, 1218.
Blin-Stoyle, R. J., and Le Tourneux, J. 1961, *Phys. Rev.*, **123**, 627.
Bromley, D. A., Kuehner, J. A., and Almqvist, E. 1960, *Proceedings of the International Conference on Nuclear Structure at Kingston, Canada*, ed. D. A. Bromley and E. W. Vogt (Toronto: University of Toronto Press; Amsterdam: North-Holland Publishing Co.).
Burbidge, E. M., Burbidge, G. R., Fowler, W. A., and Hoyle, F. 1957, *Revs. Mod. Phys.*, **29**, 547; referred to hereafter as "B²FH (1957)."
Cabibbo, N. 1963, *Phys. Rev. Letters*, **10**, 531.
Cameron, A. G. W. 1959*a*, *Ap. J.*, **130**, 452.
———. 1959*b*, *ibid.*, p. 884.
Caughlan, G. R., and Fowler, W. A. 1962, *Ap. J.*, **136**, 453.
Chandrasekhar, S. 1939, *An Introduction to the Study of Stellar Structure* (Chicago: University of Chicago Press).
Chandrasekhar, S., and Henrich, L. R. 1942, *Ap. J.*, **95**, 288.
Chiu, H.-Y., 1961*a*, *Ann. Phys.*, **15**, 1.
———. 1961*b*, *ibid.*, **16**, 321.
———. 1961*c*, *Phys. Rev.*, **123**, 1040.
———. 1963, *Ap. J.*, **137**, 343.
Chiu, H.-Y., and Morrison, P. 1960, *Phys. Rev. Letters*, **5**, 573.
Chiu, H.-Y., and Stabler, R. 1961, *Phys. Rev.*, **122**, 1317.
Clayton, D. D., Fowler, W. A., Hull, T. E., and Zimmerman, B. A. 1961, *Ann. Phys.*, **12**, 331.
Clifford, F. E., and Tayler, R. 1964, *Memoirs R.A.S.* (in press).
Colgate, S. A., and Johnson, M. H. 1960, *Phys. Rev. Letters*, **5**, 235.
Danby, G., Gaillard, J-M., Goulianos, K., Lederman, L. M., Mistry, N., Schwartz, M., and Steinberger, J. 1962, *Phys. Rev. Letters*, **9**, 36.
Deinzer, W., and Salpeter, E. E. 1964, *Ap. J.*, **140**, 499.
Dennison, D. M. 1954, *Phys. Rev.*, **96**, 378.
Eddington, A. S. 1930, *The Internal Constitution of the Stars* (Cambridge: Cambridge University Press).
Endt, P. M., and Leun, C. van der. 1962, *Nuclear Phys.*, **34**, 1.

Feynman, R. P., and Gell-Mann, M. 1958*a*, *Phys. Rev.*, **109**, 193.
———. 1958*b*, *Proceedings of the Second United Nations International Conference on the Peaceful Uses of Atomic Energy*, Vol. **30** (Geneva: United Nations).
Freeman, J. M., Montague, J. H., West, D., and White, R. E. 1962, *Phys. Rev. Letters*, **3**, 136.
Freeman, J. M., Montague, J. H., Murray, G., White, R. E., and Burcham, W. E. 1964, *ibid*, **8**, 115.
Fregeau, J. H. 1956, *Phys. Rev.*, **104**, 225.
Gamow, G., and Schönberg, M. 1941, *Phys. Rev.*, **59**, 539.
Gandel'man, G. M., and Pinaev, V. S. 1959, *Zhur. Eksp. i Teoret. Fiz.*, **37**, 1072; *Soviet Phys.—J.E.T.P.*, **10**, 764 (1960).
Gell-Mann, M. 1958, *Phys. Rev.*, **111**, 362.
———. 1961, *Phys. Rev. Letters*, **6**, 70.
Gove, H. E. Litherland, A. E., and Ferguson, A. J. 1961, *Phys. Rev.*, **124**, 1943.
Hahn, B., Ravenhall, D. G., and Hofstadter, R. 1956, *Phys. Rev.*, **101**, 1131.
Hall, I., and Tanner, N. W. 1964, *Nuclear Physics*, **53**, 673.
Hamada, T., and Salpeter, E. E. 1961, *Ap. J.*, **134**, 683.
Harrison, B. K., Wakano, M., and Wheeler, J. A. 1958, *La Structure et l'évolution de l'universe* (Brussels: R. Stoops).
Hoot, C., Kondo, M., and Rickey, M. 1963, *Bull. Am. Phys. Soc.*, **8**, 598.
Hoyle, F. 1946, *M.N.*, **106**, 343.
———. 1954, *Ap. J. Suppl.*, **1**, 121.
Hoyle, F., and Fowler, W. A. 1960, *Ap. J.*, **132**, 565.
Hoyle, F., Fowler, W. A., Burbidge, E. M., and Burbidge, G. R. 1964, *Ap. J.*, **139**, 909; referred to hereafter as "HFB[2] (1964)."
Iben, I., Jr. 1963, *Ap. J.*, **138**, 1090.
Kameny, S. L. 1956, *Phys. Rev.*, **103**, 358.
Konopinski, E. J., 1959, *Ann. Rev. Nuclear Sci.*, **9**, 99.
Lee, T. D. 1962, *Phys. Rev.*, **128**, 899.
Lee, Y. K., Mo, L. W., and Wu, C. S. 1963, *Phys. Rev. Letters*, **10**, 253.
Levine, M. 1960, private communication.
———. 1963, unpublished Ph.D. thesis, California Institute of Technology.
Matinyan, S. G., and Tsilosani, N. N. 1961, *Zhur. Eksp. i Teoret. Fiz.*, **41**, 1681; *Soviet Phys.—J.E.T.P.*, **14**, 1195 (1962).
Mayer-Kuckuk, T., and Michel, F. C. 1961, *Phys. Rev. Letters*, **7**, 167.
———. 1962, *Phys. Rev.*, **127**, 545.
Michel, F. C. 1964, *Phys. Rev.*, **133**, B329.
Miller, R. G., Kavanagh, R. W., and Goldring, G. 1963, *Bull. Am. Phys. Soc.*, **8**, 599.
Morton, D. C. 1964, *Ap. J.*, **140**, 460.
Mott, N. F., and Massey, H. S. W. 1949, *The Theory of Atomic Collisions* (2d ed.; Oxford: Clarendon Press), chap. v.
Nakamura, S., and Sato, S. 1963, *Prog. Theoret. Phys. (Kyoto)*, **29**, 325.
Nordberg, M. E., Jr., Morinigo, F. B., and Barnes, C. A. 1960, *Phys. Rev. Letters*, **5**, 321.
———. 1962, *Phys. Rev.*, **125**, 321.
Ohyama, N. 1963, *Prog. Theoret. Phys. (Kyoto)*, **30**, 170.
Ôno, Y., Sakashita, S., and Ohyama, N. 1961, *Prog. Theoret. Phys. Suppl.*, No. 20.
Oppenheimer, J. R., and Volkoff, G. M. 1939, *Phys. Rev.*, **55**, 374.
Peterson, V. L., and Bahcall, J. N. 1963, *Ap. J.*, **138**, 452.
Pinaev, V. S. 1963, *Zhur. Eksp. i Teoret. Fiz.*, **45**, 548; *Soviet Phys.—J.E.T.P.*, **18**, 377 (1964).
Pontecorvo, B. 1959, *Zhur. Eksp. i Teoret. Fiz.*, **36**, 1615; *Soviet Phys.—J.E.T.P.*, **9**, 1148.
Preston, M. A. 1962, *Physics of the Nucleus* (Reading: Addison-Wesley Publishing Co.)
Reeves, H., and Salpeter, E. E. 1959, *Phys. Rev.*, **116**, 1505.
Reines, F. 1960, *Ann. Rev. Nuclear Sci.*, **10**, 1.
Reitz, J. R. 1950, *Phys. Rev.*, **77**, 10.
Ritus, V. I. 1961, *Zhur. Eksp. i Teoret. Fiz.*, **41**, 1285; *Soviet Phys.—J.E.T.P.*, **14**, 915 (1962).
Rose, M. E., Dismuke, N. M., Perry, C. L., and Bell, P. R. 1955, *Beta and Gamma Ray Spectroscopy*, ed. K. Seigbahn (Amsterdam: North-Holland Publishing Co.), Appendix II.
Rosenberg, L. 1963, *Phys. Rev.*, **129**, 2786.
Roth, B., and Wildermuth, K. 1960, *Nuclear Phys.*, **20**, 10.
Saakyan, G. S. 1963, *Soviet Astr.*, **1**, 60.
Sakurai, J. J. 1958, *Nuovo cimento*, **7**, 649.
Salpeter, E. E. 1954, *Australian J. Phys.*, **7**, 373.
———. 1960, *Ann. Phys.*, **11**, 393.
Sampson, D. H. 1962, *Ap. J.*, **135**, 261.
Schönberg, M., and Chandrasekhar, S. 1942, *Ap. J.*, **96**, 161.
Seeger, P. A., and Kavanagh, R. W. 1963, *Nuclear Phys.*, **46**, 577.
Stothers, R. 1963, *Ap. J.*, **137**, 770.
Stothers, R., and Chiu, H.-Y. 1962, *Ap. J.*, **135**, 963.

Sudarshan, E. C. G., and Marshak, R. E. 1958, *Phys. Rev.*, **109**, 1860.
Suess, H. E., and Urey, H. C. 1956, *Revs. Mod. Phys.*, **28**, 53.
Swann, C. P., and Metzger, F. R. 1957, *Phys. Rev.*, **108**, 982.
Talbot, R. J. 1964, private communication.
Tuttle, R. J. 1952, private communication.
Vogt, E. 1962, *Revs. Mod. Phys.*, **34**, 723.
Way, K., Gove, N. B., McGinnis, C. L., and Nakasima, R. 1961, *Landolt-Börnstein* N.S., Group 1: Vol. 1, edited by A. M. Hellwege and K. H. Hellwege (Berlin: Springer-Verlag).
Wells, D. O., Blatt, S. L., and Meyerhof, W. E. 1963, *Phys. Rev.*, **130**, 1961.
Wu, C. S. 1961, *The Neutrino: Theoretical Physics in the Twentieth Century: A Memorial Volume to Wolfgang Pauli*, ed. M. Fierz and V. F. Weisskopf (New York: Interscience Publishers, Inc.), pp. 249–303.

Note added in proof: Since the discussion of the numerical value for G on p. 210 was written, it has generally come to be believed that the difference between the muon coupling constant and the polar-vector beta-decay coupling constant is to be understood in terms of the hypothesis of Feynman and Gell-Mann (1958*b*) and of Cabibbo (1963). It is thus preferable to use the muon coupling constant as the universal one for all leptons including electrons. In this case the correct G for $e^+ + e^- \rightarrow \nu + \bar{\nu}$ is the muon coupling constant which is 1.5 per cent greater than the polar-vector beta-decay coupling constant used in this paper. Numerical coefficients in all equations involving G^2, such as equations (3), (6), (19), (20), etc., should be increased by 3.0 per cent. This change should *not* be made in Appendix A, where the polar-vector beta-decay coupling constant still applies.